University of Tehran
College of Engineering
School of Chemical Engineering

ACTA

VU University Amsterdam
Academic Centre for Dentistry Amsterdam
MOVE Research Institute Amsterdam

Improved endothelialization by silicone surface modification and fluid hydrodynamics modulation: Implications for oxygenator biocompatibility

Nasim Salehi Nik

Under supervision of: Prof.dr. Jenneke Klein Nulend
Prof.dr. Ghassem Amoabediny
Co-supervisors: Dr. Behrouz Zandieh Doulabi
Prof.dr. Mohammad Ali Shokrgozar

Improved endothelialization by silicone surface modification and fluid hydrodynamics modulation: Implications for oxygenator biocompatibility

Nasim Salehi Nik

Commitment of the thesis originality

I hereby attest that the material included in this thesis is the result of my work conducted at the School of Chemical Engineering, College of Engineering, University of Tehran, Tehran, Iran, in collaboration with Academic Centre for Dentistry Amsterdam, University of Amsterdam and VU University Amsterdam, MOVE Research Institute Amsterdam, Amsterdam, The Netherlands, and that this thesis has referred to any scientific material adopted from other research according to the regulations. This thesis has not been submitted before to obtain the same or higher level certificates.

First and last name of the student: Nasim Salehi-Nik

Student's signature: 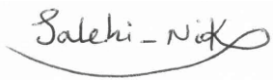

University of Tehran
College of Engineering
School of Chemical Engineering

VU University Amsterdam
Academic Centre for Dentistry Amsterdam
MOVE Research Institute Amsterdam

Improved endothelialization by silicone surface modification and fluid hydrodynamics modulation: Implications for oxygenator biocompatibility

Nasim Salehi Nik

Under supervision of: Prof.dr. Ghassem Amoabediny
Prof.dr. Jenneke Klein Nulend
Co-supervisors: Prof.dr. Mohammad Ali Shokrgozar
Dr. Behrouz Zandieh Doulabi

A thesis submitted to the Graduate Studies Office in fulfillment of the requirements for the degree of Doctorate in Chemical Engineering

The studies described in this thesis were carried out at the School of Chemical Engineering, College of Engineering, University of Tehran, Tehran, Iran, in collaboration with Academic Centre for Dentistry Amsterdam, University of Amsterdam and VU University Amsterdam, MOVE Research Institute Amsterdam, Amsterdam, The Netherlands.

The printing of this thesis was kindly supported by:
ACTA onderzoeksinstituut

Layout design: Nasim Salehi-Nik
Printed by: GVO drukkers & vormgevers B.V.
ISBN: 978-90-6464-945-5

UNIVERSITY OF TEHRAN
VRIJE UNIVERSITEIT AMSTERDAM

Improved endothelialization by silicone surface modification and fluid hydrodynamics modulation: Implications for oxygenator biocompatibility

ACADEMISCH PROEFSCHRIFT

ter verkrijging van de graad Doctor aan
de Vrije Universiteit Amsterdam
en de graad Doctor aan de University of Tehran,
op gezag van de rectores magnifici
prof.dr. V. Subramaniam en prof.dr. M. Nili-Ahmadabadi

in het openbaar te verdedigen
ten overstaan van de gezamenlijke promotiecommissie
van de Faculteit der Tandheelkunde van de Vrije Universiteit Amsterdam en
de Faculteit Chemical Engineering van de University of Tehran
op 21 september 2015 om 16:00 uur te Teheran, en
op 14 december 2015 om 13:45 uur
in de aula van de universiteit,
De Boelelaan 1105 te Amsterdam

door
Nasim Salehi Nik
geboren te Teheran, Iran

promotoren:	prof.dr. J. Klein Nulend
	prof.dr. G. Amoabediny
copromotoren:	dr. B. Zandieh Doulabi
	prof.dr. M.A. Shokrgozar

Dit proefschrift is tot stand gekomen op basis van een daartoe tussen de Vrije Universiteit en de University of Tehran, Iran, overeengekomen samenwerkingsverband ter regeling van een gezamenlijke promotie als bedoeld in het Promotiereglement Vrije Universiteit, hetgeen mede tot uiting wordt gebracht door de weergave van de beeeldmerken van beide universiteiten op deze pagina.

بنام خدا

دانشگاه تهران

پردیس دانشکده های فنی

دانشکده مهندسی شیمی

گواهی دفاع از رساله دکتری

هیات داوران رساله دکتری خانم **نسیم صالحی نیک** به شماره دانشجویی **۸۱۰۴۸۸۴۳۶** در رشته مهندسی شیمی با عنوان **"اصلاح سطح سیلیکون و اثر هیدرودینامیک سیال در افزایش پوشش‌دهی با سلول‌های اندوتلیال جهت کاربرد در زیست‌سازگاری ریه‌مصنوعی"** را در تاریخ **۱۳۹۴/۰۶/۳۰** با درجه **عالی** ارزیابی نمود.

ردیف	مشخصات هیات داوران	نام و نام خانوادگی	مرتبه دانشگاهی	دانشگاه	امضاء
۱	استاد راهنمای اول	دکتر قاسم عموعابدینی	دانشیار	تهران	
۲	استاد راهنمای دوم	*Prof.dr. Jenneke Klein-Nulend*	استاد	*VU University Amsterdam*	
۳	استاد مشاور اول	دکتر محمدعلی شکرگزار	استاد	انستیتو پاستور ایران	
۴	استاد مشاور دوم	دکتر بهروز زندیه دولابی	استادیار	*VU University Amsterdam*	
۵	استاد مدعو داخلی	دکتر رضا ضرغامی	دانشیار	تهران	
۶	استاد مدعو داخلی	دکتر محمدرضا مهرنیا	دانشیار	تهران	
۷	استاد مدعو خارجی	نوشین حقیقی‌پور	استادیار	انستیتو پاستور ایران	
۸	استاد مدعو خارجی	دکتر حسین قنبری	استادیار	علوم پزشکی تهران	
۹	نماینده کمیته تحصیلات تکمیلی دانشکده مهندسی شیمی	دکتر رضا ضرغامی	دانشیار	تهران	

دانشکده مهندسی شیمی
معاونت پژوهشی و تحصیلات تکمیلی

GENERAL ABSTRACT

Endothelialization of hollow fibers in new types of artificial lungs, so-called biohybrid artificial lungs, is promising to decrease thrombotic complications resulting from blood flow through these devices. This thesis aimed to develop a stable and anti-thrombotic functional endothelial cell layer on the surface of silicone hollow fibers using silicone surface modification and fluid hydrodynamics modulation. We started by collagen immobilization on the inside surface of silicone tubes using different functional groups. Collagen-immobilized silicone tubes with amine or carboxyl groups increased the number of endothelial cells by 3-4-fold after 6 days of culture and stimulated nitric oxide release by endothelial cells by approximately 3-fold. Collagen immobilization with carboxyl groups was applied to the outside surface of silicone hollow fibers, but 27% of the cells still detached at a high fluid shear stress of 30 dyn/cm^2. Therefore, flow preconditioning of endothelial cells with 12 dyn/cm^2 fluid shear stress in a parallel-plate flow chamber for 24 h was used to stimulate cell monolayer retention under high fluid shear stress. Flow preconditioning of endothelial cells decreased cell detachment under high fluid shear stress of 30 dyn/cm^2 by 8-fold, compared with un-preconditioned cells. Shear stress simulation at the cell's surface by COMSOL software coupled with cell experimental results showed that flow preconditioning of endothelial cells tailors a smooth surface of the cells, which resulted in a more homogenous shear stress distribution at the cell's surface, and decreased cell detachment.

The ultimate success of developing biocompatible materials depends on the anti-thrombogenicity of the surface and the degree of confluency of the endothelial cell layer. Therefore, sodium nitrite as an anti-thrombotic agent and/or growth hormone as a growth-inducing agent in free-form or in nanoliposomes were blended with collagen solution, and immobilized on silicone tubes. Sodium nitrite-collagen conjugate with 25 μM initial sodium nitrite maximally increased endothelial cell number by 28% after 6 days of culture. Five hundred μM initial sodium nitrite maximally decreased platelet adhesion by 3-fold compared with collagen coating. The biomimetic nanoliposomal sodium nitrite (nNitrite)-nanoliposomal growth hormone (nGH)-collagen (Col) coatings resulted in endothelial cell confluency of 83-119%, and decreased platelet adhesion by 50-76% after 6 days of endothelial cell culture.

The application potential of the biomimetic nNitrite-nGH-Col coating on the outside surface of silicone hollow fibers was also assessed under blood flow shear stress with the aim to improve the performance of biohybrid artificial lungs. Quantification of the nitrite production from surface-modified fibers under different shear stresses coupled with simulations of nitrite transport in a parallel-plate flow chamber using COMSOL software were used to determine nitrite bioavailability at the hollow fiber-blood interface, which is of crucial importance to inhibit thrombus

formation. Our results showed that nitrite bioavailability has a direct effect on thrombus deposition on surface-modified fibers under shear stress.

Coating of fibers with nNitrite-nGH-Col conjugate not only increased endothelial cell proliferation and stability, but also increased nitrite bioavailability and inhibited thrombus formation even under high shear stress, suggesting that this conjugate coating is highly promising to improve the biocompatibility of biohybrid artificial lungs. This, together with new insights in the effects of fluid shear stress on increasing cell stability, and anti-thrombotic functionality, as well as on modifying the bioavailability of anti-thrombotic biomolecules and thrombus deposition, improves our understanding of how surface modification and fluid hydrodynamics modulation increase material biocompatibility under flow condition. These insights could contribute to the development of biocompatible silicone to use in biohybrid artificial lungs and other blood-contacting devices.

CONTENTS

CHAPTER 1

General Introduction

GENERAL INTRODUCTION

From an engineering perspective, the lung is a paradigm of design efficiency. A gas transfer surface area of approximately 70 m^2 accomplishes efficient oxygen and carbon dioxide transfer [1, 2]. In mammals, oxygen is transferred via diffusion through pulmonary alveoli which is then distributed to different tissues by red blood cells. On the other hand, carbon dioxide produced by living cells is absorbed by the blood flow and is transferred to the pulmonary capillaries from where it penetrates into the alveoli and is finally discharged through the airways [1-3]. A membrane of 0.4-2 μm thickness separates air-carrying alveoli from the pulmonary capillaries (Figure 1).

There has been modest success in decellularization and recellularization of rat lung and also in organizing cells into small-scale structures to mimic pulmonary tissue, but scale-up and creating effective connect between such structures require further research [3]. There is a prominent need to develop new and more effective therapies for cardiopulmonary support or treatment of end-stage lung failure due to different lung-related diseases, e.g. acute respiratory distress syndrome [4, 5], chronic obstructive pulmonary disease [6], pulmonary fibrosis, pulmonary hypertension, and cystic fibrosis, mostly involving people in developing countries and mainly resulting from increasing rates of tobacco smoking and pollutants of urbanization [6].

Current treatment options to provide respiratory support (chronic aid) during cardiac surgery or for patients with end-stage pulmonary failure are mainly limited to extracorporeal membrane oxygenation (ECMO) [5, 6]. An ECMO device can only give partial respiratory support because of the low blood volumes that can be bypassed externally. This treatment can avert the death of the patient, but is generally used only temporarily until lung transplantation is possible [4, 6]. ECMO devices utilize an external circuit consisting of a blood pump, an oxygenator, a heat exchanger, and several feet of tubing. The membrane oxygenator component of ECMO devices, also called artificial lung, typically takes the form of a bundle of microporous hollow fibres fabricated from different synthetic polymers such as polypropylene, silicone, etc (Figure 1). Blood flows around the outside of the hollow fibers and oxygen flows through the lumen of the hollow fibers. ECMO circuits are primarily designed for open-heart surgical procedures (4–8 h), and require high levels of anticoagulation [5]. The limits of the current technology are found at the interface of the gas and blood sides of synthetic hollow fibers. Long term usage of hollow fibers is limited by plasma-wetting, and biocompatibility issues associated with thrombosis and/or bleeding [1, 5]. Plasma-wetting is the penetration of liquid into the fiber pores, which inhibits gas exchange. The plasma-wetting problem can be solved by using non-porous membrane hollow fibers or diffusive capillary-form hollow spheres [5, 7]. However, the poor biocompatibility of hollow fibers is still a

key limitation for clinical application of artificial lungs [1, 3]. Blood proteins adsorb to the synthetic hollow fibers surfaces, which can trigger the activation of immune cells and deposition of clots onto the fibers, resulting in a tendency toward bleeding, when the blood reenters the patient [1]. Therefore high levels of anticoagulants, such as heparin, are required during ECMO to attempt to minimize thrombus formation associated with blood contact to a foreign surface, which greatly restricts patient mobility and quality of life, and is associated with high mortality [1].

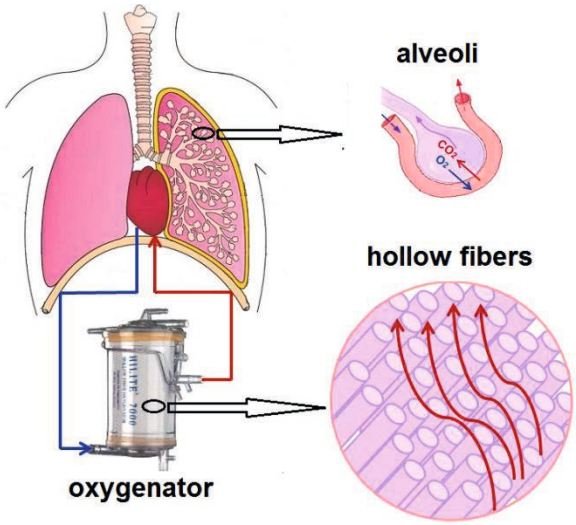

Figure 1. The native lung provides approximately 70 m^2 of gas transfer area in alveoli with actively anticoagulant endothelial surfaces lining the blood vessels. Membrane oxygenators commonly include a pack of hollow fibers across which blood flows. Blood protein deposits on the synthetic hollow fibers lead to the need for anticoagulation therapy.

Fortunately, recent advancements in the field of tissue engineering and biomaterials have increased the biocompatibility of current artificial lungs. A landmark achievement of recent developments is the design of biohybrid artificial lungs. Biohybrid artificial lungs may become a first stepping stone towards introducing regenerative medicine techniques in the treatment of chronic lung disease. Endothelialization of blood contacting surfaces of hollow fibers is a key step to generate a biohybrid artificial lung [3, 5, 6]. Although imitating the delicate structures of the human lung will not be possible in the foreseeable future, the cells that are necessary to create a single cell layer are on hand. These endothelialized

synthetic hollow fibers might mimic the native pulmonary vasculature and minimize the need for anticoagulants [1, 6]. Synthetic hollow-fiber membranes currently used in artificial lungs do not support endothelial cell adhesion and needs to be surface-modified. After endothelial cell seeding, hollow fibers are bundled and rotated in an oxygenator to create mixing and subsequently reduce boundary layer limits on gas transfer efficiency [1, 5]. If endothelialized hollow fibers in biohybrid artificial lungs can simulate native thromboresistant endothelial surfaces, a major goal will be achieved.

Blood-hollow fibers surface interactions: thrombogenicity

It is well known that shortly after contacting blood (minutes to hours) during ECMO, synthetic hollow fibers are covered with a layer of plasma proteins, predominately albumin, fibrinogen, IgG, fibronectin, and von Willebrand factor prior to the accumulation of inflammatory cells. As this occurs, platelets flowing near the surface end up adhering to the surface followed by activation, thus creating a cascade of events that results in thrombus formation. Platelets do not act in isolation, but as this thrombus formation process is underway, so is the activation of the coagulation cascade by the intrinsic pathway resulting in the release of inflammatory mediators and the production of thrombin, the pivotal agent in the process of thrombosis. Thrombin activates fibrinogen to form the insoluble cross-linked fibrin, which together with activated platelets and red blood cells ultimately leads to thrombus formation [8, 9]. For a detailed explanation of the cellular and molecular mediators of the host foreign body response to biomaterials, see a review by Anderson et al. [10]. In the case of artificial lungs, cell-mediated inflammatory responses and deposition of clots onto hollow fibers can result in bleeding when the blood reenters the patient.

Numerous approaches aimed at developing more blood compatible polymeric materials are currently being investigated in many research laboratories worldwide. Among these, approaches that mimic the highly thromboresistant properties of the normal endothelium appear to be most promising [11-13]. The endothelium is in intimate contact with the blood flow and consists of a single layer of endothelial cells, which functions as a dynamic organ and covers the entire surface of the circulating system from the heart to the smallest capillary [14]. Platelet adhesion/activation and thrombus formation do not readily occur on the surface of a healthy endothelium layer [11, 12]. Then the question to be asked is how normal endothelium does prevent thrombus formation when it is needed within the body. The endothelial cells produce, secrete, and/or express over 12 different inhibitors and activators that affect platelet function, the coagulation cascade, or both [11]. Amongst these factors, nitric oxide (NO) (generated from l-arginine by nitric oxide synthase (NOS) within the endothelial cell), thrombomodulin, prostaglandin I_2 (PGI_2), and heparins have been investigated most [9, 12].

Integrating these factors into/on polymer matrices in such a way that they are either released from the polymers [12, 13, 15], or as immobilized forms of the biologically active factors on the polymer surfaces [15-18] should result in a truly biomimetic coating that more closely resembles a layer of functional endothelial cells. What is unique to these inhibitors, as opposed to those used clinically for platelet inhibition, such as heparin, aspirin, and dipyridamol, is that this inhibition is not permanent for the platelet's life, but rather is similar to "anesthesia" of the platelet, so that once the platelet is no longer exposed to these inhibitors, it resumes normal function [11].

Endothelialization of hollow fibers

Despite extensive research to develop a non thrombogenic surface that mimics the endothelium, platelet activation still occurs, thus these modifications have not completely solved the clinical challenges of platelet passivation [11]. Endothelialized hollow fibers have been suggested as a means to improve artificial lung biocompatibility in new types of artificial lungs, so-called biohybrid artificial lungs [5, 19, 20]. This approach seeks to mimic the *in vivo* function of vascular endothelial cells to yield a biocompatible surface, actively inhibiting platelet activation and deposition, for long term ECMO support of the lung. By endothelializing hollow fibers that constitute the major blood contacting surface area of the device, the biohybrid artificial lung prototype seeks to significantly reduce or eliminate the need for chronic anticoagulation or anti-platelet agents. The attached endothelial layer provides a naturally occurring biocompatible surface for blood interaction if the cells are maintained as a non-inflammatory, anti-thrombotic phenotype [1, 3, 5].

Surface modification of hollow fiber surfaces to improve endothelialization

The successful development of biohybrid artificial lungs is challenged by the hydrophobic nature of the polymers typically used to make the hollow fibers in ECMO devices, e.g. silicone, which restricts the degree of cell adhesion [5, 6]. Surface modification through physicochemical approaches or bonding biologically adhesive proteins to the hollow fiber surface is required to guarantee endothelial cell attachment and to create a cell monolayer that is robust enough to blood flow shear stress [6, 20].

In the natural endothelium, cells are in intimate contact with the extracellular matrix (ECM), which is formed by a complex connection of proteins, glycoproteins, and proteoglycans, that have a cell-binding domain connecting the ECM–binding sites with intracellular focal adhesion plaques [14, 21]. In this respect the process of endothelial cell adhesion and spreading on hollow fibers *in vitro* has been shown to be facilitated by pre-coating of substrata with the main ECM protein, collagen [17, 18]. The ability of collagen to support cell adhesion and to trigger

signals promoting cell proliferation has been shown to be dependent on its quantity, conformation, and activity, which are influenced by the surface properties of the underlying substratum [22, 23]. Despite of its positive effects on cell adhesion and proliferation, collagen is highly thrombogenic, and induces both platelet adhesion and aggregation as well as activation of the intrinsic coagulation cascade in areas which are not fully covered by endothelial cells [24]. Therefore, promotion of endothelial cell growth by ECM molecules causes the blood compatibility to deteriorate, whereas improvement of antithrombogenicity by the anticoagulant molecules inhibits endothelial cell growth [16]. Most studies focus on one aspect of biocompatibility, i.e. blood compatibility by anti-thrombotic agents, or cytocompatibility by endothelialization [11-13], while less reports exist considering both aspects [16-18, 24]. NO is an important inhibitor of platelet adhesion [11-15]. Treatment of endothelial cells by shear stress, cold temperature, and aspirin stimulates NO production and decreases thrombus formation [25]. NO-releasing material coatings suppress thrombogenic problems in the absence of endothelial cells or in areas which are not fully covered by endothelial cells [12, 13]. Nitrite, the stable end-product of NO metabolism, may represent a potential source of NO in an acidic environment [26, 27]. Therefore conjugation of collagen with NO-donor molecules might increase endothelial cell attachment and decrease thrombotic properties of collagen when it is not completely covered by endothelial cells.

The ultimate success of endothelialization of materials depends on the confluency of the cellular layer [24, 28]. Several hundreds of millions of cells are needed to coat the hollow fibers of one meter squared artificial lung [29]. Therefore, it takes a long period of time to reach confluency of the cell layer on hollow fibers when cells are seeded at low cell densities. Sustained release of growth-inducing agents, e.g. growth factors or growth hormones, may possibly accelerate the formation of a confluent cell layer [24]. Endothelial cells could then be seeded at a density forming a sub-confluent layer on hollow fibers, and subsequently be stimulated by growth-inducing agents to rapidly form a confluent monolayer. Growth hormone, also known as somatropin, is such a growth-inducing agent, since it is a mitogen for a variety of cell types, including smooth muscle cells, fibroblasts, adipocytes, macrophages, lymphocytes, and endothelial cells [30]. Growth hormone treatment of endothelial cells reduces intracellular reactive oxygen species production and regulates the synthesis of multiple mRNA species, including that of insulin-like growth factor-1 and eNOS [30].

Current therapeutic use of anti-thrombotic or growth-inducing agents is limited by their short half life, renal toxicity, physical and chemical instability, and rapid clearance [31]. These limitations might be overcome by controlled prolonged release of biological agents from liposome-based particles. Liposome-based particles, especially nanoliposomes, have gained considerable attention as drug delivery carriers because they are biocompatible, biodegradable, and capable of

releasing encapsulated drugs in a sustained manner by changing environmental conditions and transporting drugs across biological membranes [15, 31-33]. A biomaterial surface simultaneously co-immobilized with different liposome-based biomolecules possessing anticoagulant and growth-inducing properties, might improve both anticoagulation and endothelialization, which may provide a potential application for long-term usage of blood-contacting devices. Biomaterials co-immobilized with different biomolecules have been shown to possess the properties of each individual biomolecule [16-18].

The stability of collagen or collagen-containing conjugate coatings under blood flow forces is still a common limitation to their clinical use [16, 34]. To study the interaction between conjugate coatings and blood constituents or cultured cells, well defined and stable coatings are required [34-36]. Immobilization of conjugate coatings onto a surface can be done by e.g. physical adsorption, encapsulation, entrapment, and covalent or ionic binding [16]. The advantages of covalent immobilization using carbodiimide bonds are that the immobilized biomolecules are robust enough to withstand blood flow shear stresses [16]. For covalent immobilization of conjugate coatings onto polymer surfaces, functional groups such as amine, carboxyl, hydroxyl, isocyanate, or epoxy are required. Since most conventional polymers do not have such functional groups on their surface, they should be modified to allow reactive group formation for covalent immobilization of active molecules [34-36].

Plasma glow discharge and plasma graft polymerization are two effective methods to introduce functional groups to the material's surface and subsequently affect surface properties, e.g. wettability, and charge [22, 37, 38]. Plasma is composed of highly excited atomic, molecular, ionic, and radical species, and creates surfaces with specific oxygen or nitrogen containing groups in the presence of various vapours [8, 37]. Plasma treatment modifies the outermost surface of polymers without changing the bulk characteristics of the material. The chemical composition of gas-plasma modified surfaces depends on both the gas used and the experimental conditions [22]. Plasma graft polymerization is another attractive way of modifying the surface chemistry and chemically immobilize compounds onto the surface of a biomaterial [34-36, 38]. A desired monomer may be polymerized onto the surface of a plasma-treated material resulting in the formation of a grafted layer on the material surface, avoiding drawbacks of monomer detachment by providing long-term stability. The grafted surfaces may then provide active sites for the binding of collagen or collagen-containing conjugate molecules. This method is highly surface selective, where the modification is confined to a depth of a few nanometers without modification of the bulk properties [38].

Shear stress conditioning of endothelial cell-seeded hollow fibers

In addition to stable collagen conjugate coating, cell retention on surface-modified hollow fibers is important, since cell detachment might lead to the formation of platelet aggregates in regions where blood is in direct contact with protein coating, instead of endothelial cells [21, 24]. A promising way to enhance endothelial cell retention onto a surface-modified material is shear stress preconditioning of cells with shear stresses lower than those present in the biomedical device [21, 39-41]. Under chronic shear stress, endothelial cells flatten, structurally remodel to spread the shear stress over greater surface area, and therefore increase their adherence to the substratum through focal contacts [42, 43]. The production of endothelial cell-derived anti-inflammatory agents, e.g. NO and PGI_2, can increase by fluid shear stress [25, 44, 45].

Parallel-plate flow chambers are the most commonly used devices used to investigate the cellular response to fluid shear stress [44-47]. Calculating the exact amount of applied shear stress in these devices by mathematical modeling is very important to gain a quantitative relationship between fluid changes and cell biologic responses. A common mathematical model used to predict shear stresses in these devices employs the use of the Navier-Stokes equation for steady, pressure-driven flow between two parallel-plates with a no slip boundary condition applied to the surface of the plates, resulting in parabolic Poiseuillian flow [48]. In such models of flat plate flow, the calculation of the wall shear stress may be easily accomplished from a known velocity gradient normal to the surface. However, when various types of surface roughness, such as presence of hollow fibers or considering endothelial cell layer, are incorporated into the plate, the flow at the surface is altered and direction normal to the surface is not the same in all locations, increasing the complexity in the determination of wall shear stress [46]. To better realize the effect of flow in these complicated environments, computational fluid dynamics (CFD) has been used as a reliable technique [49-52]. CFD can reveal a detailed profile of pressure, velocity, flow fields, shear stresses, and oxygen transfer in cell or tissue culture chambers of various bioreactor designs [52]. This is useful for the design optimization of internal geometric configurations of bioreactors.

Since the local fluid dynamics, especially the shear stress arising from the blood flow, cannot be analyzed experimentally, CFD is essential for estimating the blood shear stress which acts on platelets when developing blood-contacting devices [49, 50]. The blood flow pattern in artificial lungs is complicated and difficult to measure, and thus CFD has been extensively used to study the effects of packing of hollow fibers, and structure of the artificial lung on the oxygen transfer and blood trauma [53, 54]. In biohybrid artificial lungs a detailed flow field computation represents a unique opportunity to gain a qualitative correlation between the specific wall shear stress distribution over the endothelial cell-seeded hollow fibers and the biological behavior typical for endothelial cells under

controlled experimental conditions, e.g. stability, morphology, and anti-thrombotic functionality, thereby predicting experimental flow rates that provide optimal device performance [6]. Bioavailability of different biologically active factors released by surface-modified materials or produced by endothelial cells under shear stress can also be assessed using diffusion-convection physics of CFD [55].

Aim and outline of this thesis

The aim of the studies presented in this thesis was to improve the endothelialization of silicone hollow fibers used in artificial lungs and subsequently increase their biocompatibility by surface modification and fluid hydrodynamic modulation. To achieve this goal, the following questions were addressed:

1. Which functional group, e.g. peroxide, carboxyl and amine, allows strong collagen immobilization and improvement of endothelialization, cell stability, and anti-thrombotic functionality?
2. What is the influence of flow preconditioning of endothelial cells seeded on surface-modified silicone in a parallel-plate flow chamber on cell stability and anti-thrombotic functionality?
3. Does immobilization of nitrite and acidified nitrite generating nitrite sodium-collagen conjugate on acrylic acid-grafted silicone increase the number of endothelial cells as well as growth hormone production and decrease platelet adhesion?
4. Does sustained local release of sodium nitrite (as an anti-thrombotic agent) and growth hormone (as a growth-inducing agent) from nanoliposomes incorporated into collagen coating enhance endothelialization of silicone by increasing the number of endothelial cells, as well as by decreasing platelet adhesion?
5. Is it possible to achieve enhanced bioavailability of anti-thrombotic agents released by surface coating or by endothelial cells under shear stress?

To seek answers to these questions, we started by surface modification of the inside of large diameter silicone tubes with the same chemical composition as silicone hollow fibers used in artificial lungs. In **Chapter 2**, silicone tubes with three different chemical functional groups, i.e. peroxide, carboxyl, and amine, but similar wettability, were compared to determine the surface chemical entity that allows strong collagen immobilization and improvement of endothelialization, cell stability, and anti-thrombotic functionality. Plasma pre-modification was performed to introduce peroxide groups acting as initiators for graft polymerization. Then silicone tubes containing peroxide groups were graft polymerized with acrylic acid (AAc) to introduce carboxyl groups, or with aminosilane (AmS) to introduce amine groups. Collagen was stably immobilized using carbodiimide bonds on silicone tubes with carboxyl or amine functional groups.

A challenge to the successful development of biohybrid artificial lungs is to solve the problem of detachment of endothelial cells from the outside surface of hollow fibers when exposed to circulating blood flow. Although a stable collagen coating can be obtained by surface modification methods, cell retention on the outside surface of collagen-coated small diameter hollow fibers used in artificial lungs should be taken into account since cell detachment might leave parts of the thrombogenic collagen coating exposed to blood and subsequently induces platelet adhesion. In **Chapter 3**, flow preconditioning of endothelial cells seeded on collagen-immobilized AAc-grafted silicone hollow fibers is used to support the endothelial cell monolayer to withstand high fluid shear stress resulting from circulating blood flow. To examine the efficiency of collagen immobilization before cells were seeded, and flow preconditioning of cells after cells were seeded, on the stability and anti-thrombotic functionality of endothelial cells seeded on the outside surface of small diameter hollow fibers under shear stress, a parallel-plate flow chamber was designed and constructed. The precise shear stress distribution in the parallel-plate flow chamber was determined by COMSOL to gain a quantitative correlation between the shear stress and behavior of endothelial cells, e.g. cell detachment and anti-thrombotic function, under controlled experimental conditions.

Collagen is highly thrombogenic, and accelerates platelet aggregation in those areas of a material which are not fully covered by endothelial cells. NO is an important inhibitor of platelet adhesion. NO-releasing material coatings suppress thrombogenic problems in the absence of endothelial cells or in areas which are not fully covered by endothelial cells. As mentioned before, nitrite, the stable end-product of NO metabolism, may represent a potential source of NO in an acidic environment. Whether acidified nitrite indeed prevents platelet adhesion and increases endothelial cell growth has been assessed in **Chapter 4**. Sodium nitrite-collagen conjugate was immobilized on the inside surface of AAc-grafted large diameter silicone tubes and the effect of nitrite and acidified nitrite release on blood compatibility and endothelialization of silicone tubes was investigated.

A biomaterial surface simultaneously co-immobilized with different biolmolecules can possess the properties of each individual biomolecule. In addition, sustained release of biomolecules from nanoliposomes improves their biological effect. Therefore, in **Chapter 5**, it was hypothesized that co-immobilization of nanoliposomes possessing anti-thrombotic and growth-inducing properties improves both anticoagulation and endothelialization. Nanoliposomal sodium nitrite (as an anti-thrombotic agent) and nanoliposomal growth hormone (as a growth-inducing agent) were prepared, blended with collagen solution, and then co-immobilized on the inside surface of AAc-grafted large diameter silicone tubes. The amount of nitrite, acidified nitrite, and growth hormone released from surface-modified silicone tubes was determined. Sodium nitrite or growth hormone in the collagen conjugate at concentrations allowing improvement of endothelial cell

proliferation, anti-thrombotic function, as well as decreased platelet adhesion were applied for surface modification of the outside surface of small diameter silicone hollow fibers.

The bioavailability of nitrite, an anti-thrombotic agent, near the surface of hollow fibers in biohybrid artificial lungs is very important to inhibit platelet adhesion. By applying blood flow circulation in biohybrid artificial lungs, the shear stress acting on the endothelial cell layer as well as mass transport characteristics at the fluid-endothelial layer interface will be altered. These changes affect the transport of nitrite released by the endothelial cell layer and from the nitrite-donor surface coating. The bioavailability of nitrite depends strongly on diffusion and convection. In **Chapter 6**, we modeled nitrite bioavailability, expressed as nitrite concentration, on the outside surface of silicone hollow fibers coated with nanoliposomal sodium nitrite-nanoliposomal growth hormone-collagen conjugate under varying fluid shear stress magnitudes. The nitrite production rate of endothelialized surface-modified silicone hollow fibers was determined experimentally under fluid shear stress in a parallel-plate flow chamber. Laminar flow and convection-diffusion partial equations in COMSOL were used to simulate nitrite transport within the parallel-plate flow chamber, and nitrite bioavailability on the fiber-blood interface. Finally in **Chapter 7**, we discuss how our results fit with the hypothesis that silicone surface modification and hydrodynamics modulation improves endothelialization in order to postulate future directions of research and clinical application of biohybrid artificial lungs.

REFERENCES

1 Wagner WR, Griffith BP. Reconstructing the lung. Science 2010;329:519-521.
2 Galletti PM, Colton CK. Artificial lungs and blood-gas exchange devices, in Biomedical engineering handbook. Bronzino JD, Ed. CRC Press LLC, 2000.
3 Song JJ, Ott HC. Bioartificial lung engineering. Am J Transplant 2012;12:283-288.
4 Zwischenberger BA, Clemson LA, Zwischenberger JB. Artificial lung: Progress and prototypes. Expert Rev Med Devices 2006;3:485-497.
5 Polk AA, Maul TM, McKeel DT, Snyder TA, Lehocky CA, Pitt B, Stolz DB, Federspiel WJ, Wagner WR. A biohybrid artificial lung prototype with active mixing of endothelialized microporous hollow fibers. Biotechnol Bioeng 2010;106:490-500.
6 Lemon G, Lim ML, Ajalloueian F, Macchiarini P. The development of the bioartificial lung. Br Med Bull 2014;110:35-45.
7 Khachab A, Tabesh H, Kashefi A, Mottaghy Kh. Novel concept for pure diffusive capillary membrane oxygenators: Silicone hollow sphere (SiHSp) fibers. ASAIO J 2013;59:162-168.
8 Thevenot P, Hu W, Tang L. Surface chemistry influence implant biocompatibility. Curr Top Med Chem 2008;8:270-280.
9 Bridges AW, García AJ. Anti-Inflammatory polymeric coatings for implantable biomaterials and devices. J Diabetes Sci Technol 2008;2:984-994.
10 Anderson JM, Rodriguez A, Chang DT. Foreign body reaction to biomaterials. Semin Immunol 2008;20:86-100.
11 Reynolds MM, Annich GM. The artificial endothelium. Organogenesis 2011;7:42-49.
12 Wu B, Gerlitz B, Grinnell BW, Meyerhoff ME. Polymeric coatings that mimic the endothelium: Combining nitric oxide release with surface-bound active thrombomodulin and heparin. Biomaterials 2007;28:4047-4055.
13 Zhou Zh, Meyerhoff ME. Preparation and characterization of polymeric coatings with combined nitric oxide release and immobilized active heparin. Biomaterials 2005;26:6506-6517.
14 de Mel A, Cousins BG, Seifalian AM. Surface modification of biomaterials: A quest for blood compatibility. Int J Biomater 2012;2012: 707-863.
15 Naghavi N, de Mel A, Alavijeh OS, Cousins BG, Seifalian AM. Nitric oxide donors for cardiovascular implant applications. Small 2013;9:22-35.
16 Li G, Yang P, Qin W, Maitz MF, Zhou S, Huang N. The effect of coimmobilizing heparin and fibronectin on titanium on hemocompatibility and endothelialization. Biomaterials 2011;32:4691-4703.
17 Li J, Zhang K, Wu F, He Z, Yang P, Huang N. Constructing bio-functional layers of hyaluronan and type IV collagen on titanium surface for improving endothelialization. J Mater Sci 2015;50:3226-3236.
18 Zhang K, Li J, Deng K, Liu T, Chen JY, Huang N. The endothelialization and hemocompatibility of the functional multilayer on titanium surface constructed with type IV collagen and heparin. Colloid Surface B 2013;108:295-304.
19 Sawa Y, Ohata T, Takagi M, Matsuda H. Hybrid artificial lung: current status and perspective. J Artif Organs 1998;27:765-768.
20 Takagi M, Shiwaku K, Inoue T, Shirakawa Y, Sawa Y, Matsuda H, Yoshida T. Hydrodynamically stable adhesion of endothelial cells onto a polypropylene hollow fiber membrane by modification with adhesive protein. J Artif Organs 2003;6:222-226.
21 Dardik A, Liu A, Ballermann BJ. Chronic in vitro shear stress stimulates endothelial cell retention on prosthetic vascular grafts and reduces subsequent in vivo neointimal thickness. J Vasc Surg 1999;29:157-167.
22 Solouk A, Cousins BG, Mirzadeh H, Seifalian AM. Application of plasma surface modification techniques to improve hemocompatibility of vascular grafts: A review. Biotechnol Appl Biochem 2011;58:311-327.

23 Tzoneva R, Faucheux N, Groth T. Wettability of substrata controls cell–substrate and cell–cell adhesions. Biochim Biophys Acta 2007;1770:1538-1547.
24 Wissink MJ, Beernink R, Poot AA, Engbers GH, Beugeling T, van Aken WG, Feijen J. Improved endothelialization of vascular grafts by local release of growth factor from heparinized collagen matrices. J Control Release 2000;64:103-114.
25 Kabirian F, Amoabediny G, Haghighipour N, Salehi-Nik N, Zandieh-Doulabi B. Nitric oxide secretion by endothelial cells in response to fluid shear stress, aspirin, and temperature. J Biomed Mater Res A 2014;103:1231-1237.
26 Lundberg JO, Weitzberg E. NO generation from nitrite and its role in vascular control. Arterioscler Thromb Vasc Biol 2005;25:915-922.
27 Egemnazarov B, Schermuly RT, Dahal BK, Elliott GT, Hoglen NC, Surber MW, Weissmann N, Grimminger F, Seeger W, Ghofrani HA. Nebulization of the acidified sodium nitrite formulation attenuates acute hypoxic pulmonary vasoconstriction. Respir Res 2010;11:81-93.
28 Herring M, Smith J, Dalsing M, Glover J, Compton R, Etchberger K, Zollinger T. Endothelial cell seeding of polytetrafluoroethylene femoral popliteal bypasses: The failure of low-density seeding to improve patency. J Vasc Surg 1994;20:260-265.
29 Maurer AN, Matheis G. The artificial lung, in Advances in tissue engineering. Polak J, Ed. Imperial College Press, 2008.
30 Lincoln DT, Singal PK, Al-Banaw A. Growth hormone in vascular pathology: Neovascularization and expression of receptors is associated with cellular proliferation. Anticancer Res 2007;27:4201-4218.
31 Elbayoumi TA, Torchilin VP. Current trends in liposome research, Methods. Mol Biol 2010;605:1-27.
32 Jain RA. The manufacturing techniques of various drug loaded biodegradable poly(lactide-co-glycolide) (PLGA) devices. Biomaterials 2000;21:2475-2490.
33 Scott RC, Rosano JM, Ivanov Z, Wang B, Chong PL, Issekutz AC, Crabbe DL, Kiani MF. Targeting VEGF-encapsulated immunoliposomes to MI heart improves vascularity and cardiac function. FASEB J 2009;23:3361-3367.
34 Sano Sh, Kato K, Ikada Y. Introduction of functional groups onto the surface of polyethylene for protein immobilization. Biomaterials 1993;14:817-822.
35 Lee SD, Hsiue GH, Chang PCT, Kao CY. Plasma-induced grafted polymerization of acrylic acid and subsequent grafting of collagen onto polymer film as biomaterials. Biomaterials 1996;17:1599-1608.
36 Siow KS, Britcher L, Kumar S, Griesser HJ. Plasma methods for the generation of chemically reactive surfaces for biomolecule immobilization and cell colonization-A review. Plasma Process Polym 2006;3:392-418.
37 Solouk A, Cousins BG, Mirahmadi F, Mirzadeh H, Jalali Nadoushan MR, Shokrgozar MA, Seifalian AM. Biomimetic modified clinical-grade POSS-PCU nanocomposite polymer for bypass graft applications: a preliminary assessment of endothelial cell adhesion and haemocompatibility. Mater Sci Eng C Mater Biol Appl 2015;46:400-408.
38 Gupta B, Plummer C, Bisson I, Frey P, Hilborn J. Plasma-induced graft polymerization of acrylic acid onto poly(ethylene terephthalate) films: characterization and human smooth muscle cell growth on grafted films. Biomaterials 2002;23:863-871.
39 Isenberg BC, Williams C, Tranquillo RT. Endothelialization and flow conditioning of fibrin-based media-equivalents. Ann Biomed Eng 2006;34:971-985.
40 Ott MJ, Ballermann BJ. Shear stress-conditioned, endothelial cell-seeded vascular grafts: improved cell adherence in response to in vitro shear stress. Surgery 1995;117:334-339.
41 Baguneid M, Murray D, Salacinski HJ, Fuller B, Hamilton G, Walker M, Seifalian AM. Shear-stress preconditioning and tissue-engineering-based paradigms for generating arterial substitutes. Biotechnol Appl Biochem 2004;39:151-157.

42 Tzima E, del Pozo MA, Shattil SJ, Chien S, Schwartz MA. Activation of integrins in endothelial cells by fluid shear stress mediates Rho-dependent cytoskeletal alignment. EMBO J 2001;20:4639-4647.
43 McIlhenny SE, Hager ES, Grabo DJ, DiMatteo C, Shapiro IM, Tulenko TN, DiMuzio PJ. Linear shear conditioning improves vascular graft retention of adipose-derived stem cells by upregulation of the α5β1 integrin. Tissue Eng Part A 2010;16:245-255.
44 Hsieh HJ, Liu CA, Huang B, Tseng AH, Wang DL. Shear-induced endothelial mechanotransduction: the interplay between reactive oxygen species (ROS) and nitric oxide (NO) and the pathophysiological implications. J Biomed Sci 2014;21:3-18.
45 Okahara K, Sun B, Kambayashi J. Upregulation of prostacyclin synthesis-related gene expression by shear stress in vascular endothelial cells. Arterioscler Thromb Vasc Biol 1998;18:1922-1926.
46 Brown A, Burke G, Meenan BJ. Modeling of shear stress experienced by endothelial cells cultured on microstructured polymer substrates in a parallel-plate flow chamber. Biotechnol Bioeng 2011;108:1148-1158.
47 Kaur H, Carriveau R, Mutus B. A simple parallel-plate flow chamber to study effects of shear stress on endothelial cells. Am J Biomed Sci 2012;4:70-78.
48 Gaver DP, Kute SM. A theoretical model study of the influence of fluid stresses on a cell adhering to a microchannel wall. Biophys J 1998;75: 721-733.
49 Hajiali Z, Dabagh M, Jalali P. A Computational model to assess poststenting wall stresses dependence on plaque structure and stenosis severity in coronary artery. Math Probl Eng 2014;2014:1-12.
50 LaDisa JF, Guler I, Olson LE, Hettrick DA, Kersten JR, Warltier DC, Pagel PS. Three-dimensional computational fluid dynamics modeling of alterations in coronary wall shear stress produced by stent implantation. Ann Biomed Eng 2003;31:972-980.
51 Anisi F, Salehi-Nik N, Amoabediny G, Pouran B, Haghighipour N, Zandieh-Doulabi B. Applying shear stress to endothelial cells in a new perfusion chamber: hydrodynamic analysis. J Artif Organs 2014;17:329-336.
52 Salehi-Nik N, Amoabediny G, Pouran B, Tabesh H, ,Shokrgozar MA, Haghighipour N, Khatibi N, Anisi F, Mottaghy K, Zandieh-Doulabi B. Engineering parameters in bioreactor's design: a critical aspect in tissue engineering. Biomed Res Int 2013;2013:Article ID 762132,15 pages.
53 Zhang J, Nolan TDC, Zhang T, Griffith BP, Wu ZJ. Characterization of membrane blood oxygenation devices using computational fluid dynamics. J Membrane Sci 2007;288:268-279.
54 Taskin ME, Fraser KH, Zhang T, Griffith BP, Wu ZJ. Micro-scale modeling of flow and oxygen transfer in hollow-fiber membrane bundle. J Membrane Sci 2010;362:172-183.
55 Plata AM, Sherwin SJ, Krams R. Endothelial nitric oxide production and transport in flow chambers: The importance of convection. Ann Biomed Eng 2010;38:2805-2816.

CHAPTER 2

Surface Modification of Silicone Tubes by Functional Carboxyl and Amine, but not Peroxide Groups Followed by Collagen Immobilization Improves Endothelial Cell Stability and Functionality

Nasim Salehi-Nik[1,2], Ghassem Amoabediny[1,2], Mohammad Ali Shokrgozar[3], Khosrow Mottaghy[4], Jenneke Klein-Nulend[5], Behrouz Zandieh-Doulabi[5]

[1] School of Chemical Engineering, College of Engineering, University of Tehran, Tehran, Iran

[2] Department of Biomedical Engineering, Research Center for New Technologies in Life Science Engineering, University of Tehran, Tehran, Iran

[3] National Cell Bank, Pasteur Institute of Iran, Tehran, Iran

[4] Institute of Physiology, Medical Faculty, RWTH Aachen University, Aachen, Germany

[5] Department of Oral Cell Biology, Academic Centre for Dentistry Amsterdam, University of Amsterdam and VU University Amsterdam, MOVE Research Institute Amsterdam, Amsterdam, The Netherlands

Biomedical Materials 2015;10:015024

ABSTRACT

Surface modification by functional groups promotes endothelialization in biohybrid artificial lungs, but whether it affects endothelial cell stability under fluid shear stress, and release of anti-thrombotic factors, e.g. nitric oxide (NO), is unknown. We aimed to test whether surface-modified silicone tubes containing different functional groups, but similar wettability, improve collagen immobilization, endothelialization, cell stability and cell-mediated NO release. Peroxide, carboxyl, and amine-groups increased collagen immobilization (41-76%). Only amine-groups increased ultimate tensile strength (2-fold). Peroxide and amine enhanced (1.5-2.5 fold), but carboxyl-groups decreased (2.9-fold) endothelial cell number after 6 days. After collagen immobilization, cell number was enhanced by all group-modifications (2.8-3.8 fold). Cells were stable under 1 h fluid shear stress on amine, but not carboxyl or peroxide-group-modified silicone (>50% cell detachment), while cells were also stable on carboxyl-group-modified silicone with immobilized collagen. NO-release was increased by peroxide and amine (1.1-1.7 fold), but decreased by carboxyl-group-modification (9.8-fold), while it increased by all group-modifications after collagen immobilization (1.8-2.8 fold). Only amine-group-modification changed silicone stiffness and transparency. In conclusion, silicone-surface modification of blood-contacting parts of artificial lungs with carboxyl and amine, but not peroxide-groups followed by collagen immobilization allows formation of a stable functional endothelial cell layer. Amine-group-modification seems undesirable since it affected silicone's physical properties.

Keywords
Silicone, Functional groups, Collagen immobilization, Endothelialization, Cell stability, NO release

INTRODUCTION

Extracorporeal membrane oxygenation using blood oxygenators, e.g. microporous hollow fiber membrane oxygenators, also called artificial lungs, is a strategy used to support the function of natural lungs [1-3]. Long term usage of microporous hollow fibers is limited, since plasma-wetting causes plasma to break through the micropores of the capillaries into the gas phase, and poor biocompatibility of hollow fibers causes thrombosis [1, 4, 5]. The plasma-wetting problem can be solved by using non-porous silicone membrane hollow fibers or diffusive capillary-form silicone hollow spheres [6]. However the poor biocompatibility of silicone membranes is still a key limitation for clinical application of silicone-based artificial lungs [5, 7].

Tissue engineering is used to increase the biocompatibility of silicone membranes in new types of artificial lungs, so-called biohybrid artificial lungs [4, 5, 8]. The blood-contacting parts of silicone membranes in biohybrid artificial lungs are seeded with endothelial cells to provide a naturally occurring biocompatible surface for blood interaction [8-10]. The success of endothelialization of blood-contacting silicone membranes is highly dependent on the interaction of endothelial cells with the material's surface (i.e. cell adhesion, proliferation, stability, anti-thrombotic functionality) [11] depend on material surface reactive groups [12, 13], surface charge [11, 14], and immobilized adhesive proteins such as collagen, gelatin, and fibronectin [15-17]. The silicone surface is hydrophobic with a low surface energy, chemically inert, and nonpolar, and does not support the growth and function of adhesion-dependent cells [12]. Therefore principal surface modification is needed to improve cell-silicone interactions [15, 18]. Plasma graft modification involves surface activation with plasma followed by substrate exposure to a grafting monomer [19-22], and provides different functional groups with different surface charges based on the monomer used. The functional groups are main reactive groups amenable for covalent immobilization of extracellular matrix proteins [16, 17]. These proteins enhance the attachment and proliferation of endothelial cells [14, 15, 17, 23].

Plasma graft polymerization creates a strong covalent surface modification, which is essential to obtain surfaces that are robust enough to withstand circulating blood flow shear stresses in biohybrid artificial lungs [5]. This fluid shear stress has been estimated 1–3 N/m^2, except at the entrance point of the device, where the shear stress is much higher [24]. Cell detachment from the material surface as a result of fluid shear stress might result in platelet formation in regions that are not fully covered with endothelial cells [25, 26]. Not only stable endothelial cell adhesion and proliferation, but also endothelial cell functionality on surface-modified materials is important when endothelial cell seeding is used to improve the biocompatibility of artificial lungs. Since NO inhibits platelet aggregation and

adhesion, the ability of endothelial cells seeded on surface-modified silicone membranes in artificial lungs to secrete NO could be used as a measure for the anti-thrombotic property of the cell-seeded material [11, 27].

Surface modification of materials with functional groups peroxide, carboxyl, amine, and hydroxyl result in different wettability and chemistry, which are the main parameters affecting the interaction of cells with a material's surface [13, 14]. These functional groups have been claimed to improve endothelialization [16, 17], but their effect on endothelial cell stability under fluid shear stress and cell anti-thrombotic functionality, e.g. cell-mediated NO release, have been not thoroughly investigated. In the present study, silicone tubes with three different chemical functional groups, i.e. peroxide, carboxyl, and amine, but similar wettability, were developed to determine the surface chemical entity that allows strong collagen immobilization and improvement of endothelialization, cell stability, and anti-thrombotic functionality. Plasma pre-modification was performed to introduce peroxide groups acting as initiators for graft polymerization [13, 21]. Then silicone tubes containing peroxide groups were graft polymerized with acrylic acid to introduce carboxyl groups, or with aminosilane to introduce amine groups. The contact time of monomer with silicone tubes was variable to achieve the same wettability of the silicone tubes. We compared the graft density, immobilized collagen amount, mechanical properties, endothelialization (e.g. cell attachment, cell proliferation), cell stability under fluid shear stress, and cell-mediated NO release, between surfaces with carboxyl and amine groups, and between surfaces with peroxide groups, which are the initiator groups of carboxyl and amine groups in the plasma graft polymerization process.

MATERIALS AND METHODS

Materials

Surface modification and cell studies were performed in the lumen of large diameter tubular silicone (Si) membranes (inner diameter 2 mm) donated by Raumedic (Helmbrechts, Germany), with the same chemical composition as silicone membrane hollow fibers used in artificial lungs. (3-Aminopropyl) trimethoxysilane (APTES) as an aminosilane (AmS) agent was supplied by Sigma-Aldrich (Schnelldorf, Germany). Acrylic acid (AAc) was obtained from Fluka (Buchs, Switzerland) and redistilled under vacuum to remove impurities and stabilizers. Chemicals for the Griess assay were obtained from Merck (Kenilworth, NJ, USA), and were of the highest purity available. De-ionized water was used in all experiments.

Plasma pre-modification of silicone tubes

The surfaces of unmodified silicone tubes were cleaned three times with 70% (v/v) ethanol, and once with water for 5 min. Unmodified silicone tubes were placed at the bottom of a reaction chamber (Seren R600, Anatech ltd, Union City, CA, USA), which was evacuated to 0.6 mbar, and pretreated with 60 W of oxygen plasma for 0.5 min. After plasma surface modification, silicone tubes were exposed to air for 5 min to generate peroxide groups on the surface ("plasma surface-modified silicone (PSM Si) tubes"). Peroxide groups contacting air are more unstable and fade away faster than peroxide groups contacting water [21]. Therefore PSM Si tubes were either immediately (within 3 min) used for carboxyl and amine functionalization, or stored up to 2 days in water for characterization tests.

Carboxyl functionalization of silicone tubes

PSM Si tubes were immersed in 30% AAc in water for 30 min at room temperature, air-dried at 40ºC for 5 min, and placed in a reaction chamber for plasma graft copolymerization for 3 min to prepare AAc-grafted silicone tubes (AAc Si). The residual monomers and homopolymers were removed by 24 h incubation in water [20, 21, 28]. The grafted amount of AAc was calculated by a gravimetric method according to the following equation:

$$\text{Grafted amount } (\mu g/cm^2) = \frac{W_g - W_0}{A}$$

Where W_g is the dry weight of grafted silicone tube, W_0 is the dry weight of unmodified silicone tube, and A is the inner surface area of silicone tube [21].

Amine functionalization of silicone tubes

Aminosilanization of PSM Si tubes was carried out as described earlier [29, 30]. In short, PSM Si tubes were immersed in 5% APTES in chloroform for 12 h at room temperature under nitrogen gas. For hydrolytic stabilization of amine layers, the aminosilane-grafted silicone (AmS Si) tubes were submerged in water for 48 h before use in cell experiments. The grafted amount of AmS was also calculated by a gravimetric method [21].

Collagen immobilization on silicone tubes

AAc Si, and AmS Si tubes were immersed into 30 ml 5 mM 2-(N-morpholino)ethanesulfonic acid (MES) buffer solution containing 48 mg 1-Ethyl-3-[3-dimethylaminopropyl] carbodiimide hydrochloride (EDC) and 15 mg N-hydroxysuccinimide (NHS; Fluka, Neu-Ulm, Germany) before collagen immobilization [31]. The solution was gently stirred for 5 h at 4°C to activate the functional groups on silicone tubes. Then Si, PSM Si, AAc Si with activated carboxyl groups, and AmS Si tubes with activated amine groups were filled with 1 mg ml^{-1} collagen (acid soluble collagen type I, Pasteur Institute of Iran, Tehran,

Iran) in 0.02 M acetic acid to immobilize collagen at 4°C for 24 h. Unbound collagen was removed by washing the collagen-immobilized silicone tubes with water. Collagen-adsorbed silicone (Si-Col), collagen-immobilized plasma surface-modified silicone (PSM Si-Col), collagen-immobilized AAc-grafted silicone (AAc Si-Col), and collagen-immobilized AmS-grafted silicone (AmS Si-Col) tubes were dried at room temperature and stored at 4°C before use. Some tubes were washed extensively twice with water to assess the stability of the collagen linked to the tubes. The amount of immobilized collagen on the tubes before and after washing was determined by a Bradford protein assay (Bradford, Hercules, CA, USA) using an Eppendorf biophotometer D30 (Eppendorf, Hamburg, Germany) following the manufacturer's instructions [18]. Concentrations of immobilized collagen on modified silicone tubes were assessed by comparison with a standard curve.

Characterization of surface-modified silicone tubes

The effect of peroxide, carboxyl, and amine groups on mechanical properties of silicone tubes was evaluated by holding both ends of each Si, PSM Si, AAc Si, and AmS Si tube (length 9 mm) in a specific grip of an in-house fabricated uniaxial testing instrument, and pulling uniaxially until tension break. The ultimate tensile strength was determined based on the peak load and the initial surface area of each tube. The percent elongation-at-break was obtained from the ratio between the elongated length at the time of failure (l) and initial length (l_0) of each silicone tube [32, 33].

The wettability of unmodified and surface-modified silicone tubes (i.e. Si, PSM Si, AAc Si, AmS Si, PSM Si-Col, AAc Si-Col, and AmS Si-Col) was probed by static water contact angle measurement [21, 34] using Kruss G10 goniometer contact-angle measurement equipment (Krüss GmbH, Hamburg, Germany). Tubes were cut longitudinally, glued on a microscope glass slide, and mean values of five water contact angle measurements on randomly chosen areas of each tube were calculated.

Endothelial cell seeding, adherence, and proliferation

Human umbilical vein endothelial cells (HUVECs) were obtained from the National Cell Bank, Pasteur Institute of Iran (Tehran, Iran), and used between passages 3 and 6 to evaluate cell attachment and proliferation on unmodified and surface-modified silicone tubes. Hundred µl endothelial cell suspension containing 300 cells/µl Dulbecco's modified Eagle's medium (DMEM)/F12 with 10% fetal bovine serum (Gibco, Renfrewshire, Scotland) was infused from one end into the lumen of each sterile tube using a syringe. During cell seeding for 4 h, the tubes were rotated every 30 min to promote homogeneous cell adhesion to the inner surface of the tubes. Cells were either cultured for 6 days in a humidified atmosphere of 5% CO_2 in air at 37°C, with medium replacement every 2 days, or used to determine

cell attachment at 4 h. The attached cells were washed with phosphate buffered saline (PBS), released with trypsin/ethylene diamine tetraacetic acid (EDTA; Merck, Kenilworth, NJ, USA), and stained with 0.4% trypan blue (Sigma-Aldrich, St. Louis, MO, USA) to determine viable cell number in a Neubauer cell chamber. The percentage of adherent cells was calculated from the cell counts upon seeding and after 4 h of culture [11, 22].

Endothelial cell proliferation on the surface-modified silicone tubes at days 2, 4, and 6 was estimated by using the 3-(4,5-dimethylthiazol-2-yl)-2,5 diphenyltetrazolium bromide (MTT) assay (Sigma-Aldrich, St. Louis, MO, USA) as described elsewhere [9, 12, 33]. The absorbance was measured at 545 nm using an ELISA Reader (Stat Fax-2100, Miami, FL, USA). The number of endothelial cells was quantified using a calibration curve with known cell numbers.

Endothelial cell morphology

The morphology of endothelial cells attached to either unmodified or surface-modified silicone tubes was visualized after 6 days culture by scanning electron microscopy (SEM) using an Essen Philips XL 30 ESEM Environmental electron microscope (Philips, Amsterdam, The Netherlands). The tubes were cut longitudinally to allow observation of cell morphology in the lumen of cell-seeded silicone tubes. Tubes with adherent cells were rinsed with PBS, fixed with 4% (v/v) glutaraldehyde solution in PBS at 4°C for 30 min, washed once with ultrapure water, dehydrated in a series of ethanol/distilled water solution (10% ethanol increments; each step 3 min), and finally dried at room temperature [35]. The optimum parameters for SEM imaging were 20 kV electron accelerating voltage, 15 mm working distance, and 500x magnification.

Fluid shear stress treatment of endothelialized silicone tubes

To compare the different surface-modified silicone tubes for their ability to support cell attachment under fluid shear stress, an in-house designed and fabricated circulating flow loop was used. After 6 days of culture, tubes with adhered cells were washed with PBS and mounted on a holder. Endothelial cells on silicone tubes were exposed to a fluid shear stress of 1.5 N m^{-2} for 1 h using a peristaltic pump (Heidolph, Schwabach, Germany). Polyvinyl chloride tubing was used to link the medium reservoir, pump, and silicone tube. Three-way valves were used to stop entering fluid into the silicone tubes at the end of an experiment (Figure 1). The percentage of detached cells was assessed by detracting the number of cells after shear conditioning from the number before shear conditioning using the MTT assay.

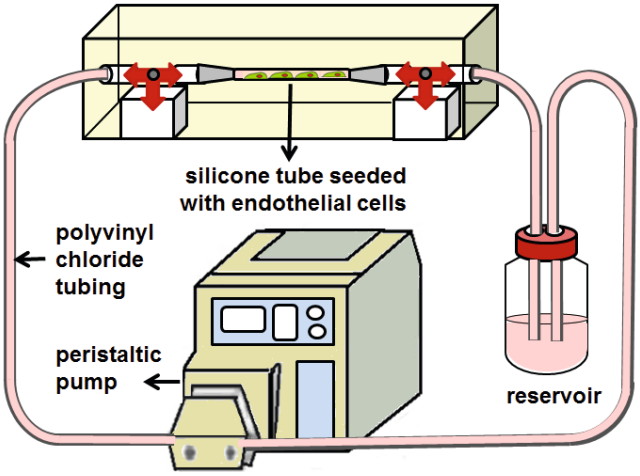

Figure 1. Flow loop chamber used for assessing the stability of endothelial cells on unmodified and surface-modified silicone tubes under fluid shear stress.

NO quantification

NO release by endothelial cells was measured as nitrite (NO_2^-) accumulation in the medium after 6 days of culture, using Griess reagent including 1% sulfanilamide, 0.1% naphtylethelene-diamine-dihydrochloride, and 2.5 M H_3PO_4 [36-39]. The absorbance was measured at 545 nm with a microplate reader (Stat Fax-2100, Miami, FL). Serial dilutions of $NaNO_2$ in the medium were used as standard curve.

Statistical analysis

All data were expressed as means ± standard deviation (SD). To compare any significant differences between unmodified and surface-modified silicone tubes, one-way analysis of variance was used. The significance of differences among means was determined by post-hoc comparisons, using Bonferroni's method. Two way analysis of variance with pairwise comparison was used to assess differences among means between groups and over time. A probability (p) value of less than 0.05 ($p<0.05$) was taken as the level of significance.

RESULTS

In this study surface modification of silicone tubes was performed to introduce peroxide (–OO), carboxyl (–COOH) or amine ($–NH_2$) functional groups with or without immobilized collagen for improvement of endothelialization, cell stability,

and anti-thrombotic functionality. Figure 2 shows a schematic of the reactions of plasma modification and graft polymerization (with AmS or AAc) followed by collagen immobilization on silicone tubes. The abbreviations used for surface-modified silicone tubes are provided in Table 1.

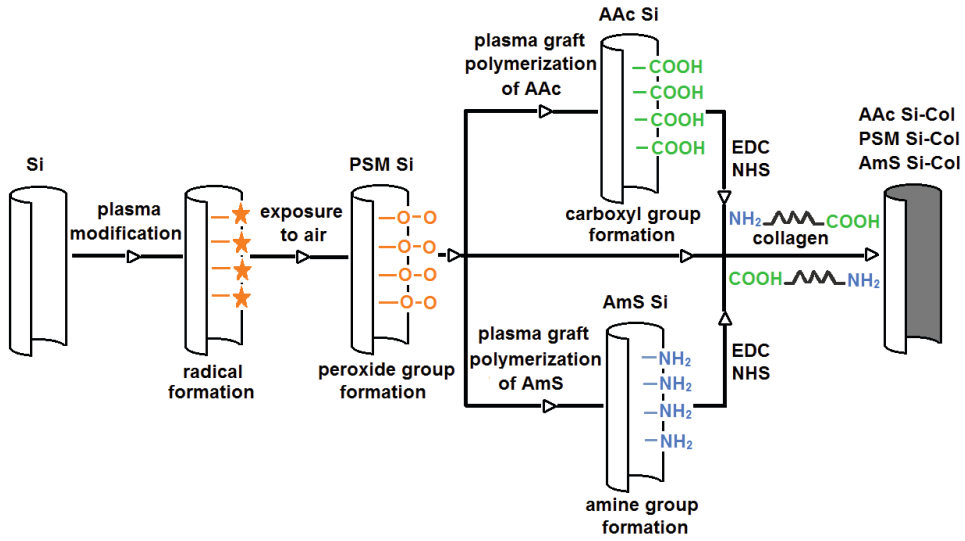

Figure 2. Schematic illustration of plasma surface modification, plasma graft polymerization, and collagen immobilization in the lumen of silicone tubes. Peroxide group formation: silicone tubes were exposed to air for 10 min after plasma modification. Carboxyl group formation: plasma surface-modified silicone tubes were immersed in an aqueous solution of AAc followed by plasma graft polymerization on a reabsorbed layer of AAc on silicone. Amine group formation: plasma surface-modified silicone tubes were immersed in an aqueous solution of APTES for aminosilanization followed by submerging in distilled water.

Grafted monomer and immobilized collagen density on surface-modified silicone tubes

The peroxide groups initiated the formation of carboxyl groups by graft polymerization of AAc, or the formation of amine groups by graft polymerization of AmS on the silicone surface. The graft mass density of AAc was much lower than of AmS (AAc: 420±28 μg cm^{-2}; AmS: 987±43 μg cm^{-2}, mean±SD), but since the molecular weight of AAc was also lower than AmS (AAc: 72.06 g mol^{-1}; AmS: 221.37 g mol^{-1}), the graft molar densities weree similar (Table 2). The negatively charged carboxyl groups on AAc Si tubes interacted with the positively charged amine groups on collagen, and the positively charged amine groups on AmS Si

tubes interacted with the negatively charged carboxyl groups on collagen, to form carbodiimide bonds through which collagen ionically crosslinked on silicone tubes (Figure 2). AmS Si tubes adsorbed 76% more collagen than Si tubes, 67% more than PSM Si tubes, and 41% more than AAc Si tubes (Table 2). Although PSM Si and Si tubes were capable of linking with collagen, ~20% (PSM Si) and 33% (Si tubes) of the collagen adsorbed was washed out after two times severe washing with water.

Table 1. Abbreviations used for different surface-modified silicone tubes.

Tube, surface modification	Tube, abbreviation
silicone	Si
plasma surface-modified silicone	PSM Si
acrylic acid-grafted silicone	AAc Si
aminosilane-grafted silicone	AmS Si
collagen-adsorbed silicone	Si-Col
collagen-immobilized plasma surface-modified silicone	PSM Si-Col
collagen-immobilized aminosilane-grafted silicone	AmS Si-Col
collagen-immobilized acrylic acid-grafted silicone	AAc Si-Col

Table 2. Graft density and collagen adsorbed on unmodified and surface-modified silicone tubes before and after washing. Values are mean ± standard deviation for 3 independent experiments. Si-Col, collagen-adsorbed silicone; PSM Si-Col, collagen-immobilized plasma surface-modified silicone; AAc Si-Col, collagen-immobilized AAc-grafted silicone; AmS Si-Col, collagen-immobilized AmS-grafted silicone.

Tube, surface modification	Graft density (mol cm^{-2})	Collagen adsorbed before washing (μg cm^{-2})	Collagen adsorbed after washing (μg cm^{-2})
Si-Col	-	15.3 ± 1.7	10.2 ± 3.2
PSM Si-Col	-	16.2 ± 2.1	13.0 ± 1.1
AAc Si-Col	$5.8 \pm 0.4 \times 10^{-6}$	19.1 ± 3.0	18.8 ± 1.7
AmS Si-Col	$4.4 \pm 0.2 \times 10^{-6}$	27.0 ± 1.8	27.3 ± 1.2

Mechanical properties of surface-modified silicone tubes

The ultimate tensile strength of AmS Si tubes was 1.8-fold higher than that of Si, 2-fold higher than that of PSM Si, and 1.6-fold higher than that of AAc Si tubes, showing that silicone tubes stiffened after surface modification with amine groups (Figure 3a). The percent elongation at break was more than 100% for Si, PSM Si, AAc Si, and AmS Si tubes, with no statistically significant differences observed between tubes (Figure 3b). The ultimate tensile strength and elongation at break of PSM Si and AAc Si tubes were similar to Si tubes.

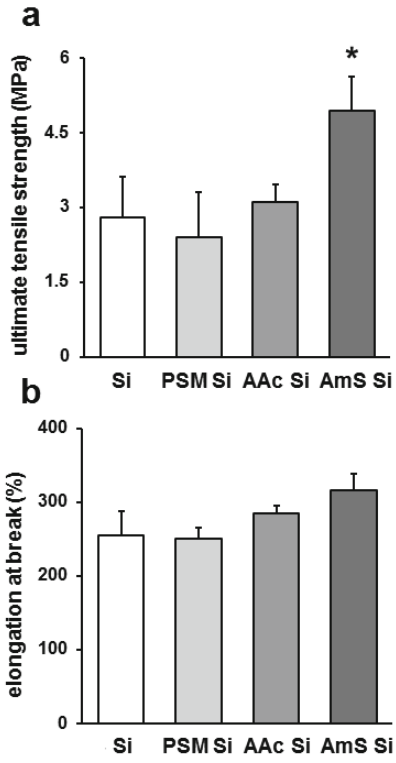

Figure 3. Mechanical properties of unmodified and surface-modified silicone tubes. (a) Ultimate tensile strength, (b) Elongation-at-break of silicone tubes. n=3. The ultimate tensile strength of AmS Si tubes was 1.8-fold higher than Si tubes, showing that silicone tubes became more stiff after surface modification with amine groups. Elongation-at-break of different surface-modified tubes was not statistically different. Si, silicone; PSM Si, plasma surface-modified silicone; AAc Si, acrylic acid-grafted silicone; AmS Si, aminosilane-grafted silicone. *Significant effect of surface modification, $p < 0.05$.

Wettability of surface-modified silicone tubes

To assess the hydrophilicity of different surface-modified silicone tubes, the water contact angles were measured by the sessile drop method (Table 3). We found that the water contact angles decreased after plasma surface modification and monomer grafting on silicone tubes (Si: 102±4º; PSM Si: 38±3º, AAc Si: 42±2º, and AmS Si: 49±3º), while the amount of water contact angles were not significantly different ($p>0.05$) for all surface-modified silicone tubes. Collagen addition slightly

increased the contact angles compared with ones without collagen (PSM Si-Col: 53 ± 5°; AAc Si-Col: 56 ± 2°; AmS Si-Col: 61 ± 4°). AAc and AmS grafting resulted in moderate contact angles, especially after collagen immobilization.

Endothelial cell adhesion on surface-modified silicone tubes

Maximal cell adhesion was found on collagen-immobilized silicone tubes independent of pretreatment with peroxide, carboxyl, or amine groups (Table 3). More endothelial cells adhered on Ams Si than on PSM Si or AAc Si tubes without immobilized collagen. The number of cells adhered on AmS Si tubes was 1.7-fold higher than on Si tubes. Carboxyl groups in AAc Si tubes decreased cell adhesion by 3-fold. Increased cell adhesion was observed on peroxide groups in PSM Si tubes, albeit 1.4-fold lower than cell adhesion on positively charged amine groups in AmS Si tubes.

Table 3. Wettability, endothelial cell adhesion, and endothelial cell detachment of Si, PSM Si, AAc Si, AmS Si, PSM Si-Col, AAc Si-Col, and AmS Si-Col tubes after 1 h exposure to 1.5 N m^{-2} fluid shear stress. Values are mean ± standard deviation for 3 independent experiments. Si, silicone; PSM Si, plasma surface-modified silicone; AAc Si, AAc-grafted silicone; AmS Si, AmS-grafted silicone; PSM Si-Col, collagen-immobilized plasma surface-modified silicone; AAc Si-Col, collagen-immobilized AAc-grafted silicone; AmS Si-Col, collagen-immobilized AmS-grafted silicone.

Tube, surface modification	Wettability, water contact angle (º)	Cell adhesion (%)	Cell detachment (%)
Si	102.1 ± 4.0	46 ± 2	75 ± 2
PSM Si	38.5 ± 3.1	56 ± 3	62 ± 4
AAc Si	42 ± 2	15 ± 2	98 ± 2
AmS Si	49 ± 3	80 ± 4	7 ± 3
PSM Si-Col	53 ± 5	77 ± 2	37 ± 2
AAc Si-Col	56 ± 2	85 ± 4	5 ± 1
AmS Si-Col	61 ± 4	83 ± 5	3 ± 2

Endothelial cell proliferation on surface-modified silicone tubes

Endothelial cell proliferation on Si, PSM Si, AAc Si, AmS Si, PSM Si-Col, AAc Si-Col, and AmS Si-Col tubes was compared after 2, 4, and 6 days of culture (Figure 4). The number of cells was higher on collagen-immobilized silicone tubes than on tubes without immobilized collagen at all time points measured, with the highest cell proliferation rate observed on AmS Si-Col tubes. The cell number on AmS Si-

Col tubes was 1.5-fold ($p<0.05$, day 2), 1.2-fold ($p<0.05$, day 4), and 1.1-fold ($p<0.05$, day 6) increased compared with AAc Si-Col tubes. Cell proliferation was highest on Ams Si tubes compared with other tubes without immobilized collagen (i.e. PSM Si, and AAc Si tubes). The number of cells on AmS Si tubes was increased by 82% at day 4 ($p<0.005$), and 151% at day 6 ($p<0.0005$), compared with Si tubes. The cell number on AAc Si tubes was significantly decreased by 4-fold ($p<0.0005$, day 4) and 3-fold ($p<0.005$, day 6) compared with Si tubes. The cell number on PSM Si tubes was similar as on Si tubes at days 2 and 4, but increased at day 6 of culture (1.5-fold, $p<0.05$).

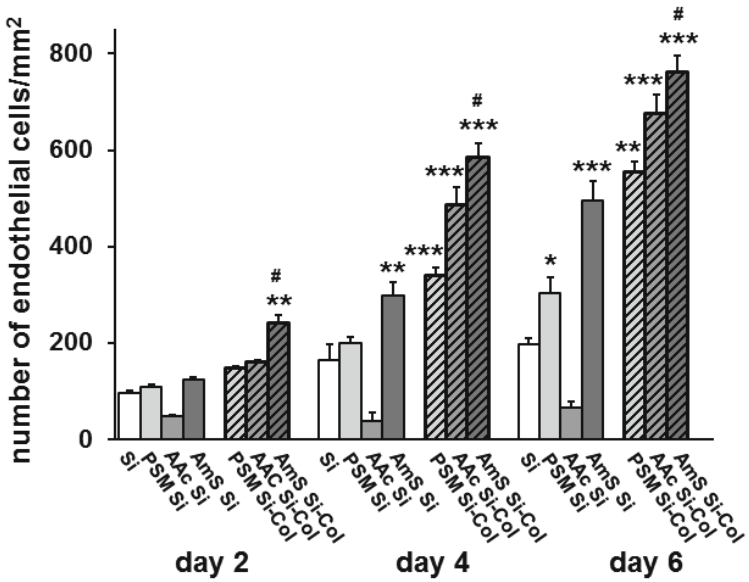

Figure 4. Endothelial cell proliferation on Si, PSM Si, AAc Si, AmS Si, PSM Si-Col, AAc Si-Col, and AmS Si-Col tubes after 2, 4, and 6 days of culture. Cell proliferation on collagen-immobilized silicone tubes was increased compared with Si. Maximum cell number was observed on AmS Si-Col at all time points. Cell proliferation was decreased on AAc Si but increased on PSM Si and AmS Si tubes compared with Si tubes at all time points. Si, silicone; PSM Si, plasma surface-modified silicone; AAc Si, AAc-grafted silicone; AmS Si, AmS-grafted silicone; PSM Si-Col, collagen-immobilized plasma surface-modified silicone; AAc Si-Col, collagen-immobilized AAc-grafted silicone; AmS Si-Col, collagen-immobilized AmS-grafted silicone. *Significant effect of surface modification, $p<0.05$, **$p<0.005$, ***$p<0.0005$, #Significantly different from AAc Si-Col tubes, $p<0.05$.

Morphology of endothelial cells on surface-modified silicone tubes

SEM micrographs of endothelial cells cultured for 6 days on unmodified and surface-modified silicone tubes showed that the cell morphology was dependent on the surface modification method used (Figure 5).

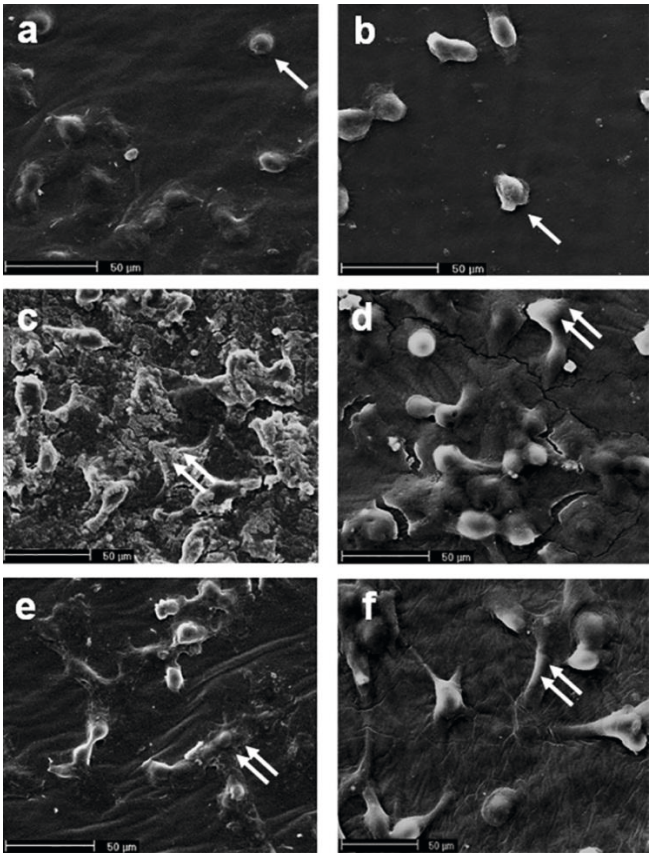

Figure 5. Scanning electron microscopy (SEM) showing morphology of endothelial cells seeded on Si, PSM Si-Col, AAc Si, AAc Si-Col, AmS Si, AmS Si-Col surfaces after 6 days of culture. (a) Si, (b) AAc Si, (c) AmS Si , (d) PSM Si-Col, (e) AAc Si-Col, (f) AmS Si-Col. Magnification x500. Endothelial cells on unmodified Si tubes and on AAc Si tubes exhibited "round" cell bodies (a, b). Endothelial cells on collagen-immobilized and AmS Si tubes displayed a flat, spindle-shaped morphology, while no “round” cells were present (c, d, e, f). Si, silicone; AAc Si, AAc-grafted silicone; AmS Si, AmS-grafted silicone; PSM Si-Col, collagen-immobilized plasma surface-modified silicone; AAc Si-Col, collagen-immobilized AAc-grafted silicone; AmS Si-Col, collagen-immobilized AmS-grafted silicone. Single arrow: round cell; double arrows: spindle-shaped cell.

Cells on Si tubes did not spread well (Figure 5a). Only few cells were attached on AAc Si tubes, exhibiting "round" morphology (Figure 5b). In contrast, cells attached onto AmS Si tubes kept their natural spindle-shaped morphology (Figure 5c). Cells on PSM Si-Col (Figure 5d), AAc Si-Col (Figure 5e), and AmS Si-Col (Figure 5f) tubes showed a spindle-shaped morphology. This suggests that a collagen coating provides a highly compatible substratum for endothelial cells.

Endothelial cell detachment from endothelialized silicone tubes after shear stress

The percentage of detached cells was determined after 1 h fluid shear stress treatment (Table 3). Cell detachment from AmS Si-Col and AAc Si-Col tubes was negligible, while 37% of the cells detached from PSM Si-Col tubes. Cell detachment from AmS Si tubes was decreased (91%, $p<0.005$), but increased from AAc Si tubes (31%, $p<0.05$) compared with Si tubes. Seventy-five % of cells on Si tubes detached after fluid shear stress treatment.

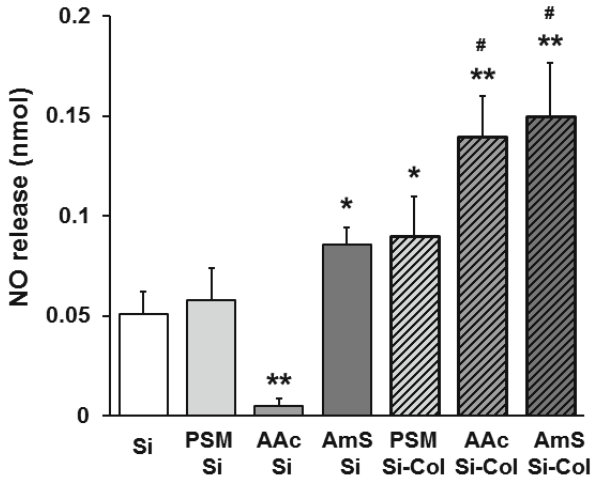

Figure 6. NO release by endothelial cells on Si, PSM Si, AAc Si, AmS Si, PSM Si-Col, AAc Si-Col, and AmS Si-Col tubes after 2 days of culture. The NO release by endothelial cells cultured on AmS Si-Col tube was about 1.7-fold higher than on PSM Si-Col tubes, while no significant difference was observed between NO release by cells on AmS Si-Col and AAc Si-Col tubes. Si, silicone; PSM Si, plasma surface-modified silicone; AAc Si, AAc-grafted silicone; AmS Si, AmS-grafted silicone; PSM Si-Col, collagen-immobilized plasma surface-modified silicone; AAc Si-Col, collagen-immobilized AAc-grafted silicone; AmS Si-Col, collagen-immobilized AmS-grafted silicone. n=3. *Significant effect of surface modification, $p<0.05$, **$p<0.005$, $^{\#}$Significantly different from PSM Si-Col tubes, $p<0.05$.

NO release by endothelial cells

NO release by endothelial cells cultured for 6 days on collagen-immobilized silicone tubes was much higher than that from cells on tubes without immobilized collagen (Figure 6). NO release by cells cultured on AmS Si-Col tubes was 2.9-fold higher ($p<0.005$) than on Si tubes, and 1.7-fold higher ($p<0.05$) than on PSM Si-Col tubes, while no significant difference was observed between NO released by cells on AmS Si-Col and AAc Si-Col tubes. Cells on PSM Si tubes released similar NO levels as on Si tubes, but they only released a very small amount of NO on AAc Si tube. The amount of NO released by endothelial cells on AAc Si tubes was 9.7-fold lower ($p<0.005$) than on Si tubes.

DISCUSSION

Endothelialization of blood contacting parts of hollow fibers would be a key milestone in the development of biohybrid artificial lungs, which may become a first stepping stone towards the introduction of regenerative medicine techniques in the treatment of lung disease [4, 7]. Silicone membrane hollow fibers are widely used for artificial lungs, but they do not support cell attachment and/or proliferation due to their surface hydrophobicity and inertness [40]. Therefore principal surface modification is needed to improve cell-silicone interactions, as this is strongly influenced by the physicochemical properties of the silicone surface [15, 18]. Plasma graft polymerization in the presence of different reactive chemical materials to introduce functional peroxide, carboxyl, hydroxyl, amine, or aldehyde groups has received much attention. The functional groups are main chemically reactive groups amenable for covalent immobilization of collagen, that enhance endothelial cell attachment and proliferation [9, 14, 15, 17, 23]. In this study, plasma pre-modified silicone tubes containing peroxide groups were used to initiate graft polymerization of two different monomers, i.e. AAc and AmS. We investigated whether the presence of different functional groups on silicone tubes, i.e. peroxide groups by oxygen plasma pre-modification, carboxyl groups by AAc grafting, and amine groups by AmS grafting, but similar wettability enhanced interaction with endothelial cells leading to a stable cell layer with anti-thrombotic properties. Peroxide groups resulting from plasma pre-modification act as initiators in plasma graft polymerization [13, 21]. The density of grafted monomers directly depends on the peroxide concentration on plasma pre-modified surfaces [21]. Therefore we used constant parameters of plasma pre-modification to achieve the same peroxide density before grafting of AAc or AmS. Silicone plasma pre-modification using our parameters (60 W oxygen plasma for 0.5 min) has been reported to result in maximum peroxide density (~7×10^{-8} mol cm^{-2}) on a silicone's surface [21]. After plasma pre-modification of silicone tubes, the contact time of monomers with

silicone tube was adjusted to achieve the same wettability on AAc-grafted and AmS-grafted silicone tubes, which also resulted in similar graft molar density of carboxyl and amine groups. It is well known that graft density affects collagen adsorption, which directly affects cell adhesion [18, 20, 41].

The hydrophilic nature of a material in general prevents protein adsorption, although amine functional groups do not only increase material hydrophilicity but also protein adsorption. On the other hand, collagen has more carboxyl groups than amine groups in its chemical structure, causing it to easily react with amine functional groups on a material surface to produce carbodiimide bonds [11, 14, 42]. Our data shows that the introduction of amine groups on silicone increases the immobilized collagen concentration compared with carboxyl or peroxide groups. This observation corresponds to the increased collagen-endothelial cell interaction, cell adherence and number on AmS Si-Col compared with PSM Si-Col or AAc Si-Col tubes.

Mechanical and physical properties of AmS Si but not PSM Si and AAc Si tubes significantly changed compared to Si tubes. This represents an important advantage of PSM Si and AAc Si rather than AmS Si tubes for clinical usage. The shelf life of plasma surface-modified and AmS-grafted materials is limited, with post-plasma oxidation reactions leading to the loss of peroxide and amine groups from the material surface [17]. Aging of AAc-grafted materials is not a problem, probably because carboxyl groups are a product of post-plasma oxidative reactions anyway [17, 21]. A relatively long shelf life of AAc-grafted materials compared with plasma-modified or AmS-grafted materials can be considered another advantage of AAc Si tubes for clinical use.

Introduction of functional groups to a material surface results in decreased water contact angles [16, 34]. We found a considerable decrease in water contact angles of silicone tubes after plasma modification, AAc grafting, and AmS grafting, which resulted in increased hydrophilicity of silicone tubes. The decrease in wettability of silicone tubes after collagen immobilization could be inherent to the fact that collagen is more hydrophobic than AAc or AmS [18, 20, 40]. Materials with moderate water contact angle optimally support cell adhesion and consequently improve their biocompatibility [43-46]. Therefore AAc Si-Col and AmS Si-Col tubes, having moderate water contact angles, might be favorable for endothelial cell attachment and proliferation.

Endothelial cells are sensitive to material surface characteristics, e.g. wettability and surface charge. In the current study, endothelial cells showed poor adhesion on negatively charged AAc Si tubes, which agrees with published data showing that carboxyl groups grafted on a material surface inhibit cell adhesion and proliferation [11, 14, 17]. Our results also agree with data by Lee et al. (1994), who observed optimal chinese hamster ovary (CHO) cell adhesion, growth, and spreading on positively charged (amine group-grafted) polyethylene surfaces, while

negatively charged (carboxylic group-grafted) surfaces showed poor cell growth [13]. Moreover, positively charged groups also attract negatively charged cells. This may explain why AmS Si-Col tubes showed the highest density of cells initially adhering compared to the other surface-modified tubes tested. The cell density on collagen-immobilized silicone tubes was higher than on tubes without immobilized collagen. This result agrees well with data by others that endothelial cell adhesion is facilitated by pre-coating of the substratum with extracellular matrix proteins such as collagen [16, 17, 40], although the ability of adhesive proteins to support cell adhesion is dependent on cell quantity and activity, which is influenced by the surface properties of the underlying substratum [34]. Taken together, AmS Si tubes were more favorable for collagen immobilization compared with AAc Si tubes, which directly increased endothelial cell growth on AmS Si-Col tubes.

Endothelial cells proliferated well on all types of collagen-immobilized silicone tubes. The number of cells on AmS Si-Col tubes was slightly higher than on AAc Si-Col tubes at all time points measured. Cell proliferation on AmS Si tubes without immobilized collagen was increased compared to Si tubes. Moreover, cells cultured on surface-modified silicone tubes grew rapidly, whereas cells on unmodified tubes grew slowly. The number of cells was increased on AmS Si tubes containing amine functionalities, but the cell number was very low on AAc Si tubes. This agrees with published data showing that negatively charged surfaces are not suitable for endothelial cell proliferation [17, 18].

Excellent cell spreading indicates strong cell-material interaction, while round cells on a material indicate weak cell–material contact, which might cause cell death. Endothelial cell morphology was undesirably affected by the negatively charged carboxyl groups resulting in round cell morphology. In contrast, positively charged amine groups supported cell contact well, resulting in a spindle-shaped cell morphology. This is likely due to the negative charges on silicone introduced by AAc, which are toxic for endothelial cells. Positive charges introduced by AmS provided an appropriate substratum for endothelial cells.

AmS Si-Col and AAc Si-Col tubes maintained a high cell density after fluid shear stress treatment. A high percentage (37%) of cells detached from PSM Si-Col tubes, which likely resulted from a weak linkage of collagen on these tubes, unlike the collagen immobilized with carbodiimide bonds on silicone tubes with amine or carboxyl groups. Fluid shear stress caused a cell loss of 75% from unmodified silicone tubes. Cells on AmS Si tubes were firmly attached, but cells on AAc Si tubes were easily removed from the surface.

The success of endothelization of a synthetic material surface can also be assessed by measuring the secretion of anti-thrombotic factors such as NO [11]. The high NO release by endothelial cells on collagen-immobilized silicone tubes indicated excellent anti-thrombotic functionality. Immobilized collagen could suitably link with amine or carboxyl groups on the silicone tubes, and provided an

excellent substratum for cell growth and function. Higher amounts of NO released by endothelial cells cultured on AmS Si than on AAc Si tubes revealed that cells functioned well on amine group-modified tubes.

CONCLUSIONS

AmS Si and PSM Si but not AAc Si tubes were favorable for endothelial cell attachment and proliferation even without collagen immobilization. Collagen-immobilized silicone tubes pretreated with peroxide, carboxyl, or amine groups enhanced endothelial cell attachment, proliferation, and NO release compared to tubes without immobilized collagen. Cells were more stable under fluid shear stress on AAc Si-Col and AmS Si-Col tubes containing carbodiimide bonds between functional groups and collagen than on PSM Si-Col tubes. Although AmS Si-Col tubes allowed excellent cell behavior, the amine groups extremely changed silicone's physical properties. This suggests that collagen immobilization after AAc grafting, but not oxygen modification or AmS grafting is preferable for endothelialization of blood-contacting parts of artificial lungs.

ACKNOWLEDGEMENTS

The authors are grateful to Dr. Jhamak Noormohammadi and Dr. Atefeh Solouk for valuable advice on plasma graft polymerization of silicone tubes. The authors declare that there is no conflict of interest.

REFERENCES

1 Betit P. Extracorporeal membrane oxygenation: Quo vadis?. Respir Care 2009;54:948-957.
2 Nolan H, Wang D, Zwischenberger JB. Artificial lung basics: Fundamental challenges, alternative designs and future innovations. Organogenesis 2011;7:23-27.
3 Zwischenberger BA, Clemson LA, Zwischenberger JB. Artificial lung: progress and prototypes. Expert Rev Med Devices 2006;3:485-497.
4 Polk AA, Maul TM, McKeel DT, Snyder TA, Lehocky CA, Pitt B, Stolz DB, Federspiel WJ, Wagner WR. A biohybrid artificial lung prototype with active mixing of endothelialized microporous hollow fibers. Biotechnol Bioeng 2010;106:490-500.
5 Wagner WR, Griffith BP. Reconstructing the lung. Science 2010;329:519-521.
6 Khachab A, Tabesh H, Kashefi A, Mottaghi Kh. Novel concept for pure diffusive capillary membrane oxygenators: silicone hollow sphere (SiHSp) fibers. ACAIO J 2013;59:162-168.
7 Song JJ, Ott HC. Bioartificial lung engineering. Am J Transplant 2012;12:283-288.
8 Sawa Y, Ohala T, Takagi M, Suhara H, Matsuda H. Development of hybrid artificial lung with gene transfected biological cells. J Artif Organs 2000;3:1-4.
9 Lim HR, Baek HS, Lee MH, Woo YI, Han DW, Han MH. Surface modification for enhancing behaviors of vascular endothelial cells onto polyurethane films by microwave-induced argon plasma. Surf Coat Technol 2008;202:5768-5772.
10 Mel A, Cousins BG, Seifalian AM. Surface modification of biomaterials: A quest for blood compatibility. Int J Biomater 2012;2012:707-863.
11 Tzoneva R, Seifert B, Alberecht W, Richau K, Lendlein A, Gruth T. Poly(ether imide) membranes: studies on the effect of surface modification and protein pre-adsorption on endothelial cell adhesion, growth and function. J Biomat Sci-Polym E 2008;19:837-852.
12 Hamerli P, Weigel T, Groth T, Paul D. Surface properties of and cell adhesion onto allylamine-plasma coated polyethylenterephtalat membranes. Biomaterials 2003;24:3989-3999.
13 Lee JH, Jung HW, Kang IK, Lee HB. Cell behaviour on polymer surfaces with different functional groups. Biomaterials 1994;15:705-711.
14 Thevenot P, Hu W, Tang L. Surface chemistry influence implant biocompatibility. Curr Top Med Chem 2008;8:270-280.
15 Ai H, Mills DK, Jonathan AS, Jones SA. Gelatin-gelatardehyde cross-linking on silicone rubber to increase endothelial cell adhesion and growth. In Vitro Cell Dev-An 2002;38:487-492.
16 Sano S, Kato K, Ikada Y. Introduction of functional groups onto the surface of polyethylene for protein immobilization. Biomaterials 1993;14:817-822.
17 Siow KS, Britcher L, Kumar S, Griesser HJ. Plasma methods for the generation of chemically reactive surfaces for biomolecule immobilization and cell colonization-A review. Plasma Process Polym 2006;3:392-418.
18 Lee SD, Hsiue GH, Chang PCT, Kao CY. Plasma-induced grafted polymerization of acrylic acid and subsequent grafting of collagen onto polymer film as biomaterials. Biomaterials 1996;17:1599-1608.
19 Choi HS, Kim YS, Zhang Y, Tang S, Myung SW, Shin BC. Plasma-induced graft co-polymerization of acrylic acid onto the polyurethane surface. Surf Coat Tech 2004;182:55-64.
20 Gupta B, Plummer C, Bisson I, Frey P, Hilborn J. Plasma-induced graft polymerization of acrylic acid onto poly(ethylene terephthalate) films: characterization and human smooth muscle cell growth on grafted films. Biomaterials 2002;23:863-871.
21 Karkhaneh A, Mirzadeh H, Ghaffariyeh A. Simultaneous graft copolymerization of 2-hydroxyethyl methacrylate and acrylic acid onto polydimethylsiloxane surfaces using a two-step plasma treatment. J Appl Polym Sci 2007;105:2208-2217.
22 Blanchemain N, Aguilar MR, Chai F, Jimenez M, Jean-Baptiste E, El-Achari A, Martel B, Hildebrand HF, San Roman J. Selective biological response of human pulmonary microvascular

endothelial cells and human pulmonary artery smooth muscle cells on cold-plasma-modified polyester vascular prostheses. Biomed Mater 2011;6:065003
23 Bordenave L, Lefebvre F, BareilXe R, Rouais F, Baquey Ch, Rabaud M. New artificial connective matrix-like structure: thrombogenicity and use as endothelial cell culture support. Biomaterials 1992;13:439-447.
24 Takagi M, Shiwaku K, Inoue T, Shirakawa Y, Sawa Y, Matsuda H, Yoshida T. Hydrodynamically stable adhesion of endothelial cells onto a polypropylene hollow fiber membrane by modification with adhesive protein. J Artif Organs 2003;6:222-226.
25 Bouten CVC, Dankers PYW, Driessen-Mol A, Pedron S, Brizard AMA, Baaijens FPT. Substrates for cardiovascular tissue engineering. Adv Drug Deliv Rev 2011;63:221-241.
26 Lin Q, Ding X, Qiu F, Song X, Fu G, Ji J. In situ endothelialization of intravascular stents coated with an anti-CD34 antibody functionalized heparin–collagen multilayer. Biomaterials 2010;31:4017-4025.
27 Jozkowicz A, Cooke JP, Guevara I, Huk I, Funovics P, Pachinger O, Weidinger F, Dulak J. Genetic augmentation of nitric oxide synthase increases the vascular generation of VEGF. Cardiovasc Res 2001;51:773-783.
28 Solouk A, Solati-Hashjin M, Najarian S, Mirzadeh H, Seifalian AM. Optimization of acrylic acid grafting onto POSS-PCU nanocomposite using response surface methodology. Iran Polym J 2011;20:91-107.
29 Howarter JA, Youngblood JP. Surface modification of polymers with 3-aminopropyltriethoxysilane as a general pretreatment for controlled wettability. Macromolecules 2007;40:1128-1132.
30 Williams RL, Wilson DJ, Rhodes NP. Stability of plasma-treated silicone rubber and its influence on the interfacial aspects of blood compatibility. Biomaterials 2004;25:4659-4673.
31 Solouk A, Cousins BG, Mirahmadi F, Mirzadeh H, Jalali Nadoushan MR, Shokrgozar MA, Seifalian AM. Biomimetic modified clinical-grade POSS-PCU nanocomposite polymer for bypass graft applications: A preliminary assessment of endothelial cell adhesion and haemocompatibility. Mater Sci Eng C Mater Biol Appl 2015;46:400-408.
32 McGuigan AP, Sefton MV. The influence of biomaterials on endothelial cell thrombogenicity. Biomaterials 2007;28:2547-2571.
33 Park K, Ju YM, Son JS, Ahn KD, Han DK. Surface modification of biodegradable electrospun nanofiber scaffolds and their interaction with fibroblasts. J Biomat Sci-Polym E 2007;18:369-382.
34 Tzoneva R, Faucheux N, Groth T. Wettability of substrata controls cell–substrate and cell–cell adhesions. Biochim Biophys Acta 2007;1770:1538-1547.
35 Kannan RY, Salacinski HJ, Sales KM, Butler PE, Seifalian AM. The endothelialization of polyhedral oligomeric silsesquioxane nanocomposites. Cell Biochem Biophys 2006;45:1-8.
36 Bacabac RG, Smit TH, Van Loon JJWA, Zandieh-Doulabi B, Helder MN, Klein-Nulend J. Bone cell responses to high-frequency vibration stress: does the nucleus oscillate within the cytoplasm?. FASEB J 2006;20:858-864.
37 Kabirian F, Amoabediny G, Haghighipour N, Salehi-Nik N, Zandieh-Doulabi B. Nitric oxide secretion by endothelial cells in response to fluid shear stress, aspirin, and temperature. J Biomed Mater Res A 2015;103:1231-1237.
38 Mullender MG, Dijcks SJ, Bacabac RG, Semeins CM, Van Loon JJWA, Klein-Nulend J. Release of nitric oxide, but not prostaglandin E_2, by bone cells depends on fluid flow frequency. J Orthop Res 2006;24:1170-1177.
39 Prasad CK, Krishnan LK. Regulation of endothelial cell phenotype by biomimetic matrix coated on biomaterials for cardiovascular tissue engineering. Acta Biomater 2008;4:182-191.
40 Farhadi M, Mirzadeh H, Solouk A, Asghari A, Jalessi M, Ghanbari H, Yazdanifard P. Collagen-immobilized patch for repairing small tympanic membrane perforations: In vitro and in vivo assays. J Biomed Mater Res A 2012;100:549-553.
41 Li H, et al. Aminosilane micropatterns on hydroxyl-terminated substrates: fabrication and applications. Langmuir 2010;26:5603-5609.

42 Keselowsky BG, Collard DM, Garcia AJ. Surface chemistry modulates focal adhesion composition and signals through changes in integrin binding. Biomaterials 2004;25:5947-5954.
43 Bodas D, Khan-Malek C. Hydrophilization and hydrophobic recovery of PDMS by oxygen plasma and chemical treatment-An SEM investigation. Sensor Actuat B-Chem 2007;123:368-373.
44 Kaar JL, Oh HI, Russell AJ, Federspiel WJ. Towards improved artificial lungs through biocatalysis Biomaterials 2007;28:3131-3139.
45 Pareta RA, Reising AB, Miller T, Storey D, Webster TJ. Increased endothelial cell adhesion on plasma modified nanostructured polymeric and metallic surfaces for vascular stent applications. Biotechnol Bioeng 2009;103:459-471.
46 Yamamoto H, Shibata Y, Miyazaki T. Anode glow discharge plasma treatment of titanium plates facilitates adsorption of extracellular matrix proteins to the plates. J Dent Res 2005;84:668-671.

CHAPTER 3

Flow Preconditioning of Endothelial Cells on Collagen-Immobilized Silicone Fibers Enhances Cell Retention and Anti-Thrombotic Function

Nasim Salehi-Nik[1,2], Seyedeh Parnian Banikarimi[1,2], Ghassem Amoabediny[1,2], Behdad Pouran[3,4], Mohammad Ali Shokrgozar[5], Behrouz Zandieh-Doulabi[6], Jenneke Klein-Nulend[6]

[1] School of Chemical Engineering, College of Engineering, University of Tehran, Tehran, Iran

[2] Department of Biomedical Engineering, Research Center for New Technologies in Life Science Engineering, University of Tehran, Tehran, Iran

[3] Department of Orthopedics, University Medical Center Utrecht, Utrecht, The Netherlands

[4] Department of Biomechanical Engineering, Faculty of Mechanical, Maritime, and Materials Engineering, Delft University of Technology, Delft, The Netherlands

[5] National Cell Bank, Pasteur Institute of Iran, Tehran, Iran

[6] Department of Oral Cell Biology, Academic Centre for Dentistry Amsterdam, University of Amsterdam and VU University Amsterdam, MOVE Research Institute Amsterdam, Amsterdam, The Netherlands

Submitted for publication

ABSTRACT

Stability and anti-thrombotic functionality of endothelial cells on silicone hollow fibers are critical in the development of biohybrid artificial lungs. Here we aimed to enhance endothelial cell retention and anti-thrombotic function by low (12 dyn/cm^2, 24 h) fluid shear stress ("flow") preconditioning of endothelial cells seeded on collagen-immobilized silicone hollow fibers. The response of endothelial cells, either or not preconditioned, on hollow fibers to high (30 dyn/cm^2, 1 h) fluid shear stress was assessed in a parallel-plate flow chamber. Finite element (FE) modeling was used to simulate shear stress within the flow chamber. We found that collagen immobilization on hollow fibers using carbodiimide bonds provided sufficient stability to high shear stress. Flow preconditioning for 24 h before treatment with high shear stress for 1 h on collagen-immobilized hollow fibers increased cell retention (1.3-fold). The FE model showed that cell flattening due to flow preconditioning reduced maximum shear stress on cells by 32%. Flow preconditioning prior to exposure to high fluid shear stress enhanced the production of nitric oxide (1.2-fold) and prostaglandin I_2 (1.1-fold). In conclusion, flow preconditioning of endothelial cells on collagen-immobilized silicone hollow fibers enhanced cell retention and anti-thrombotic function, which could significantly improve current biohybrid artificial lungs.

Keywords
Anti-thrombotic function, Biohybrid artificial lung, Collagen immobilization, Endothelialization, Finite element modeling, Fluid shear stress

INTRODUCTION

Hollow fiber membrane oxygenators, also called artificial lungs, contain hollow fibers across which patient blood is passed for artificial oxygenation during open-heart surgery [1]. Blood-contacting parts of hollow fibers are functionally limited due to biocompatibility issues associated with thrombosis [1-3]. Endothelialization of hollow fibers down-regulates the thrombogenic response of blood platelets in so-called biohybrid artificial lungs, which have been developed in recent decade [2, 3]. The hydrophobicity of silicone hollow fibers which are typically used in artificial lungs impedes endothelial cell adhesion. Therefore, surface modification through physical, chemical, or physicochemical methods might be required to enhance stable cell attachment [4-6]. Deposition of extracellular matrix (ECM) proteins, e.g. collagen, has been widely used to promote cell attachment on silicone sheets or tubes [7, 8]. Earlier we have shown that acrylic acid (AAc) grafting of silicone tubes before collagen immobilization results in strong carbodiimide bonding between amine groups of collagen and carboxyl groups of AAc-grafted silicone tubes, making it resistant to fluid shear stress [8].

Endothelial cell retention on collagen-coated hollow fibers in artificial lungs is important since endothelial cell detachment might expose cell-free regions to blood flow and consequently induce platelet adhesion [9, 10]. Controlled exposure of endothelial cells seeded on surface-modified materials to low fluid shear stress, so-called flow preconditioning, remarkably stimulates endothelial cell monolayer retention under fluid shear stress [11-15]. This is likely due to integrin activation [15, 16], increased binding affinity of integrins to ECM ligands [15, 16], and/or cell flattening which increases the cell surface area involved in integrin-mediated adhesion and limits cell surface shear stress gradients [14, 17, 18].

In addition to enhanced endothelial cell adhesion on surface-modified materials, anti-thrombotic functionality of endothelial cells account for improved biocompatibility of artificial lungs. Since nitric oxide (NO) and prostaglandin I_2 (PGI_2) inhibit platelet aggregation and adhesion [19, 20], the ability of endothelial cells seeded on surface-modified silicone hollow fibers to produce these factors can be used to assess the anti-thrombotic capacity of biohybrid artificial lungs. Flow preconditioning of endothelial cells has been shown to increase cell retention under high shear stresses, but its effect on endothelial cell anti-thrombotic functionality, e.g. cell-mediated NO and PGI_2 release, has been not thoroughly investigated. To correlate shear stress with the cell responses, e.g. cell detachment and anti-thrombotic functionality, the precise amount of shear stress experienced by cells should be determined. Mathematical and computational models are often used particularly in problems involving complex geometries to obtain shear stress distribution at the endothelial cell surface [17, 21].

The current study aimed to investigate whether endothelial cell retention and anti-thrombotic function on silicone hollow fibers under high shear stress can be improved by collagen immobilization on these fibers and flow preconditioning of endothelial cells. Endothelial cells seeded on collagen-adsorbed and collagen-immobilized silicone hollow fibers with or without preconditioning were exposed to 1-30 dyn/cm^2 shear stress in a custom-made parallel-plate flow chamber. Shear-induced endothelial cell responses, i.e. cell detachment, as well as NO and PGI_2 production were assessed by experiment. A FE model was developed to determine the inlet fluid flow rate through the parallel-plate flow chamber corresponding to the desired shear stress on surface-modified silicone hollow fibers and to obtain the fluid shear stress distribution on endothelial cells with or without preconditioning. The combination of experiments and FE model enables correlating the biological response of the endothelial cells with the applied fluid shear stress and finding the optimal surface modification method and mechanical conditioning within the parallel-plate flow chamber.

MATERIALS AND METHODS

Materials

Cylindrical silicone hollow fibers (inner diameter 0.6 mm, thickness 0.1 mm) were kindly donated by Raumedic (Helmbrechts, Germany). Twenty nine silicone hollow fibers were glued together with a biocompatible silicone glue to prepare one large silicone hollow fiber (SiHF) patch (25 mm x 60 mm). Ninety SiHF patches were prepared and split into three groups: 1) Collagen-adsorbed SiHF patches without endothelial cells (n=21 patches) and with endothelial cells (n=21 patches); 2) Collagen-immobilized SiHF patches without endothelial cells (n=21 patches) and with endothelial cells (n=21 patches); 3) Collagen-immobilized SiHF patches with flow preconditioned (12 dyn/cm^2 fluid shear stress for 24 h in a parallel-plate flow chamber) endothelial cells (n=6 patches).

The effect of collagen immobilization on SiHF patches using carbodiimide bonds on collagen stability, endothelial cell retention and anti-thrombotic function was investigated by comparing collagen and cell detachment from collagen-adsorbed, and collagen-immobilized SiHF patches after exposure to fluid shear stress of 1, 6, 12, 18, 24, and 30 dyn/cm^2 for 1 h. The effect of flow preconditioning of endothelial cells on cell retention and antithrombotic function of collagen-immobilized SiHF patches at high shear stress (30 dyn/cm^2) was investigated and compared with cell stability on collagen-immobilized SiHF patches without flow preconditioning of the cells.

Surface modification of SiHF patches

SiHF patches were cleaned 3 times with 70% (v/v) ethanol, and once with de-ionized water for 5 min. Forty two SiHF patches were put in a solution of 1 mg/ml collagen (acid soluble collagen type I; Pasteur Institute of Iran, Tehran, Iran) in 0.02 M acetic acid (Fluka, Buchs, Switzerland) at 4°C for 24 h to achieve collagen-adsorbed SiHF (SiHF-Col) patches. Another 48 SiHF patches were placed on the bottom of a reaction chamber (Seren R600, Anatech ltd, Union city, CA, USA), which was evacuated to 0.6 mbar, and pretreated with 60 W of oxygen plasma for 0.5 min. The plasma-treated SiHF patches were immersed in a solution containing 30% AAc in de-ionized water for 30 min at room temperature. After removal from the solution, the patches were air-dried at 40°C for 5 min. The dried patches with a pre-adsorbed surface layer of reactive AAc monomers were placed into the reaction chamber for plasma graft copolymerization for 3 min to produce AAc-grafted SiHF patches. The residual monomers and homopolymers were removed by washing twice with warm de-ionized water in a water bath, followed by incubation in distilled water for 24 h [8, 22]. AAc-grafted SiHF patches were immersed in 30 ml 5 mM 2-(N-morpholino)ethanesulfonic acid (MES) buffer solution containing 48 mg 1-ethyl-3-[3-dimethylaminopropyl] carbodiimide hydrochloride (EDC) and 15 mg N-hydroxysuccinimide (NHS; Fluka, Neu-Ulm, Germany) before collagen immobilization [22]. The solution was gently stirred for 5 h at 4°C to activate the carboxyl groups on the patches. Then AAc-grafted SiHF patches were put into a solution of 1 mg/ml collagen in 0.02 M acetic acid to immobilize collagen at 4°C for 24 h. Finally, collagen-immobilized AAc-grafted SiHF (AAc SiHF-Col) patches were washed in distilled water for 1 min to remove unbound collagen, and stored at 4°C until further use.

To investigate the stability of collagen coating, 18 SiHF-Col patches and 18 AAc SiHF-Col patches were exposed to shear stresses of 1, 6, 12, 18, 24, and 30 dyn/cm^2 for 1 h in an in-house fabricated parallel-plate flow chamber with a closed loop system by pumping 50 ml distilled water with a peristaltic pump (pump for low flow rates was from Rainin Dynamax, San Diego, CA, USA; pump for high flow rates from Heidolph, Schwabach, Germany (Figure 1)). Polyvinyl chloride tubing was used to link the fluid reservoir, pump, and flow chamber. Three patches in each group served as static control. The amount of collagen on the patches was determined by a Bradford protein assay (Bradford, Hercules, CA, USA) using an Eppendorf biophotometer D30 (Eppendorf, Hamburg, Germany) following the manufacturer's instructions. The concentration of immobilized collagen on the patches was assessed by comparison with a standard curve.

Endothelial cell seeding and culture on surface-modified SiHF patches

Human umbilical vein endothelial cells (HUVECs) from the National Cell Bank, Pasteur Institute of Iran (Tehran, Iran) were used between passages 3 and 6 to

examine endothelial cell retention and anti-thrombotic function on SiHF patches. Surface-modified SiHF patches, i.e. SiHF-Col, and AAc SiHF-Col, were put into petri dishes, sterilized with UV, washed twice with phosphate-buffered saline (PBS) solution, and washed once with culture medium before cell seeding (see below).

Endothelial cells were seeded on surface-modified SiHF patches at 10^5 cells/cm^2 in an in-house fabricated seeding well containing 3 ml Dulbecco's Minimal Essential Medium (DMEM)/F12 (1/1, v/v) with 10% fetal bovine serum (Gibco, Renfrewshire, Scotland; Figure 1), and cultured in a humidified atmosphere of 5% CO_2 in air at 37°C for 2 days.

Exposure of cultured endothelial cells on surface-modified SiHF patches to fluid shear stress

After two days of cell culture, 18 SiHF-Col patches and 18 AAc SiHF-Col patches were exposed to fluid shear stress of 1, 6, 12, 18, 24, and 30 dyn/cm^2 for 1 h within a parallel-plate flow chamber with a closed loop system by pumping 50 ml DMEM/F12 medium over the cells (Figure 1). Cell detachment generally occurs during the first 30-45 min [23], and therefore 1 h shear stress exposure was used to assess cell retention. Three patches per group served as static control to assess the cell number in the absence of fluid shear stress. To investigate the effect of flow preconditioning on endothelial cell attachment and function, cells were seeded and incubated overnight on 6 AAc SiHF-Col patches. Then the cells were preconditioned (12 dyn/cm^2 fluid shear stress for 24 h) in a parallel-plate flow chamber. Once a patch with cells was mounted in the flow chamber for flow preconditioning, the flow loop system was moved to a 37°C incubator, and the flow rate was initiated at 10 ml/min and ramped up to the desired flow rate in increments of 10 ml/min every 15 min. Endothelial cells were exposed for 24 h to fluid shear stress after the target flow rate equivalent to a fluid shear stress of 12 dyn/cm^2 was achieved (see "shear stress modeling" for details). To assess the response of preconditioned endothelial cells to high fluid shear stress, i.e. cell retention and anti-thrombotic function, three of the patches with preconditioned cells were exposed to 30 dyn/cm^2 for 1 h, and another three patches served as static control.

Shear stress modeling in a parallel-plate flow chamber

To estimate the inlet flow rate corresponding to the desired shear stress on surface-modified SiHF patches, as well as the fluid shear stress distribution on the one raw of endothelial cells with or without preconditioning, a three-dimensional FE model was developed using commercially available software, COMSOL Multiphysics (Ver. 4.4, COMSOL Inc., TU Delft, Delft, The Netherlands). First, a section of the parallel-plate flow chamber consisting of a SiHF patch (25 mm x 66 mm x 1.4 mm) without considering endothelial cells was constructed in COMSOL (Figure 2a), with 1541300 tetrahedral mesh elements (Figure 2b) to achieve the

inlet flow rate for each desired shear stress. Table 1 summarizes the model geometry and other parameters used in the simulation. The model solution was confirmed to be mesh-independent by comparing solutions based on different meshing schemes.

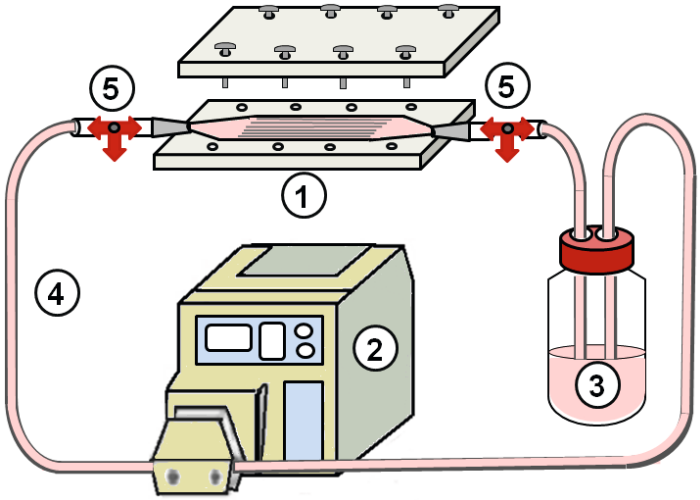

Figure 1. Schematic of a closed loop system used to expose endothelial cells to fluid shear stress of different magnitude. (1) Parallel-plate flow chamber containing cell-seeded silicone hollow fiber patch, (2) Peristaltic pump, (3) Medium reservoir, (4) Polyvinylchloride tubing, (5) Check valves.

Table 1. A list and description of the symbols used in the simulation.

Symbol	Value, units	Description
L	66 mm	Length of the flow chamber
W	25 mm	Width of the flow chamber
H	1.4 mm	Height of the flow chamber
D	0.8 mm	Outer diameter of silicone hollow fiber
D_h	0.65 mm	Hydraulic diameter
μ	0.001 Pa s	Dynamic viscosity of the culture medium at 37°C
ρ	1000 kg/m^3	Density of the culture medium at 37°C
τ_w	dyn/cm^2	Wall shear stress

Navier-Stokes (Equation 1) and Continuity (Equation 2) were solved simultaneously to compute the flow field within the flow chamber [24]:

$$\rho(u.\nabla)u=\nabla.[-p+\mu(\nabla u)]+\rho g \quad (1)$$

$$\rho\nabla.(u)=0 \quad (2)$$

where u is the local velocity, μ is the fluid dynamic viscosity, p is the fluid pressure, and g is the gravity constant. The fluid inlet velocity boundary condition is given as [17]:

$$u(z)=6\,V_m\,(z/H)(1-z/H) \quad (3)$$

where V_m is the averaged input velocity, z is the direction normal to the flow direction, and H is the height of the parallel-plate flow chamber. The inlet flow was considered to be non-oscillatory which is consistent with the pump characteristics used in the experiments. Fluid pressure was set to zero at the outlet of the parallel-plate flow chamber. No-slip boundary condition was used for all surfaces. The culture medium was modeled as a Newtonian fluid with a density of 1000 kg/m^3 and a viscosity of 0.001 Pa.s similar to the actual experimental condition. The Reynolds number was calculated using the hydraulic diameter (D_h):

$$Re=\frac{\rho V_m D_h}{\mu},\ D_h=\frac{4A}{P} \quad (4)$$

where ρ is the fluid density, μ is the fluid viscosity, A is the cross-sectional area of the flow chamber, and P is the wetted premeter. A and P were calculated by considering the presence of a SiHF patch in the parallel-plate flow chamber (Figure 2a):

$$A=A_{chamber}-A_{SiHF\ patch}=(W\times H)-(29\times\frac{\pi D^2}{4}) \quad (5)$$

$$P=P_{SiHF\ patch}+P_{chamber}=(29\times\pi D)+(2\times(H-\frac{D}{2})+2\times W) \quad (6)$$

where W is the width of the chamber, H is the height of the chamber, and D is the outer diameter of silicone hollow fiber. Reynolds number at all velocities used in this study was below 70, which is well below the laminar Reynolds number threshold (Reynolds number = 2300).

Flow preconditioning of cells affects their morphology [25-27]. To investigate flow alteration in the presence of cells with different morphologies, a row of cells on 1 mm of a single fiber was created in Solidworks (Version 2011, TU Delft, Delft, The Netherlands) as a wavy surface using the dimensions described by Barbee et al. (1994; Cells without flow preconditioning: average height 3.4 μm, length 31 μm; flow preconditioned cells: average height 1.8 μm, length 40 μm;

Figure 3) [26]. Then, the fiber together with overlying cells was imported to COMSOL, placed into a small chamber (1.4 x 1 x 0.9 mm) and meshed using 21300 tetrahedral elements. Boundary conditions were imposed exactly the same as for the entire parallel-plate flow chamber, and the shear stress distribution was quantified in the flow direction along the centerline of the row of cells.

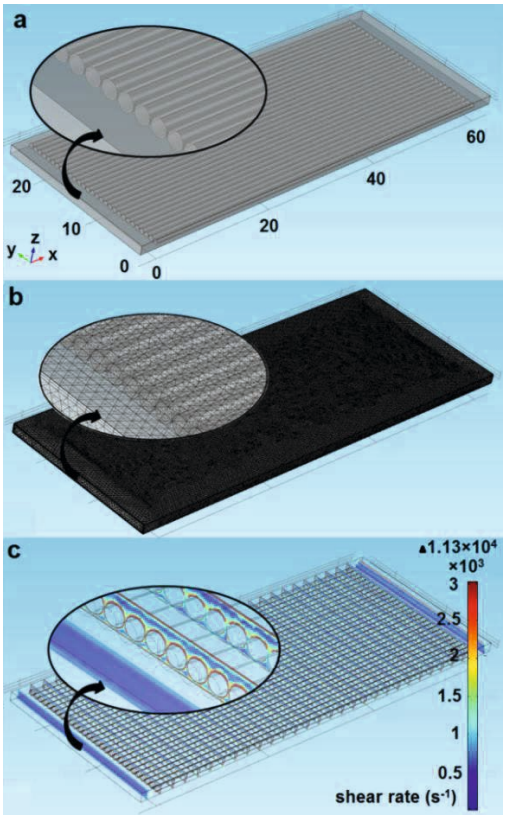

Figure 2. FE modeling of fluid shear stress rate on a SiHF patch in a parallel-plate flow chamber. (a) Geometry, (b) FE mesh grid, and (c) Shear rate distribution at a mean shear stress of 30 dyn/cm^2. The shear rate is higher on the top surface of the fibers compared with the space between the fibers. FE, finite element.

Effect of fluid shear stress on endothelial cell detachment from surface-modified SiHF patches

Confluent (100%) endothelial cell monolayers on surface-modified SiHF patches were subjected to fluid shear stress. A critical shear stress ($\tau_{critical}$) was defined at which 10% of cells were detached from the patches. The optimal fluid shear stress driven by fluid (τ_D) was assumed to be lower than $\tau_{critical}$ to retain cell confluency on the patches (confluency> 90%):

$\tau_D < \tau_{critical}$

After exposure to fluid shear stress, the attached cells on each static (control) or fluid shear stress-exposed SiHF-Col and AAc SiHF-Col patches were washed with PBS, released with trypsin/EDTA (Merck, Kenilworth, NJ, USA), and stained with 0.4% trypan blue (Sigma-Aldrich, St. Louis, MO, USA) to determine the number of viable cells in a Neubauer cell counting chamber. The percentage of detached cells was calculated from the cell counts on shear stress-exposed patches and on control patches.

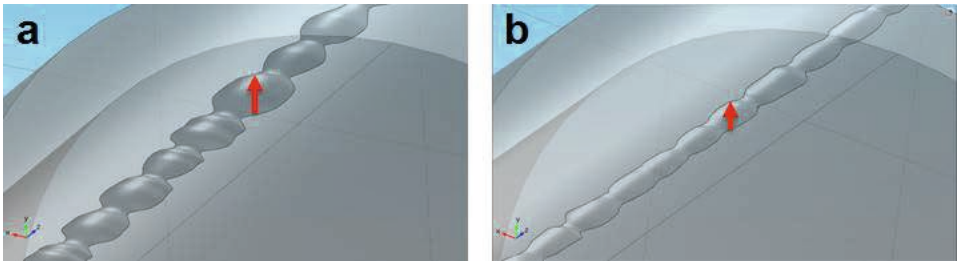

Figure 3. Model geometry of a row of endothelial cells on part of one hollow fiber in a parallel-plate flow chamber. (a) Cells without preconditioning with an average height of 3.4 µm and length of 31 µm, and (b) Preconditioned cells by 12 dyn/cm^2 shear stress with an average height of 1.8 µm and length of 40 µm. The arrows point toward the cell surface with their base touching the fiber's surface.

NO and PGI_2 determination

After exposure of each endothelial cell-seeded SiHF-Col, and AAc SiHF-Col patches to 12 or 30 dyn/cm^2 shear stress for 1 h, 0.5 ml of the medium was collected from the medium reservoir (Figure 1) to determine NO and PGI_2 production. NO production was measured as nitrite (NO_2^-) accumulation in the medium, using Griess reagent containing 1% sulfanilamide, 0.1% naphtylethelene-diamine-dihydrochloride, and 2.5 M H_3PO_4 [28]. Serial dilutions of $NaNO_2$ in medium were used to generate the standard curve. The absorbance was measured at 545 nm with a microplate reader (Stat Fax-2100, Miami, FL, USA). PGI_2 production was measured by measuring the concentration of its stable metabolite 6-keto-prostaglandin $F_{1\alpha}$ (6-keto-$PGF_{1\alpha}$) using a 6-keto-$PGF_{1\alpha}$ enzyme immunoassay kit (Enzo, Lorrach, Germany) according to the manufacturer's protocol [29]. Results were normalized for the number of attached cells on the SiHF-Col and AAc SiHF-Col patches. Endothelial cell detachment, as well as NO and PGI_2 release was also determined for preconditioned endothelial cells on AAc SiHF-Col patches after exposure to 30 dyn/cm^2 shear stress and compared with the response of endothelial cells without flow preconditioning.

Statistical analysis
All data were expressed as means ± standard deviation (SD). To compare any significant differences between surface-modified SiHF patches, one-way analysis of variance was used. The significance of differences among means was determined by post-hoc comparisons, using Bonferroni's method. A probability (p) value of less than 0.05 ($p<0.05$) was taken as the level of significance.

RESULTS

Modeling of fluid shear stress in a parallel-plate flow chamber
The inlet flow rate corresponding to the desired shear stress within the parallel-plate flow chamber was calculated by the FE model. The magnitude of the inlet flow rate (5, 24, 51, 78, 99 and 120 ml/min) was determined based on the target mean fluid shear stress (1, 6, 12, 18, 24, and 30 dyn/cm^2) in the parallel-plate flow chamber including SiHF patch. The geometry, mesh and fluid shear rate contour on the SiHF patch at 30 dyn/cm^2 shear stress are illustrated (Figure 2a-c). Spatial inhomogeneity of the fluid shear rate at 30 dyn/cm^2 in different regions of silicone hollow fibers was observed (Figure 2c).

Introduction of carboxyl groups before collagen immobilization on SiHF patches increased collagen stability under fluid shear stress
Quantification of the collagen content of surface-modified SiHF patches showed that AAc SiHF-Col patches adsorbed 30% more collagen (21.3±3.0 μg/cm^2) compared with SiHF-Col patches (16.3±1.4 μg/cm^2, $p<0.05$; Figure 4). Application of 1, 6, 12, 18, 24, and 30 dyn/cm^2 shear stress did not affect the collagen content of AAc SiHF-Col patches, but there was a shear stress dependent decrease in the amount of collagen on SiHF-Col patches (Figure 4). At 30 dyn/cm^2 shear stress, 64% of the initial collagen content was lost from SiHF-Col patches.

Collagen immobilization increased endothelial cell retention under fluid shear stress
The percentage of detached endothelial cells from surface-modified SiHF patches, i.e. SiHF-Col and AAc SiHF-Col, was determined after 1 h exposure to 1, 6, 12, 18, 24, and 30 dyn/cm^2 fluid shear stress (Figure 5). Cell detachment from SiHF-Col and AAc SiHF-Col patches resulting from 1 or 6 dyn/cm^2 shear stress was similar, while cell detachment from AAc SiHF-Col patches was lower than that from SiHF-Col patches at shear stress magnitudes above 12 dyn/cm^2 (Figure 5). At 30 dyn/cm^2 fluid shear stress, cell detachment from AAc SiHF-Col patches (27%) was 2-fold lower ($p<0.005$) than from SiHF-Col patches (54%). Moreover, $\tau_{critical}$ of AAc

SiHF-Col patches (13 dyn/cm^2) was 1.7-fold higher than SiHF-Col patches (8 dyn/cm^2).

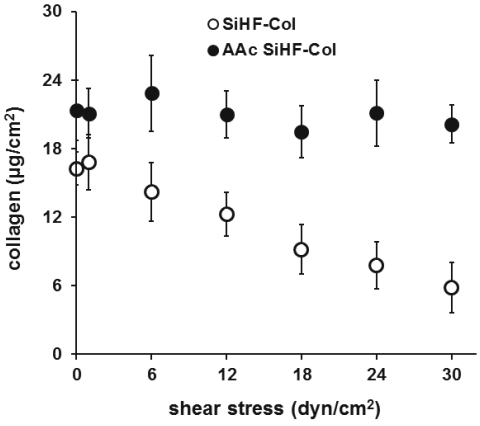

Figure 4. Collagen content of SiHF-Col and AAc SiHF-Col patches after 1 h exposure to 0-30 dyn/cm^2 fluid shear stress. Fluid shear stress did not change the collagen content of AAc SiHF-Col patches, but it decreased the collagen content of SiHF-Col patches. n=3. SiHF-Col, collagen-adsorbed silicone hollow fiber;AAc SiHF-Col, collagen-immobilized AAc-grafted silicone hollow fiber.

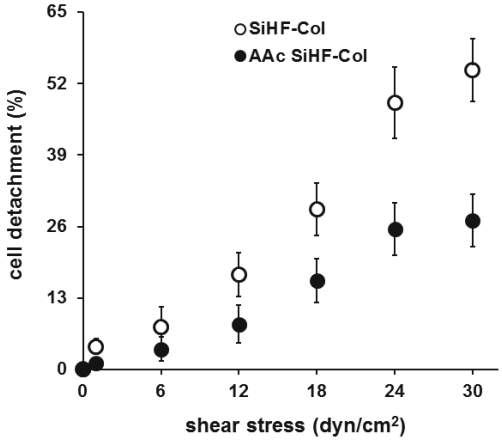

Figure 5. Cell detachment from SiHF-Col and AAc SiHF-Col patches after 1 h exposure to 0-30 dyn/cm^2 fluid shear stress. Cell detachment from SiHF-Col and AAc SiHF-Col patches at 1 or 6 dyn/cm^2 fluid shear stress was similar, but at higher shear stress, cell detachment from AAc SiHF-Col patches was significantly lower than from SiHF-Col patches. n=3. SiHF-Col, collagen-adsorbed silicone hollow fiber; AAc SiHF-Col, collagen-immobilized AAc-grafted silicone hollow fiber.

Flow preconditioning of endothelial cells increased their retention on AAc SiHF-Col patches under fluid shear stress

The total number of endothelial cells on AAc SiHF-Col patches after 2 days of culture and before exposure to shear stress was 795 ± 46 cells/mm^2 (Table 2). After treatment of endothelial cells with 30 dyn/cm^2 fluid shear stress for 1 h, 27% of the cells on AAc SiHF-Col patches were detached. Preconditioning of endothelial cells cultured on AAc SiHF-Col patches decreased cell detachment

under 30 dyn/cm^2 fluid shear stress by 8.2-fold compared with endothelial cells without preconditioning (Table 2). The percentage of detached cells from flow preconditioned AAc SiHF-Col patches under 30 dyn/cm^2 fluid shear stress (3.3%) was significantly below the chosen threshold value of 10%, which shows that $\tau_{critical}$ for preconditioned cells on AAc SiHF-Col patches did rise to values above 30 dyn/cm^2.

Table 2. Endothelial cell number on AAc SiHF-Col patches and cell detachment with or without flow preconditioning after 1 h exposure to 30 dyn/cm^2 shear stress. n=3. AAc SiHF-Col, collagen-immobilized AAc-grafted silicone hollow fiber; Preconditioning, exposure of endothelial cells to 12 dyn/cm^2 fluid shear stress for 24 h.

	Preconditioning	
	Without	With
Cell number on static cultured patch (cells/mm^2)	795 ± 46	795 ± 46
Cell detachment after shear stress conditioning (%)	27.2 ± 4.7	3.3 ± 2.1

To investigate the effect of cell morphology changes due to flow preconditioning on fluid shear stress distribution on endothelial cells and consequently on cell detachment, shear stress contour maps under 30 dyn/cm^2 target fluid shear stress were obtained for cells without preconditioning (average height 3.4 μm; Figures 3a and 6a) and for preconditioned cells (average height 1.8 μm; Figures 3b and 6b). Histograms of fluid shear stress on the endothelial cells with and without preconditioning were obtained from the FE model (Figure 6c). Cells without preconditioning experienced a wide range of shear stress values on their surface as a result of the increased cell height. Flow preconditioning on the other hand tailors a smoother surface of the cells, which results in a more homogenous shear stress distribution on the cell's surface (Figure 6c).

The mean, maximum, and minimum shear stress exerted by fluid flow over the hollow fibers was calculated (Table 3). Cells on a hollow fiber increased the maximum shear stress (57% increase for cells without preconditioning, $p<0.005$; 7% increase for preconditioned cells, not significant) and decreased the minimum shear stress (41% decrease for cells without preconditioning, $p<0.005$; 16% decrease for preconditioned cells, $p<0.05$) compared with a hollow fiber without cells. The highest value of the maximum shear stress (48.9 dyn/cm^2) and the lowest value of the minimum shear stress (17.3 dyn/cm^2) were experienced by cells without preconditioning. Reduction in cell height after flow preconditioning decreased the maximum shear stress to 32% ($p<0.005$) and increased the minimum shear stress to 43% ($p<0.005$).

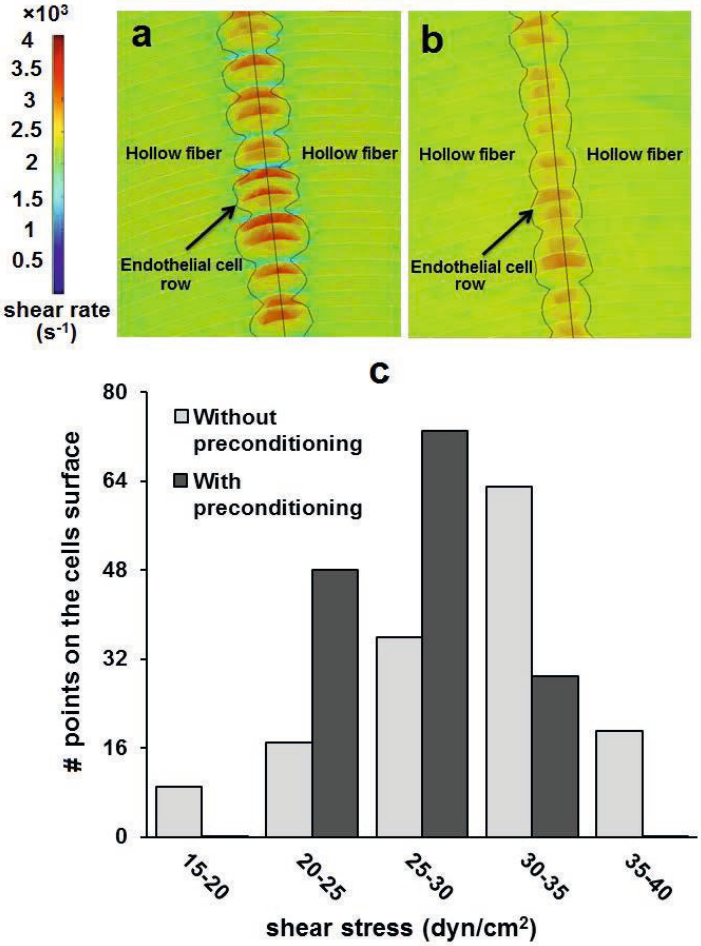

Figure 6. FE modeled shear stress distribution along a hollow fiber of 1 mm at mean fluid shear stress of 30 dyn/cm^2. (a) Fluid shear stress distribution on cells without preconditioning with average height of 3.4 μm, (b) Shear stress distribution on flow preconditioned cells with average height of 1.8 μm, and (c) Histograms of shear stress on the surface of a row of cells either preconditioned or without preconditioning. Higher inhomogeneity of the cell surface without flow preconditioning resulted in a wider shear stress distribution, whereas smoother cell surface associated with preconditioning resulted in a more uniform shear stress distribution. FE, finite element.

Table 3. Mean, maximum, and minimum fluid shear stress experienced by endothelial cells on silicone hollow fiber with and without preconditioning calculated using FE model. As a control, values are also reported for silicone hollow fiber without cells. Preconditioning, exposure of endothelial cells to 12 dyn/cm^2 fluid shear stress for 24 h. *Significant effect after considering cells in the model, p<0.05, **p<0.005, ##Significantly different from endothelial cells on fiber without preconditioning, p<0.005.

	No cells	Preconditioning	
		Without	With
Mean shear stress (dyn/cm^2)	30.0 ± 1.1	34.2 ± 2.1	28.4 ± 1.7
Maximum shear stress (dyn/cm^2)	31.2 ± 2.3	48.9 ± 2.2 **	33.3 ± 2.2 ##
Minimum shear stress (dyn/cm^2)	29.3 ± 1.9	17.3 ± 1.0 **	24.7 ± 2.0 * ##

Collagen immobilization on SiHF patches followed by flow preconditioning increased NO and PGI_2 production under fluid shear stress

The basal NO production by endothelial cells cultured on SiHF-Col and AAc SiHF-Col patches during 1 h static incubation at 37°C was similar (Figure 7). Treatment of cells with 12 dyn/cm^2 fluid shear stress for 1 h increased NO production by 6.1-fold (p<0.0005) by endothelial cells on AAc SiHF-Col patches, and 3.2-fold (p<0.05) by cells on SiHF-Col patches. Treatment with 30 dyn/cm^2 fluid shear stress increased NO production by 1.2-fold (p<0.05) by endothelial cells on AAc SiHF-Col patches, but decreased NO production by 2.3-fold (p<0.05) by cells on SiHF-Col, compared with 12 dyn/cm^2 shear stress treatment.

Basal PGI_2 production by endothelial cells on AAc SiHF-Col and SiHF-Col patches after 1 h static culture was similar (Figure 8). After 1 h of 12 dyn/cm^2 fluid shear stress treatment, PGI_2 production by endothelial cells increased by 2.5-fold (p<0.005) on both SiHF-Col and AAc SiHF-Col patches compared with static controls. After 1 h of 30 dyn/cm^2 fluid shear stress treatment, PGI_2 production was slightly, but not significantly, increased (1.1-fold, p>0.05) on AAc SiHF-Col patches. PGI_2 production by endothelial cells dropped by 1.8-fold (p<0.005) on SiHF-Col patches after exposure to 30 dyn/cm^2 fluid shear stress compared with 12 dyn/cm^2 fluid shear stress.

Thirty dyn/cm^2 fluid shear stress stimulated NO production (1.2-fold, p<0.05) as well as PGI_2 production (1.1-fold, p<0.05) by flow preconditioned endothelial cells on AAc SiHF-Col patches compared with cells without flow preconditioning (Table 4).

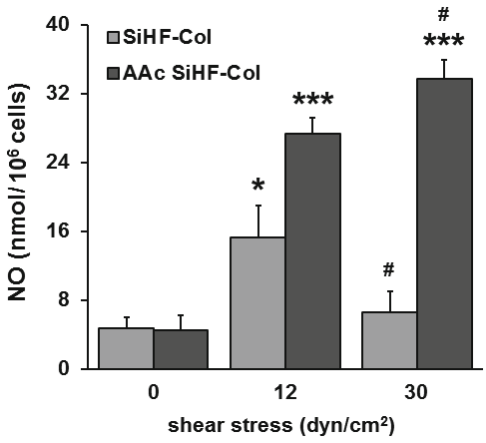

Figure 7. NO produced by endothelial cells on SiHF-Col and AAc SiHF-Col patches after 1 h with or without exposure to 12 and 30 dyn/cm^2 fluid shear stress. Basal NO production by endothelial cells on AAc SiHF-Col and SiHF-Col patches was similar. By increasing the fluid shear stress from 12 to 30 dyn/cm^2, NO production increased by 1.2-fold on AAc SiHF-Col patches, but decreased by 2.3-fold on SiHF-Col patches. n=3. SiHF-Col, collagen-adsorbed silicone hollow fiber; AAc SiHF-Col, collagen-immobilized AAc-grafted silicone hollow fiber. *Significant effect of fluid shear stress, $p<0.05$, ***$p<0.0005$, $^{\#}$Significantly different from patches exposed to 12 dyn/cm^2, $p<0.05$.

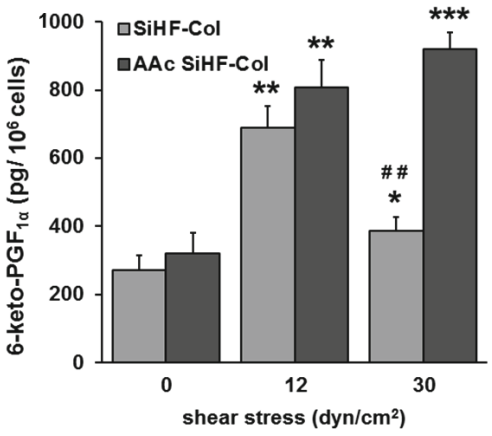

Figure 8. PGI_2 production by endothelial cells on SiHF-Col and AAc SiHF-Col patches after 1 h with or without exposure to 12 and 30 dyn/cm^2 fluid shear stress. Basal PGI_2 production (measured as 6-keto-$PGF_{1\alpha}$, the stable metabolite of PGI_2) by endothelial cells on AAc SiHF-Col and SiHF-Col patches was similar. By increasing the fluid shear stress from 12 to 30 dyne/cm^2, PGI_2 release increased by 1.1-fold on AAc SiHF-Col patches, but decreased by 1.8-fold on SiHF-Col patches. n=3. SiHF-Col, collagen-adsorbed silicone hollow fiber; AAc SiHF-Col, collagen-immobilized AAc-grafted silicone hollow fiber. *Significant effect of fluid shear stress, $p<0.05$, **$p<0.005$, ***$p<0.0005$, $^{\#\#}$Significantly different from patches exposed to 12 dyn/cm^2, $p<0.005$.

Table 4. NO and PGI_2 production by endothelial cells on AAc SiHF-Col patches with and without preconditioning after 1 h exposure to 30 dyn/cm^2 fluid shear stress. n=3. AAc SiHF-Col, collagen-immobilized AAc-grafted silicone hollow fiber; Preconditioning, exposure of endothelial cells to 12 dyn/cm^2 fluid shear stress for 24 h. *Significantly different from endothelial cells on AAc SiHF-Col patches without preconditioning, $p<0.005$.

	Preconditioning	
	Without	With
NO (nmol/10^6 cells)	33.6 ± 2.2	42.3 ±3.1*
6-keto-$PGF_{1\alpha}$ (pg/10^6 cells)	918.7 ± 50.6	1053.3 ± 45.3*

DISCUSSION

Endothelial cell seeding of blood contacting parts of SiHFs in artificial lungs is a first stepping stone towards developing biohybrid artificial lungs [3]. The attached endothelial cell layer provides a biocompatible surface for blood-cell interaction if the cells are maintained in a stable, anti-thrombotic phenotype [6]. However, rapid loss of cells after exposure to fluid shear stress during blood circulation in biohybrid artificial lungs causes a problem. Coating of SiHFs with collagen, the main ECM protein, improves endothelial cell adhesion [6, 8]. The stability of a collagen coating is a major issue, since collagen detachment from a SiHF's surface initiates cells detachment. Flow preconditioning of endothelial cells stimulates their retention on SiHFs under high shear stress similar to that observed in vascular grafts [11-15].

To our best of knowledge, we are the first to investigate the effect of surface modification of SiHFs by collagen immobilization and flow preconditioning of endothelial cells on endothelial cell retention and anti-thrombotic function. Collagen was immobilized on SiHF patches using AAc grafting as described earlier [8]. SiHF patches with adsorbed collagen was used for comparison. Collagen-surface binding stability and cell retention under 1 to 30 dyn/cm^2 shear stress was assessed. Preconditioning with 12 dyn/cm^2 fluid shear stress for 24 h of endothelial cells on surface-modified SiHF patches encased in a custom-made parallel-plate flow chamber was performed to investigate whether preconditioning affects cell retention and/or anti-thrombotic function. FE modeling allowed to correlate the fluid shear stress distribution on the cell surface with the cell biological response.

Collagen did not detach from AAc SiHF-Col patches after treatment with 1 to 30 dyn/cm^2 fluid shear stress, showing that carbodiimide bonds between carboxyl groups of AAc-grafted SiHF patches and amine groups of collagen are stable enough to withstand shear stress. However, detached collagen from SiHF-Col patches depends on the magnitude of the applied fluid shear stress. The $\tau_{critical}$, fluid shear stress at which 10% of the cells were detached was higher for AAc

SiHF-Col patches than for SiHF-Col patches, showing that AAc SiHF-Col patches better support cell retention under high fluid shear stress compared with SiHF-Col patches. More than 30% of endothelial cells on SiHF-Col patches detached at fluid shear stress of 18 dyn/cm^2 or higher. It is possible that the cells got detached as a result of collagen detachment, which was relatively weakly bound to the SiHF-Col patches. AAc SiHF-Col patches retained cells well under different levels of fluid shear stress, but 27% of cells did still detach at the maximum shear stress of 30 dyn/cm^2 as used in this study. Since collagen did not detach from AAc SiHF-Col patches under 30 dyn/cm^2 fluid shear stress, cell detachment might not have occurred due to collagen detachment, but rather as a result of weak bonds between cellular integrins and collagen under high shear stress.

Flow preconditioning of endothelial cells increases cell binding affinity to a collagen coating thereby increasing cell retention [11-15]. Furthermore, exposure to fluid shear stress influences endothelial cell morphology, mechanical properties, phenotype, ability to adhere to a surface, viability, proliferation, and differentiation [13]. Fluid shear stress affects cellular organization and cell biological responses [25-27]. For example, aortic endothelial cells show increased local elasticity (from 0.87±0.23 to 1.75 ±0.43 kPa) [30], and decreased height-to-length ratio (from 0.11±0.02 to 0.05±0.01 μm) [26] after applying 12 dyn/cm^2 fluid shear stress. Our results suggest that 24 h preconditioning of endothelial cells on AAc SiHF-Col patches with 12 dyn/cm^2 fluid shear stress significantly increased cell retention by 33%.

The cell adhesion force should be higher than the hydrodynamic forces generated by a fluid flow to allow the creation of a stable layer of endothelial cells. Integrin-mediated cell adhesion force depends on the number of integrins per cell, as well as on the cell surface area involved in attachment by integrins [31]. Flow preconditioning of endothelial cells induces conformational activation of integrins and increased binding to ECM ligands [15, 16]. It also increases cell surface area involved in integrin-mediated adhesion as a consequence of cell flattening [14, 17]. In addition, cell flattening after flow preconditioning might reduce shear stress gradients at the cell surface, resulting in decreased cell detachment [17, 26]. To investigate the effect of cell flattening on fluid shear stress distribution on hollow fibers, two rows of cells corresponding to cells with and without preconditioning were modeled using COMSOL. The control situation where no cells were seeded on hollow fibers was also studied for comparison. Our results showed that by decreasing the cell height after flow preconditioning, the mean and maximum shear stress experienced by the cells also decreased, and therefore a more homogeneous fluid shear stress distribution was obtained. The fluid shear stress simulation values on hollow fibers without cells showed 1.8 dyn/cm^2 difference between maximum and minimum shear stress, while they showed 31.6 dyn/cm^2 difference between maximum and minimum shear stress after considering cells

without flow preconditioning. This shows that the presence of cells leads to a wider shear stress distribution than when cells were not considered. However, by decreasing the cell height following flow preconditioning, the difference between maximum and minimum shear stress decreased to 8.6 dyn/cm^2. These values indicate that cell geometry changes in different conditions are critical when analyzing cellular biologic responses.

The anti-thrombotic phenotype of endothelial cells cultured on surface-modified, and/or flow preconditioned SiHF patches under fluid shear stress was determined by measuring NO and PGI_2 production. Both NO and PGI_2 are known for their anti-thrombotic effect [19, 32, 33]. Fluid shear stress stimulates the release of NO, C-type natriuretic peptide, and PGI_2 through elevated intracellular Ca^{2+} and increased transcription of endothelial NO synthase mRNA and C-type natriuretic peptide mRNA [20, 29]. Our data suggest that NO and PGI_2 production by endothelial cells cultured on surface-modified SiHF patches increased after applying 12 dyn/cm^2 fluid shear stress. These findings are in agreement with numerous other reports demonstrating increased endothelial-derived anti-thrombotic factors in response to laminar shear stress [32, 33]. High shear stress (30 dyn/cm^2) stimulated NO and PGI_2 production by endothelial cells cultured on AAc SiHF-Col patches, but decreased production of these factors by cells on SiHF-Col patches. An explanation for this observation might be an altered response of loosely attached endothelial cells on the surface of SiHF-Col patches compared with stably attached endothelial cells on the surface of AAc SiHF-Col patches. Flow preconditioning of endothelial cells with 12 dyn/cm^2 shear stress for 24 h significantly increased NO and PGI_2 production when subjected to high fluid shear stress, showing that flow preconditioning not only increases cell retention under high shear stress, but also enhances anti-thrombotic capability of endothelial cells.

In conclusion, endothelial cell stability and anti-thrombotic function was enhanced after collagen immobilization of SiHF patches and flow preconditioning at 12 dyn/cm^2 fluid shear stress for 24 h. FE modeling of fluid shear stress experienced by endothelial cells did establish a quantitative relation between fluid shear stress and endothelial cell behavior, which might be important to ensure a stable, functional, and effective endothelial cell layer on hollow fibers and in developing biohybrid artificial lungs. Our findings can also be extended to adoption of optimal fluid flow rates in geometrically similar parallel-plate flow chambers to maximize their functionality and efficacy for applications in biological and medical field.

ACKNOWLEDGMENTS

The authors are grateful to Dr Atefeh Solouk for valuable advice on plasma graft polymerization of silicone tubes and Mr. Javad Akbari for good tips in the simulation process.

REFERENCES

1 Betit P. Extracorporeal membrane oxygenation: Quo vadis? Respir Care 2009;54:948-957.
2 Lemon G, Lim ML, Ajalloueian F, Macchiarini P. The development of the bioartificial lung. Br Med Bull 2014;110:35-45.
3 Polk AA, Maul TM, McKeel DT, Snyder TA, Lehocky CA, Pitt B, Stolz DB, Federspiel WJ, Wagner WR. A biohybrid artificial lung prototype with active mixing of endothelialized microporous hollow fibers. Biotechnol Bioeng 2010;106:490-500.
4 Thevenot P, Hu W, Tang L. Surface chemistry influence implant biocompatibility. Curr Top Med Chem 2008;8:270-280.
5 Solouk A, Cousins BG, Mirzadeh H, Seifalian AM. Application of plasma surface modification techniques to improve hemocompatibility of vascular grafts. Biotechnol Appl Biochem 2011;58:311-327.
6 Takagi M, Shiwaku K, Inoue T, Shirakawa Y, Sawa Y, Matsuda H, Yoshida T. Hydrodynamically stable adhesion of endothelial cells onto a polypropylene hollow fiber membrane by modification with adhesive protein. J Artif Organs 2003;6:222-226.
7 Hauser J, Zietlow J, Köller M, Esenwein SA, Halfmann H, Awakowicz P, Steinau HU. Enhanced cell adhesion to silicone implant material through plasma surface modification. J Mater Sci Mater Med 2009,20:2541-2548.
8 Salehi-Nik N, Amoabediny G, Shokrgozar MA, Mottaghy K, Klein-Nulend J, Zandieh-Doulabi B. Surface modification of silicone tubes by functional carboxyl and amine, but not peroxide groups followed by collagen immobilization improves endothelial cell stability and functionality. Biomed Mater 2015;10:015024.
9 Lin Q, Ding X, Qiu F, Song X, Fu G, Ji J. In situ endothelialization of intravascular stents coated with an anti-CD34 antibody functionalized heparin–collagen multilayer. Biomaterials 2010;31:4017-4025.
10 Wissink MJB, Beernink R, Poot AA, Engbers GH, Beugeling T, van Aken WG, Feijen J. Improved endothelialization of vascular grafts by local release of growth factor from heparinized collagen matrices. J Control Release 2000;64:103-114.
11 Isenberg BC, Williams C, Tranquillo RT. Endothelialization and flow conditioning of fibrin-based media-equivalents. Ann Biomed Eng 2006;34:971-985.
12 Ott MJ, Ballermann BJ. Shear stress-conditioned, endothelial cell-seeded vascular grafts: improved cell adherence in response to in vitro shear stress. Surgery 1995;117:334-339.
13 Vara DS, Punshon G, Sales KM, Sarkar S, Hamilton G, Seifalian AM. Endothelial cell retention on a viscoelastic nanocomposite vascular conduit is improved by exposure to shear stress preconditioning prior to physiological flow. Artif Organs 2008;32:977-981.
14 Dardik A, Liu A, Ballermann BJ. Chronic in vitro shear stress stimulates endothelial cell retention on prosthetic vascular grafts and reduces subsequent in vivo neointimal thickness. J Vasc Surg 1999;29:157-167.
15 McIlhenny SE, Hager ES, Grabo DJ, DiMatteo C, Shapiro IM, Tulenko TN, DiMuzio PJ. Linear shear conditioning improves vascular graft retention of adipose-derived stem cells by upregulation of the $\alpha_5\beta_1$ integrin. Tissue Eng Part A 2010;16:245-255.
16 Tzima E, del Pozo MA, Shattil SJ, Chien S, Schwartz MA. Activation of integrins in endothelial cells by fluid shear stress mediates Rho-dependent cytoskeletal alignment. EMBO J 2001;20:4639-4647.
17 Brown A, Burke G, Meenan BJ. Modeling of shear stress experienced by endothelial cells cultured on microstructured polymer substrates in a parallel plate flow chamber. Biotechnol Bioeng 2011;108:1148-1158.
18 Choi HW, Barakat AI. Modulation of ATP/ADP concentration at the endothelial cell surface by flow: Effect of cell topography. Ann Biomed Eng 2009;37:2459-2468.

19 Traub O, Berk BC. Laminar shear stress: mechanisms by which endothelial cells transduce an atheroprotective force. Arterioscler Thromb Vasc Biol 1998;18:677-685.
20 Frangos JA, Eskin SG, McIntire LV, Ives CL. Flow effects on prostacyclin production by cultured human endothelial cells. Science 1985;227:1477-1479.
21 Qin KR, Xiang C, Xu Z, Cao LL, Ge SS, Jiang ZL. Dynamic modeling for shear stress induced ATP release from vascular endothelial cells. Biomech Model Mechanobiol 2008;7:345-353.
22 Solouk A, Cousins BG, Mirahmadi F, Mirzadeh H, Jalali Nadoushan MR, Shokrgoza MA, Seifalian AM. Biomimetic modified clinical-grade POSS-PCU nanocomposite polymer for bypass graft applications: A preliminary assessment of endothelial cell adhesion and haemocompatibility. Mater Sci Eng C Mater Biol Appl 2015;46:400-408.
23 Feugiera P, Black RA, Hunt JA, How TV. Attachment, morphology and adherence of human endothelial cells to vascular prosthesis materials under the action of shear stress. Biomaterials 2005;26:1457-1466.
24 Huo Y, Choy JS, Svendsen M, Sinha AK, Kassab JS. Effects of vessel compliance on flow pattern in porcine epicardial right coronary arterial tree. J Biomech 2009;42:594-602.
25 Ohashi T, Sato M. Remodeling of vascular endothelial cells exposed to fluid shear stress: experimental and numerical approach. Fluid Dyn Res 2005;37:40-59.
26 Barbee KA, Davies PF, Lal R. Shear stress-induced reorganization of the surface topography of living endothelial cells imaged by atomic force microscopy. Circ Res 1994;74:163-171.
27 Barbee KA. Role of subcellular shear–stress distributions in endothelial cell mechanotransduction. Ann Biomed Eng 2002;30:472-482.
28 Salehi-Nik N, Amoabediny G, Solouk A, Shokrgozar MA, Zandieh-Doulabi B, Klein-Nulend J. Biomimetic modification of silicone tubes using sodium nitrite-collagen immobilization accelerates endothelialization. J Biomed Mater Res B 2015;In press.
29 Noris M, Morigi M, Donadelli R, Aiello S, Foppolo M, Todeschini M, Orisio S, Remuzzi G, Remuzzi A. Nitric oxide synthesis by cultured endothelial cells is modulated by flow conditions. Circ Res 1995;76:536-543.
30 Ohashi T, Ishii Y, Ishikawa Y, Matsumoto T, Sato M. Experimental and numerical analyses of local mechanical properties measured by atomic force microscopy for sheared endothelial cells. Biomed Mater Eng 2002;12:319-327.
31 Shao JY, Xu G. The adhesion between a microvillus-bearing cell and a ligand-coated substrate: A monte carlo study. Ann Biomed Eng 2007;35:397-407.
32 Hsieh HJ, Liu CA, Huang B, Tseng AH, Wang DL. Shear-induced endothelial mechanotransduction: the interplay between reactive oxygen species (ROS) and nitric oxide (NO) and the pathophysiological implications. J Biomed Sci 2014;21:3-18.
33 Kabirian F, Amoabediny G, Haghighipour N, Salehi-Nik N, Zandieh-Doulabi B. Nitric oxide secretion by endothelial cells in response to fluid shear stress, aspirin, and temperature. J Biomed Mater Res A 2015;103:1231-1237.

CHAPTER 4

Biomimetic Modification of Silicone Tubes Using Sodium Nitrite-Collagen Immobilization Accelerates Endothelialization

Nasim Salehi-Nik[1,2], Ghassem Amoabediny[1,2], Atefeh Solouk[3], Mohammad Ali Shokrgozar[4], Behrouz Zandieh-Doulabi[5], Jenneke Klein-Nulend[5]

[1] School of Chemical Engineering, College of Engineering, University of Tehran, Tehran, Iran

[2] Dept of Biomedical Engineering, Research Center for New Technologies in Life Science Engineering, University of Tehran, Tehran, Iran

[3] Dept of Biomedical Engineering, Amirkabir University of Technology, Tehran, Iran

[4] National Cell Bank, Pasteur Institute of Iran, Tehran, Iran

[5] Dept of Oral Cell Biology, Academic Centre for Dentistry Amsterdam, University of Amsterdam and VU University Amsterdam, MOVE Research Institute Amsterdam, Amsterdam, The Netherlands

Biomedical Materials Research Part B: Applied Biomaterials (in press)

ABSTRACT

Biomimetic coatings to increase endothelialization of blood-contacting materials in biomedical devices are promising to improve the biocompatibility of these devices. Although a stable extracellular matrix protein coating on a biomaterial's surface is a prerequisite for endothelial cell attachment, it also stimulates platelet adhesion. Therefore anti-thrombotic additives such as nitric oxide donors to a stable protein coating might lead to successful endothelialization of a material's surface. We aimed to test whether immobilized bioactive nitrite and acidified nitrite-generating sodium nitrite-collagen conjugate on silicone tubes enhances endothelialization by increasing the number of endothelial cells as well as growth hormone production, and by decreasing platelet adhesion. Stable collagen immobilization on acrylic acid-grafted silicone tubes decreased the water contact angle from 102° to 56°. Initial 25 μM sodium nitrite in conjugate resulted in maximal growth hormone production (2.5 fold increase), and endothelial cell number (1.8 fold increase) after 2 days. A 95% confluent endothelial cell monolayer on sodium nitrite-collagen conjugate coating was obtained after 6 days. Maximum (2.7 fold) inhibition of platelet adhesion was reached with initial 500 μM sodium nitrite in conjugate. Our data showing that sodium nitrite-collagen conjugate coating with 25-50 μM sodium nitrite on silicone tubes increases the number of endothelial cells attached and inhibits platelet adhesion, suggest that this coating is highly promising for use in blood-contacting parts of biomedical devices.

Keywords
Surface modification, Acrylic acid grafting, Collagen, Sodium nitrite, Endothelial cells

INTRODUCTION

Endothelial cell seeding of blood-contacting parts of biomedical devices to mimic the function of the normal vascular endothelium is promising to decrease thrombotic complications resulting from blood flows through these devices [1, 2]. The surface of most commercially available materials used in biomedical devices, such as silicone, is highly hydrophobic and does not support endothelial cell attachment [1]. To overcome this limitation, several physicochemical techniques have been employed to improve the properties of silicone through surface modification [2, 3].

A widely used surface modification method is plasma graft polymerization of acrylic acid (AAc), which introduces functional carboxyl groups on an inert silicone surface [4-7]. Nowadays biomimetic coatings incorporating bioactive molecules that can be bound successfully to the carboxyl groups of AAc, such as collagen and gelatin [4, 6], insulin [8], and anticoagulants such as thrombodulin [9], albumin [10], and heparin [9, 11, 12] are extensively used. AAc-grafted materials show improved wettability [4-7], but they negatively affect many cell types when in direct contact [4, 6]. On the other hand, covalent immobilization of collagen onto AAc-grafted materials, through chemical bonds between amino-groups of collagen and carboxyl functional groups of AAc, enhances cell adhesion, proliferation, and differentiation [3, 4, 6]. However, collagen is highly thrombogenic, and accelerates platelet aggregation in those areas of a material which are not fully covered by endothelial cells [11].

Nitric oxide (NO) is an important inhibitor of platelet adhesion [13, 14]. Recently we have shown that treatment of endothelial cells by shear stress, cold temperature, and aspirin stimulates NO production and decreases thrombus formation [15]. NO-releasing material coatings suppress thrombogenic problems in the absence of endothelial cells or in areas which are not fully covered by endothelial cells [13, 14, 16]. In addition to inhibition of platelet adhesion and activation [13, 14], NO regulates amongst others (a.o.) vascular cell proliferation and migration [17], and the production of vascular endothelial growth factor (VEGF) [18] and/or growth hormone (GH) [19]. Nitrite, the stable end-product of NO metabolism, may represent a potential source of NO in an acidic environment [20, 21]. Whether acidified nitrite indeed prevents thrombus formation and increases endothelial cell growth has not yet been unequivocally established.

In this study we aimed to investigate whether incorporation of the nitrite donor sodium nitrite in a collagen coating immobilized on AAc-grafted silicone tubes increases the number of endothelial cells as well as decreases platelet adhesion. A two-step plasma treatment was used to graft AAc on silicone [7]. Collagen and sodium nitrite-collagen conjugate with different initial concentrations of sodium nitrite were added to the lumen of AAc-grafted silicone tubes to allow

collagen immobilization. Collagen content, nitrite and acidified nitrite release, water contact angles of the surface-modified silicone tubes, as well as endothelial cell attachment were determined. The effect of nitrite and acidified nitrite release from the sodium nitrite-collagen conjugate coating on the number of endothelial cells and GH production after 2 days of culture, as well as platelet adhesion, was assessed.

MATERIALS AND METHODS

Materials

Medical grade tubular silicone rubber (inner diameter 2 mm) was kindly donated by Raumedic (Helmbrechts, Germany). AAc was supplied by Fluka (Buchs, Switzerland), and purified by distillation under vacuum to remove impurities and stabilizers. De-ionized water was used in all experiments. Chemicals for the Griess assay were obtained from Merck (Kenilworth, NJ, USA), and were of the highest purity available.

Plasma graft polymerization of AAc onto silicone tubes

A two-step plasma treatment was used to prepare AAc-grafted silicone (AAc Si) tubes [4-7], i.e. plasma pretreated silicone tubes were immersed in an aqueous solution of 30% AAc in water followed by plasma graft copolymerization on a reabsorbed layer of AAc on silicone. A reaction chamber (Seren R600, Anatech ltd, Union City, CA, USA) evacuated to 0.6 mbar and pretreated with 60 W of oxygen plasma was used for 0.5 min plasma pretreatment and for 3 min plasma graft copolymerization of AAc on silicone tubes. The residual monomers and homopolymers were removed by incubation in water for 24 h. The grafted amount of AAc was calculated after weighing the samples before and after graft polymerization as described by Karkhaneh et al [7].

Collagen and sodium nitrite-collagen conjugate immobilization on AAc Si tubes

Sodium nitrite stock solution ($NaNO_2$; Merck, Kenilworth, NJ, USA) at 0.01 M was used to prepare 5, 10, 25, 50, 100, 250, and 500 µM of sodium nitrite in water containing 1 mg/ml collagen (acid soluble collagen type I; Pasteur Institute of Iran, Tehran, Iran) and 0.02 M acetic acid. Solutions were gently shaken for 1 h at 4°C to obtain homogeneous sodium nitrite-collagen conjugates.

AAc Si tubes were immersed into 30 ml 5 mM 2-(N-morpholino) ethanesulfonic acid (MES) buffer solution containing 48 mg 1-Ethyl-3-[3-dimethylaminopropyl] carbodiimide hydrochloride (EDC) and 15 mg N-hydroxysuccinimide (NHS; Fluka, Neu-Ulm, Germany) [22]. The solution was

gently stirred for 5 h at 4°C to activate the carboxyl groups on AAc Si tubes. Then AAc Si tubes with activated carboxyl groups were filled with collagen or sodium nitrite-collagen conjugate for collagen immobilization at 4ºC for 24 h. Collagen-immobilized AAc-grafted silicone (AAc Si-Col) tubes and sodium nitrite-collagen conjugate immobilized AAc-grafted silicone (AAc Si-Nitrite-Col) tubes were washed in water for 1 min to remove unbound proteins and sodium nitrites, and stored at 4ºC. To assess the stability of collagen linked to the tubes, the lumen of AAc Si-Col and AAc Si-Nitrite-Col tubes was washed extensively three times with 5 ml water for 5 min by infusion from one end into the lumen of the tubes using a syringe. The amount of immobilized collagen on AAc Si-Col tubes as well as on AAC Si-Nitrite-Col tubes before and after washing was determined by using a Bradford protein assay (Bradford, MA, USA) according to the manufacturer's instructions [4], followed by quantification in an Eppendorf biophotometer D30 (Eppendorf, Hamburg, Germany). Concentrations of immobilized collagen on surface-modified silicone tubes were assessed by comparison with a standard curve consisting of serial dilutions of collagen.

To verify indirectly that sodium nitrite-collagen conjugate was bound to the silicone, nitrite and acidified nitrite release from AAc Si-Nitrite-Col tubes was measured by Griess assay. The AAc Si-Nitrite-Col tubes were filled with Dulbecco's minimal essential medium/F12 (1/1, v/v) (Gibco, Life Technologies, Grand Island, NY), and incubated for 4 h and 48 h. Nitrite and acidified nitrite release was measured as nitrite (NO_2^-) accumulation in the medium, using Griess reagent containing 1% sulfanilamide, 0.1% naphtylethelene-diamine-dihydrochloride, and 2.5 M H_3PO_4 [23, 24]. Serial dilutions of $NaNO_2$ in the medium were used as standard curve. The absorbance was measured at 540 nm with a microplate reader (Stat Fax-2100, Miami, FL, USA). Nitrite and acidified nitrite release from AAc Si-Nitrite-Col tubes was also expressed as the percentage of the initial sodium nitrite in conjugate (i.e. the total amount of nitrite in the medium divided by the total amount of sodium nitrite in conjugate x100%).

Characterization of surface-modified silicone tubes

Surface-modified silicone tubes were dried for 2 h at room temperature, cut longitudinally, and glued on glass microscope slides to determine surface wettability by the sessile drop method. Five µl double-distilled water droplets were placed on each tube, and the water contact angle was recorded after 1 min using Kruss G10 goniometer contact-angle measurement equipment (Krüss GmbH, Hamburg, Germany). The results are mean values of five water contact angle measurements performed at randomly chosen areas of each silicone tube.

Endothelial cell seeding, adherence, and culture

Human umbilical vein endothelial cells (HUVECs) were obtained from the National Cell Bank, Pasteur Institute of Iran (Tehran, Iran), and used between passages 3 and 6. After surface modification, triplicates of unmodified and surface-modified tubes (inner diameter 0.2 cm, length 3 cm, surface area 1.88 cm^2) were put into petri dishes, sterilized with UV light, and washed twice with PBS and once with culture medium before endothelial cell seeding. One hundred microliters of an endothelial cell suspension containing $3x10^5$ endothelial cells/ml Dulbecco's minimal essential medium/F12 medium with 10% fetal bovine serum (GIBCO, Renfrewshire, Scotland) was added to the lumen of the tubes, which were rotated every 30 min for 4 h to promote homogeneous cell adhesion. Endothelial cells were either cultured in a humidified atmosphere of 5% CO_2 in air at 37°C for 6 days, with medium replacement every 2 days, or used to determine cell attachment at 4 h.

The attached cells were fixed, dehydrated in graded ethanol series, and stained with 5% Giemsa for optical microscopic examination. The number of adhered endothelial cells was determined by using an image-processing system (Image Pro Plus, version 6, Media Cybernetics, Bethesda, MD, USA). Three objective fields were randomly chosen in central and peripheral regions of each tube and the mean number of adhered cells determined. All attachment assays were run in duplicate.

Endothelial cell proliferation and GH production

The MTT (Sigma, St. Louis, MO, USA) assay was used to evaluate endothelial cell proliferation at days 2, 4, and 6 on unmodified and surface-modified silicone tubes as described previously [15, 25]. A calibration curve with known endothelial cell numbers was used to determine the number of cells. At day 6, attached cells were stained with 5% Giemsa, and three random photographs were taken in central and peripheral regions of each tube. The surface area of 50 cells from each photograph was determined by Image Pro Plus 6 software using the pixels per micrometer provided. The area covered with cells of each silicone tubes was determined by multiplying the mean individual cell area by number of cells counted. Cell confluency was expressed as percent of tube surface covered with cells, and was calculated as follows [1]:

% Confluency = [(area covered with cells (mm^2)/total surface area (mm^2)] x100

GH production by endothelial cells cultured on AAc Si-Col or AAc Si Nitrite-Col tubes was determined by electrochemiluminescence. After 2 days of culture the medium was harvested, and GH concentrations quantified using an automatic analyzer (Roche Elecsys 2010, Hitachi, Tokyo, Japan).

Endothelial cell morphology

The morphology of endothelial cells attached to unmodified or surface-modified silicone tubes was assessed by using scanning electron microscopy (SEM; Essen Philips XL 30 ESEM Environmental, Philips, Amsterdam, The Netherlands). The tubes were cut longitudinally to observe cell morphology in the lumen of cell-seeded silicone tubes. After 6 days of culture, the tubes with adhered cells were rinsed with PBS, fixed with 4% (v/v) glutaraldehyde in PBS for 30 min at 4°C, washed with ultrapure water, dehydrated in graded ethanol series, and dried at room temperature. The tubes were mounted on SEM stubs, and gold-coated (10-20 nm thickness) by vapor deposition using a sputter coater with a gold (Au) target for conductance and high resolution imaging. SEM imaging was performed using 20 kV electron accelerating voltage, 15 mm working distance, and magnifications x200, and x1000.

Platelet adhesion on AAc Si-Nitrite-Col tubes

Platelet-rich plasma (PRP) was obtained from the Iranian Blood Transfusion Organization. A final concentration of $15x10^4$ platelets/mm^3 was used, with a viscosity of 1 cp, which is the same as the viscosity of culture medium [26]. Polyethylene glycol-grafted silicone (PEG Si) tubes were prepared as described previously [27] and used as a negative control. In short, plasma pretreated silicone tubes were immersed in PEG/ethanol solution (20 g/l) and physically adsorbed PEG was grafted on silicone using plasma treatment for 3 min. Un-grafted PEG on the silicone surface was removed by washing tubes by methanol.

Each Si, AAc Si, AAc Si-Col, AAc Si-Nitrite-Col, and PEG Si tube added to a centrifuge tube containing 2 ml PRP, and centrifuged at 700xg for 1 h at 37°C. Each tube was run in triplicate. Then silicone tubes were removed from the centrifuge tubes. The number of platelets in the PRP solution was measured by using a blood cell counter (Medonic CA 530, E. Merck, Darmstadt, Germany). Adhesion of platelets to the silicone tubes was calculated as follows [26]:

% Platelet Adhesion= $[(P_s-P_c)/P_s] \times 100$

in which P_s is the number of platelets in the PRP solution before, and P_c is the number of platelets in the same PRP solution after incubation with silicone tube.

Statistical analysis

All data are expressed as mean ± standard deviation. Data were analyzed using one-way analysis of variance, and the significance of differences among means was determined by post-hoc comparisons, using Bonferroni's method. Two way analysis of variance with pairwise comparison was used to assess differences among means between groups and over time. Differences were considered significant if $p<0.05$.

RESULTS

Collagen immobilization on AAc Si tubes

An AAc graft density of 420±28 μg/cm^2 was achieved with 0.5 min pretreatment and 3 min copolymerization. Moreover, the amount of collagen immobilized onto AAc Si-Col tubes was 19.1 μg/cm^2 before extensive washing with water, and 18.8 μg/cm^2 after washing, indicating stable collagen bonding on the AAc Si tubes (Table 1). There was no significant difference between the amount of collagen immobilized on AAc Si-Col tubes and on AAc Si-Nitrite-Col tubes with 500 μM sodium nitrite (the highest concentration used in this study) in conjugate before ($p=0.36$) and after ($p=0.7$) washing.

Table 1. Collagen adsorbed on AAc Si-Col, and AAc Si-Nitrite-Col tubes with 500 μM sodium nitrite in conjugate before and after washing. Values are mean ± standard deviation for 3 independent experiments.

Tube, surface modification	Abbreviation	Acrylic acid graft density (μg/cm^2)	Collagen adsorbed before washing (μg/cm^2)	Collagen adsorbed after washing (μg/cm^2)
Collagen immobilized acrylic acid-grafted silicone	AAc Si-Col	420 ± 28	19.1 ± 3.0	18.8 ± 1.7
Sodium nitrite-collagen conjugate immobilized acrylic acid-grafted silicone	AAc Si-Nitrite-Col	420 ± 28	21.2 ± 1.9	18.1 ± 2.6

Nitrite and acidified nitrite release from AAc Si-Nitrite-Col tubes

A scheme of the suggested mechanism for the conjugation of sodium nitrite to collagen and release of nitrite and acidified nitrite from the sodium nitrite-collagen conjugate immobilized on silicone tubes is depicted in Figure 1. The absolute amount of nitrite and acidified nitrite released from AAc Si-Nitrite-Col tubes with 0-500 μM sodium nitrite in conjugate was measured as nitrite accumulation in the medium at 4 h (Figure 2A), and 48 h (Figure 2B). At both 4 and 48 h, there was a dose-dependent relationship between the initial sodium nitrite concentration in the sodium nitrite-collagen conjugate coating of AAc Si-Nitrite-Col tubes and the amount of nitrite and acidified nitrite released (Figure 2). Nitrite and acidified nitrite release from AAc Si-Nitrite-Col tubes with 0-500 μM sodium nitrite in conjugate at 4

and 48 h was also expressed as percentage of the initial sodium nitrite concentration in conjugate (Figure 2C,D). The percentage nitrite and acidified nitrite released of the initial sodium nitrite in conjugate from AAc Si-Nitrite-Col tubes was ranging from 6% (AAc Si-Nitrite-Col tubes with 500 µM sodium nitrite in conjugate) to 12% (AAc Si-Nitrite-Col tubes with 10 µM sodium nitrite in conjugate) at 4 h (Figure 2C), and from 46% (AAc Si-Nitrite-Col tubes with 50 µM sodium nitrite in conjugate) to 57% (AAc Si-Nitrite-Col tubes with 100 µM sodium nitrite in conjugate) at 48 h (Figure 2D).

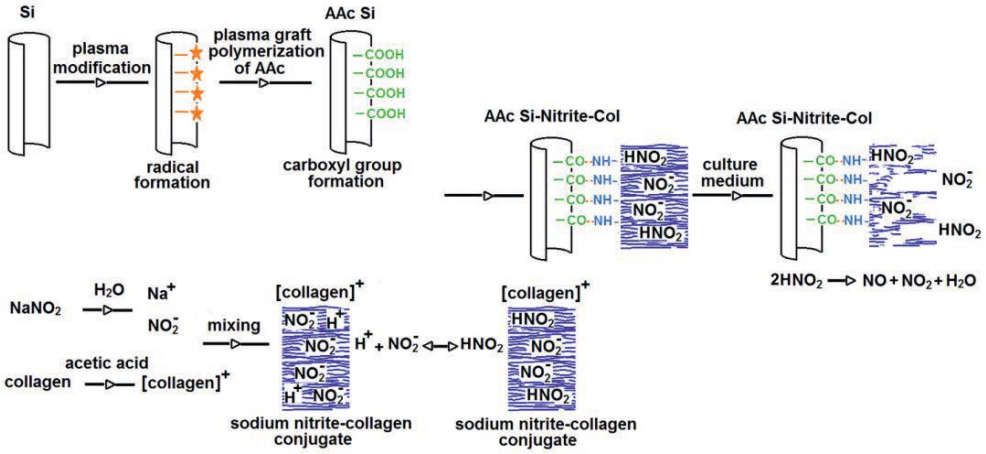

Figure 1. Sodium nitrite ($NaNO_2$) dissociates into ions (Na^+, NO_2^-) after dissolving in water. The acetic acid used to dissolve collagen in water causes an acidic condition (pH~3) resulting in positively charged amino acids along the collagen molecule, thereby making the entire collagen molecule positively charged. After adding sodium nitrite solution to the collagen solution, the negatively charged NO_2^- ions are electrostatically entrapped within positively charged collagen chain entanglements, and sodium nitrite-collagen conjugate is made. Some of the entrapped NO_2^- ions convert to nitrous acid (HNO_2) in the acidic environment of the collagen solution. Conjugate mixing at 4°C prevents fast decomposition of HNO_2. By adding the sodium nitrite-collagen conjugate into AAc Si tubes, the carboxyl groups of AAc generate carbodiimide bonds with collagen, and help to immobilize sodium nitrite-collagen conjugate on the silicone surface. By filling the AAc Si-Nitrite-Col tubes with aqueous cell culture medium, the polymeric collagen might swell resulting in the release of the entrapped NO_2^- and HNO_2. HNO_2 can then easily decompose into NO, NO_2, and H_2O at 37°C.

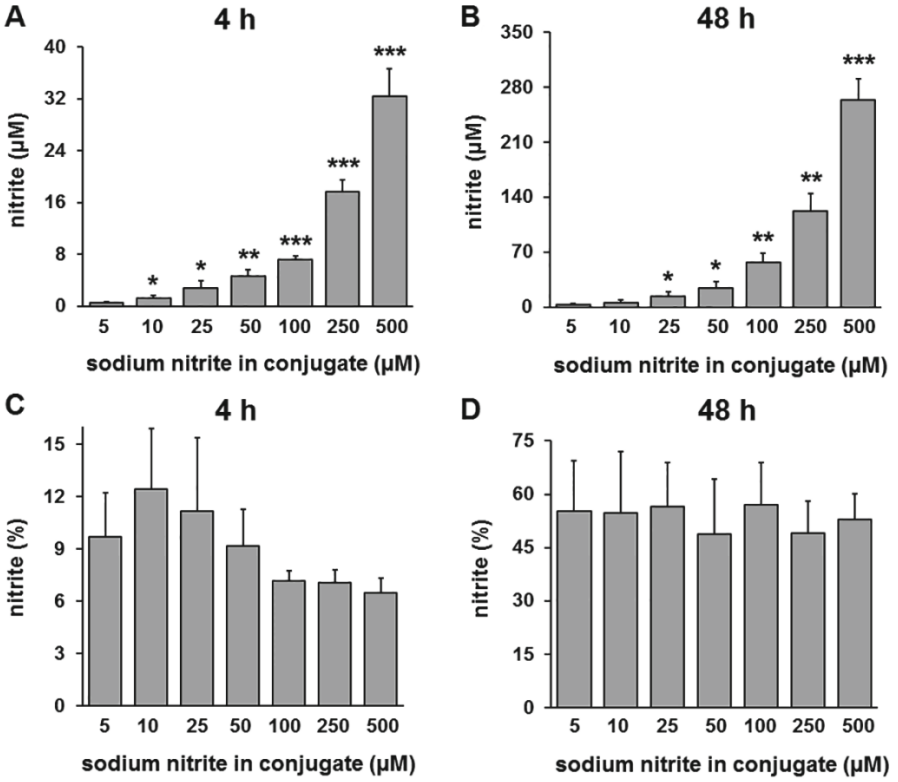

Figure 2. Nitrite and acidified nitrite release from AAc Si-Nitrite-Col tubes measured as nitrite accumulation in the culture medium at 37°C after 4 and 48 h. Nitrite and acidified nitrite release (in µM) from AAc Si-Nitrite-Col tubes increased with increasing the initial sodium nitrite concentrations in conjugate at (A) 4 h and (B) 48 h. Nitrite and acidified nitrite release (in % of the amount of initial sodium nitrite in conjugate) from AAc Si-Nitrite-Col tubes ranged from 6% to 12% at (C) 4 h, and from 46% to 57% at (D) 48 h. n=3. AAc Si-Nitrite-Col, sodium nitrite-collagen conjugate immobilized AAc-grafted silicone. *Significantly different from 5 µM sodium nitrite in conjugate, $p<0.05$, **$p<0.005$, and ***$p<0.0005$.

Wettability and endothelial cell adhesion on surface-modified silicone tubes

The wettability and cell adhesion on surface-modified tubes, e.g. AAc Si, AAc Si-Col, and AAc Si-Nitrite-Col, were assessed and compared with Si tubes (Table 2). The average water contact angle of silicone tubes was >50% decreased after AAc grafting (Si: 102°±4°; AAc Si: 42°±2°). Collagen coating of AAc Si tubes increased the water contact angle from 42°±2° (AAc Si) to 56°±2° (AAc Si-Col). The water contact angles of AAc Si-Col tubes and AAc Si-Nitrite-Col tubes with 5-500 µM

sodium nitrite in conjugate were similar, ranging from 51° to 56°. The number of endothelial cells attached to AAc Si-Col tubes and AAc Si-Nitrite-Col tubes with 5-500 µM sodium nitrite in conjugate was also similar, ranging from 98 cells/mm^2 to 115 cells/mm^2. The number of endothelial cells attached to AAc Si-Nitrite-Col tubes with 500 µM sodium nitrite in conjugate was similar to the number of cells attached to AAc Si-Col tubes, and 1.8-fold higher ($p<0.005$) than the number of cells attached to Si tubes (AAc Si-Nitrite-Col tubes: 110±8 cells/mm^2; AAc Si-Col tubes: 115±14 cells/mm^2; Si tubes: 63±12 cells/mm^2, mean±SD). Only few endothelial cells were attached to AAc Si tubes; the number of cells attached to Si tubes was 3-fold higher ($p<0.005$) than the number of cells attached to AAc Si tubes (Si tubes: 63±12 cells/mm^2; AAc Si tubes: 21±5 cells/mm^2, mean±SD).

Table 2. Wettability and endothelial cell attachment to Si, AAc Si, AAc Si-Col, and AAc Si-Nitrite-Col tubes with 5-500 µM sodium nitrite in conjugate. Inner diameter silicone tube: 2 mm; length tube: 30 mm. Tubes were incubated with 3x10^5 endothelial cells/ml, and cell attachment was determined after 4 h. Listed are also the abbreviations used for the different surface modifications used in this study. Values are mean ± standard deviation for 3 independent experiments.

Tube, surface modification	Abbreviation	Wettability, water contact angle (°)	Number of adhered cells, (cells/mm^2)
Silicone	Si	102.1 ± 4.0	63 ± 12
Acrylic acid-grafted silicone	AAc Si	42.2 ± 2.0	21 ± 5
Collagen immobilized acrylic acid-grafted silicone	AAc Si-Col	56.3 ± 2.0	115 ± 14
Sodium nitrite-collagen conjugate immobilized acrylic acid-grafted silicone with different sodium nitrite concentrations in conjugate (µM)	AAc Si-Nitrite-Col		
5 µM		53.1 ± 1.5	101 ± 10
10 µM		54.4 ± 3.5	112 ± 5
25 µM		56.2 ± 4.0	104 ± 3
50 µM		51.5 ± 3.1	100 ± 13
100 µM		52.2 ± 1.8	115 ± 9
250 µM		54.3 ± 2.7	98 ± 11
500 µM		55.2 ± 3.0	110 ± 8

AAc Si-Nitrite-Col tubes affect GH production by endothelial cells

AAc Si-Nitrite-Col tubes with different concentrations of sodium nitrite caused a dose-dependent increase in GH production by endothelial cells, with a maximum effect at 25 μM initial sodium nitrite in the conjugate (Figure 3). The amount of GH produced by endothelial cells on AAc Si-Nitrite-Col tubes with 25 μM initial sodium nitrite was 2.5-fold higher ($p<0.005$) than on AAc Si-Col tubes, 1.6-fold higher ($p<0.05$) than on AAc Si-Nitrite-Col tubes with 50 μM initial sodium nitrite, and 2-fold higher ($p<0.05$) than on AAc Si-Nitrite-Col tubes with 500 μM initial sodium nitrite in the conjugate.

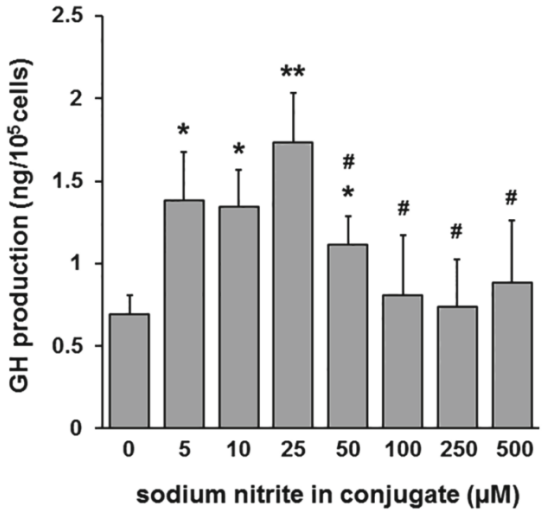

Figure 3. Effect of the initial sodium nitrite concentration in a sodium nitrite-collagen conjugate coating of AAc Si-Nitrite-Col tubes on GH production by endothelial cells after 2 days of culture. Initial sodium nitrite concentration of 5-50 μM in sodium nitrite-collagen conjugate coating resulted in enhanced GH production, with a maximum effect at 25 μM sodium nitrite in the conjugate. AAc Si-Nitrite-Col, sodium nitrite-collagen conjugate immobilized AAc-grafted silicone. *Significant effect of sodium nitrite in conjugate compared to control without sodium nitrite, $p<0.05$, **$p<0.005$, #Significantly different from 25 μM sodium nitrite in conjugate, $p<0.05$.

AAc Si-Nitrite-Col tubes affect endothelial cell proliferation

Initial sodium nitrite concentrations of 5-50 μM in the conjugate increased, but concentrations higher than 50 μM sodium nitrite did not affect endothelial cell number on AAc Si-Nitrite-Col tubes (Figure 4). Maximal stimulation of cell number

after 2 days was obtained when cells were cultured on AAc Si-Nitrite-Col tubes with 25 μM initial sodium nitrite in the conjugate. The number of endothelial cells on AAc Si-Nitrite-Col tubes with 25 μM initial sodium nitrite was 1.8-fold higher ($p<0.005$) than on AAc Si-Col tubes, 1.3-fold higher ($p<0.05$) than on AAc Si-Nitrite-Col tubes with 50 μM initial sodium nitrite, 1.8-fold higher ($p<0.05$) than on AAc Si-Nitrite-Col tubes with 100 μM initial sodium nitrite, 2.1-fold higher ($p<0.005$) than on AAc Si-Nitrite-Col tubes with 250 μM initial sodium nitrite, and 2.3-fold higher ($p<0.005$) than on AAc Si-Nitrite-Col tubes with 500 μM initial sodium nitrite in the sodium nitrite-collagen conjugate.

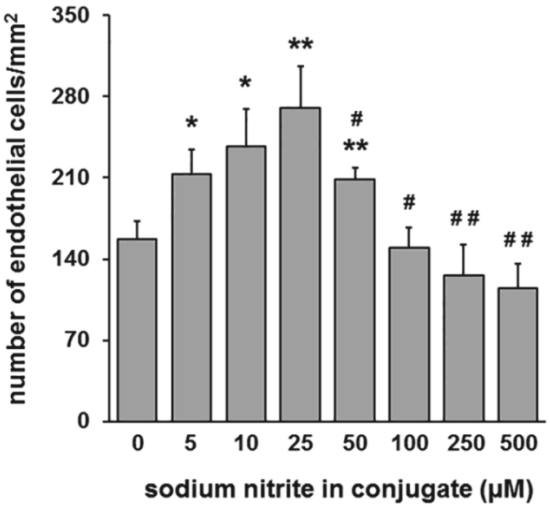

Figure 4. Effect of the initial sodium nitrite concentration in a sodium nitrite-collagen conjugate coating of AAc Si-Nitrite-Col tubes on the number of endothelial cells after 2 days of culture. AAc Si-Nitrite-Col tubes with 50 μM or less initial sodium nitrite in conjugate showed an increase in the number of endothelial cells, with a maximum effect at 25 μM sodium nitrite in the conjugate. The number of cells on AAc Si-Nitrite-Col tubes with initial 25 μM sodium nitrite was 1.8-fold higher than on AAc Si-Col tubes. AAc Si-Nitrite-Col, sodium nitrite-collagen conjugate immobilized AAc-grafted silicone; AAc Si-Col, collagen immobilized AAc-grafted silicone. *Significant effect of sodium nitrite in conjugate compared to control without sodium nitrite, $p<0.05$, **$p<0.005$, $^{\#}$Significantly different from 25 μM sodium nitrite in conjugate, $p<0.05$, $^{\#\#}p<0.005$.

Endothelial cell proliferation on Si, AAc Si, AAc Si-Col, and AAc Si-Nitrite-Col (with 25 μM initial sodium nitrite in the conjugate) tubes was compared after 2, 4, and 6 days of culture (Figure 5A). The number of endothelial cells on AAc Si

tubes was significantly decreased compared with Si tubes by 4-fold ($p<0.0005$, day 4) and 3-fold ($p<0.005$, day 6). On the other hand, the number of endothelial cells on AAc Si-Col tubes was 3-fold ($p<0.0005$, day 4) and 3.4-fold ($p<0.0005$, day 6) increased compared with the number of cells on Si tubes. Nitrite incorporation in AAc Si-Nitrite-Col tubes further increased the number of endothelial cells by 68% at day 2 ($p<0.05$), 34% at day 4 ($p<0.05$), and 28% at day 6 ($p<0.005$), compared with AAc Si-Col tubes. Thus endothelial cells showed the highest proliferation rate on AAc Si-Nitrite-Col tubes at all time points measured. The number of endothelial cells increased on AAc Si-Col tubes and AAc Si-Nitrite-Col tubes with increased incubation time, while such an increase over time was not observed with Si and AAc Si tubes.

Optical micrographs of endothelial cells attached to Si, AAc Si, AAc Si-Col, and AAc Si-Nitrite-Col tubes were used to assess endothelial cell confluency at day 6 (Figure 5Ba-d). Cell confluency differed dependent on the surface modification used. The number of cells on Si tubes was very low, as well as cell confluency (22%) within 6 days (Figure 5Ba). Most cells did not adhere while attached cells showed poor proliferation on AAc Si tubes in the absence of collagen coating, resulting in increased cell death (data not shown). As a result, cells were only scarcely covering the silicone surface (7%; Figure 5Bb). Cell layers were more confluent (74%) on AAc Si-Col tubes than on Si and AAc Si tubes (Figure 5Bc). Although endothelial cells on AAc Si-Col tubes proliferated well, they did not form a confluent monolayer on the silicone surface. The high rate of endothelial cell proliferation on AAc Si-Nitrite-Col tubes resulted in 95% cell confluency within 6 days (Figure 5Bd).

Morphology of endothelial cells on surface-modified silicone tubes

The morphology of attached endothelial cells on unmodified and surface-modified silicone tubes was different after 6 days of culture, dependent on the type of surface modification (Figure 6). SEM images revealed that cells on Si tubes did not spread well (Figure 6a). Only few cells were attached on AAc Si tubes, exhibiting "round" morphology (Figure 6b). In contrast, cells attached onto AAc Si-Col tubes kept their natural spindle-shaped morphology (Figure 6c). This suggests that a collagen coating provides a highly compatible substratum for endothelial cells. Endothelial cells on AAc Si-Nitrite-Col tubes displayed a flat, cobble stone-shaped morphology, while no “round” cells were seen (Figure 6d).

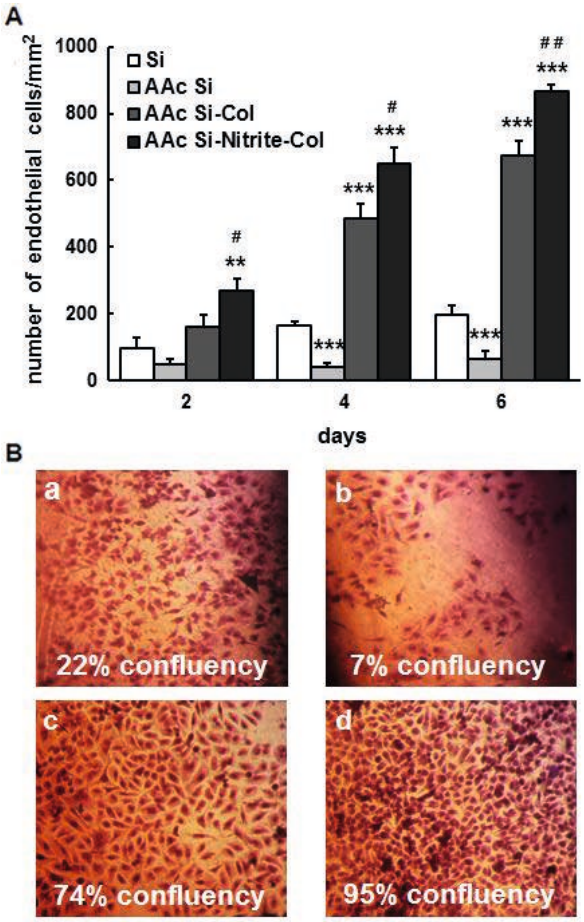

Figure 5. Endothelial cell proliferation and confluency on Si, AAc Si, AAc Si-Col, and AAc Si-Nitrite-Col tubes with 25 μM sodium nitrite in conjugate after 2, 4, and 6 days of culture. (A) Endothelial cell proliferation at days 2, 4, and 6. Cell number on AAc Si tubes decreased compared with that on Si tubes at all time points. Cell number on AAc Si-Col tubes increased compared with Si tubes, and even further increased on AAc Si-Nitrite-Col tubes. (B) Optical micrographs showing endothelial cell confluency after 6 days. (a) Si, (b) AAc Si, (c) AAc Si-Col, (d) AAc Si-Nitrite-Col tubes. Magnification x200. Cell confluency was low (22%) on Si tubes, and even lower on AAc Si tubes (7%) in the absence of a collagen coating. Cell coverage was rather high on collagen-coated tubes (74% confluency), and even higher when sodium nitrite was incorporated in the collagen coating (95% confluency). Si, silicone; AAc Si, AAc-grafted silicone; AAc Si-Col, collagen immobilized AAc-grafted silicone; AAc Si-Nitrite-Col, sodium nitrite-collagen conjugate immobilized AAc-grafted silicone. **Significantly different from Si tubes, $p<0.005$, ***$p<0.0005$, $^{\#}$Significant effect of sodium nitrite in conjugate, $p<0.05$, $^{\#\#}p<0.005$.

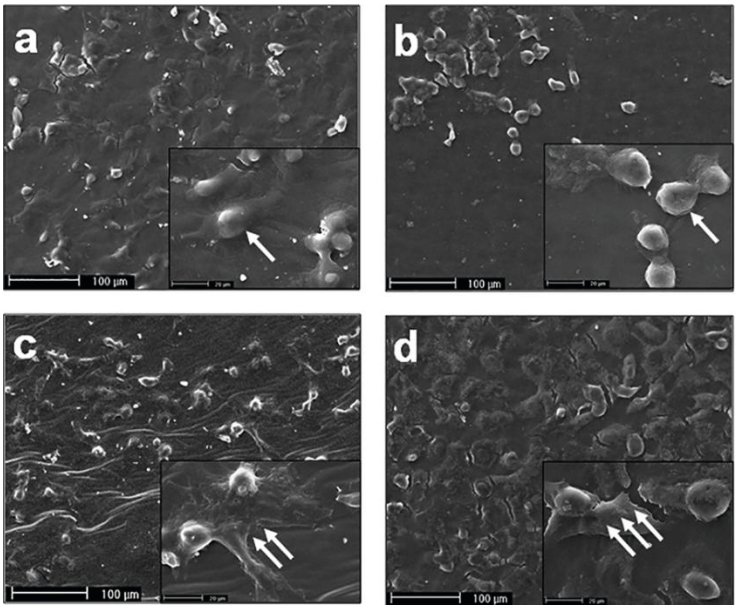

Figure 6. Scanning electron microscopy (SEM) showing morphology of endothelial cells seeded on Si, AAc Si, AAc Si-Col, and AAc Si-Nitrite-Col tubes with 25 µM sodium nitrite in conjugate after 6 days of culture. (a) Si, (b) AAc Si, (c) AAc Si-Col, (d) AAc Si-Nitrite-Col. Magnification x200. Insert: SEM image of endothelial cells, magnification x1000. Endothelial cells on Si tubes and on AAc Si tubes exhibited "round" cell bodies (a, b). Endothelial cells on AAc Si-Col tubes displayed a flat, spindle-shaped morphology while no “round” cells were present (c). Cell morphology was changed to cobblestone-like morphology on AAc Si-Nitrite-Col tubes (d). Si, silicone; AAc Si, AAc-grafted silicone; AAc Si-Col, collagen immobilized AAc-grafted silicone; AAc Si-Nitrite-Col, sodium nitrite-collagen conjugate immobilized AAc-grafted silicone. Single arrow: round cell; double arrows: spindle-shaped cell; triple arrows: cobblestone-shaped cell.

Platelet adhesion on surface-modified silicone tubes

Platelet adhesion was decreased by 20% on AAc Si tubes compared with Si tubes ($p<0.05$). In contrast, platelet adhesion on AAc Si-Col tubes was increased by 27% compared with Si tubes ($p<0.05$; Figure 7). AAc Si-Nitrite-Col tubes with 25 to 500 µM initial sodium nitrite suppressed platelet adhesion compared with AAc Si-Col tubes. The higher the initial concentration of sodium nitrite in sodium nitrite-collagen conjugate, the more platelet adhesion on AAc Si-Nitrite-Col tubes was reduced. Platelet adhesion to AAc Si-Nitrite-Col tubes with an initial sodium nitrite concentration of 500 µM provided maximal inhibition by 63% ($p<0.005$) compared with adhesion to AAc Si-Col tubes. Platelet deposition onto PEG Si tubes, that

were used as a reference matrix, was very low com pared to other unmodified and surface-modified silicone tubes ($p<0.0005$).

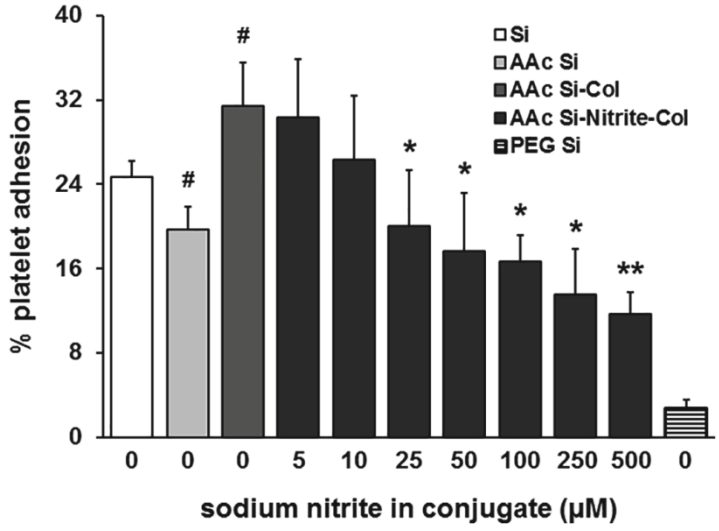

Figure 7. Effect of surface modification on platelet adhesion onto silicone tubes. Adhesion of platelets on the silicone tubes was expressed as percentage of the total number of platelets present in the PRP solution. AAc Si-Nitrite-Col tubes with 25-500 µM initial sodium nitrite in conjugate decreased platelet adhesion compared with AAc Si-Col tubes. Si, silicone; AAc Si, AAc-grafted silicone; AAc Si-Col, collagen immobilized AAc-grafted silicone; AAc Si-Nitrite-Col, sodium nitrite-collagen conjugate immobilized AAc-grafted silicone; PEG Si, polyethylene glycol-grafted silicone. *Significant effect of sodium nitrite in conjugate, $p<0.05$, **$p<0.005$, #Significant effect of AAc grafting or collagen immobilization on silicone tube, $p<0.05$.

DISCUSSION

Endothelial cell seeding on a silicone surface is generally known to improve blood compatibility of silicone-based medical devices. Silicone is a hydrophobic and inert material that does not facilitate endothelial cell adhesion and/or proliferation. In general, surface coating of biomaterials with extracellular matrix proteins such as collagen enhances cell growth [4, 6]. Collagen has excellent properties that allow cell attachment, but also undesired platelet adhesion causing thrombosis [11]. To suppress the thrombogenic properties of collagen, several anti-thrombotic factors such as heparin, aspirin, or NO donors have been immobilized on collagen [8-12].

Nitrite, the stable end-product of NO, has also been shown to have anti-thrombogenic properties in acidic environments [13-15], and therefore we investigated whether the combination of sodium nitrite, as a nitrite donor, with collagen in the presence of acetic acid improves endothelialization of silicone tubes by increasing the number of endothelial cells and GH production, as well as by decreasing platelet adhesion. The sodium nitrite concentrations were chosen based on the following published data. NO-generating sodium nitroprusside (SNP) at low concentration (1 μM) [28] but not at high concentration (>100 μM) [29] increases endothelial cell proliferation. Also, endothelial cells exposed to 0.1-100 μM SNP show increased proliferation with a maximal effect at 10 μM [30]. Finally NO release by NO-generating S-nitroso-N-acetylpenicillamine (SNAP; 50 μM) also stimulates endothelial cell proliferation [31]. Therefore, we used sodium nitrite-collagen conjugates with 0.5-500 μM initial sodium nitrite for coating of silicone tubes. Since the amount of nitrite and acidified nitrite released from coated silicone tubes containing less than 5 μM initial sodium nitrite in the conjugate was negligible, we used >5 μM initial sodium nitrite in the conjugate in the current study.

To study the interaction between a sodium nitrite-collagen conjugate coating with endothelial cells, a well-defined and stable collagen coating is required. A stable collagen coating can be obtained by carbodiimide bonds between the functional groups of collagen and the functional groups introduced to the surface of silicone tubes by plasma graft polymerization of a specific monomer [4-7]. Different functional groups, i.e. amine, carboxyl, and hydroxyl groups, have been introduced to the surface of silicone to facilitate collagen immobilization [4, 6]. In this study, collagen and sodium nitrite-collagen conjugate were immobilized onto silicone tubes by ionic interaction with a pre-determined AAc graft density. The amount of collagen immobilized on AAc Si tubes before washing and after washing was not significantly different, indicating that the carboxyl groups of AAc Si were tightly bound to the amino groups of collagen. In addition, incorporation of sodium nitrite (at all concentrations tested) in the collagen conjugate did not change the amount of immobilized collagen.

Nitrite and acidified nitrite release from AAc Si-Nitrite-Col tubes increased with increasing initial sodium nitrite concentrations in the conjugate. However, the amount of nitrite and acidified nitrite released from the AAc Si-Nitrite-Col tubes was low compared with the amount of initial sodium nitrite in conjugate at 4 h. At 500 μM initial sodium nitrite (the highest concentration used in this study), only 7% of the initial nitrite was released. This release was low in comparison to the 50% released from initially loaded diazeniumdiolate NO donor in the backbone of polyurethane after 4 h in another study [16]. The difference in release kinetics between the studies might be explained by the differences in the NO donor used (NO gas and nitrite-donor), the hydrophilicity/structure of the substratum used (AAc-grafted silicone and backbone of polyurethane), and the chemistry utilized to

bond NO/nitrite-donor to the substratum. The AAc grafting on silicone tubes before sodium nitrite-collagen conjugate immobilization, and the hydrogel-like nature of polyAAc might help the immobilized sodium nitrite molecules to retain their biological activity for a prolonged period of time [32]. Our study shows that almost half of the initial sodium nitrite in conjugate was released at 48 h (46-57%) at all initial sodium nitrite concentrations tested. This is comparable to the 70% released from initially loaded diazeniumdiolate NO donor in the backbone of polyurethane after 48 h as has been reported by others [16].

AAc grafting has been shown to create a hydrophilic surface with a low water contact angle, while linking collagen increases the water contact angle [4-7]. Our results are in accordance with these observations; we found that the water contact angle was considerably decreased on AAc Si tubes. The wettability of AAc Si-Col and AAc Si-Nitrite-Col tubes was even less than that of AAc Si tubes. This is inherent to the fact that collagen is more hydrophobic than AAc [4, 22]. Our data showing that collagen immobilization on AAc-grafted silicone tubes led to moderate wettability is a favorable condition for endothelial cell attachment, since a material surface with either a very high or a very low contact angle is not suitable for cell attachment [4-6].

Several reports claimed that, carboxyl functional groups create a higher negative surface charge than other commonly used surface functional groups, which causes inhibition of cell attachment [4, 6]. We found that endothelial cells in direct contact with carboxyl groups of AAc did not attach and showed poor proliferation. On the other hand, the immobilized collagen on the tubes created an adequate environment for endothelial cell attachment. Collagen is a main protein in the extracellular matrix responsible for cell binding to the material surface. The integrin family of cell adhesion receptors contains four collagen receptors that are involved in cell-matrix interactions [22, 23]. The presence of these receptors implicates that collagen is suitable as a matrix for endothelial cell growth *in vitro*, and might be the reason for increased endothelial cell attachment on AAc Si-Col tubes compared with AAc Si tubes. Although AAc Si tubes had toxic effects on endothelial cells in the absence of collagen immobilization, our results also indicate that these tubes can be used as substratum for collagen immobilization and then provide a favorable surface for endothelialization (AAc Si-Col tubes).

NO is known to inhibit platelet adhesion, and to inhibit or stimulate endothelial cell proliferation dependent on the concentration [28-31]. We found that sodium nitrite-collagen conjugate coating of AAc Si-Nitrite-Col tubes increased the number of endothelial cells. Interestingly, GH production by endothelial cells was stimulated on AAc Si-Nitrite-Col tubes containing 5-50 μM initial sodium nitrite in conjugate. Twenty-five μM initial sodium nitrite in the conjugate maximally stimulated GH production. GH is known to stimulate endothelial cell growth [34, 35]. This might explain the maximal stimulation by sodium nitrite-collagen

conjugate coating of AAc Si-Nitrite-Col tubes on the number of endothelial cells with 25 μM initial sodium nitrite in the conjugate. Endothelial cell proliferation on different surface-modified silicone tubes at 2, 4, and 6 days also showed that AAc decreases the number of endothelial cells at all time points, probably by causing an acid environment [4, 6]. This was in contrast to the high increase in cell number observed on tubes with immobilized collagen. The number of endothelial cells on AAc Si-Nitrite-Col tubes with 50 μM or less initial sodium nitrite in the conjugate was increased compared with the number of cells on AAc Si-Col tubes after 2 days of culture, with a maximum effect at 25 μM initial sodium nitrite. Therefore sodium nitrite-collagen conjugate coating with 5 to 50 μM initial sodium nitrite accelerates endothelialization of silicone tubes even more than collagen coating alone.

Endothelial cells cultured on AAc Si-Nitrite-Col tubes formed a perfect confluent (95%) monolayer, but confluency was not achieved on AAc Si-Col tubes after 6 days of culture. The morphology of endothelial cells cultured on AAc Si-Col tubes was spindle-shaped, while a round morphology was observed on AAc Si tubes. Endothelial cells on AAc Si-Nitrite-Col tubes had changed to cobblestone-like morphology. Thus sodium nitrite-collagen conjugate coating was compatible with endothelial cells providing the possibility of improved endothelialization. AAc grafting increases material surface hydrophilicity thereby preventing platelet adhesion [36]. Collagen is highly thrombogenic and induces platelet adhesion on a material surface [11]. Our data agree with these observations, since we found reduced platelet adhesion on AAc Si tubes, and increased platelet adhesion on AAc Si-Col tubes. We also observed that after incorporation of sodium nitrite into collagen in the presence of acetic acid, the use of this nitrite and acidified nitrite-generating coating with 25 to 500 μM initial sodium nitrite significantly suppressed the thrombogenic properties of collagen by decreasing platelet adhesion on the silicone surface, especially when a high initial concentration of sodium nitrite in conjugate was used. The presence of acetic acid in the sodium nitrite-collagen conjugate might change some nitrite molecules to nitrous acid, that easily decomposes into NO; that is known to inhibit platelet adhesion [20, 21]. Although AAc Si-Nitrite-Col tube with 500 μM sodium nitrite in conjugate prevented more platelet adhesion, it did not affect endothelial cell growth. These results agree with data reported by others showing that NO inhibits as well as stimulates endothelial cell proliferation dependent on the concentration [28-31]. Low NO concentrations (μmolar or sub-mmolar range) stimulate cell proliferation of a.o. fibroblasts, pancreatic tumours, myoblasts, keratinocytes, and endothelial cells [28, 30, 31, 37], while NO in the mmolar range inhibits cell proliferation [29, 38, 39]. The reason for this biphasic effect is not well understood, but it has been suggested that the NO-mediated increase in endothelial cell proliferation requires the production of reactive oxygen species (ROS), since superoxide dismutase and catalase suppress in part the stimulatory effect of NO on cell proliferation [28, 39]. NO at a

low concentration (1 μM) increases endothelial cell proliferation [28], whereas NO at a high concentration (>100 μM) has no effect [29]. SNP at 0.1-100 μM increases endothelial cell proliferation, with a maximal effect at 10 μM [30]. The release of NO by SNAP at 50 μM, but not 10 μM, stimulates endothelial cell proliferation [31]. Overall, these studies support the concept that the effect of NO on endothelial cell proliferation is concentration-dependent [39].

CONCLUSIONS

Our data shows that a nitrite and acidified nitrite-generating sodium nitrite-collagen conjugate coating of AAc Si-Nitrite-Col tubes with 5 to 50 μM initial sodium nitrite increased the number of endothelial cells, more than collagen coating alone, probably via GH production, with a maximum effect at 25 μM initial sodium nitrite, resulting in a confluent endothelial cell monolayer on a silicone surface. In addition, AAc Si-Nitrite-Col tubes with 25 to 500 μM initial sodium nitrite suppressed platelet adhesion in areas that were not fully covered with endothelial cells. Since AAc Si-Nitrite-Col tubes with 25 to 50 μM initial sodium nitrite increases endothelial cell proliferation and inhibits platelet aggregation, this suggests that sodium nitrite-collagen conjugate coatings are highly promising to promote endothelialization of silicone materials in blood-contacting devices.

ACKNOWLEDGMENTS

The authors are grateful to Dr. Nooshin Haghighipour for valuable advice on cell seeding, and Dr. Azadeh Hashemi for help in image-processing. The authors also thank Dr. Astrid D. Bakker for critically reading the manuscript.

REFERENCES

1 Polk AA, Maul TM, McKeel DT, Snyder TA, Lehocky CA, Pitt B, Stolz DB, Federspiel WJ, Wagner WR. A biohybrid artificial lung prototype with active mixing of endothelialized microporous hollow fibers. Biotechnol Bioeng 2010;106:490-500.

2 de Mel A, Cousins BG, Seifalian AM. Surface modification of biomaterials: A quest for blood compatibility. Int J Biomater 2012;2012:707-863

3 Farhadi M, Mirzadeh H, Solouk A, Asghari A, Jalessi M, Ghanbari H, Yazdanifard P. Collagen-immobilized patch for repairing small tympanic membrane perforations: In vitro and in vivo assays. J Biomed Mater Res A 2012;100:549-553.

4 Lee SHD, Hsiue GH, Chang PCT, Kao CHY. Plasma-induced grafted polymerization of acrylic acid and subsequent grafting of collagen onto polymer film as biomaterials. Biomaterials 1996;17:1599-1608.

5 Salehi-Nik N, Amoabediny G, Shokrgozar MA, Mottaghy K, Klein-Nulend J, Zandieh-Doulabi B. Surface modification of silicone tubes by functional carboxyl and amine, but not peroxide groups followed by collagen immobilization improves endothelial cell stability and functionality. Biomed Mater 2015;10:015024.

6 Gupta B, Plummer Ch, Bisson I, Frey P, Hilborn J. Plasma-induced graft polymerization of acrylic acid onto poly(ethylene terephthalate) films: characterization and human smooth muscle cell growth on grafted films. Biomaterials 2002;23:863-871.

7 Karkhaneh A, Mirzadeh H, Ghaffariyeh A. Simultaneous graft copolymerization of 2-hydroxyethyl methacrylate and acrylic acid onto polydimethylsiloxane surfaces using a two-step plasma treatment. J Appl Polym Sci 2007;105:2208-2217.

8 Kang IK, Choi SH, Shin DS, Yoon SC. Surface modification of polyhydroxyalkanoate films and their interaction with human fibroblasts. Int J Biol Macromol 2011;28:205-212.

9 Wu B, Gerlitz B, Grinnell BW, Meyerhoff ME. Polymeric coatings that mimic the endothelium: combining nitric oxide release with surface-bound active thrombomodulin and heparin. Biomaterials 2007;28:4047-4055.

10 Jingrun R, Jin W, Hong S, Nan H. Surface modification of polyethylene terephthalate with albumin and gelatin for improvement of anticoagulation and endothelialization. Appl Surf Sci 2008;255:263-266.

11 Wissink MJB, Beernink R, Poot AA, Engbers GH, Beugeling T, van Aken WG, Feijen J. Improved endothelialization of vascular grafts by local release of growth factor from heparinized collagen matrices. J Control Release 2000;64:103-114.

12 Zhao J, Falotico R, Nguyen T, Cheng Y, Parker T, Dave V, Rogers C, Riesenfeld J. A nonelutable low-molecular weight heparin stent coating for improved thromboresistance. J Biomed Mater Res B 2012;100:1274-1282.

13 Reynolds MM, Annich GM. The artificial endothelium. Organogenesis 2011;7:42-49.

14 Wu Y, Zhou Zh, Meyerhoff ME. In vitro platelet adhesion on polymeric surfaces with varying fluxes of continuous nitric oxide release. J Biomed Mater Res A 2007;81:956-963.

15 Kabirian F, Amoabediny G, Haghighipour N, Salehi-Nik N, Zandieh-Doulabi B. Nitric oxide secretion by endothelial cells in response to fluid shear stress, aspirin, and temperature. J Biomed Mater Res A 2015;103:1231-1237.

16 Taite LJ, Yang P, Jun H, West JL. Nitric oxide-releasing polyurethane–PEG copolymer containing the YIGSR peptide promotes endothelialization with decreased platelet adhesion. J Biomed Mater Res B 2008;84:108-116.

17 Murohara T, Witzenbichler B, Spyridopoulos I, Asahara T, Ding B, Sullivan A, Losordo DW, Isner JM. Role of endothelial nitric oxide synthase in endothelial cell migration. Arterioscler Thromb Vasc Biol 1999;19:1156-1161.

18 Jozkowicz A, Cooke JP, Guevara I, Huk I, Funovics P, Pachinger O, Weidinger F, Dulak J. Genetic augmentation of nitric oxide synthase increases the vascular generation of VEGF. Cardiovasc Res 2001;51:773-783.
19 Pinilla L, Tena-Sempere M, Aguilar E. Nitric oxide stimulates growth hormone secretion *in vitro* through a calcium- and cyclic guanosine monophosphate-independent mechanism. Horm Res 1999;51:242-247.
20 Lundberg JO, Weitzberg E. NO generation from nitrite and its role in vascular control. Arterioscler Thromb Vasc Biol 2005;25:915-922.
21 Egemnazarov B, Schermuly RT, Dahal BK, Elliott GT, Hoglen NC, Surber MW, Weissmann N, Grimminger F, Seeger W, Ghofrani HA. Nebulization of the acidified sodium nitrite formulation attenuates acute hypoxic pulmonary vasoconstriction. Respir Res 2010;11:81-93.
22 Solouk A, Cousins BG, Mirahmadi F, Mirzadeh H, Jalali Nadoushan MR, Shokrgozar MA, Seifalian AM. Biomimetic modified clinical-grade POSS-PCU nanocomposite polymer for bypass graft applications: A preliminary assessment of endothelial cell adhesion and haemocompatibility. Mater Sci Eng C Mater Biol Appl 2015;46:400-408.
23 Mullender MG, Dijcks SJ, Bacabac RG, Semeins CM, Van Loon JJWA, Klein-Nulend J. Release of nitric oxide, but not prostaglandin E2, by bone cells depends on fluid flow frequency. J Orthop Res 2006;24:1170-1177.
24 Bacabac RG, Smit TH, Van Loon JJWA, Zandieh-Doulabi B, Helder MN, Klein-Nulend J. Bone cell responses to high-frequency vibration stress: does the nucleus oscillate within the cytoplasm?. FASEB J 2006;20:858-864.
25 Zhang Q, Shen Y, Tang C, Wu X, Yu Q, Wang G. Surface modification of coronary stents with SiCOH plasma nanocoatings for improving endothelialization and anticoagulation. J Biomed Mater Res B 2015;103:464-472.
26 Yeganeh H, Orang F, Solouk A, Rafienia M. Synthesis, characterization and preliminary investigation of blood compatibility of novel epoxy-modified polyurethane networks. J Bioact Compat Pol 2008;23:276-300.
27 Abednejad AS, Amoabediny G, Ghaee A. Surface modification of polypropylene membrane by polyethylene glycol graft polymerization. Mat Sci Eng C 2014;42:443-450.
28 Luczak K, Balcerczyk A, Soszyński M, Bartosz G. Low concentration of oxidant and nitric oxide donors stimulate proliferation of human endothelial cells in vitro. Cell Biol Int 2004;28:483-486.
29 Heller R, Polack T, Grabner R, Till U. Nitric oxide inhibits proliferation of human endothelial cells via a mechanism independent of cGMP. Atherosclerosis 1999;144:49-57.
30 Ziche M, Morbidelli L, Masini E, Granger H, Geppetti P, Ledda F. Nitric oxide promotes DNA synthesis and cyclic GMP formation in endothelial cells from postcapillary venules. Biochem Biophys Res 1993;192:1198-1203.
31 Leo S, Nuydens R, Meert TF. Opioid-induced proliferation of vascular endothelial cells. J Pain Res 2009;2:59-66.
32 Keshvari H, Mirzadeh H, Mansoori P, Orang F, Khorasani M. Collagen immobilization onto acrylic acid laser-grafted silicone for using as artificial skin: In vitro. Iran Polym J 2008;17:171-182.
33 Jokinen J, Dadu E, Nykvist P, Kapyla J, White DJ, Ivaska J, Vehvilainen P, Reunanen H, Larjava H, Hakkinen L, Heino J. Integrin-mediated cell adhesion to type I collagen fibrils. J Biol Chem 2004;279:31956-31963.
34 Rymaszewski Z, Cohen RM, Chomczynski P. Human growth hormone stimulates proliferation of human retinal microvascular endothelial cells in vitro. Proc Natl Acad Sci USA 1991;88:617-621.
35 Lincoln DT, Singal PK, Al-Banaw A. Growth hormone in vascular pathology: Neovascularization and expression of receptors is associated with cellular proliferation. Anticancer Res 2007;27:4201-4218.
36 Mirzadeh H, Dadsetan M, Sharifi-Sanjani N. Platelet adhesion on laser-induced acrylic acid–grafted polyethylene terephthalate. J Appl Polym Sci 2002;86: 3191-3196.

37 Jones DA, Khambata RS, Mathur A, Ahluwalia A. A sodium nitrite promotes the viability and proliferation of endothelial cells but inhibits the growth of smooth muscle cells under hypoxia. Nitric Oxide 2013;31:S13-S48.
38 Gooch KJ, Dangler CA, Frangos JA. Exogenous, basal, and flow-induced nitric oxide production and endothelial cell proliferation. J Cell Physiol 1997:171;252-258.
39 Napoli C, Paolisso G, Casamassimi A, Al-Omran M, Barbieri M, Sommese L, Infante T, Ignarro LJ. Effects of nitric oxide on cell proliferation. J Am Coll Cardiol 2013;62:89-95.

CHAPTER 5

Sustained Release of Growth Hormone and Sodium Nitrite from Biomimetic Collagen Coating Immobilized on Silicone Tubes Improves Endothelialization

Nasim Salehi-Nik[1,2], Zahra Malaie-Balasi[1,2], Ghassem Amoabediny[1,2], Seyedeh Parnian Banikarimi[1,2], Mohammad Ali Shokrgozar[3], Behrouz Zandieh-Doulabi[4], Jenneke Klein-Nulend[4]

[1] School of Chemical Engineering, College of Engineering, University of Tehran, Tehran, Iran

[2] Department of Biomedical Engineering, Research Center for New Technologies in Life Science Engineering, University of Tehran, Tehran, Iran

[3] National Cell Bank, Pasteur Institute of Iran, Tehran, Iran

[4] Department of Oral Cell Biology, Academic Centre for Dentistry Amsterdam, University of Amsterdam and VU University Amsterdam, MOVE Research Institute Amsterdam, Amsterdam, The Netherlands

Submitted for publication

ABSTRACT

Biocompatibility of biomedical devices can be improved by endothelialization of blood-contacting parts mimicking the vascular endothelium's function. Improved endothelialization might be obtained by using biomimetic coatings that allow local sustained release of biologically active molecules, e.g. anti-thrombotic and growth-inducing agents, from nanoliposomes. We aimed to test whether incorporation of growth-inducing nanoliposomal growth hormone (nGH) and anti-thrombotic nanoliposomal sodium nitrite (nNitrite) into collagen coating of silicone tubes enhances endothelialization by stimulating endothelial cell proliferation and inhibiting platelet adhesion.

Collagen coating stably immobilized on acrylic acid-grafted silicone tubes decreased the water contact angle from 102° to 56°. Incorporation of 50 or 500 nmol/ml nNitrite and 100 or 1000 ng/ml nGH into collagen coating decreased the water contact angle further to 48°. Endothelial cell number was increased after surface coating of silicone tubes with collagen by 1.6-fold, and with nNitrite-nGH-collagen conjugate by 1.8-3.9-fold after 2 days. After 6 days, endothelial cell confluency in the absence of surface coating was 22%, with collagen coating 74%, and with nNitrite-nGH-collagen conjugate coating 83-119%. In the absence of endothelial cells, platelet adhesion was stimulated after collagen coating by 1.3-fold, but inhibited after nNitrite-nGH-collagen conjugate coating by 1.6-3.7-fold. The release of anti-thrombotic prostaglandin I_2 from endothelial cells was stimulated after nNitrite-nGH-collagen conjugate coating by 1.7-2.2-fold compared with collagen coating.

In conclusion, our data shows improved endothelialization using nNitrite-nGH-collagen conjugate coating on silicone tubes suggesting that these coatings are highly suitable for use in blood-contacting parts of biomedical devices.

Keywords
Biomimetic coating, Endothelialization, Growth hormone, Nanoliposome, Sodium nitrite

INTRODUCTION

The biocompatibility of synthetic materials is of crucial importance in the development of biomedical devices that are in continuous contact with blood, such as artificial lungs, vascular grafts, heart valves, stents, etc. [1, 2]. Endothelial cell seeding of blood-contacting parts of biomedical devices minimizes the need for anticoagulants when using these devices [3, 4]. The surface of most commercially available synthetic materials used in biomedical devices, such as silicone, is highly hydrophobic and therefore not suitable for endothelial cell seeding. Modification of silicone surface by chemical surface treatment [5], glow discharge treatment [4], or coating with extracellular matrix proteins [6, 7], may improve endothelial cell adhesion and proliferation.

Collagen, the main protein in the extracellular matrix of connective tissue, is often used for tissue engineering purposes due to its key role in cell adhesion to the synthetic material surface, which involves integrins. The integrin family of cell adhesion receptors contains four collagen receptors that are involved in cell-matrix interactions [7, 8]. The presence of these receptors implicates that collagen has excellent properties that allow cell attachment, but also undesired platelet adhesion in areas of a collagen coating that are not fully covered by endothelial cells, which causes thrombosis [9]. A practical solution to the problem of collagen thrombogenicity is the creation of collagen conjugate coatings that release anticoagulants such as heparin [9, 10], aspirin [11], hirudin [12], thrombomodulin [13], and nitric oxide (NO) [9, 14] at the blood-polymer interface. We have previously shown that nitrite and acidified nitrite released from biomimetic sodium nitrite-collagen conjugate coatings significantly decreases platelet adhesion and increases endothelialization of silicone tubes [15]. The rate of endothelialization can be improved by immobilization of specific exogenous growth factors or growth hormones. Endothelial cells seeded at low density on a material surface can be stimulated by growth-inducing agents to rapidly form a confluent monolayer in a few days [16]. Growth hormone (GH), also known as somatropin, is a mitogen for a variety of cell types, including smooth muscle cells, fibroblasts, adipocytes, macrophages, lymphocytes, and endothelial cells [17]. It plays a role in controlling cell metabolism, balanced growth, and differentiation by modulating the synthesis of multiple mRNA species such as insulin-like growth factor 1 [17].

Biomaterials co-immobilized with different biomolecules to improve endothelialization, e.g. anti-thrombotic and cell growth-inducing biomolecules, show simultaneously anti-thrombotic and growth-inducing properties [16, 18]. Currently the use of anti-thrombotic or growth-inducing agents is limited by their short half-life, renal toxicity, physical and chemical instability, and rapid clearance. Prolonged release of anti-thrombotic or growth-inducing agents from liposomes, that function as drug delivery carriers, has gained considerable attention, since

liposomes are biocompatible, biodegradable, and capable of releasing encapsulated drugs in a sustained manner, and transporting drugs across biological membranes [19, 20].

In this study, we aimed to test whether sustained release of the anti-thrombotic agent sodium nitrite and the growth-inducing agent GH from collagen conjugate improves endothelialization by inhibiting platelet adhesion when silicone is not yet fully covered by endothelial cells, and by stimulating fast endothelial cell coverage of the silicone. First a stable collagen conjugate coating able to withstand fluid shear stress on silicone tubes was developed as described earlier [21]. Collagen solution blended with nNitrite and/or nGH, was co-immobilized on the internal surface of acrylic acid (AAc)-grafted silicone tubes. The release of nitrite and/or GH from the surface-modified silicone tubes was determined, and the effect of the released molecules on endothelial cell proliferation and prostaglandin I_2 (PGI_2) release, as well as on platelet adhesion assessed.

MATERIALS AND METHODS

Materials

Medical grade tubular silicone rubber (inner diameter 2 mm) was kindly donated by Raumedic (Helmbrechts, Germany). AAc was supplied by Fluka (Buchs, Switzerland), and purified by distillation under vacuum to remove impurities and stabilizers. Sodium nitrite and other chemicals for the Griess assay were obtained from Merck (Kenilworth, NJ, USA), and were of the highest purity available. Somatropin (GH) was obtained from Novo Nordisk (Aalborg, Denmark). 1,2 Distearoyl-sn-glycero-3-phosphoethanolamine-N-[amino(polyethyleneglycol)-2000] (amino-PEG lipid) and dipalmitoyl phosphatidylcholine (DPPC) were purchased from Lipoid Gmbh (Ludwigshafen, Germany). Cholesterol and sucrose were purchased from Sigma Aldrich (Gillingham, Dorset UK). Chloroform was obtained from Duksan (Gyeonggi, Korea).

Plasma graft polymerization of AAc onto silicone tubes

Silicone tubes were cleaned three times with 70% (v/v) ethanol, and one time with de-ionized water for 5 min. They were placed on the bottom of a reaction chamber (Seren R600, Anatech ltd, CA, USA), which was evacuated to 0.6 mbar, and pretreated with 60 W of oxygen plasma for 0.5 min. Plasma surface-modified tubes were immersed in a solution containing 30% AAc in de-ionized water for 30 min at room temperature. Then the tubes were removed from the solution and air-dried at 40°C for 5 min. Tubes with a pre-adsorbed surface layer of reactive AAc monomers were placed into a reaction chamber for plasma graft copolymerization for 3 min to produce AAc-grafted silicone tubes (AAc Si). The residual monomers

and homopolymers were removed by washing twice with warm de-ionized water in an ultrasonic water bath, followed by incubation in distilled water for 24 h [15, 21].

nNitrite and nGH preparation

Sodium nitrite solution at 0.01 M was prepared by dissolving sodium nitrite in water containing 0.02 M acetic acid at 4ºC. Some of the nitrite ions in the solution convert to acidified nitrite (nitrous acid; HNO_2) in the presence of acetic acid. Preparation of the solution at 4°C prevents fast decomposition of HNO_2 into NO, NO_2, and H_2O [15]. From now on we refer to the total amount of nitrite and acidified nitrite as “nitrite". GH at 90 µg/ml was prepared by dissolving somatropin in water.

nNitrite and nGH were prepared using the thin-film hydration technique as described earlier [22, 23]. A lipid phase (total weight: 10 times the sodium nitrite or GH weight) was prepared from a lipid mixture of DPPC, cholesterol, and amino-PEG (molar percentage ratio: 83:15:2), and dissolved in chloroform (1 ml chloroform/20 mg of lipid phase) in a round bottom flask. The solvent was removed in an IKA RV10 rotary evaporator (IKA, Deutschland, Germany) at 150 rpm, 50ºC, during 30 min under reduced pressure. Subsequently, nitrogen was blown over the dried lipid film for 5 min to remove residual solvent.

Dry thin lipid film was hydrated with 10 ml sodium nitrite or GH solution. Afterwards, sucrose powder (6 mg sucrose/1 mg lipid phase) was added, and the dispersion obtained was gently shaken for 30 min allowing the formation of multilamellar vesicles containing sodium nitrite or GH. The multilamellar vesicles were put in an ice bath and sonicated using a probe type ultrasonicator (Misonix sonicator s94000, QSONICA, Newtown, CA, USA) to produce nanoliposomes. Sonication was performed at a net power of 20 W and a frequency of 20 KHz, 20 sec on and 10 sec off, with a total process time of 30 min. Unwanted titanium particles that possibly disparted from the probe of the sonicator in the nanoliposome solution were removed by centrifugation in a Hettich Universal 320 R centrifuge (Buckinghamshire, UK) at 9000 rpm for 20 min.

To assess the encapsulation efficiency of nNitrite or nGH, the liposomal suspension was transferred to the upper chamber of an Amicon centrifugal filter tube (EMD Millipore, Darmstadt, Germany) and centrifuged at 5000 rpm for 30 min. The amount of non-encapsulated sodium nitrite or GH was determined by measuring the concentration of sodium nitrite or GH in the suspension in the lower chamber of the centrifugal filter tube. Encapsulation efficiency of nNitrite or nGH was calculated as the percentage of the total sodium nitrite ($NaNO_2$) or GH concentration using the following equation [23]:

$$\text{encapsulation efficiency} = \frac{\text{total } [NaNO_2] \text{ or } [GH] - \text{non-encapsulated } [NaNO_2] \text{ or } [GH]}{\text{total } [NaNO_2] \text{ or } [GH]} \times 100\%$$

The mean hydrodynamic diameter of the liposomes was determined by the dynamic light scattering technique (DLS) in a Zeta sizer Nano ZS (Malvern Instruments, CO, Malvern, UK) equipped with a 633 nm laser source [23]. The nanoliposomal solution was diluted with phosphate buffered saline (PBS) to reach a viscosity of 0.933 cP. DLS analysis was performed at room temperature using a refraction index of 1.33. All liposome hydrodynamic diameter measurements were run in triplicate. Finally nNitrite and nGH were stored at 4ºC until use. For cell culture experiments, nNitrite and nGH were sterilized using 0.2 µm filters (EMD Millipore, Darmstadt, Germany).

nNitrite-collagen and/or nGH-collagen conjugate immobilization on AAc Si tubes

nNitrite stock solution (0.01 M) and nGH stock solution (90 µg/ml) were used to prepare conjugates with 50 or 500 nmol/ml nNitrite, 100 or 1000 ng/ml nGH, a combination of 50 nmol/ml nNitrite and 100 ng/ml nGH, 50 nmol/ml nNitrite and 1000 ng/ml nGH, 500 nmol/ml nNitrite and 100 ng/ml nGH, and 500 nmol/ml nNitrite and 1000 ng/ml nGH in water containing 1 mg/ml collagen (acid soluble collagen type I; Pasteur Institute of Iran, Tehran, Iran) and 0.02 M acetic acid. Solutions were gently shaken for 1 h at 4°C to obtain homogeneous nNitrite-collagen (nNitrite-Col), nGH-collagen (nGH-Col), and nNitrite-nGH-collagen (nNitrite-nGH-Col) conjugates.

AAc Si tubes were immersed in 30 ml of 5 mM 2-(N-morpholino) ethanesulfonic acid (MES) buffer solution containing 48 mg 1-Ethyl-3-[3-dimethylaminopropyl] carbodiimide hydrochloride (EDC) and 15 mg N-hydroxysuccinimide (NHS; Fluka, Neu-Ulm, Germany) [7]. The solution was stirred for 5 h at 4°C to activate the carboxyl groups on AAc Si tubes. Then collagen immobilization on AAc Si tubes with activated carboxyl groups was achieved by filling the tubes with nNitrite-Col, nGH-Col, or nNitrite-nGH-Col conjugate at 4ºC for 24 h. nNitrite-Col conjugate immobilized AAc-grafted silicone (AAc Si-nNitrite-Col) tubes, nGH-Col conjugate immobilized AAc-grafted silicone (AAc Si-nGH-Col) tubes, and nNitrite-nGH-Col conjugate immobilized AAc-grafted silicone (AAc Si-nNitrite-nGH-Col) tubes were washed with water for 1 min to remove unbound collagen and/or nanoliposomes, and stored at 4ºC.

Characterization of surface-modified silicone tubes

Unmodified and surface-modified silicone tubes, i.e. Si, AAc Si, AAc Si-nNitrite-Col, AAc Si-nGH-Col, and AAC Si-nNitrite-nGH-Col, were dried with nitrogen gas, cut longitudinally, and glued on glass microscope slides to determine surface wettability by the sessile drop method [24]. Five µl double-distilled water droplets were placed on each tube, and the water contact angle was recorded after 1 min using Kruss G10 goniometer contact-angle measurement equipment (Krüss

GmbH, Hamburg, Germany). The results are mean values of five water contact angle measurements performed at randomly chosen areas of each silicone tube.

The effect of nNitrite-Col, nGH-Col, or nNitrite-nGH-Col conjugate immobilization on the mechanical properties of silicone tubes was evaluated by holding both ends of each tube (length 9 mm) in a specific grip of an in-house fabricated uniaxial testing instrument, and pulling uniaxially until tension break. The ultimate tensile strength was determined based on the peak load and the initial surface area of each tube. The percent elongation-at-break was obtained from the ratio between the elongated length at the time of failure (l) and initial length (l_0) of each silicone tube [25].

To verify (indirectly) the binding of nNitrite and nGH to silicone, and to assess the continuous release of nitrite and/or GH, the amount of nitrite released from AAc Si nNitrite-Col tubes, and the amount of GH released from AAc Si-nGH-Col tubes were determined after 4, 12, 24, 48, 72, 96, and 120 h of incubation with Dulbecco's minimal essential medium (DMEM)/F12 (1/1, v/v) (Gibco, Life Technologies, Grand Island, NY, US). To investigate a possible effect of nanoliposomes on sodium nitrite or GH release, the amount of nitrite or GH released from nNitrite or nGH was compared with that from the free form of sodium nitrite or GH in the conjugates with collagen. The free form of sodium nitrite at 50 or 500 nmol/ml, or GH at 100 or 1000 ng/ml were mixed with collagen, gently shaken for 1 h at 4°C to obtain homogeneous sodium nitrite-collagen (Nitrite-Col) or GH-collagen (GH-Col) conjugates, and immobilized on AAc-grafted silicone tubes to prepare AAc Si-Nitrite-Col or AAc Si-GH-Col tubes. Nitrite release from AAc Si-nNitrite-Col and AAc Si-Nitrite-Col tubes was measured as nitrite (NO_2^-) accumulation in the culture medium, using Griess reagent containing 1% sulfanilamide, 0.1% naphtylethelene-diamine-dihydrochloride, and 2.5 M H_3PO_4 [15, 26]. Serial dilutions of $NaNO_2$ in medium were used as standard curve. The absorbance was measured at 545 nm with a microplate reader (Stat Fax-2100, Miami, FL, USA). Nitrite release was expressed as the percentage of the initial sodium nitrite in conjugate (i.e. the total amount of nitrite in the medium divided by the total amount of sodium nitrite in conjugate x100%). GH release from AAc Si-nGH-Col and AAc Si-GH-Col tubes was determined by electrochemiluminescence. The GH concentration in the medium was quantified using an automatic analyzer (Roche Elecsys 2010, Hitachi, Tokyo, Japan).

The stability of the nNitrite or nGH on surface-modified silicone tubes was assessed after storage for 1, 2, and 3 months at 4°C, to assure that storage after preparation until clinical use does not affect nanoliposome stability. For this purpose, the AAc Si-nNitrite-nGH-Col tubes with 500 nmol/ml nNitrite and 1000 ng/ml nGH in conjugate were stored. After 1, 2, and 3 months of storage at 4°C, the tubes were put in culture medium at 37°C, and the release of nitrite and GH

was determined after 4, 12, 24, 48, 72, 96, and 120 h of incubation with culture medium and calculated as a function of the storage time [23].

Endothelial cell seeding, viability, and proliferation

Human umbilical vein endothelial cells (HUVECs) from the National Cell Bank, Pasteur Institute of Iran (Tehran, Iran), were used between passages 3 and 6 to evaluate cell attachment and proliferation on modified silicone tubes. After surface modification, triplicates of unmodified and surface-modified silicone tubes were put into petri dishes, sterilized with UV, washed twice with PBS solution, and washed once with culture medium before cell seeding. Hundred µl of endothelial cell suspension with $3x10^5$ cells/ml DMEM/F12 medium containing 10% fetal bovine serum (Gibco, Renfrewshire, Scotland) was infused from one end into the lumen of each sterile silicone tube using a syringe. Silicone tubes with endothelial cells were then rotated every 30 min for 4 h to promote homogeneous cell adhesion to the inner surface of the tubes. Then cells were cultured for 6 days in a humidified atmosphere of 5% CO_2 in air at 37°C, with medium replacement every 2 days.

The cytotoxicity of nanoliposomes was assessed by a live/dead assay. Unmodified silicone tubes were seeded with endothelial cells, and either filled with culture medium or with 10% (v/v) empty nanoliposomes in culture medium. After 48 h of culture, cell viability was observed using acridine orange-propidium iodide staining. Silicone tubes containing endothelial cells were incubated with an acridine orange-propidium iodide mixture for 10 min, and monitored under a fluorescence microscope. Live cells stained green while dead cells stained red [27].

Endothelial cell proliferation on surface-modified silicone tubes was estimated at days 2, 4, and 6 by using the 3-(4,5-dimethylthiazol-2-yl)-2,5 diphenyltetrazolium bromide (MTT) assay (Sigma-Aldrich, St. Louis, MO, USA) as described elsewhere [11, 27]. The absorbance was measured at 545 nm using an ELISA reader (Stat Fax-2100, Miami, FL, USA). The number of endothelial cells was quantified using a calibration curve with known cell numbers. At day 6, the attached cells were fixed, dehydrated in graded ethanol series, and stained with 5% Giemsa for optical microscopic examination. Three random photographs were taken in central and peripheral regions of each tube, and the surface area of 50 cells from each photograph was determined by an image-processing system (Image Pro Plus, version 6, Media Cybernetics, Bethesda, MD, USA) using the pixels per µm provided. The area covered with cells on each silicone tube was determined by multiplying the mean individual cell area by the number of cells counted. Cell confluency was expressed as percent of the tube surface covered with cells, and calculated as follows [28]:

$$\text{Confluency} = [(\text{area covered with cells } (mm^2)/\text{total surface area } (mm^2)] \times 100\%$$

NO and PGI_2 release by endothelial cells cultured on surface-modified silicone tubes

After 2 days of endothelial cell culture on unmodified or surface-modified silicone tubes, i.e. Si, AAc Si-Col, AAc Si-nNitrite-Col, AAc Si-nGH-Col, and AAc Si-nNitrite-nGH-Col, 0.5 ml medium was harvested for NO and PGI_2 determination. NO release by endothelial cells was measured as nitrite (NO^{2-}) accumulation in the medium, using the Griess method. PGI_2 production was determined by measuring the concentration of its stable metabolite 6-keto-prostaglandin $F_{1\alpha}$ (6-keto-$PGF_{1\alpha}$) using a 6-keto-$PGF_{1\alpha}$ enzyme immunoassay kit (Enzo, Lorrach, Germany) according to the manufacturer's protocol [29].

Statistical analysis

All data are expressed as mean ± standard deviation. Data were analyzed using one-way analysis of variance, and the significance of differences among means was determined by post-hoc comparisons, using Bonferroni's method. Two-way analysis of variance with pairwise comparison was used to assess differences among means between groups and over time. Differences were considered significant if the probability value (p)<0.05.

RESULTS

Biomimetic modification of silicone tubes using nNitrite-Col, nGH-Col, and nNitrite-nGH-Col conjugates was successfully established. Figure 1 shows the possible mechanism for the immobilization of nNitrite-Col, nGH-Col, and nNitrite-nGH-Col conjugates on silicone tubes, and the release of nitrite and/or GH from surface-modified silicone tubes. The abbreviations used for surface-modified silicone tubes are provided in the legend of Figure 1.

Encapsulation efficiency and size of nanoliposomes

The encapsulation efficiency of sodium nitrite or GH into nanoliposomes was 91.3±1.4% for sodium nitrite, and 98.1±2.1% for GH. The average size of nNitrite (diameter 112 nm) and nGH (diameter 117 nm) was similar.

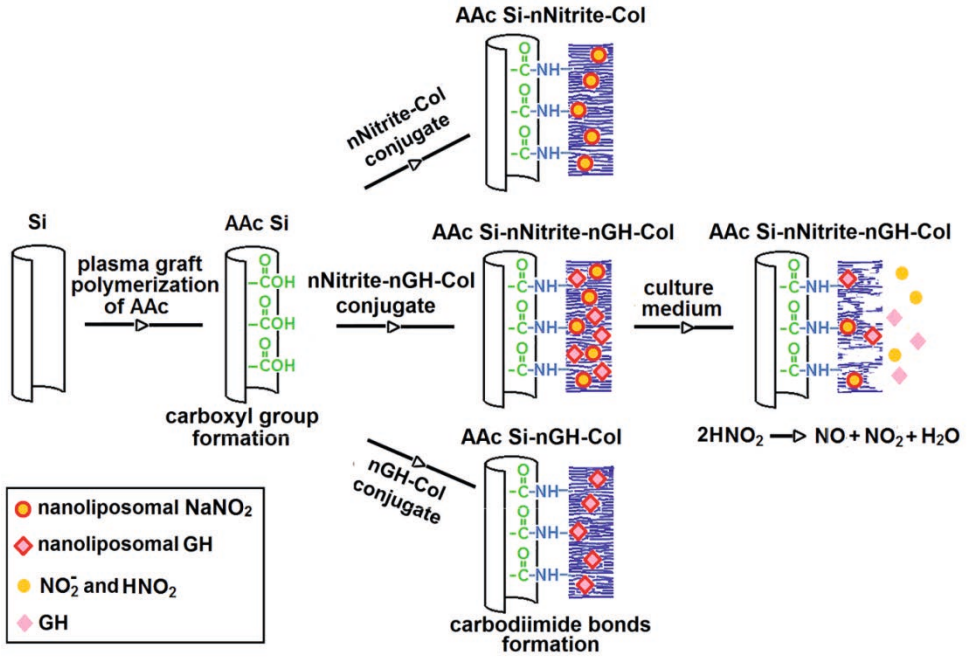

Figure 1. Schematic illustration of biomimetic modification of silicone tubes. Plasma surface-modified silicone tubes were immersed in an aqueous solution of AAc followed by plasma graft polymerization on a reabsorbed layer of AAc on silicone. AAc Si tubes with activated carboxyl groups were filled with nNitrite-Col conjugate to produce AAc Si-nNitrite-Col tubes, or with nGH-Col conjugate to produce AAc Si-nGH-Col tubes or with nNitrite-nGH-Col conjugate to produce AAc Si-nNitrite-nGH-Col tubes, and stored for 24 h at 4ºC for conjugate immobilization. AAc provides reactive carboxyl groups for generating carbodiimide bonds with amine groups on both nanoliposomes and collagen molecules. By filling the AAc Si-nNitrite-nGH-Col tubes with aqueous culture medium, the polymeric collagen might swell resulting in the release of the entrapped nGH and nNitrite particles. Si, silicone; AAc Si, acrylic acid-grafted silicone; AAc Si-Col, collagen immobilized acrylic acid-grafted silicone; AAc Si-nNitrite-Col, nanoliposomal sodium nitrite-collagen conjugate immobilized acrylic acid-grafted silicone; AAc Si-nGH-Col, nanoliposomal growth hormone-collagen conjugate immobilized acrylic acid-grafted silicone; AAc Si-nNitrite-nGH-Col, nanoliposomal sodium nitrite-nanoliposomal growth hormone-collagen conjugate immobilized acrylic acid-grafted silicone.

Wettability and mechanical properties of surface-modified silicone tubes

The hydrophilicity of unmodified and surface-modified silicone tubes, e.g. Si, AAc Si-Col, AAc Si-nNitrite-Col, AAc Si-nGH-Col, and AAc Si-nNitrite-nGH-Col, was assessed by measuring the water contact angles (Table 1). We found that the

water contact angles decreased after collagen immobilization via AAc grafting (Si: 102±4º; AAc Si-Col: 56±2º). nNitrite-Col conjugate coating with 500 nmol/ml nNitrite in conjugate, and nGH-Col conjugate coating with 1000 ng/ml nGH in conjugate significantly decreased the water contact angle compared with AAc Si-Col tubes (AAc Si-nNitrite-Col: 51±2º; AAc Si-nGH-Col: 50±2º, $p<0.05$). The water contact angles of AAc Si-nNitrite-nGH-Col tubes with different nNitrite and nGH concentrations were similar, ranging from 47° to 49°. These water contact angles were slightly lower than those of tubes with nNitrite-Col or nGH-Col coatings.

The ultimate tensile strength of AAc Si-nNitrite-nGH-Col tubes with different nNitrite and nGH concentrations ranged from 3.9 to 4.1 MPa, and was not significantly different from the ultimate tensile strength of AAc Si-Col tubes (3.6±0.5 MPa, $p<0.05$; Table 1). The percent elongation at break was more than 100% for Si, AAc Si-Col, AAc Si-nNitrite-Col, AAc Si-nGH-Col, and AAc Si-nNitrite-nGH-Col tubes, with no statistically significant differences observed between coatings (Table 1).

Table 1. Wettability and mechanical characteristics of unmodified and surface-modified silicone tubes, i.e. Si, AAc Si, AAc Si-nNitrite-Col, AAc Si-nGH-Col, and AAc Si-nNitrite-nGH-Col tubes. Values are mean ± standard deviation for 3 independent experiments. *Significantly different from AAc Si-Col tubes.

Tube, surface modification	nNitrite (nmol/ml)	nGH (ng/ml)	Wettability, water contact angle (º)	Ultimate tensile strength (MPa)	Elongation at break (%)
Si	0	0	102.1 ± 4.0	2.8 ± 0.8	255 ± 32
AAc Si-Col	0	0	56.3 ± 2.0	3.6 ± 0.5	305 ± 17
AAc Si-nNitrite-Col	50	0	51.4 ± 4.0	3.7 ± 0.3	280 ± 13
	500	0	50.7 ± 2.5*	4.0 ± 0.4	302 ± 11
AAc Si-nGH-Col	0	100	52.3 ± 1.3	3.9 ± 0.6	300 ± 9
	0	1000	49.7 ± 2.0*	3.8 ± 0.7	297 ± 12
AAc Si-nNitrite-nGH-Col	50	100	49.2 ± 4.2	3.9 ± 0.4	274 ± 10
	50	1000	47.4 ± 2.7*	4.0 ± 0.3	282 ± 11
	500	100	48.5 ± 3.2*	4.0 ± 0.6	307 ± 18
	500	1000	47.9 ± 1.9*	4.1 ± 0.3	310 ± 15

Nitrite and/or GH release from nanoliposomes immobilized on silicone tubes

To assess the sustained release ability of nNitrite, the percentage nitrite released from AAc Si-nNitrite-Col tubes with 500 nmol/ml nNitrite in conjugate was measured, and compared with the percentage nitrite released from AAc Si-Nitrite-Col tubes with 500 nmol/ml of the free form of sodium nitrite in conjugate (Figure 2a). For AAc Si-Nitrite-Col tubes, most nitrite was released during the first 24 h, but not anymore thereafter. The nNitrite on AAc Si-nNitrite-Col tubes gradually released nitrite during 72 h to a lower amount than from AAc Si-Nitrite-Col tubes. However, after 72 h the release of nitrite from AAc Si-nNitrite-Col tubes increased and was even higher than the release from AAc Si-Nitrite-Col tubes. After 120 h incubation, 58% nitrite was released from AAc Si-nNitrite-Col tubes and 48% from AAc Si-Nitrite-Col tubes. By adding 100 or 1000 ng/ml nGH to the conjugate in AAc Si-nNitrite-nGH-Col tubes, the release of nitrite slightly, but not significantly, decreased compared with AAc Si-nNitrite-Col tubes (data not shown).

The percentage of GH released from AAc Si-nGH-Col tubes with 1000 ng/ml nGH in conjugate was compared to that released from the AAc Si-GH-Col tubes (Figure 2b). nGH on AAc Si-nGH-Col tubes gradually released GH during 120 h of incubation. This GH release was higher than from AAc Si-GH-Col tubes. The release of GH from AAc Si-GH-Col tubes stoped at 72 h. After 120 h incubation, 22% GH was released from AAc Si-nGH-Col tubes, while only 10% GH was released from AAc Si-GH-Col tubes. By adding 50 or 500 nmol/ml nNitrite to the conjugate in AAc Si-nNitrite-nGH-Col tubes, the release of GH was not significantly changed compared with AAc Si-nGH-Col tubes (data not shown).

Stability of nanoliposomes on AAc Si-nNitrite-nGH-Col tubes during a 3 months storage period

A possible effect of storage of AAc Si-nNitrite-nGH-Col tubes at 4°C for 1, 2, or 3 months on the release potential of nNitrite and nGH was assessed (Figure 2c,d). There were no changes in the percentage of nitrite released from nNitrite as a result of storage at 4°C for 1 month (Figure 2c, $p>0.05$). After 2 months of storage, the percentage of nitrite released from nanoliposomes significantly decreased compared with the release from fresh nanoliposomes ($p<0.05$, at all-time points measured). After 3 months of storage, the percentage of nitrite released did decrease even more compared with the release from fresh nanoliposomes, with no release anymore after 48 h (Figure 2c). The percentage of GH released from AAc Si-nNitrite-nGH-Col tubes after storage showed that nanoliposomes loaded with GH were stable until 2 months (Figure 2d). After 2 months of storage, GH was continuously released until 96 h, but not anymore thereafter. After 3 months of storage, the release of GH significantly decreased compared with that from fresh nanoliposomes. This indicates that the nanoliposomes in nNitrite-nGH-Col conjugate coating of AAc Si-nNitrite-nGH-Col tubes was not stable after storage for

2 and 3 months at 4°C. Therefore, these surface-modified tubes should only be stored for a period up to 1 month at 4°C.

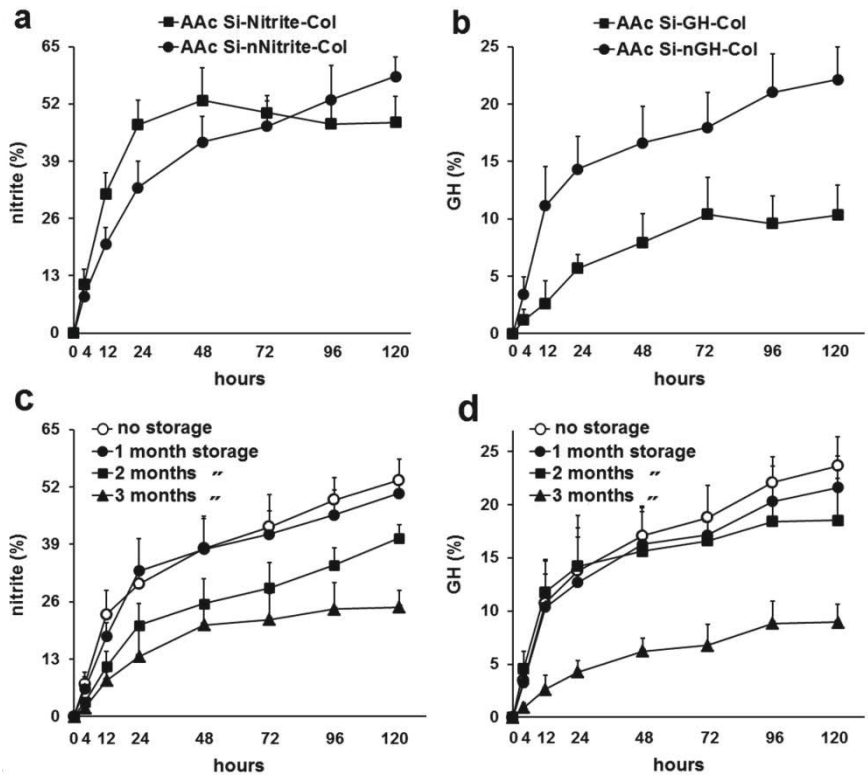

Figure 2. Nitrite and GH release from surface-modified silicone tubes in the culture medium at 37°C, immediately after preparation and storage for 1, 2, or 3 months at 4°C. (a) Nitrite release from AAc Si-nNitrite-Col and AAc Si-Nitrite-Col tubes with 500 nmol/ml nNitrite or Nitrite in conjugate immediately after preparation. (b) GH release from AAc Si-nGH-Col and AAc Si-GH-Col tubes with 1000 ng/ml nGH or GH in conjugate immediately after preparation. (c) Nitrite, and (d) GH release from AAc Si-nNitrite-nGH-Col tubes with 500 nmol/ml nNitrite and 1000 ng/ml nGH in conjugate after storage for 1, 2, or 3 months at 4°C. The nanoliposomes in nNitrite-nGH-Col conjugate coating of AAc Si-nNitrite-nGH-Col tubes were stable after 1 month storage at 4°C, but not after longer storage periods. Nitrite and GH release were expressed as % of the initial amount of sodium nitrite and GH in nanoliposomes or in conjugate. n=3. nNitrite, nanoliposomal sodium nitrite; nGH, nanoliposomal growth hormone; AAc Si-nNitrite-Col, nNitrite-collagen conjugate immobilized AAc-grafted silicone; AAc Si-nGH-Col, nGH-collagen conjugate immobilized AAc-grafted silicone; AAc Si-nNitrite-nGH-Col, nNitrite-nGH-collagen conjugate immobilized AAc-grafted silicone.

No cytotoxic effects of nanoliposomes on endothelial cells

The cytotoxicity of prepared nanoliposomes was assessed by live/dead assay after 48 h incubation with seeded endothelial cells (Figure 3a). Cell viability on silicone tubes filled with culture medium containing 10% (v/v) empty nanoliposomes was 96%, which was comparable with cell viability on silicone tubes filled with pure culture medium (98%; Figure 3a).

Nitrite and/or GH release from surface-modified silicone tubes affected endothelial cell proliferation and confluency

Collagen immobilization on silicone tubes (AAc Si-Col) increased endothelial cell numbers by 1.6-fold compared with unmodified silicone tubes after 2 days of culture ($p<0.05$, Figure 3b). Fifty nmol/ml nNitrite in conjugate stimulated by 1.7-fold ($p<0.05$), but 500 nmol/ml nNitrite did not change endothelial cell number on AAc Si-nNitrite-Col tubes compared with AAc Si-Col tubes. More endothelial cells were present on AAc Si-nGH-Col tubes compared with AAc Si-nNitrite-Col tubes (Figure 3b). By increasing the concentration of nGH from 100 to 1000 ng/ml on AAc Si-nGH-Col tubes, the endothelial cell number increased by 1.4-fold ($p<0.005$) after two days of culture. The number of endothelial cells on AAc Si-nGH-Col tubes with 1000 ng/ml nGH in conjugate was 2.6-fold higher ($p<0.0005$) than on AAc Si-Col tubes, 1.5-fold higher ($p<0.005$) than on AAc Si-nNitrite-Col tubes with 50 nmol/ml nNitrite, and 2.8-fold higher ($p<0.0005$) than on AAc Si-nNitrite-Col tubes with 500 nmol/ml nNitrite in the conjugate. The presence of 100 ng/ml nGH in nNitrite-nGH-Col conjugate coating with 50 or 500 nNitrite did not affect endothelial cell number on AAc Si-nNitrite-nGH-Col tubes compared with AAc Si-nNitrite-Col tubes. However, 1000 ng/ml nGH in nNitrite-nGH-Col conjugate increased cell number compared with AAc Si-nNitrite-Col tubes with 50 nmol/ml nNitrite (1.4-fold, $p<0.05$) or 500 nmol/ml nNitrite in conjugate (2.3-fold, $p<0.005$; Figure 3b).

Optical micrographs of endothelial cells attached on Si, AAc Si-Col, and AAc Si-nNitrite-nGH-Col tubes with 50 or 500 nmol/ml nNitrite, and 100 or 1000 ng/ml nGH in conjugate, were used to assess endothelial cell confluency after 6 days of culture (Figure 4a-f). The level of cell confluency was dependent on the surface modification used. The number of endothelial cells on Si tubes was very low, as well as cell confluency (22%) after 6 days of culture (Figure 4a). Cell confluency was 74% on AAc Si-Col tubes (Figure 4b). Although endothelial cells on AAc Si-Col tubes did show excellent proliferation, they did not form a confluent monolayer on the silicone surface. The level of cell confluency on silicone tubes with a collagen coating containing 50 nmol/ml nNitrite and 100 ng/ml nGH increased to 98% (Figure 4c). By increasing the amount of nNitrite to 500 nmol/ml, cell confluency decreased to 83% (Figure 4d). Increasing the initial amount of nGH to 1000 ng/ml in conjugate coating of AAc Si-nNitrite-nGH-Col tubes resulted in >100% cell confluency within 6 days (Figure 4e,f).

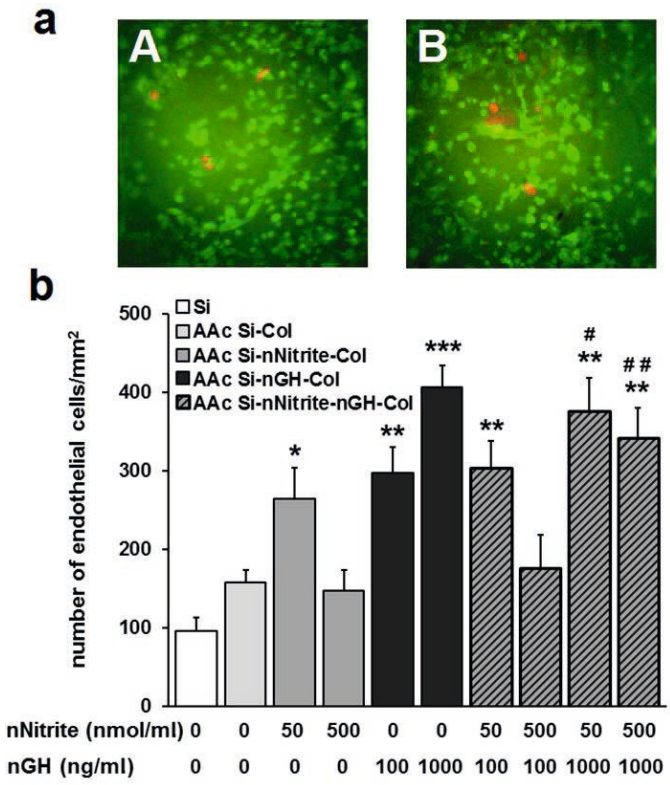

Figure 3. Cytotoxicity of nanoliposomes and effect of nNitrite and/or nGH conjugation with collagen coating on endothelial cell numbers after 2 days of culture. (a) Acridine orange-propidium iodide staining of endothelial cells cultured for 2 days on silicone tubes filled with culture medium with or without nanoliposomes. (A) Endothelial cells incubated with culture medium, and (B) Endothelial cells incubated with 10% (v/v) empty nanoliposomes in culture medium. (b) Effect of surface-modified silicone tubes with different nNitrite and/or nGH in the conjugate coating, i.e. AAc Si-Col, AAc Si-nNitrite-Col, AAc Si-nGH-Col, and AAc Si-nNitrite-nGH-Col, on the number of endothelial cells after 2 days of culture. Maximum cell number was observed on AAc Si-nGH-Col and AAc Si-nNitrite-nGH-Col tubes with 1000 ng/ml nGH in conjugate coating. nNitrite, nanoliposomal sodium nitrite; nGH, nanoliposomal growth hormone; Si, silicone; AAc Si-Col, collagen immobilized AAc-grafted silicone; AAc Si-nNitrite-Col, nNitrite-collagen conjugate immobilized AAc-grafted silicone; AAc Si-nGH-Col, nGH-collagen conjugate immobilized AAc-grafted silicone; AAc Si-nNitrite-nGH-Col, nNitrite-nGH-collagen conjugate immobilized AAc-grafted silicone. *Significantly different from AAc Si-Col tubes, $p<0.05$, **$p<0.005$, ***$p<0.0005$; $^{\#}$Significantly different from AAc Si-nNitrite-Col tubes, $p<0.05$, $^{\#\#}p<0.005$.

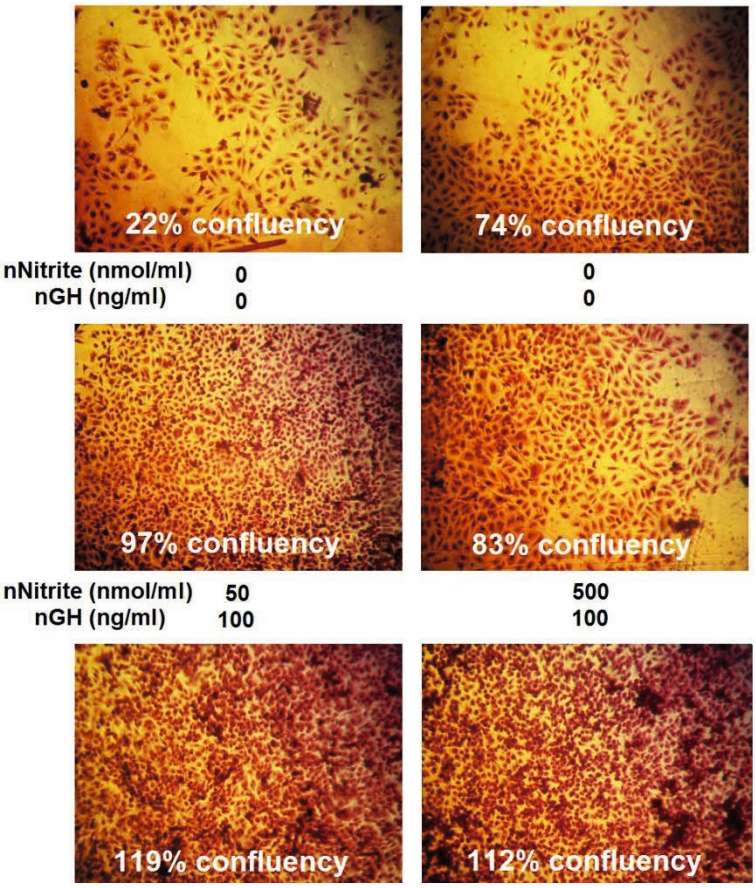

Figure 4. Optical micrographs showing endothelial cell confluency after 6 days culture. (a) Si, (b) AAc Si-Col, (c) AAc Si-nNitrite-nGH-Col with 50 nmol/ml nNitrite and 100 ng/ml nGH in conjugate, (d) AAc Si-nNitrite-nGH-Col with 500 nmol/ml nNitrite and 100 ng/ml nGH in conjugate, (e) AAc Si-nNitrite-nGH-Col with 50 nmol/ml nNitrite and 1000 ng/ml nGH in conjugate, and (f) AAc Si-nNitrite-nGH-Col with 500 nmol/ml nNitrite and 1000 ng/ml nGH in conjugate. AAc Si-nNitrite-nGH-Col tubes with 50 or 500 nmol/ml nNitrite and 1000 ng/ml nGH in conjugate resulted in >100% cell confluency within 6 days. Magnification x200. nNitrite, nanoliposomal sodium nitrite; nGH, nanoliposomal growth hormone; Si, silicone; AAc Si-Col, collagen immobilized AAc-grafted silicone; AAc Si-nNitrite-nGH-Col, nNitrite-nGH-collagen conjugate immobilized AAc-grafted silicone.

Platelet adhesion on unmodified and surface-modified silicone tubes

Platelet adhesion on unmodified and surface-modified silicone tubes was investigated before and after endothelialization (Figure 5). Without endothelial cell seeding, platelet adhesion on AAc Si-Col tubes was increased by 27% compared with Si tubes ($p<0.05$, Figure 5a). AAc Si-nNitrite-Col tubes suppressed platelet adhesion compared with AAc Si-Col tubes by 2.1-fold when 50 nmol/ml nNitrite was present in nNitrite-Col conjugate ($p<0.005$), and by 3.5-fold with 500 nmol/ml nNitrite in conjugate ($p<0.005$). There was a linear relationship between the initial concentration of nNitrite in nNitrite-Col conjugate with the degree of platelet adhesion on AAc Si-nNitrite-Col tubes. Platelet adhesion to AAc Si-nGH-Col tubes was slightly but not significantly lower than AAc Si-Col tubes. The combination of nNitrite and nGH at different concentrations in the collagen coating decreased platelet adhesion compared with collagen coating alone. AAc Si-nNitrite-nGH-Col tubes with 500 nmol/ml nNitrite and 1000 ng/ml nGH inhibited platelet adhesion by 78% ($p<0.005$) compared with AAc Si-Col tubes. Platelet adhesion onto PEG Si tubes, used as controls, was low compared to other unmodified and surface-modified silicone tubes ($p<0.05$, Figure 5a).

Endothelialization of silicone tubes decreased the percentage of platelet adhesion on unmodified and surface-modified tubes by 50-75% compared with silicone tubes without endothelial cells (Figure 5b). Platelet adhesion to AAc Si-Col tubes and Si tubes after endothelialization was similar. AAc Si-nNitrite-Col tubes suppressed platelet adhesion compared with AAc Si-Col tubes by 1.8-fold when 50 nmol/ml nNitrite was present in the nNitrite-Col conjugate ($p<0.05$), and by 2.3-fold with 500 nmol/ml nNitrite in conjugate ($p<0.005$). Platelet adhesion to AAc Si-nGH-Col tubes with 100 ng/ml nGH decreased slightly, but not significantly, by 13% ($p>0.05$), and with 1000 ng/ml by 31% ($p<0.05$) compared with AAc Si-Col tubes. Platelet adhesion to AAc Si-nGH-Col tubes with both 100 and 1000 ng/ml nGH in conjugate before endothelialization was similar (Figure 5a). AAc Si-nNitrite-nGH-Col tubes with different nNitrite and nGH concentrations in conjugate suppressed platelet adhesion compared with collagen coating alone in the presence of endothelial cells. Platelet adhesion to AAc Si-nNitrite-nGH-Col tubes with 1000 ng/ml nGH decreased by 76% ($p<0.005$) when 50 nmol/ml nNitrite was used, and by 73% ($p<0.005$) when 500 nmol/ml nNitrite was used compared with AAc Si-Col tubes.

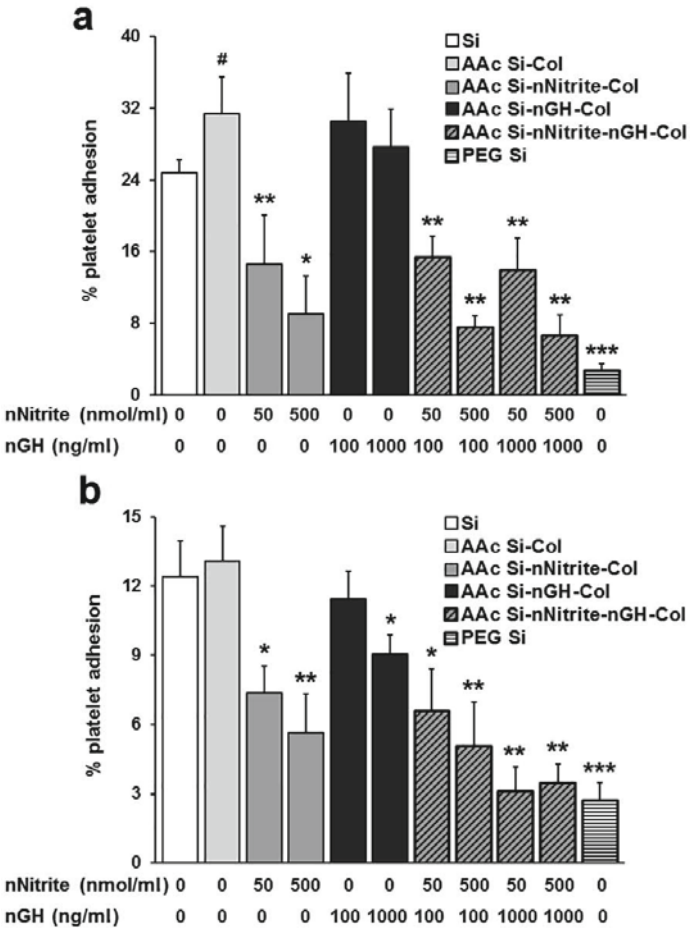

Figure 5. Effect of surface modification on platelet adhesion onto silicone tubes in the absence and presence of endothelial cells. (a) Platelet adhesion (expressed as % of the initial amount of platelet numbers in PRP solution) on surface-modified silicone tubes in the absence of endothelial cells. (b) Platelet adhesion (expressed as % of the initial amount of platelet numbers in PRP solution) on surface-modified silicone tubes in the presence of endothelial cells. AAc Si-nNitrite-nGH-Col tubes with 500 nmol/ml nNitrite and 1000 ng/ml nGH in conjugate inhibited platelet adhesion by 79% in the absence of endothelial cells, and by 73% in the presence of endothelial cells compared with AAc Si-Col tubes. nNitrite, nanoliposomal sodium nitrite; nGH, nanoliposomal growth hormone; Si, silicone; AAc Si-Col, collagen immobilized AAc-grafted silicone; AAc Si-nNitrite-Col, nNitrite-collagen conjugate immobilized AAc-grafted silicone; AAc Si-nGH-Col, nGH-collagen conjugate immobilized AAc-grafted silicone; AAc Si-nNitrite-nGH-Col, nNitrite-nGH-collagen conjugate immobilized AAc-grafted silicone. *Significantly different from AAc Si-Col tubes, $p<0.05$, **$p<0.005$, ***$p<0.0005$, $^{\#}$Significantly different from Si tubes, $p<0.05$.

GH release from AAc Si-nGH-Col or AAc Si-nNitrite-nGH-Col tubes stimulated endothelial cell-derived NO

Silicone tubes with coatings containing nNitrite (an anti-thrombotic agent) reduced platelet adhesion in the absence or presence of endothelial cells (Figure 5). However, unmodified or surface-modified silicone tubes without nNitrite in the coating, i.e. Si, AAc Si-Col, and AAc Si-nGH-Col tubes, also decreased platelet adhesion in the presence of endothelial cells. Since NO inhibits platelet aggregation and adhesion, the ability of endothelial cells seeded on these tubes to secrete NO indicates the anti-thrombotic property of these cell-seeded tubes. Endothelial cells cultured on Si tubes released low amounts of NO (0.51 nmol/ml; Figure 6). Collagen immobilization on silicone tubes increased NO release by endothelial cells by 3.5-fold compared with NO release by endothelial cells on Si tubes ($p<0.05$). GH released from AAc Si-nGH-Col tubes stimulated NO release by endothelial cells. NO release by endothelial cells cultured on AAc Si-nGH-Col tubes with 1000 ng/ml nGH, but not 100 ng/ml nGH in the conjugate significantly increased by 4.5-fold ($p<0.005$) compared with AAc Si-Col tubes.

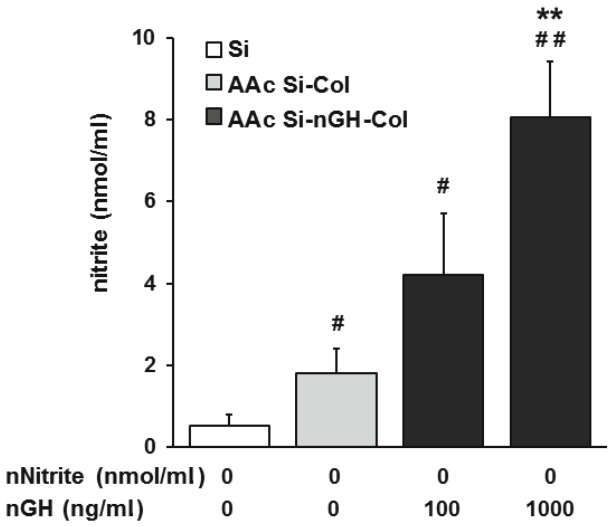

Figure 6. Effect of GH release from AAc Si-nGH-Col tubes on endothelial cell-derived NO production after 2 days cell culture. AAc Si-nGH-Col tubes with 1000 ng/ml nGH increased NO release by endothelial cells by 4.5-fold compared with AAc Si-Col tubes. nNitrite, nanoliposomal sodium nitrite; nGH, nanoliposomal growth hormone; AAc Si-Col, collagen immobilized AAc-grafted silicone; AAc Si-nGH-Col, nGH-collagen conjugate immobilized AAc-grafted silicone. **Significantly different from AAc Si-Col tubes, $p<0.005$, #Significantly different from Si tubes, $p<0.05$, ##$p<0.005$.

Nitrite released from AAc Si-nNitrite-nGH-Col tubes stimulated $PGF_{1\alpha}$ production by endothelial cells

AAc Si-nNitrite-Col tubes with 500 nmol/ml, but not 50 nmol/ml nNitrite in conjugate increased $PGF_{1\alpha}$ production by 1.8-fold ($p<0.05$) in endothelial cells, compared with AAc Si-Col tubes (Figure 7). GH released from AAc Si-nGH-Col tubes with both 100 and 1000 ng/ml nGH in conjugate had no significant effect on $PGF_{1\alpha}$ production. AAc Si-nNitrite-nGH-Col tubes stimulated $PGF_{1\alpha}$ production by 1.7-fold (AAc Si-nNitrite-nGH-Col tubes with 50 nmol/ml nNitrite and 100 ng/ml nGH in conjugate; $p<0.05$) to 2.2-fold (AAc Si-nNitrite-nGH-Col tubes with 500 nmol/ml nNitrite and 1000 ng/ml nGH in conjugate; $p<0.005$) compared with AAc Si-Col tubes.

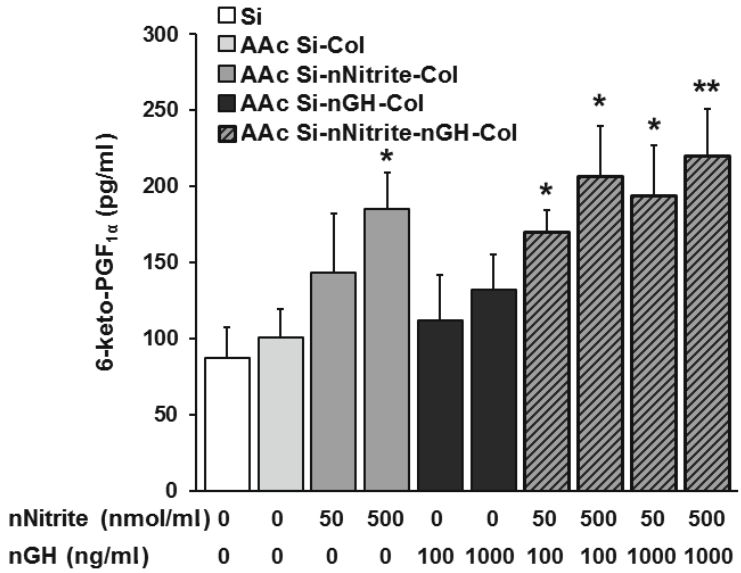

Figure 7. Effect of surface modification of silicone tubes on endothelial cell-derived $PGF_{1\alpha}$ production. $PGF_{1\alpha}$ production was quantified by measuring the concentration of its stable metabolite 6-keto-prostaglandin $F_{1\alpha}$ (6-keto-$PGF_{1\alpha}$). $PGF_{1\alpha}$ production by endothelial cells on AAc Si-nNitrite-nGH-Col tubes with 500 nmol/ml nNitrite and 1000 ng/ml nGH in conjugate was 2.2-fold higher than on AAc Si-Col tubes. nNitrite, nanoliposomal sodium nitrite; nGH, nanoliposomal growth hormone; AAc Si-Col, collagen immobilized AAc-grafted silicone; AAc Si-nNitrite-nGH-Col, nNitrite-nGH-collagen conjugate immobilized AAc-grafted silicone. *Significantly different from AAc Si-Col tubes, $p<0.05$, **$p<0.005$.

DISCUSSION

Endothelium is the perfect natural blood compatible surface which secretes various substances affecting platelet adhesion and aggregation [3, 4]. Therefore, creating a functional lining of endothelial cells on blood-contacting parts of medical devices might increase the biocompatibility of these devices. Currently available synthetic materials used in medical devices, such as silicone, are unsuitable as a substrate for endothelial cell seeding and need to be surface modified [3]. The immobilization of different biomolecules on material surfaces improves blood compatibility [12-14], and enhances cell attachment and proliferation [16, 18, 21]. Anti-coagulant molecules act as anti-thrombotic agents, but are not suitable for endothelial cell attachment and growth. Promotion of endothelial cell attachment and growth by extracellular matrix molecules causes deterioration of blood compatibility [18]. Thus a biomaterial surface immobilized with different biomolecules possessing anti-thrombotic and growth-inducing properties might improve both anti-coagulation and endothelialization, thus providing a potential application for long-term use of blood-contacting medical devices [16, 18].

It is generally accepted that collagen, the main protein in the extracellular matrix, is suitable as a coating for endothelial cell attachment and growth [8]. However, collagen is highly thrombogenic, and accelerates platelet aggregation in those areas of a material which are not fully covered by endothelial cells [16]. Therefore, suppression of the thrombogenic properties of collagen by using anti-thrombotic agents on the one hand, and promotion of endothelial cell growth using growth-inducing agents to achieve a confluent cell layer on the material surface on the other hand, may result in improved blood-contacting medical devices performance. We aimed to develop a collagen coating on silicone tubes that prevents platelet adhesion by sustained release of nitrite, and that induces endothelial cell growth by sustained release of GH.

Nanoliposomes loaded with sodium nitrite or GH were used to control the sustained release of these anti-thrombotic and growth-inducing agents. The encapsulation efficiency achieved was high, i.e. >90% for both sodium nitrite and GH, showing the effectiveness of the thin-film hydration technique used for the preparation of nanoliposomes. The presence of PEG in the nanoliposome structure increased the hydrophilicity of the nanoliposomes, which efficiently hinders hydrophilic drug escape to outer water, and results in a high encapsulation efficiency [30]. The slightly higher GH encapsulation efficiency than sodium nitrite encapsulation efficiency is probably due to the higher molecular weight of GH (sodium nitrite: 69 g/mol; GH: 22124 g/mol), that likely hindered its escape to the outer solution during solvent evaporation [30].

To study the interaction between endothelial cells and nNitrite-nGH-Col conjugate coating, a well-defined and stable coating is required. Therefore, AAc

was graft polymerized on silicone tubes, providing a surface with reactive carboxyl groups to form carbodiimide bonds with amine groups on both collagen and nanoliposomes. A covalent immobilization of biological agents through carbodiimide bonds is more stable and shows improved resistance to fluid shear stress, and its biofunction lasts longer than with other bonding methods, such as physical adsorption, entrapment, etc. [18, 31, 32]. Therefore, in this study nNitrite-nGH-Col conjugate was co-immobilized on AAc-grafted silicone tubes to provide a stable coating that offers both anti-thrombotic and growth-inducing properties.

Drug liposomal formulations provide improved drug solubility, longer drug circulation times, and focused drug delivery, compared to free drugs [19, 22, 23, 33]. Our observations on nitrite released from nNitrite-Col conjugate agree with observations by others on the interaction between a lipid bilayer of nanoliposomes and collagen fibrils, that offers improved stability and decreased permeability of nitrite compared with nitrite released from Nitrite-Col conjugate [33]. AAc Si-nGH-Col tubes released GH at a higher rate than AAc Si-GH-Col tubes. This can be explained by the fact that GH is a high molecular weight peptide, and when in free form combined with collagen, the chains of GH get completely stuck with the chains of collagen, which makes it hard for GH molecules to be released. Encapsulation of GH in nanoliposomes hindered the direct mixing of GH with collagen, which led to more rapid release of GH from the AAc Si-nGH-Col tubes than from AAc Si-GH-Col tubes. The faster release of sodium nitrite than GH from nanoliposomes can be explained by the lower molecular weight of sodium nitrite than GH.

The surface-modified silicone tubes containing nNitrite and nGH were stable for 1 month storage at 4°C. The presence of cholesterol and amino-PEG in the lipid phase of nanoliposomes increases nanoliposome stability, and controls the release rate [34]. Rapid leakage of the low-molecular weight sodium nitrite from the nanoliposomes during storage for 2 months at 4°C significantly decreased nitrite released from nanoliposomes. After 3 months of storage at 4°C, the release of nitrite and GH from the nanoliposomes decreased significantly, which indicates that the surface-modified silicone tubes can be stored for 1 month at 4°C, but not for longer time periods.

It is generally accepted that hydrophilic materials support cell adhesion and consequently improve their biocompatibility [21, 24]. The hydrophilicity of silicone tubes improved after collagen immobilization, especially with collagen conjugates with nNitrite, and/or nGH. A material surface with either a very high or a very low contact angle is not suitable for cell attachment [24]. Therefore the moderate wettability of the surface-modified silicone tubes in this study makes them suitable substrates for endothelial cell attachment.

Not only cell attachment onto a material, but also cell growth is important to reach cell confluency on material surface. NO has been shown to stimulate

endothelial cell proliferation, while reducing platelet adhesion [15, 35]. Nitrite, the stable end-product of NO metabolism, may represent a potential source of NO and can be used as a NO donor under hypoxia conditions or in an acidic environment [15, 36]. We have shown previously that nitrite-generating sodium nitrite-collagen conjugate coating of silicone tubes with 5 to 50 μM sodium nitrite increases the number of endothelial cells more than collagen coating alone, probably via GH production [15]. In this study, we show that conjugation of collagen with 50 nmol/ml nNitrite increased the number of endothelial cells after 48 h of culture. Although the amount of nitrite released from nNitrite-Col conjugate was lower than from Nitrite-Col conjugate during 72 h, the slow but continuous release of nano-sized nitrite was more effective to stimulate endothelial cell proliferation.

GH treatment of endothelial cells reduces intracellular reactive oxygen species (ROS) production and regulates the synthesis of multiple mRNA species, including that of insulin-like growth factor-1 (IGF-1) and endothelial nitric oxide synthase (eNOS) [17, 37]. GH (200 pg/l) stimulates proliferation of cultured human retinal microvascular endothelial cells but not HUVECs [37]. Our study also shows that endothelial cells respond to GH with enhanced proliferation. The stimulatory effect of GH released from AAc Si-nGH-Col tubes with 1000 ng/ml nGH in conjugate on endothelial cell proliferation was higher than that nitrite released from AAc Si-nNitrite-Col tubes with 50 nmol/ml nNitrite in conjugate. Combination of nNitrite with nGH-Col conjugate in AAc Si-nNitrite-nGH-Col tubes did not hamper GH release from nGH as indicated by the increased number of endothelial cells on AAc Si-nNitrite-nGH-Col tubes compared with AAc Si-Col tubes.

The adhesion and activation of platelets on a biomaterial surface often leads to coagulation and thrombus formation [13]. NO is widely recognized as a potent inhibitor of platelet adhesion and activation [13, 14]. The extraordinarily thromboresistant nature of blood vessel inner walls is, in part, due to the continuous production of NO by the endothelial cells lining the blood vessels [13]. Improved blood compatibility of NO-releasing polymeric materials has been shown in animal studies [13, 14]. Previously we showed that sodium nitrite-collagen conjugate coating of silicone tubes with 500 nmol/ml sodium nitrite exerts strong anti-platelet activity [15]. Interestingly, sustained release of nitrite from nNitrite-Col conjugate more strongly inhibited platelet adhesion than nitrite release from Nitrite-Col conjugate. Sodium nitrite stimulates NO production by endothelial cells lining the vessel wall in a NOS-independent manner [38]. Therefore by endothelial cell seeding of AAc Si-nNitrite-Col tubes, not only nitrite released from nNitrite-Col conjugate, but also NO release by endothelial cells helps in increased anti-platelet activity of these tubes.

GH released from nGH-Col conjugate in AAc Si-nGH-Col tubes did not significantly inhibit platelet adhesion in the absence of endothelial cells. The presence of the anti-thrombotic polymer PEG in the nanoliposome's structure

prevents platelet adhesion [39]. Therefore, all surface-modified silicone tubes containing nanoliposomes in their coatings, even without anti-thrombotic agent (e.g. AAc Si-nGH-Col tubes), showed reduced platelet adhesion. Although platelet inhibition caused by nanoliposomes themselves on AAc Si-nGH-Col tubes was not significant. After endothelialization of surface-modified silicone tubes, platelet adhesion was decreased on AAc Si-nGH-Col tubes compared with platelet adhesion on the same tubes in the absence of endothelial cells. This indicates that GH might increase the anti-thrombotic function of endothelial cells, which includes anti-coagulation, prevention of inflammatory cytokines production, and adhesion of the inflammatory cells, which is mostly controlled by the release of functional factors, such as NO, PGI_2, and thrombomodulin, by endothelial cells [13, 16].

The GH released resulted in increased NO release by endothelial cells on AAc Si-nGH-Col tubes. This indicates that GH not only affects endothelial cell proliferation, but also the anti-thrombotic function. Our results agree with data by others showing that somatropin treatment of endothelial cells increases NO production through eNOS activation [40]. High somatropin concentrations (100-1000 ng/ml) enhance eNOS mRNA expression, whereas NO production was only increased with GH at the highest dose of 1000 ng/ml [40]. We have shown earlier that nitrite release, which can continuously convert to NO, stimulates GH production by endothelial cells [15]. Since nitrite stimulates GH production by endothelial cells, and because GH released enhances NO production by endothelial cells, preparation of a surface with the ability to release nitrite and GH may play a significant role in endothelialization of blood-contacting parts of biomedical devices.

GH released from nGH-Col conjugate on AAc Si-nGH-Col tubes did not significantly affect $PGF_{1\alpha}$ production, independent of the concentration in the conjugate. nNitrite at 500 nmol/ml in AAc Si-nNitrite-Col tubes significantly increased the production of $PGF_{1\alpha}$ by endothelial cells, which agrees with data published by others [41]. Conjugation of nNitrite with nGH and collagen in AAc Si-nNitrite-nGH-Col tubes stimulated $PGF_{1\alpha}$ production by endothelial cells. This shows excellent functionality of endothelial cells on AAc Si-nNitrite-nGH-Col tubes, which is important when endothelial cell seeding is used to improve the biocompatibility of blood-contacting medical devices.

CONCLUSIONS

Encapsulation of sodium nitrite or GH in nanoliposomes followed by addition of nNitrite and/or nGH to the surface coating of silicone tubes increased the sustained release as well as the effectiveness, and bioavailability of these bioactive compounds. Nanoliposomes also allowed stability of surface-modified silicone

tubes after storage. AAc Si-nNitrite-nGH-Col tubes with nNitrite (500 nmol/ml) and nGH (1000 ng/ml) in conjugate coating provided full endothelial coverage, and low platelet adhesion even in the absence of endothelial cells, suggesting that nNitrite-nGH-Col conjugate coatings are highly promising to promote endothelialization of silicone materials in blood-contacting devices.

ACKNOWLEDGMENTS

The authors are grateful to Dr. Atefeh Solouk for valuable advice on plasma graft polymerization of silicone tubes, and Dr. Nooshin Haghighipour for help in cell seeding.

REFERENCES

1 Anderson JM. Biological responses to materials. Annu Rev Mater Res 2001;31:81-110.
2 Busch R, Strohbach A, Rethfeldt S, Walz S, Busch M, Petersen S, Felix S, Sternberg K. New stent surface materials: The impact of polymer-dependent interactions of human endothelial cells, smooth muscle cells, and platelets. Acta Biomater 2014;10:688-700.
3 Polk AA, Maul TM, McKeel DT, Snyder TA, Lehocky CA, Pitt B, Stolz DB, Federspiel WJ, Wagner WR. A biohybrid artificial lung prototype with active mixing of endothelialized microporous hollow fibers. Biotechnol Bioeng 2010;106:490-500.
4 Lim HR, Baek HS, Lee MH, Woo YI, Han DW, Han MH. Surface modification for enhancing behaviors of vascular endothelial cells onto polyurethane films by microwave-induced argon plasma. Surf Coat Technol 2008;202:5768-5772.
5 Tiller JC, Bonner G, Pan LC, Klibanov AM. Improving biomaterial properties of collagen films by chemical modification. Biotechnol Bioeng 2001;73:246-252.
6 Sano S, Kato K, Ikada Y. Introduction of functional groups onto the surface of polyethylene for protein immobilization. Biomaterials 1993:14:817-822.
7 Solouk A, Cousins BG, Mirahmadi F, Mirzadeh H, Jalali Nadoushan MR, Shokrgozar MA, Seifalian AM. Biomimetic modified clinical-grade POSS-PCU nanocomposite polymer for bypass graft applications: A preliminary assessment of endothelial cell adhesion and haemocompatibility. Mater Sci Eng C Mater Biol Appl 2015;46:400-408.
8 Jokinen J, Dadu E, Nykvist P, Kapyla J, White DJ, Ivaska J, Vehvilainen P, Reunanen H, Larjava H, Hakkinen L, Heino J. Integrin-mediated cell adhesion to type I collagen fibrils. J Biol Chem 2004;279:31956-31963.
9 Suchyta DJ, Handa H, Meyerhoff ME. A nitric oxide-releasing heparin conjugate for delivery of a combined antiplatelet/anticoagulant agent. Mol Pharm 2014;11:645-650.
10 Ding Y, Yang M, Yang Z, Luo R, Lu X, Huang N, Huang P, Leng Y. Cooperative control of blood compatibility and re-endothelialization by immobilized heparin and substrate topography. Acta Biomater 2015;15:150-163.
11 Kabirian F, Amoabediny G, Haghighipour N, Salehi-Nik N, Zandieh-Doulabi B. Nitric oxide secretion by endothelial cells in response to fluid shear stress, aspirin, and temperature. J Biomed Mater Res A 2014;103:1231-1237.
12 Phaneuf MD, Berceli SA, Bide MJ, Quist WC, LoGerfo FW. Covalent linkage of recombinant hirudin to poly(ethylene terephthalate): creation of a novel antithrombin surface. Biomaterials 1997;18:755-765.
13 Wu B, Gerlitz B, Grinnell BW, Meyerhoff ME. Polymeric coatings that mimic the endothelium: Combining nitric oxide release with surface-bound active thrombomodulin and heparin. Biomaterials 2007;28:4047-4055.
14 Jun HW, Taite LJ, West JL. Nitric oxide-producing polyurethanes. Biomacromolecules 2005;6:838-844.
15 Salehi-Nik N, Amoabediny G, Solouk A, Shokrgozar MA, Zandieh-Doulabi B, Klein-Nulend J. Biomimetic modification of silicone tubes using sodium nitrite-collagen immobilization accelerates endothelialization. J Biomed Mater Res B 2015;In press.
16 Wissink MJB, Beernink R, Poot AA, Engbers GH, Beugeling T, van Aken WG, Feijen J. Improved endothelialization of vascular grafts by local release of growth factor from heparinized collagen matrices. J Control Release 2000;64:103-114.
17 Lincoln DT, Singal PK, Al-Banaw A. Growth hormone in vascular pathology: Neovascularization and expression of receptors is associated with cellular proliferation. Anticancer Res 2007;27:4201-4218.
18 Li G, Yang P, Qin W, Maitz MF, Zhou S, Huang N. The effect of coimmobilizing heparin and fibronectin on titanium on hemocompatibility and endothelialization. Biomaterials 2011;32:4691-4703.

19 Monteiro N, Martins M, Martins A, Fonseca NA, Moreira JN, Reis RL, Neves NM. Antibacterial activity of chitosan nanofiber meshes with liposomes immobilized releasing gentamicin. Acta Biomater 2015;18:196-205.
20 Jain RA. The manufacturing techniques of various drug loaded biodegradable poly(lactide-co-glycolide) (PLGA) devices. Biomaterials 2000;21:2475-2490.
21 Salehi-Nik N, Amoabediny G, Shokrgozar MA, Mottaghy K, Klein-Nulend J, Zandieh-Doulabi B. Surface Modification of silicone tubes by functional carboxyl and amine, but not peroxide groups followed by collagen immobilization improves endothelial cell stability and functionality. Biomed Mater 2015;10:015024.
22 Mourtas S, Kastellorizios M, Klepetsanis P, Farsari E, Amanatides E, Mataras D, Pistillo BR, Favia P, Sardella E, d'Agostino R, Antimisiaris SG. Covalent immobilization of liposomes on plasma functionalized metallic surfaces. Colloids Surfaces B 2011;184:214-220.
23 ElMeshad AN, Mortazavi SM, Mozafari MR. Formulation and characterization of nanoliposomal 5-fluorouracil for cancer nanotherapy. J Liposome Res 2014:24:1-9.
24 Tzoneva R, Faucheux N, Groth T. Wettability of substrata controls cell–substrate and cell–cell adhesions. Biochim Biophys Acta 2007;1770:1538-1547.
25 McGuigan AP, Sefton MV. The influence of biomaterials on endothelial cell thrombogenicity. Biomaterials 2007;28:2547-2571.
26 Prodanov L, Semeins CM, van Loon JJWA, te Riet J, Jansen JA, Klein-Nulend J, Walboomers XF. Influence of nanostructural environment and fluid flow on osteoblast-like cell behavior: A model for cell-mechanics studies. Acta Biomater 2013;9:6653-6662.
27 Mirahmadi F, Tafazzoli-Shadpour M, Shokrgozar MA, Bonakdar S. Enhanced mechanical properties of thermosensitive chitosan hydrogel by silk fibers for cartilage tissue engineering. Mater Sci Eng C Mater Biol Appl 2013;33:4786-4794.
28 Kim KS, Tezel TH, Del Priore LV. Minimum number of adult human retinal pigment epithelial cells required to establish a confluent monolayer in vitro. Curr Eye Res 1998;17:962-969.
29 Noris M, Morigi M, Donadelli R, Aiello S, Foppolo M, Todeschini M, Orisio S, Remuzzi G, Remuzzi A. Nitric oxide synthesis by cultured endothelial cells is modulated by flow conditions. Circ Res 1995;76:536-543.
30 Feng S, Nie L, Zou P, Suo J. Effects of drug and polymer molecular weight on drug release from PLGA-mPEG microspheres. J Appl Polym Sci 2015;132:41431.
31 Zhang L, Hong L, Yu Y, Bae SC, Granick S. Nanoparticle-assisted surface immobilization of phospholipid liposomes. J Am Chem Soc 2006;128:9026-9027.
32 Kim JM, Jung HS, Park JW, Yukimasa T, Oka H, Lee HY, Kawai T. Spontaneous immobilization of liposomes on electron-beam exposed resist surfaces. J Am Chem Soc 2005;127:2358-2362.
33 Craciunescu O, Gaspar A, Trif M, Moisei M, Oancea A, Moldovan L, Zarnescu O. Preparation and characterization of a collagen-liposome-chondroitin sulfate matrix with potential application for inflammatory disorders treatment. J Nanomater 2014;2014:Article ID 903691,9 pages.
34 Dominak LM, Omiatek DM, Gundermann EL, Heien ML, Keating CD. Polymeric crowding agents improve passive biomacromolecule encapsulation in lipid vesicles. Langmuir 2010;26:13195-13200.
35 Luczak K, Balcerczyk A, Soszynski M, Bartosz G. Low concentration of oxidant and nitric oxide donors stimulate proliferation of human endothelial cells in vitro. Cell Biol Int 2004;28:483-486.
36 Egemnazarov B, Schermuly RT, Dahal BK, Elliott GT, Hoglen NC, Surber MW, Weissmann N, Grimminger F, Seeger W, Ghofrani HA. Nebulization of the acidified sodium nitrite formulation attenuates acute hypoxic pulmonary vasoconstriction. Respir Res 2010;11:81-93.
37 Rymaszewski Z, Cohen RM, Chomczynski P. Human growth hormone stimulates proliferation of human retinal microvascular endothelial cells in vitro. Proc Natl Acad Sci USA 1991;88:617-621.
38 Alef MJ, Vallabhaneni R, Carchman E, Morris SM, Shiva S, Wang Y, Kelley EE, Tarpey MM, Gladwin MT, Tzeng E, Zuckerbraun BS. Nitrite-generated NO circumvents dysregulated arginine/NOS signaling to protect against intimal hyperplasia in Sprague-Dawley rats. J Clin Invest 2011;121:1646-1656.

39 Campbell EJ, O'Byrne V, Stratford PW, Quirk I, Vick TA, Wiles MC, Yianni YP. Biocompatible surfaces using methacryloylphosphorylcholine laurylmethacrylate copolymer. ASAIO J 1994;40:853-857.
40 Thum T, Tsikas D, Frolich JC, Borlak J. Growth hormone induces eNOS expression and nitric oxide release in a cultured human endothelial cell line. FEBS Lett 2003;555:567-571.
41 Roberto da Costa RP, Costa AS, Korzekwa AJ, Platek R, Siemieniuch M, Galvao A, Redmer DA, Silva JR, Skarzynski DJ, Ferreira-Dias G. Actions of a nitric oxide donor on prostaglandin production and angiogenic activity in the equine endometrium. Reprod Fertil Dev 2008;20:674-683.

CHAPTER 6

Nanoliposomal Growth Hormone and Sodium Nitrite Release from Silicone Fibers Reduces Thrombus Formation under Flow

Nasim Salehi-Nik[1,2], Ghassem Amoabediny[1,2], Seyedeh Parnian Banikarimi[1,2], Behdad Pouran[3,4], Behrouz Zandieh-Doulabi[5], Jenneke Klein-Nulend[5]

[1] School of Chemical Engineering, College of Engineering, University of Tehran, Tehran, Iran

[2] Department of Biomedical Engineering, Research Center for New Technologies in Life Science Engineering, University of Tehran, Tehran, Iran

[3] Department of Orthopedics, University Medical Center Utrecht, Utrecht, The Netherlands

[4] Department of Biomechanical Engineering, Faculty of Mechanical, Maritime, and Materials Engineering, Delft University of Technology, Delft, The Netherlands

[5] Department of Oral Cell Biology, Academic Centre for Dentistry Amsterdam, University of Amsterdam and VU University Amsterdam, MOVE Research Institute Amsterdam, Amsterdam, The Netherlands

Submitted for publication

ABSTRACT

Biocompatibility of artificial lungs can be improved by endothelialization of hollow fibers. Bioavailability of growth-inducing and anti-thrombotic agents on the hollow fiber-blood interface inhibits thrombosis. We investigated if nanoliposomal growth-inducing growth hormone (nGH) and anti-thrombotic sodium nitrite (nNitrite) incorporation into collagen-coating on silicone hollow fibers improves blood compatibility by increasing endothelial cell growth and nitrite bioavailability under flow. Nitrite production rate was assessed under varying fluid shear stresses. Finite element (FE) modeling was used to simulate nitrite transport within the parallel-plate flow chamber, and nitrite bioavailability on the fiber-blood interface at 1-30 dyn/cm^2 shear stress. Endothelial cell number on fibers coated with nNitrite-nGH-collagen conjugate was 1.5-fold higher than on collagen-coated fibers. For collagen-coated fibers, nitrite production reached a maximum at 18 dyn/cm^2 shear stress. When fibers were coated with nNitrite-nGH-collagen conjugate, nitrite production increased continuously by increasing shear stress. FE modeling revealed that nitrite concentrations at the fiber-blood interface were affected by shear stress-induced nitrite production, and diffusion/convection-induced nitrite removal. Highest nitrite concentrations and lowest thrombus deposition were observed on fibers coated with nNitrite-nGH-collagen conjugate exposed to 6-12 dyn/cm^2 shear stress. In conclusion, our results suggest that nNitrite-nGH-Col conjugate coatings not only promote endothelialization, but also thrombus inhibition under shear stress in biohybrid artificial lungs.

Keywords
Biomimetic collagen coating, Endothelialization, Finite element modeling, Shear stress, Nitrite bioavailability, Silicone hollow fibers, Biohybrid artificial lungs, Thrombus deposition

INTRODUCTION

Hollow fiber membrane oxygenators, also called artificial lungs, contain hollow fibers along which the patient's blood flows for oxygenation during open-heart surgery [1]. Endothelial cell seeding of blood-contacting parts of hollow fibers is a promising method to improve biocompatibility of these fibers in so-called biohybrid artificial lungs [1, 2].

Coating with extracellular matrix proteins such as collagen is a prerequisite for endothelial cell attachment [3, 4]. Growth-inducing agents, e.g. growth hormone (GH), can be encapsulated in nanoliposomes and incorporated into the collagen coating to accelerate the endothelialization rate [5, 6]. Endothelial cells seeded at low density on hollow fibers can be stimulated by sustained release of GH from nanoliposomes to rapidly (within a few days) form a confluent monolayer. The blood shear stress in artificial lungs has been estimated 1–3 N/m^2, except at the entrance region of the device, where the shear stress is much higher [7]. There is a need for anti-thrombotic agents in the collagen coating, since endothelial cell detachment might occur under high shear stress and the thrombogenicity of collagen in areas not covered by endothelial cells is another problem to overcome [5]. Sustained release of anti-thrombotic agents, e.g. nitric oxide (NO)-donors, from nanoliposomes incorporated into collagen coating of hollow fibers may guarantee blood compatibility of these fibers under high shear stress [8, 9]. We have shown previously that nitrite and acidified nitrite released from biomimetic sodium nitrite-collagen conjugate coatings significantly decreases platelet adhesion [10]. Biomimetic coatings possessing growth-inducing and anti-thrombotic properties might improve both endothelialization and anti-coagulation, thus providing a potential application for long-term use of hollow fibers [11, 12].

Co-immobilization of biomimetic coatings using carbodiimide bonds has been shown to provide resistance against blood flow shear stress [13]. Not only a stable biomimetic coating, but also the bioavailability of anti-thrombotic biomolecules on the hollow fiber-blood interface is critical to inhibit thrombus formation. Flow velocity alterations modify the mass transport characteristics at the hollow fiber-blood interface. The bioavailability of anti-thrombotic biomolecules depends strongly on transport processes, and decreases due to convection [14, 15]. Therefore, the anti-thrombotic biomolecule concentration at the hollow fiber-blood interface is regulated by the counteraction between the shear stress-dependent production of anti-thrombotic biomolecules and their removal by diffusive and convective transport [14-19].

Parallel-plate flow chambers have been used to determine the relationship between anti-thrombotic agent production by endothelial cells and the applied shear stress, as well as the effect of convection on the anti-thrombotic agent concentration at the biomaterial-fluid interface [16, 20]. The latter concentration

cannot be measured experimentally, and consequently numerical simulations based on convection-diffusion-reaction equations are useful. The production and transport of NO, as the most important anti-thrombotic agent, have been modeled in parallel-plate flow chambers [14, 15, 21, 22]. Some of these models did not consider the effect of variations in fluid flow velocity on the NO production rate or NO transport due to convection [21, 22]. Others although have considered shear stress-induced NO production and washing out of NO due to convection, they modeled NO transport within two dimensional flat parallel-plate flow chambers [14, 15].

In this study, we aimed to test whether sustained release of the growth-inducing agent GH and the anti-thrombotic agent sodium nitrite from collagen conjugate improves blood compatibility by increasing the number of endothelial cells on the silicone hollow fibers, and by enhancing the bioavailability of nitrite under flow. First a stable and confluent endothelial cell layer was developed on silicone hollow fibers using sustained release of GH. We determined a relationship between shear stress and nitrite production rate in a parallel-plate flow chamber containing endothelialized surface-modified silicone hollow fibers under 1-30 dyn/cm^2 shear stress. The effect of mass transport phenomena on nitrite bioavailability on the silicone hollow fiber surface was assessed by solving laminar flow and convection-diffusion partial differential equations under different shear stress. Real measurements of thrombus deposition on hollow fibers was used to validate the simulation results.

MATERIALS AND METHODS

Materials

Cylindrical silicone hollow fibers (inner diameter 0.6 mm, thickness 0.1 mm) were kindly donated by Raumedic (Helmbrechts, Germany). Twenty nine silicone hollow fibers were glued together with a biocompatible silicone glue to prepare one large silicone hollow fiber (SiHF) patch (25 mm x 60 mm). AAc was supplied by Fluka (Buchs, Switzerland), and purified by distillation under vacuum to remove impurities. Sodium nitrite and other chemicals for the Griess assay were obtained from Merck (Kenilworth, NJ, USA), and were of the highest purity available. Somatropin as a GH was supplied from Novo Nordisk (Aalborg, Denmark). 1,2 Distearoyl-sn-glycero-3-phosphoethanolamine-N-[amino (polyethyleneglycol)-2000] (amino-PEG lipid) and dipalmitoyl phosphatidylcholine (DPPC) were purchased from Lipoid Gmbh (Ludwigshafen, Germany). Cholesterol and sucrose were purchased from Sigma Aldrich (Gillingham, Dorset, UK). Chloroform was obtained from Duksan (Gyeonggi, Korea).

Surface modification of SiHF patches

Sodium nitrite solution at 0.01 M was prepared by dissolving sodium nitrite in water containing 0.02 M acetic acid at 4ºC. Some of the nitrite ions in the solution convert to acidified nitrite (nitrous acid; HNO_2) in the presence of acetic acid. Preparation of the solution at 4°C prevents fast decomposition of HNO_2 into NO, NO_2, and H_2O [10]. From now on we refer to the total amount of nitrite and acidified nitrite as "nitrite". GH at 90 µg/ml was prepared by dissolving somatropin in water. Nanoliposomal sodium nitrite (nNitrite) and nanoliposomal GH (nGH) were prepared using the thin-film hydration technique, as previously described [23, 24]. In short, a lipid phase was prepared from a mixture of lipids DPPC: cholesterol: amino-PEG lipid (molar percentage ratio: 83:15:2), and dissolved in a solution of chloroform in a round bottom flask. The solvent was removed in an IKA RV10 rotary evaporator (IKA, Deutschland, Germany) at 150 rpm, 50ºC, for 30 min, under reduced pressure. The resulting thin, dry lipid film was hydrated with 10 ml sodium nitrite or GH solution and by adding sucrose. The dispersion obtained was gently shaken for about 30 min at 4ºC. The formed multilamellar vesicles were directly sonicated using a probe type ultrasonic device (Misonix sonicator s94000, QSONICA, Newtown, CA, USA) with a net power of 20 W and a frequency of 20 KHz with a total process time of 30 min to produce nanoliposomes. nNitrite stock solution (0.01 M) and nGH stock solution (90 µg/ml) were used to prepare conjugates with 500 nmol/ml nNitrite, and 1000 ng/ml nGH in collagen solution, i.e. water containing 1 mg/ml collagen (acid soluble collagen type I; Pasteur Institute of Iran, Tehran, Iran) and 0.02 M acetic acid. The solution was gently shaken for 1 h at 4°C to obtain homogeneous nNitrite-nGH-collagen (nNitrite-nGH-Col) conjugate.

SiHF patches were plasma graft polymerized with acrylic acid (AAc) using a two-step plasma treatment as described earlier [10, 13]. AAc-grafted SiHF patches were immersed into 30 ml 5 mM 2-(N-morpholino)ethanesulfonic acid (MES) buffer solution containing 48 mg 1-Ethyl-3-[3-dimethylaminopropyl] carbodiimide hydrochloride (EDC) and 15 mg N-hydroxysuccinimide (NHS; Fluka, Neu-Ulm, Germany). The solution was gently stirred for 5 h at 4°C to activate the carboxyl groups on AAc-grafted patches. Then patches with activated carboxyl groups were either immersed into collagen solution or nNitrite-nGH-Col conjugate for collagen immobilization at 4ºC for 24 h. Collagen-immobilized AAc-grafted SiHF (AAc SiHF-Col) and nNitrite-nGH-Col conjugate-immobilized AAc-grafted SiHF (AAc SiHF-nNitrite-nGH-Col) patches were washed in water for 1 min to remove unbound collagen and nanoliposomes, and stored at 4ºC.

Endothelial cell seeding and proliferation on surface-modified SiHF patches

Human umbilical vein endothelial cells (HUVECs) from the National Cell Bank, Pasteur Institute of Iran (Tehran, Iran), were used between passages 3 and 6 to evaluate cell proliferation, retention, and anti-thrombotic function on surface-

modified SiHF patches, i.e. AAc SiHF-Col, and AAc SiHF-nNitrite-nGH-Col. Surface-modified SiHF patches were put into petri dishes, sterilized with UV, washed twice with phosphate buffered saline solution (PBS), and washed once with culture medium before cell seeding. Endothelial cells were seeded on surface-modified SiHF patches at a low density of $1.6x10^4$ cells/cm^2 in an in-house fabricated seeding well together with 3 ml of DMEM/F12 medium containing 10% fetal bovine serum (GIBCO, Renfrewshire, Scotland) and cultured in a humidified atmosphere of 5% CO_2 in air in a 37°C incubator for 6 days.

The MTT (Sigma, St. Louis, MO, USA) assay was used to evaluate endothelial cell proliferation after cell seeding (day 0) and at days 2, 4, and 6 of culture on AAc SiHF-Col and AAc SiHF-nNitrite-nGH-Col patches as described previously [10, 25]. A calibration curve with known endothelial cell numbers was used to determine the number of cells.

Shear stress conditioning of surface-modified SiHF patches to determine cell stability and nitrite release

To compare the stability of endothelial cells on AAc SiHF-Col and on AAc SiHF-nNitrite-nGH-Col patches under different shear stress, each endothelialized surface-modified SiHF patch was removed from the incubator after 6 days of culture and exposed to shear stress of 1, 2, 4, 6, 10, 12, 18, 24, and 30 dyn/cm^2 for 1 h within the parallel-plate flow chamber with a closed loop system while pumping DMEM/F12 medium (Figure 1). Open-heart surgical procedures in which artificial lungs are used usually take 4–8 h [26]. Therefore, the effect of flow conditioning during 2, 4, 6, and 8 h on cell detachment was investigated by applying 30 dyn/cm^2 shear stress (the maximum shear stress used in this study) on AAc SiHF-nNitrite-nGH-Col patches. One patch of each type of surface-modified SiHF patches was put in static culture to calculate the cell number before exposure to shear stress.

Flow rates required to achieve specific shear stress on SiHF patches were calculated using a three-dimensional FE model developed in COMSOL Multiphysics (Ver. 4.4, COMSOL Inc., TU Delft, Delft, The Netherlands). Details of physical properties and geometry of the parallel-plate flow chamber are provided (Table 1). Both culture medium and blood were considered Newtonian fluids since under applied shear stress conditions as described in this study, blood behaves as a Newtonian fluid [27]. Reynolds number at all velocities used in this study was below 70, which is well below the laminar Reynolds number threshold (Reynolds number = 2300).

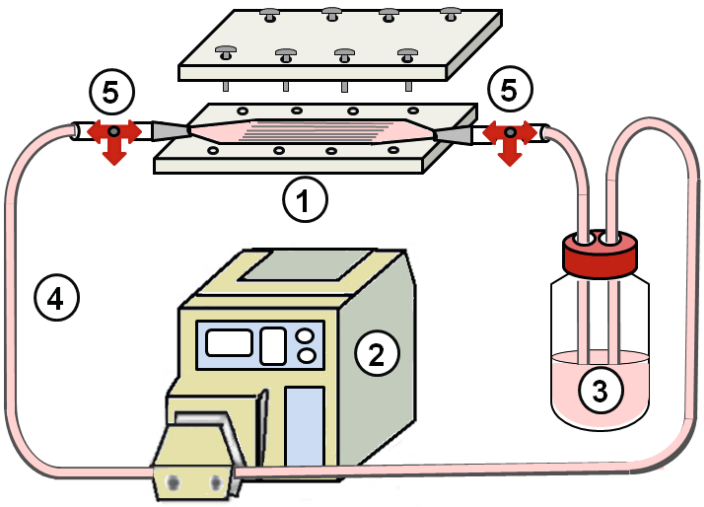

Figure 1. Schematic of a closed loop system used to expose endothelial cells to fluid shear stress of different magnitude. (1) Parallel-plate flow chamber containing an endothelialized SiHF patch, (2) Peristaltic pump, (3) Medium reservoir, (4) Polyvinylchloride tubing, (5) Check valves.

Table 1. A list and description of the symbols used in the simulation.

Symbol	Value, units	Description
L	66 mm	Length of the flow chamber
W	25 mm	Width of the flow chamber
H	1.4 mm	Height of the flow chamber
μ	0.001 Pa s	Dynamic viscosity of the culture medium at 37°C
μ_{blood}	0.003 Pa s	Dynamic viscosity of the blood at 37°C
D	3300 $\mu m^2/s$	Nitrite diffusion coefficient
τ_w	dyn/cm^2	Wall shear stress
R_N	mol/m^2 s	Nitrite production rate (flux)

After shear stress conditioning of cells, the attached cells on each static or shear stress-conditioned surface-modified patches were washed with PBS, released with trypsin/EDTA (Merck, Kenilworth, NJ, USA), and stained with 0.4% trypan blue (Sigma-Aldrich, St. Louis, MO, USA) to determine viable cell number in a Neubauer cell chamber. The percentage of detached cells was calculated by

detracting the number of cells on shear stress-conditioned patches from the number of cells in static culture. Moreover, after 1 h of shear stress application, 0.5 ml of the medium was collected from the reservoir for nitrite determination. NO release by endothelial cells or nitrite release by nNitrite in the conjugate coating was measured as nitrite (NO_2^-) accumulation in the medium, using Griess reagent containing 1% sulfanilamide, 0.1% naphtylethelene-diamine-dihydrochloride, and 2.5 M H_3PO_4 [10, 28]. Serial dilutions of $NaNO_2$ in medium were used as standard curve. The absorbance was measured at 545 nm with a microplate reader (Stat Fax-2100, Miami, FL, USA) to calculate the total nitrite concentration in mole. Results were normalized for the number of attached cells on surface-modified SiHF patches, and converted to nitrite production rate by dividing by the SiHF patch surface area and time. An equation was derived for nitrite production rate changes by shear stress using an online curve fitting program.

Nitrite convection-diffusion modeling in the parallel-plate flow chamber

Nitrite concentration in the parallel-plate flow chamber is affected by diffusion and convection (Figure 2) [14, 15]. Nitrite transport within the parallel-plate flow chamber was investigated by coupling laminar flow equations and convection-diffusion equations. A section of the parallel-plate flow chamber consisting of an endothelial cell-seeded SiHF patch (25 mm x 66 mm x 1.4 mm; Figure 2) was constructed in COMSOL, with 1541300 tetrahedral mesh elements. The model solution was confirmed to be mesh-independent by comparing solutions based on different meshing schemes. Two sets of simulations were conducted based on either culture medium or blood properties. Table 1 summarizes the model geometry and other parameters used in the simulation. In addition, the following assumptions were made:

1) The surface of surface-modified SiHF patches is modeled as a source of nitrite. This assumption is based on the fact that the thickness of the endothelium and surface coating can be neglected cf. the height of the flow chamber [15].

2) A distance of 3 mm between the entrance of the flow into the simulated region and the position of endothelialized surface-modified SiHF patch ensures exposure of endothelial cells to fully developed plane Poiseuille flow.

3) The nitrite concentration is zero at the entrance of the chamber, i.e. there is no nitrite dissolved in the culture medium or blood.

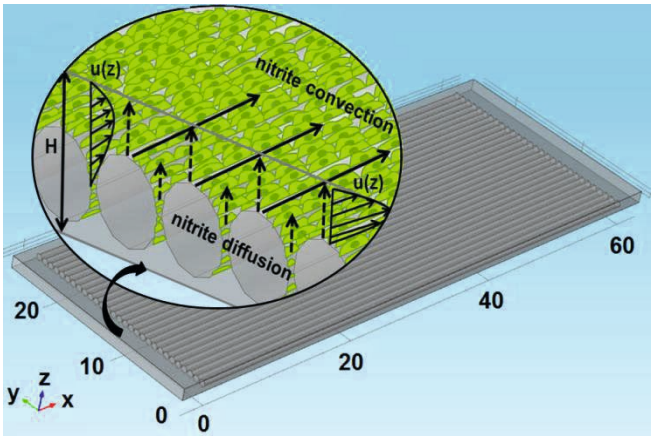

Figure 2. Schematic of nitrite production and transport in the parallel-plate flow chamber. Nitrite concentration at the hollow fiber-blood interface was determined by the balance between shear stress-dependent production of nitrite and its removal by diffusive and convective transport.

Navier-Stokes (Equation 1) and Continuity (Equation 2) were solved simultaneously to compute the flow field within the flow chamber [29]:

$$\rho(u.\nabla)u=\nabla.[-p+\mu(\nabla u)]+\rho g \quad (1)$$

$$\rho\nabla.(u)=0 \quad (2)$$

where u is the local velocity, μ is the fluid dynamic viscosity, p is the fluid pressure, and g is the gravity constant. The fluid inlet velocity boundary condition is given as [15]:

$$u(z)=6\,V_m\,(z/H)(1-z/H) \quad (3)$$

where V_m is the averaged input velocity, z is the direction normal to the flow direction, and H is the height of the parallel-plate flow chamber. Fluid pressure was set to zero at the outlet of the parallel-plate flow chamber. No-slip boundary condition was used for all surfaces. Nitrite transport is described by the following steady-state convection-diffusion equation [14, 15]:

$$0=D\nabla^2C_N-U.\nabla C_N \quad (4)$$

where C_N denotes nitrite concentration; D is the nitrite diffusion coefficient, and U is the velocity field within the simulation domain which is obtained from the laminar flow model. It was assumed that the amount of nitrite measured by sampling from

the culture medium reservoir (Figure 1) after 1 h shear stress conditioning of cells equals the amount released by cells and nNitrite incorporated into the SiHF patch coating. Since sampling was done after switching off the pump, it can be assumed that the effect of convection fades away. Nitrite production rate (R_N) at the SiHF patch surface is related to the wall shear stress as [14]:

$$R_N = \frac{a}{1+b\ \exp(d\ \tau)} \tag{5}$$

where "a" represents the maximum nitrite production rate, and "b", and "d" indicate nitrite production in response to wall shear stress. The nitrite concentration gradient at the top plate (z=H) and the outlet of the chamber (x=L) is set to be zero, thus:

$$\frac{\partial C_N}{\partial z}\Big|_{z=H} = 0 \tag{6}$$

$$\frac{\partial C_N}{\partial x}\Big|_{x=L} = 0 \tag{7}$$

At the entrance of the chamber (x=0) the nitrite concentration is zero:

$$C_N\Big|_{x=0} = 0 \tag{8}$$

Finally, at the interface of the hollow fiber surface and culture medium or blood, nitrite production equals nitrite diffusion flux, thus:

$$R_N = -D\frac{\partial C}{\partial z} \tag{9}$$

Substituting Equation 5 in Equation 9 yields:

$$\frac{a}{1+b\ \exp(d\ \tau)} = -D\frac{\partial C}{\partial z} \tag{10}$$

The shear stress profile obtained from the laminar flow model was used as τ in equation 10. The governing partial differential equations were solved by FE modeling using COMSOL.

Blood biocompatibility of endothelialized surface-modified SiHF patches

The blood biocompatibility of endothelialized surface-modified SiHF patches was evaluated by quantifying thrombus deposition from blood under static and 1, 6, 12, 18, 24, and 30 dyn/cm^2 shear stress. Citrated blood was obtained from Iranian blood transfusion organization (Tehran, Iran), mixed with 0.6 U/ml of unfractionated heparin (Baxter, Deerfield, IL, USA), re-calcified with a 1 M $CaCl_2$ solution to a final

concentration of 2–3 mM calcium and balanced to pH 7.4 with 1 M NaOH solution [26]. The viscosity of the prepared blood was measured by a viscometer. All blood was refrigerated and used within 24 h of collection. For each experiment, a reservoir was filled with 30 ml of prewarmed blood. Then the blood was flown over endothelialized AAc SiHF-Col or AAc SiHF-nNitrite-nGH-Col patches (Figure 1) for 8 h at 37°C. The flow rate required to achieve a defined amount of shear stress on the patch by blood flow was estimated by the FE model. After shear stress conditioning, SiHF patches were carefully removed from the parallel-plate flow chamber, rinsed by soaking three times in PBS, and imaged with a digital camera on an optical microscope. A threshold was applied for the red thrombus in each image, and the percentage of the image covered by the thrombus was computed in ImageJ 1.49.

Statistical analysis

All data were expressed as mean ± standard deviation (SD). To compare any significant differences between surface-modified SiHF patches, one-way analysis of variance was used. The significance of differences among means was determined by post-hoc comparison using Bonferroni's method. A probability (p) value of less than 0.05 ($p<0.05$) was taken as the level of significance

RESULTS

AAc SiHF-nNitrite-nGH-Col patches affect endothelial cell proliferation

Endothelial cell proliferation on AAc SiHF-Col and on AAc SiHF-nNitrite-nGH-Col patches was compared after seeding (0 day) and after 2, 4, and 6 days of culture (Figure 3). A similar number of endothelial cells was attached on AAc SiHF-Col and on AAc SiHF-nNitrite-nGH-Col patches after seeding. Incorporation of nGH in AAc SiHF-nGH-nNitrite-Col patches increased the number of endothelial cells by 1.8-fold at day 2 ($p<0.05$), 1.4-fold at day 4 ($p<0.05$), and 1.5-fold at day 6 ($p<0.005$), compared with AAc SiHF-Col patches.

Modeling of fluid shear stress in the parallel-plate flow chamber

The inlet flow rate of fluid corresponding to the desired shear stress on a SiHF patch within the parallel-plate flow chamber was obtained for both culture medium and blood (Table 2).

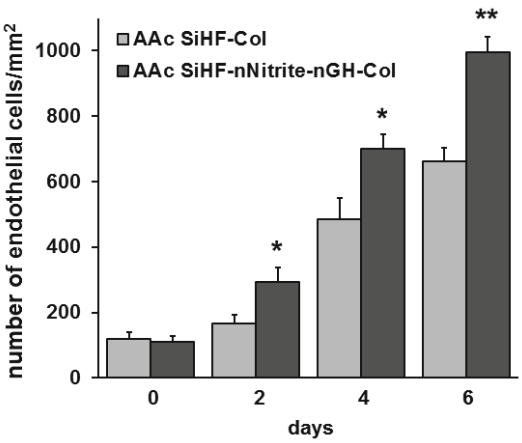

Figure 3. Endothelial cell proliferation on AAc SiHF-Col and AAc SiHF-nNitrite-nGH-Col patches after seeding (0 day) and after 2, 4, and 6 days of culture. The number of endothelial cells on AAc SiHF-nNitrite-nGH-Col patches was higher than on AAc SiHF-Col patches at all-time points. AAc SiHF-Col, collagen-immobilized AAc-grafted SiHF; AAc SiHF-nNitrite-nGH-Col, nNitrite-nGH-Col conjugate-immobilized AAc-grafted SiHF. *Significant effect of nGH in conjugate, $p<0.05$, **$p<0.005$.

Table 2. The inlet culture medium or blood flow required to achieve target mean shear stress calculated by FE modeling.

	Target shear stress (dyn/cm^2)								
	1	2	4	6	10	12	18	24	30
Inlet culture medium flow rate (ml/min)	5.3	9.7	19.6	24.5	40.4	51.1	77.9	99.5	120.8
Inlet blood flow rate (ml/min)	2.4	4.5	9.1	12.4	19.8	25.6	41.1	58.7	80.8

AAc SiHF-nNitrite-nGH-Col patches increase endothelial cell stability under fluid shear stress

After 6 days of cell culture on surface-modified SiHF patches, i.e. AAc SiHF-Col and AAc SiHF-nNitrite-nGH-Col, the patches were exposed to different shear stresses of 1, 6, 12, 18, 24, and 30 dyn/cm^2 for 1 h, and the percentage of detached cells determined (Figure 4a). The SiHF patches coated with nNitrite-nGH-Col conjugate (AAc SiHF-nNitrite-nGH-Col) demonstrated enhanced

resistance to all levels of shear stress tested compared with SiHF patches coated with collagen alone (AAc SiHF-Col patches, $p<0.05$). At 30 dyn/cm^2 shear stress, the maximal shear stress applied in this study, cell detachment from AAc SiHF-nNitrite-nGH-Col patches was 32% lower ($p<0.005$) than cell detachment from AAc SiHF-Col patches. Cell detachment from AAc SiHF-nNitrite-nGH-Col patches was also assessed during 8 h exposure to 30 dyn/cm^2 shear stress (Figure 4b). Cell detachment from AAc SiHF-nNitrite-nGH-Col patches was slightly but not significantly increased by increasing the duration of shear stress exposure. After 8 h exposure to 30 dyn/cm^2 shear stress, cell detachment was 1.3-fold higher ($p>0.05$) than after 1 h exposure (Figure 4b).

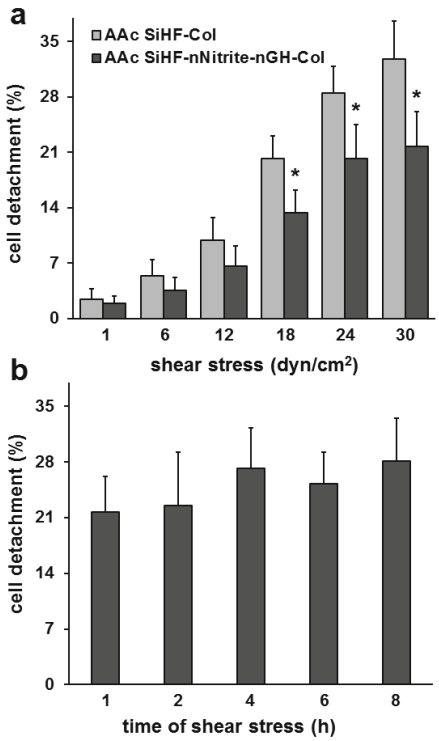

Figure 4. Endothelial cell detachment from surface-modified patches during 8 h exposure to 1-30 dyn/cm^2 fluid shear stress. (a) Cell detachment from AAc SiHF-Col and AAc SiHF-nNitrite-nGH-Col patches after 1 h exposure to 1-30 dyn/cm^2 fluid shear stress. Cell detachment from AAc SiHF-nNitrite-nGH-Col patches was significantly lower than from AAc SiHF-Col patches, especially at shear stress higher than 18 dyn/cm^2. (b) Cell detachment from AAc SiHF-nNitrite-nGH-Col patches after 1, 2, 4, 6, and 8 h exposure to 30 dyn/cm^2 fluid shear stress. Increasing the duration of shear stress exposure had no significant effect on cell detachment from AAc SiHF-nNitrite-nGH-Col patches.
AAc SiHF-Col, collagen-immobilized AAc-grafted SiHF; AAc SiHF-nNitrite-nGH-Col, nNitrite-nGH-Col conjugateimmobilized AAc-grafted SiHF. *Significantly different from AAc SiHF-Col patches, $p<0.05$, **$p<0.005$.

Nitrite production rate of endothelialized surface-modified SiHF patches under shear stress

Nitrite production rate was calculated by measuring nitrite accumulation in the culture medium resulting from NO release by endothelial cells on AAc SiHF-Col or AAc SiHF-nNitrite-nGH-Col patches plus nitrite release by nNitrite on AAc SiHF-

nNitrite-nGH-Col patches under static condition as well as under shear stress of different magnitudes (Figure 5). Nitrite production rate from AAc SiHF-nNitrite-nGH-Col patches was 3.1-fold higher ($p<0.05$) than from AAc SiHF-Col patches under static condition. For AAc SiHF-Col patches, the nitrite production rate slightly but not indefinitely increased by increasing shear stress. Maximal nitrite production was reached at 18 dyn/cm^2 shear stress. At shear stresses higher than 18 dyn/cm^2, no more nitrite accumulation was measured. However, for AAc SiHF-nNitrite-nGH-Col patches, nitrite accumulation increased continuously by increasing the shear stress. At 30 dyn/cm^2 shear stress, the nitrite production rate from AAc SiHF-nNitrite-nGH-Col patches was 3-fold higher ($p<0.005$) than from AAc SiHF-Col patches.

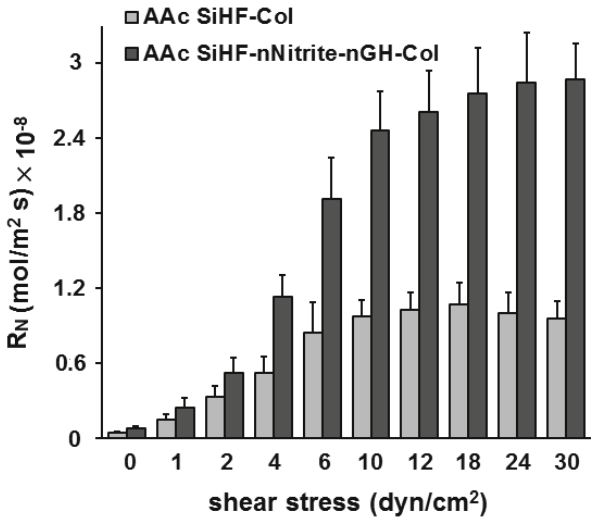

Figure 5. Nitrite production rate on AAc SiHF-Col and AAc SiHF-nNitrite-nGH-Col patches under static condition and under 1-30 dyn/cm^2 shear stress. For AAc SiHF-Col patches, nitrite production reached a maximum at 18 dyn/cm^2 shear stress. However, for AAc SiHF-nNitrite-nGH-Col patches, since R_N is related to nitrite release by nNitrite plus NO production by endothelial cells, nitrite production increased continuously by increasing the shear stress. R_N, nitrite production rate; AAc SiHF-Col, collagen-immobilized AAc-grafted SiHF; AAc SiHF-nNitrite-nGH-Col, nNitrite-nGH-Col conjugate-immobilized AAc-grafted SiHF.

The constants of the suggested sigmoidal equation for changes in nitrite production rate with shear stress magnitude were derived (Table 3) and used as a flux boundary condition (Equation 10).

Table 3. The constants of the suggested equation for the relationship between R_N from AAc SiHF-Col and AAc SiHF-nNitrite-nGH-Col patches and shear stress, $R_N=a/(1+b\times\exp(d\tau))$, derived by online curve fitting software. R_N, nitrite production rate.

	constants		
	$a\times10^{-8}$ (mol m^{-2} s^{-1})	b	d (Pa^{-1})
AAc SiHF-Col	1.06	8.36	-4.80
AAc SiHF-nNitrite-nGH-Col	2.80	13.77	-5.77

Nitrite transport in the parallel-plate flow chamber

Nitrite flux and concentration profiles are illustrated under shear stresses of 1 and 30 dyn/cm^2 in the parallel-plate flow chamber containing an endothelialized AAc SiHF-nNitrite-nGH-Col patch (Figure 6). The magnitude and distribution of nitrite flux increased in the parallel-plate flow chamber by increasing the shear stress from 1 (Figure 6a) to 30 dyn/cm^2 (Figure 6b). However, the nitrite concentration and distribution decreased by increasing the shear stress from 1 (Figure 6c) to 30 dyn/cm^2 (Figure 6d). Increasing the flow velocity affected the nitrite concentration boundary layer (Figure 7). At low shear stress (1 dyn/cm^2), more nitrite molecules remained in the parallel-plate flow chamber which resulted in a thickened nitrite concentration boundary layer on the patch surface. At high shear stress (30 dyn/cm^2), a higher transport rate of nitrite molecules out of the chamber resulted in a thin nitrite concentration boundary layer on the patch surface.

Nitrite concentration at the surface of endothelialized AAc SiHF-Col, and AAc SiHF-nNitrite-nGH-Col patches was calculated by COMSOL (Figure 8). By considering culture medium as the flowing fluid, the nitrite concentration on AAc SiHF-Col patches showed three different trends based on shear stress magnitude ranges, i.e. shear stress <4 dyn/cm^2, 4-10 dyn/cm^2, and >10 dyn/cm^2 (Figure 8a). At shear stress lower than 4 dyn/cm^2, the nitrite concentration increased by increasing shear stress, showing that the shear stress-enhanced nitrite production rate did outweigh the effect of convection. At shear stress between 4 to 10 dyn/cm^2, the nitrite concentration on AAc SiHF-Col patches did not significantly change, showing that the shear stress-enhanced nitrite production rate and convection similarly affected the nitrite concentration. By applying shear stresses higher than 10 dyn/cm^2, the nitrite concentration gradually decreased showing that the convection did outweigh the shear stress-enhanced nitrite production rate. AAc SiHF-nNitrite-nGH-Col patches showed a biphasic nitrite concentration response to increasing shear stress (Figure 8a). At shear stresses lower than 6 dyn/cm^2, the shear stress-enhanced nitrite production rate did outweigh the increase in

convection resulting in a higher nitrite concentration on AAc SiHF-nNitrite-nGH-Col patches. However, at shear stresses higher than 6 dyn/cm^2, the increased convection velocity is higher than the increased nitrite production rate leading to a lower nitrite concentration (Figure 8a). By considering blood as the fluid, the nitrite concentration on AAc SiHF-Col and on AAc SiHF-nNitrite-nGH-Col increased at all shear stresses tested compared with culture medium (Figure 8b). The maximum blood shear stress at which the shear stress-enhanced nitrite production rate on AAc SiHF-nNitrite-nGH-Col patches outweighed the convection, was 10 dyn/cm^2. The nitrite concentration on AAc SiHF-nNitrite-nGH-Col patches at 30 dyn/cm^2 blood shear stress was 1.5-fold higher than 1 dyn/cm^2 shear stress (Figure 8b).

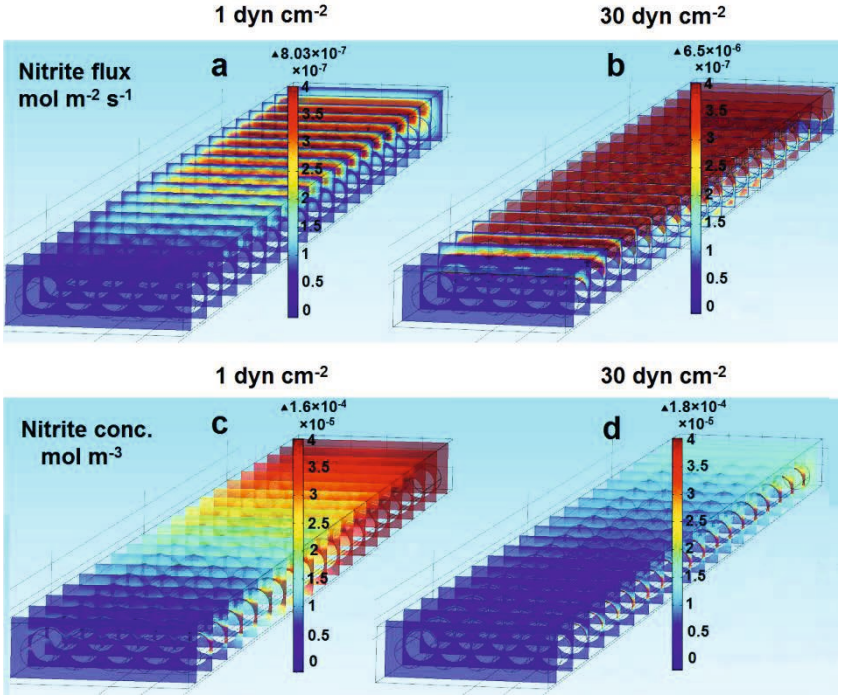

Figure 6. Nitrite flux and nitrite concentration profiles in the parallel-plate flow chamber containing a AAc SiHF-nNitrite-nGH-Col patch at 1 and 30 dyn/cm^2 shear stress. Nitrite flux profile at: (a) 1 dyn/cm^2, (b) 30 dyn/cm^2. Nitrite concentration profile at: (c) 1 dyn/cm^2, (d) 30 dyn/cm^2. An increase in fluid shear stress was associated with two opposing phenomena: 1) increased nitrite production rate, and 2) convective velocity. The counteraction between these two phenomena determined the nitrite concentration. AAc SiHF-nNitrite-nGH-Col, nNitrite-nGH-Col conjugate-immobilized AAc-grafted SiHF.

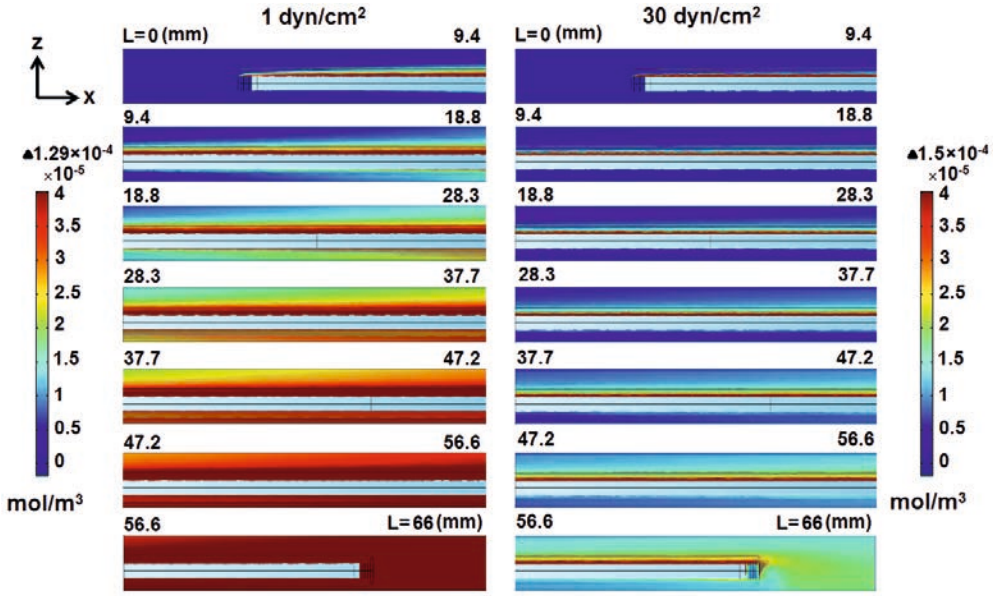

Figure 7. Nitrite concentration boundary layer over the length of the parallel-plate flow chamber (L=0-66 mm) containing a AAc SiHF-nNitrite-nGH-Col patch at 1 and 30 dyn/cm^2 shear stress. The length of the chamber was divided into seven separate areas to simplify comparison between the effects of two shear stresses on the nitrite concentration boundary layer. At low (1 dyn/cm^2) shear stress, the nitrite concentration boundary layer was thick since nitrite molecules moved with low velocity and accumulated around the patch. By increasing the shear stress to 30 dyn/cm^2, the thickness of the nitrite concentration boundary layer decreased due to rapid washing out of nitrite molecules from the chamber.

Blood biocompatibility of endothelialized surface-modified SiHF patches under shear stress

Thrombus deposition on AAc SiHF-Col patches was 1.9-fold higher than that on AAc Si-nNitrite-nGH-Col patches under static condition (Figure 9). By applying 1 dyn/cm^2 shear stress, thrombus deposition slightly but not significantly increased on AAc SiHF-Col patches. By increasing the shear stress to 6 dyn/cm^2, thrombus deposition decreased by 1.2-fold compared with static patches, and then gradually increased until 30 dyn/cm^2. Thrombus deposition on AAc SiHF-Col patches after 30 dyn/cm^2 shear stress application, was slightly but not significantly (1.1-fold, $p>0.05$) higher than that on the static patches. AAc SiHF-nNitrite-nGH-Col patches showed lower thrombus deposition compared with AAc SiHF-Col patches at all shear stresses applied (Figure 9). The lowest thrombus deposition on AAc SiHF-nNitrite-nGH-Col patches (Figure 9) and the highest nitrite concentration on the patches (Figure 8b) were observed at 6-12 dyn/cm^2 shear stress. By applying

higher shear stress, the amounts of thrombus deposition on AAc SiHF-nNItrite-nGH-Col patches increased but remained always lower than under static condition.

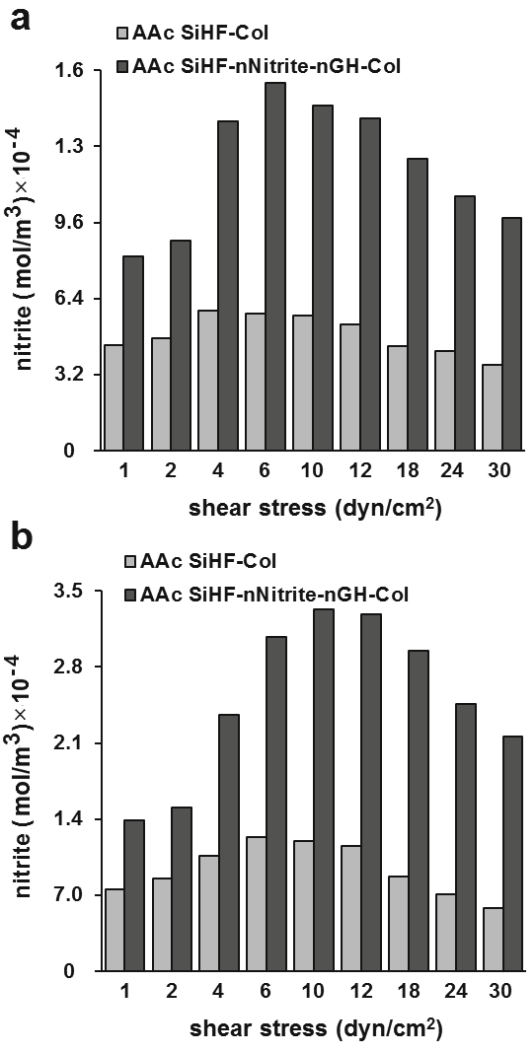

Figure 8. Average nitrite concentration on AAc SiHF-Col and AAc SiHF-nNitrite-nGH-Col patches under 1-30 dyn/cm^2 shear stress considering either (a) culture medium or (b) blood as the fluid as determined by simulation of nitrite transport. The nitrite concentration at the hollow fiber-fluid interface was determined by the balance between shear stress-dependent nitrite production rate and nitrite removal by diffusive and convective transport. The maximum shear stress magnitude at which the shear-dependent increase in nitrite production rate did outweigh the convection velocity was 6 dyn/cm^2 for culture medium and 10 dyn/cm^2 for blood.

AAc SiHF-Col, Collagen-immobilized AAc-grafted SiHF; AAc SiHF-nNitrite-nGH-Col, nNitrite-nGH-Col conjugate-immobilized AAc-grafted SiHF.

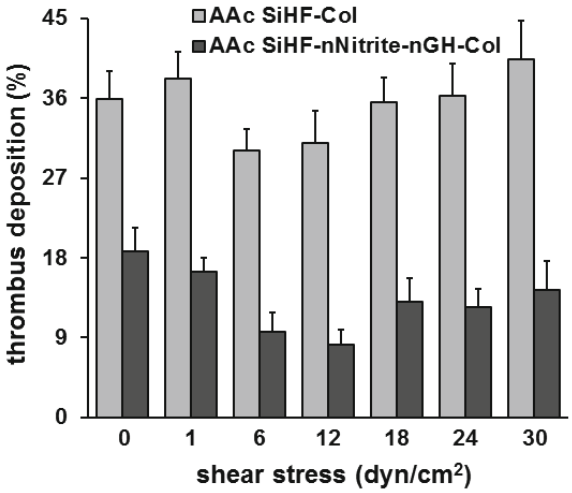

Figure 9. Thrombus deposition on AAc SiHF-Col and AAc SiHF-nNitrite-nGH-Col patches under static condition and at 1-30 dyn/cm^2 shear stress. Thrombus deposition expressed as the percentage of the SiHF patch's surface area covered with thrombus had a direct relationship with the concentration of nitrite on SiHF patch's surface. The lowest thrombus deposition was observed on AAc SiHF-nNitrite-nGH-Col patches at 6-12 dyn/cm^2 shear stress, which resulted in the highest nitrite concentration measured compared with static condition. AAc SiHF-Col, collagen-immobilized AAc-grafted SiHF; AAc SiHF-nNitrite-nGH-Col, nNitrite-nGH-Col conjugate-immobilized AAc-grafted SiHF.

DISCUSSION

Endothelial cell seeding of blood-contacting parts of hollow fibers is promising to decrease thrombotic complications in artificial lungs [2, 7]. Most commercially available materials used in artificial lungs, such as silicone, do not support endothelial cell attachment, and therefore a stable extracellular matrix protein coating, such as collagen, on their surface is required for endothelialization [2, 26]. However, there are some limitations to achieve a blood-compatible biohybrid artificial lung; several hundred millions of cells are required to fully coat all blood-contacting parts of hollow fibers in biohybrid artificial lungs. On the other hand, collagen coating used to initiate endothelial cell attachment is thrombogenic [30]. Therefore, biomimetic coatings incorporating growth-inducing and anti-thrombotic agents may improve endothelialization and blood compatibility of blood-contacting parts of silicone hollow fibers and subsequently improve performance of biohybrid artificial lungs [8, 11, 12].

In this study, a collagen coating was developed on SiHF patches to induce endothelial cell proliferation by sustained release of GH, and to prevent platelet adhesion by sustained release of nitrite. Incorporation of nGH into collagen coating significantly increased the number of endothelial cells after 2, 4, and 6 days of culture. Cell detachment from AAc SiHF-nNitrite-nGH-Col patches was lower than that from AAc SiHF-Col patches under shear stress. A higher rate of endothelial cell proliferation on AAc SiHF-nNitrite-nGH-Col patches resulted in a higher number of cells, and therefore a more confluent cell layer than on AAc SiHF-Col patches. The high number of cells increases cell-cell bond number and strength, which together with cell-collagen conjugate coating bonds creates a stable endothelial monolayer on AAc SiHF-nNitrite-nGH-Col patches.

Not only surface coating with anti-thrombotic agents, but also endothelial cells covering the material surface release anti-thrombotic biomolecules. Shear stress is the most potent physiological stimulus for anti-thrombotic function, e.g. NO and prostacyclin production, in endothelial cells [16-18]. Interestingly, our results showed that a very low level of 1 dyn/cm^2 shear stress stimulates endothelial cells to produce a much higher level of NO than under static condition, indicating that NO production by endothelial cells exhibits an exquisite sensitivity to flow. This is consistent with other studies showing that endothelial cells produce more NO under shear stress as low as 0.2 dyn/cm^2 compared with static culture [31]. For AAc SiHF-Col patches, where the measured nitrite production was just related to NO release by endothelial cells, the nitrite produced did not indefinitely increase with shear stress, but reached a plateau instead. However, for AAc SiHF-nNitrite-nGH-Col patches, where the nitrite production resulted from both endothelial cell-derived NO production and nitrite released from nNitrite in the coating, the nitrite production rate gradually increased with increasing shear stress. Since endothelial cell-derived NO production reached a saturated concentration under defined shear stress, the continuous increase in nitrite production under shear stress is likely related to the release by nNitrite in the coating of AAc SiHF-nNItrite-nGH-Col patches.

The bioavailability of anti-thrombotic factors is important to decrease platelet adhesion on a material's surface [14, 15]. The thrombogenic properties of a medical device under shear stress during clinical use are different from those under static conditions [32]. Flow alterations modify the mass transport characteristics at the fluid–material interface which affects the transport of anti-thrombotic agent. The bioavailability of anti-thrombotic agent may drop significantly due to convection [14, 15]. In this study, real measurements of the nitrite production rate under varying shear stresses coupled with simulations of nitrite transport in the parallel-plate flow chamber enabled to determine the nitrite concentration at the surface of SiHF patches under shear stress.

Increased flow velocity and thus increased fluid shear stress, is associated with two opposing phenomena: (1) Increased nitrite production rate at the SiHF patch surface, and (2) Increased convective transport [14, 17], which affect the overall nitrite concentration. To increase the nitrite concentration in the steady-state condition, the nitrite production rate must exceed the rate of removal by convective transport [17]. The results of our simulation showed that the nitrite concentration on AAc SiHF-nNitrite-nGH-Col patches follows a non-monotonic function of shear stress. The maximum shear stress causing an increase in nitrite concentration was 6 dyn/cm^2 for culture medium, and 10 dyn/cm^2 for blood.

A nitrite concentration boundary layer developed within the parallel-plate flow chamber. The thickness of such a boundary layer asymptotes to a constant value at some finite distance, which was less than the length of the chamber used in this study. At low flow velocities, the nitrite concentration boundary layer was thicker, since nitrite molecules move at low velocity and accumulate around the patch. By increasing the flow velocity, the thickness of a nitrite concentration boundary layer decreases due to rapid washing out of nitrite molecules from the chamber. Furthermore, the formation of a nitrite concentration boundary layer led to substantial differences in the effect of convection on the nitrite concentration on hollow fibers between the entrance and the exit of the flow chamber. Since the concentration boundary layer is extremely thin at the entrance of the chamber, a convective mass transfer effect on the nitrite concentration on hollow fibers is only minimal. This allows to conceive a direct effect of shear stress on nitrite production by the cells on hollow fibers located at the entrance of the chamber. However, both fluid-dynamic and mass transfer-related phenomena affect the nitrite concentration at the exit of the chamber, allowing the study of the combined effect of both phenomena on the nitrite concentration [14]. Furthermore, shear stress is higher on top of the hollow fibers than in the valleys between them. This results in more nitrite production by the cells located on the top of the fibers than in the valleys of the fibers. Higher nitrite production leads to higher nitrite concentration on fibers located at the flow entrance of the chamber, where the effect of mass transport is negligible. On the contrary, when the combined effect of fluid-dynamic and mass transport is considered (at the exit of the parallel-plate flow chamber), shear stress at high magnitude did not lead to increased nitrite concentration, because convection counteracts nitrite production thereby lowering the nitrite concentration produced on top of the fibers compared with the valleys between fibers.

Nitrite bioavailability had a direct effect on thrombotic deposition on surface-modified SiHF patches under shear stress. Shear stress conditioning of endothelialized surface-modified SiHF patches altered the bioavailability of nitrite and subsequently thrombotic deposition. This deposition on AAc SiHF-nNItrite-nGH-Col patches was lower than that on AAc SiHF-Col patches at all shear

stresses tested, which shows that nNitrite-nGH-Col conjugate coating can improve the biocompatibility of biohybrid artificial lungs.

CONCLUSIONS

Coating of SiHF patches with nNitrite-nGH-Col conjugate not only increased endothelial cell proliferation and stability, but also nitrite (as an anti-thrombotic agent) bioavailability under shear stress. An increase in blood flow rate was associated with two different phenomena: 1) increased nitrite production by the endothelialized surface-modified patches, and 2) increased rate of nitrite washing out due to convection. The simulations used in this study help to understand the range of shear stresses suitable to avoid thrombus formation on the surface of SiHFs. AAc SiHF-nNitrite-nGH-Col patches allowed high endothelial cell numbers, and low thrombus formation, even at high shear stresses, suggesting that nNitrite-nGH-Col conjugate coatings are promising to promote biocompatibility of SiHFs in biohybrid artificial lungs.

ACKNOWLEDGMENTS

The authors are thankful to the scientific support of members of the Pasteur Institute of Iran, in particular the help of Prof. Mohammad Ali Shokrgozar.

REFERENCES

1 Betit P. Extracorporeal membrane oxygenation: Quo vadis?. Respir Care 2009;54:948-957.
2 Lemon G, Lim ML, Ajalloueian F, Macchiarini P. The development of the bioartificial lung. Br Med Bull 2014;110:35-45.
3 Solouk A, Cousins BG, Mirahmadi F, Mirzadeh H, Jalali Nadoushan MR, Shokrgozar MA, Seifalian AM. Biomimetic modified clinical-grade POSS-PCU nanocomposite polymer for bypass graft applications: A preliminary assessment of endothelial cell adhesion and haemocompatibility. Mater Sci Eng C Mater Biol Appl 2015;46:400-408.
4 Jokinen J, Dadu E, Nykvist P, Kapyla J, White DJ, Ivaska J, Vehvilainen P, Reunanen H, Larjava, H, Hakkinen L, Heino J. Integrin-mediated cell adhesion to type I collagen fibrils. J Biol Chem 2004;279:31956-31963.
5 Lincoln DT, Singal PK, Al-Banaw A. Growth hormone in vascular pathology: Neovascularization and expression of receptors is associated with cellular proliferation. Anticancer Res 2007;27:4201-4218.
6 Doi K, Matsuda T. Enhanced vascularization in a microporous polyurethane graft impregnated with basic fibroblast growth factor and heparin. J Biomed Mat Res 1997;34:361-370.
7 Takagi M, Shiwaku K, Inoue T, Shirakawa Y, Sawa Y, Matsuda H, Yoshida T. Hydrodynamically stable adhesion of endothelial cells onto a polypropylene hollow fiber membrane by modification with adhesive protein. J Artif Organs 2003;6:222-226.
8 Suchyta DJ, Handa H, Meyerhoff ME. A nitric oxide-releasing heparin conjugate for delivery of a combined antiplatelet/anticoagulant agent. Mol Pharm 2014;11:645-650.
9 Jun HW, Taite LJ, West JL. Nitric oxide-producing polyurethanes. Biomacromolecules 2005;6:838-844.
10 Salehi-Nik N, Amoabediny G, Solouk A, Shokrgozar MA, Zandieh-Doulabi B, Klein-Nulend J. Biomimetic modification of silicone tubes using sodium nitrite-collagen immobilization accelerates endothelialization. J Biomed Mater Res B 2015;In press.
11 Li G, Yang P, Qin W, Maitz MF, Zhou S, Huang N. The effect of coimmobilizing heparin and fibronectin on titanium on hemocompatibility and endothelialization. Biomaterials 2011;32:4691-4703.
12 Wissink MJB, Beernink R, Poot AA, Engbers GH, Beugeling T, van Aken WG, Feijen J. Improved endothelialization of vascular grafts by local release of growth factor from heparinized collagen matrices. J Control Release 2000;64:103-114.
13 Salehi-Nik N, Amoabediny G, Shokrgozar MA, Mottaghy K, Klein-Nulend J, Zandieh-Doulabi B. Surface Modification of silicone tubes by functional carboxyl and amine, but not peroxide groups followed by collagen immobilization improves endothelial cell stability and functionality. Biomed Mater 2015;10:015024.
14 Plata AM, Sherwin SJ, Krams R. Endothelial nitric oxide production and transport in flow chambers: The importance of convection. Ann Biomed Eng 2010;38:2805-2816.
15 Fadel AA, Barbee KA, Jaron D. A computational model of nitric oxide production and transport in a parallel plate flow chamber. Ann Biomed Eng 2009;37:943-954.
16 Sprague B, Chesler NC, Magness RR. Shear stress regulation of nitric oxide production in uterine and placental artery endothelial cells: experimental studies and hemodynamic models of shear stresses on endothelial cells. Int J Dev Biol 2010;54:331-339.
17 Andrews AM, Jaron D, Buerk DG, Kirby PL, Barbee KA. Direct. Real-time measurement of shear stress-induced nitric oxide produced from endothelial cells in vitro. Nitric Oxide 2010;23:335-342.
18 Mashour GA, Boock RJ. Effects of shear stress on nitric oxide levels of human cerebral endothelial cells cultured in an artificial capillary system. Brain Res 1999;842:233-238.
19 Choi HW, Barakat AI. Modulation of ATP/ADP Concentration at the Endothelial Cell Surface by Flow: Effect of Cell Topography. Ann Biomed Eng 2009;37:2459-2468.

20 Brown A, Burke G, Meenan BJ. Modeling of shear stress experienced by endothelial cells cultured on microstructured polymer substrates in a parallel plate flow chamber. Biotechnol Bioengin 2011;108:1148-1158.
21 Kavdia M, Popel A. Wall shear stress differentially affects no level in arterioles for volume expanders and hb-based O2 carriers. Microvasc Res 2003;66:49-58.
22 Smith K, Moore L, Layton H. Advective transport of nitric oxide in a mathematical model of the afferent arteriole. Am J Physiol Renal Physiol 2003;284:1080-1096.
23 Mourtas S, Kastellorizios M, Klepetsanis P, Farsari E, Amanatides E, Mataras D, Pistillo BR, Favia P, Sardella E, d'Agostino R, Antimisiaris SG. Covalent immobilization of liposomes on plasma functionalized metallic surfaces. Colloids Surfaces B 2011;184:214-220.
24 ElMeshad AN, Mortazavi SM, Mozafari MR. Formulation and characterization of nanoliposomal 5-fluorouracil for cancer nanotherapy. J Liposome Res 2014;24:1-9.
25 Mirahmadi F, Tafazzoli-Shadpour M, Shokrgozar MA, Bonakdar S. Enhanced mechanical properties of thermosensitive chitosan hydrogel by silk fibers for cartilage tissue engineering. Mater Sci Eng C Mater Biol Appl 2013;33:4786-4794.
26 Polk AA, Maul TM, McKeel DT, Snyder TA, Lehocky CA, Pitt B, Stolz DB, Federspiel WJ, Wagner WR. A biohybrid artificial lung prototype with active mixing of endothelialized microporous hollow fibers. Biotechnol Bioeng 2010;106:490-500.
27 Perktold K, Resch M, Florian H. Pulsatile non-Newtonian flow characteristics in a three-dimensional human carotid bifurcation model. ASME J Biomech Eng 1991;113:464-475.
28 Kabirian F, Amoabediny G, Haghighipour N, Salehi-Nik N, Zandieh-Doulabi B. Nitric oxide secretion by endothelial cells in response to fluid shear stress, aspirin, and temperature. J Biomed Mater Res A 2015;103:1231-1237.
29 Huo Y, Choy JS, Svendsen M, Sinha AK, Kassab JS. Effects of vessel compliance on flow pattern in porcine epicardial right coronary arterial tree. J Biomech 2009;42:594-602.
30 Bridges AW, Garcia AJ. Anti-Inflammatory polymeric coatings for implantable biomaterials and devices. J Diabetes Sci Technol 2008;2:984-994.
31 Kanai AJ, Strauss HC, Truskey GA, Crews AL, Grunfeld S, Malinski T. Shear stress induces ATP-independent transient nitric oxide release from vascular endothelial cells, measured directly with a porphyrinic microsensor. Circ Res 1995;77:284-293.
32 Spijker HT, Graaff R, Boonstra PW, Busscher HJ, van Oeveren W. On the influence of flow conditions and wettability on blood material interactions. Biomaterials 2003;24:4717-4727.

CHAPTER 7

General Discussion

GENERAL DISCUSSION

The only current treatment option to provide respiratory support during cardiac surgery, or chronic aid for patients in end-stage pulmonary failure is extracorporeal membrane oxygenation (ECMO) [1, 2]. The membrane oxygenator component of ECMO, also called artificial lung, typically consists of a bundle of synthetic microporous hollow fibres [1]. Thrombus formation resulting from the poor biocompatibility of hollow fibers made of different synthetic polymers, e.g. silicone, is a key limitation for clinical application of artificial lungs [2, 3]. Therefore, to minimize thrombus formation associated with blood contact with synthetic materials during ECMO, high levels of anticoagulants such as heparin are required which greatly restricts patient mobility and quality of life [1-3]. During the last decade important developments in the field of biomaterials and tissue engineering have increased the biocompatibility of hollow fibers in new types of artificial lungs, so-called biohybrid artificial lungs [1-5]. The blood-contacting parts of hollow fibers in these biohybrid artificial lungs are seeded with endothelial cells to mimic the native pulmonary vasculature and to provide a naturally occurring biocompatible surface for blood interaction. In this thesis we focus on the development of a stable, anti-thrombotic endothelial cell monolayer on silicone hollow fibers by using surface modification and fluid hydrodynamics modulation to improve the biocompatibility of these fibers used in artificial lungs.

Collagen immobilization as a first step for endothelialization

The successful development of biohybrid artificial lungs is challenged by the hydrophobic nature of the polymers typically used to make the hollow fibers, which lowers the degree of cell adhesion [2, 5]. Therefore, surface modification through covalent immobilization of biologically adhesive extracellular matrix proteins, such as collagen, to the surface of the hollow fibers is needed to guarantee uniform cell attachment and growth [2, 5]. Covalent immobilization of collagen using carbodiimide bonds provides a coating that is robust enough to withstand fluid shear stress resulting from the blood flow [5-7]. The functional groups on the material's surface are mainly chemically reactive groups amenable for covalent immobilization of collagen [8-10]. Much attention has been paid to plasma graft polymerization in the presence of different reactive chemicals to introduce functional groups on the material's surface [10, 11]. We introduced different functional groups, i.e. peroxide groups by oxygen plasma pre-modification, carboxyl groups by acrylic acid (AAc) grafting, and amine groups by aminosilane (AmS) grafting, on the inert and nonpolar surface of silicone tubes to improve covalent immobilization of collagen (**Chapter 2**). The amine groups resulted in the highest concentrations of immobilized collagen on silicone tubes as well as the most optimal collagen-endothelial cell interaction, and cell number attached to the

material's surface. Endothelial cells are known to be sensitive to material surface characteristics, such as wettability and surface charge [9, 10]. Our results showed that endothelial cells poorly adhere to negatively charged carboxyl groups, which agrees with published data showing that carboxyl groups grafted on a material surface inhibit cell adhesion and proliferation [9, 10, 12]. Although the carboxyl groups on the silicone tubes did not support endothelial cell adhesion, they did improve collagen immobilization thus providing an excellent substrate for endothelial cell attachment and growth. The cell density on collagen-immobilized silicone tubes was higher than on tubes without immobilized collagen. This result agrees well with data by others that endothelial cell adhesion is facilitated by pre-coating of the substratum with extracellular matrix proteins such as collagen [8, 13]. The ability of adhesive proteins to support cell adhesion is also dependent on cell quantity and activity, which is influenced by the surface properties of the underlying substratum [14]. A relatively high percentage of the cells did detach from collagen-immobilized plasma surface-modified silicone tubes under fluid shear stress, which likely resulted from a weak linkage of collagen on these tubes, unlike the collagen immobilized with carbodiimide bonds on silicone tubes with amine or carboxyl groups. The high nitric oxide (NO) release by endothelial cells on collagen-immobilized silicone tubes indicated an excellent anti-thrombotic functionality of the cells. The collagen-immobilized AmS-grafted silicone tubes allowed excellent cell behavior, but the amine groups significantly changed the silicone's physical and mechanical properties. In addition, the shelf life of peroxide and amine groups is limited [15], which indicates an important advantage of using carboxyl groups rather than peroxide or amine groups for collagen immobilization on silicone in the clinic. Immobilized collagen suitably links with carboxyl groups on the silicone tubes, and provides an excellent and stable substratum for endothelial cell growth and function.

Flow preconditioning of endothelial cells to increase cell stability and anti-thrombotic capacity

AAc grafting was used to immobilize collagen on the outside surface of silicone hollow fibers (SiHFs). Not only a stable collagen coating, but also endothelial cell retention on collagen-immobilized SiHFs in artificial lungs is important, since endothelial cell detachment might result in cell-free regions and consequently induce platelet adhesion [16, 17]. Controlled exposure of endothelial cells seeded on surface-modified materials to fluid shear stress, so-called flow preconditioning, remarkably stimulates endothelial cell monolayer retention under fluid shear stress [18-21]. Under chronic steady shear stress, endothelial cells flatten and remodel structurally to spread the shear stress over a larger surface area [20-22]. Fluid shear stress treatment increases the production of endothelial cell-derived anti-inflammatory agents, e.g. NO and prostaglandin I_2 (PGI_2) [23-25]. In this thesis, we

tested whether endothelial cell retention and anti-thrombotic function on SiHFs under high shear stress could be improved by collagen immobilization on these fibers and flow-preconditioning of the endothelial cell layer (**Chapter 3**). Collagen did not detach from collagen-immobilized AAc-grafted SiHF patches after treatment with 1 to 30 dyn/cm^2 fluid shear stress, showing that carbodiimide bonds between carboxyl groups of AAc-grafted SiHFs and amine groups of collagen are stable enough to withstand the fluid shear stress. Collagen-immobilized AAc-grafted SiHFs retained cells well under different levels of fluid shear stress, but 27% of the cells still detached at a high fluid shear stress of 30 dyn/cm^2. This detachment of cells might have occurred as a result of weak bonds between cellular integrins and collagen under high shear stress. Our results suggest that 24 h preconditioning of endothelial cells on collagen-immobilized AAc-grafted SiHF patches with 12 dyn/cm^2 fluid shear stress in a parallel-plate flow chamber significantly increased cell retention. The cell adhesion force should be higher than the hydrodynamic forces generated by a fluid flow to allow the creation of a stable layer of endothelial cells. Flow preconditioning of endothelial cells induces conformational activation of integrins and increased binding to extracellular matrix ligands [21, 22]. It also increases cell surface area involved in integrin-mediated adhesion as a consequence of cell flattening [20, 26]. A finite element model allowed to achieve a detailed and precise flow field computation within the parallel-plate flow chamber, and to correlate the fluid shear stress distribution on the cell surface with the cellular response. Our finite element simulation results showed that by decreasing the cell height after flow preconditioning, the mean and maximum shear stress experienced by the cells also decreased, and therefore a more homogeneous fluid shear stress distribution was obtained at the cell surface, resulting in decreased cell detachment. Flow preconditioning of endothelial cells significantly increased NO and PGI_2 production when subjected to high fluid shear stress, showing that flow preconditioning not only increases cell retention under high shear stress, but also enhances anti-thrombotic capability of endothelial cells.

Incorporation of sodium nitrite into collagen conjugate coating as a practical solution to the problem of collagen thrombogenicity

Collagen has positive effects on cell adhesion and proliferation, but it is also highly thrombogenic, and induces platelet adhesion and aggregation as well as activation of a coagulation cascade in areas which are not fully covered by endothelial cells [17]. Nitrite, the stable end-product of NO, has been shown to have anti-thrombogenic properties in acidic environments [27, 28]. Therefore we investigated whether the combination of sodium nitrite, as a nitrite donor, with collagen in the presence of acetic acid improves endothelialization of silicone tubes by increasing the number of endothelial cells and growth hormone (GH) production, as well as by decreasing platelet adhesion (**Chapter 4**). Collagen and sodium nitrite-collagen

conjugates were immobilized onto silicone tubes by ionic interaction with a pre-determined AAc graft density. Incorporation of sodium nitrite in the collagen conjugate did not change the amount of immobilized collagen. A nitrite and acidified nitrite-generating sodium nitrite-collagen conjugate coating of silicone tubes with <50 μM initial sodium nitrite increased the number of endothelial cells more than collagen coating alone, probably via GH production, with a maximum effect at 25 μM initial sodium nitrite resulting in a perfect confluent endothelial cell monolayer on the silicone surface after 6 days of culture. We observed that nitrite and acidified nitrite-generating coating of sodium nitrite-collagen conjugate immobilized AAc-grafted silicone tubes with >25 μM initial sodium nitrite significantly suppressed the thrombogenic properties of collagen by decreasing platelet adhesion on the silicone surface, especially when a high initial concentration of sodium nitrite in conjugate was used. Since sodium nitrite-collagen conjugate coatings with 25-50 μM initial sodium nitrite in conjugate increased endothelial cell proliferation and also inhibited platelet aggregation, they are highly promising to promote endothelialization of silicone materials in blood-contacting devices.

Co-immobilization of growth-inducing and anti-thrombotic agents on silicone tubes offers both endothelialization and anti-coagulation

The ultimate success of endothelialization of materials depends on the degree of confluency of the formed endothelial cell layer [17, 29]. Several hundreds of millions of cells are needed to coat the hollow fibers of one meter squared artificial lung [30]. Therefore, it takes a long period of time to reach confluency of the endothelial cell layer when cells are seeded at low density. The rate of endothelialization can be improved by immobilization of specific exogenous growth factors or growth hormones. Endothelial cells seeded at low density on hollow fibers can be stimulated by growth-inducing agents to rapidly form a confluent monolayer in a few days [17, 31]. Therefore, suppression of the thrombogenic properties of collagen by using anti-thrombotic agents on the one hand, and promotion of endothelial cell growth using growth-inducing agents to achieve a confluent cell layer on the material surface on the other hand, may result in improved performance of blood-contacting medical devices [17, 32, 33]. Currently the use of anti-thrombotic or growth-inducing agents is limited by the short half-life, renal toxicity, physical and chemical instability, and rapid clearance of these agents [34]. Prolonged release of anti-thrombotic or growth-inducing agents from liposomes, that function as drug delivery carriers, has gained considerable attention, since liposomes are biocompatible, biodegradable, capable of releasing encapsulated drugs in a sustained manner, and transporting drugs across biological membranes [34, 35]. In this thesis, endothelialization of silicone tubes was improved by using sustained release of sodium nitrite as an anti-thrombotic

agent when the silicone tubes are not yet completely covered by endothelial cells, and by using sustained release of GH as a growth-inducing agent to stimulate complete surface coverage by endothelial cells (**Chapter 5**). Nanoliposomes loaded with sodium nitrite (nNitrite) or GH (nGH) were prepared and used to control the sustained release of the anti-thrombotic and growth-inducing agents. The encapsulation efficiency achieved was high for both sodium nitrite and GH, showing the effectiveness of the thin-film hydration technique used for the preparation of nanoliposomes. nNitrite-nGH-collagen conjugate was co-immobilized on AAc-grafted silicone tubes to provide a stable coating that offers both anti-thrombotic and growth-inducing properties. The surface-modified silicone tubes containing nNitrite and nGH were stable for 1 month storage at 4°C due to the presence of cholesterol and amino-PEG in the lipid phase of nanoliposomes [36]. Encapsulation of sodium nitrite or GH in nanoliposomes increased the controlled release as well as the effectiveness and bioavailability of these bioactive compounds. Our results showed that conjugation of collagen with nNitrite increased the number of endothelial cells after 48 h of culture. However, the stimulatory effect of GH released from nGH-collagen coating on endothelial cell proliferation was higher than that of nitrite and acidified nitrite released from nNitrite-collagen coating. The presence of the anti-thrombotic polymer PEG in the nanoliposome's structure prevents platelet adhesion [37]. Therefore, all surface-modified silicone tubes containing nanoliposomes in their coatings, even without anti-thrombotic agent, showed reduced platelet adhesion. Maximum platelet inhibition was observed on silicone tubes containing nNitrite in their conjugate coating. Interestingly, sustained release of nitrite and acidified nitrite from nNitrite-collagen conjugate more strongly inhibited platelet adhesion than nitrite and acidified nitrite release from sodium nitrite-collagen conjugate (**Chapter 4**). The GH released resulted in increased NO release by endothelial cells on silicone tubes coated with nGH-collagen conjugate. This indicated that GH not only affected endothelial cell proliferation, but also the anti-thrombotic function and inhibited platelet aggregation [38]. Nitrite and acidified nitrite release from silicone tubes coated with nNitrite-nGH-collagen conjugate and GH-induced NO release by endothelial cells on these tubes contributed to the increased anti-platelet activity of these tubes. Conjugation of nNitrite with nGH and collagen in coating of silicone tubes stimulated PGI_2 production by endothelial cells which showed excellent functionality of endothelial cells on surface-modified silicone tubes. nNitrite-nGH-collagen conjugate immobilized AAc-grafted silicone tubes provided full endothelial coverage, and low platelet adhesion even in the absence of endothelial cells.

Bioavailability of anti-thrombotic agents on hollow fiber-blood interface affects thrombus deposition under fluid flow

Biomimetic coatings with incorporated growth-inducing and anti-thrombotic agents improved both endothelialization and blood compatibility of silicone tubes (**Chapter 5**). The application potential of these coatings on blood-contacting parts of SiHFs was also investigated with the aim to improve the performance of biohybrid artificial lungs (**Chapter 6**). Endothelialized hollow fibers are continuously in contact with blood flow when the biohybrid artificial lung starts working [1-5]. A change in fluid flow modifies the mass transport characteristics at the hollow fiber-blood interface. The bioavailability of anti-thrombotic biomolecules on the hollow fiber-blood interface, which is of crucial importance to inhibit thrombus formation, strongly depends on transport processes and the level of the anti-thrombotic biomoleules may drop due to convection [39-42]. Therefore, the concentration of anti-thrombotic biomolecules at the hollow fiber-blood interface is determined by the balance between fluid shear stress-dependent production of anti-thrombotic biomolecules and their removal by diffusive and convective transport dependent on the applied fluid shear stress. In this thesis, we used sustained release of the growth-inducing agent GH and the anti-thrombotic agent sodium nitrite from collagen conjugate to decrease thrombus deposition by increasing the number of endothelial cells on the SiHFs as well as the bioavailability of nitrite under flow conditions (**Chapter 6**). Collagen or nNitrite-nGH-collagen conjugate were immobilized on AAc-grafted SiHFs. The percentage of cells detached from SiHFs immobilized with nNitrite-nGH-collagen conjugate was lower than from SiHFs immobilized with collagen under different fluid shear stress ranging from 1-30 dyn/cm^2. GH release from SiHFs immobilized with nNitrite-nGH-collagen conjugate resulted in a higher number of endothelial cells present compared with SiHFs immobilized with collagen after 6 days of culture. The high number of endothelial cells on SiHFs immobilized with nNitrite-nGH-collagen conjugate might have increased the number and the strength of cell-cell bonds, which together with cell-collagen bonds contribute to the development of a stable endothelial monolayer. For endothelialized SiHFs immobilized with collagen, where nitrite production was just related to endothelial cell-derived NO production, the amount of nitrite did not indefinitely increase with shear stress but reached a saturated concentration instead. However, for SiHFs immobilized with nNitrite-nGH-collagen conjugate where the nitrite production resulted from both endothelial cell-derived NO production and nitrite release from nNitrite in the coating of the fibers, the magnitude of nitrite production rate gradually increased by increasing the shear stress. Measurements of nitric production rate under different shear stresses coupled with theoretical simulations were used to determine the nitrite bioavailability measured as nitrite concentration on the surface of SiHF patches. An increase in blood flow rate was associated with two different phenomena: 1)

Increased nitrite production by the endothelialized surface-modified patches, and 2) Increased velocity of nitrite washing out from the chamber due to convection. To allow the steady-state nitrite concentration to increase with increased shear stress, the stimulated nitrite production rate must exceed the rate of removal by the increased convective transport effects [43]. Our simulation results showed that the nitrite concentration on SiHFs immobilized with nNitrite-nGH-collagen conjugate depends on the shear stress in a complex non-monotonic fashion. Nitrite bioavailability had a direct effect on thrombus deposition on surface-modified SiHF patches under shear stress. The bioavailability of nitrite and subsequently the thrombus deposition was modified by shear stress conditioning of endothelialized surface-modified SiHF patches. Thrombus deposition on SiHFs immobilized with nNitrite-nGH-collagen conjugate was lower than on SiHFs immobilized with collagen under shear stress application. Coating of SiHFs with nNitrite-nGH-collagen conjugate not only increased endothelial cell proliferation and stability, but also increased nitrite (as an anti-thrombotic agent) bioavailability and inhibited thrombus formation even under high shear stress, suggesting that nNitrite-nGH-collagen conjugate coatings are highly promising to improve the biocompatibility of biohybrid artificial lungs.

CONCLUSIONS

Endothelial cell seeding of blood-contacting parts of hollow fibers in artificial lungs to mimic the function of the normal vascular endothelium is promising to decrease thrombotic complications resulting from blood flow through these devices. In this thesis, we aimed to improve the endothelialization of silicone hollow fibers used in artificial lungs and subsequently their biocompatibility by surface modification and fluid hydrodynamic modulation. Our results showed that carboxyl groups introduced by AAc grafting on silicone surface suitably links with amine groups of collagen, and provides an excellent and stable substratum for endothelial cell growth and function (**Chapter 2**). Controlled exposure of endothelial cells seeded on collagen-immobilized silicone to fluid shear stress, so-called flow preconditioning, remarkably stimulated endothelial cell monolayer retention and anti-thrombotic function under fluid shear stress (**Chapter 3**). The thrombogenicity of collagen was suppressed by incorporation of sodium nitrite in the collagen coating of silicone. Nitrite and acidified nitrite-generating sodium nitrite-collagen conjugate coating on silicone increased the number of endothelial cells and decreased platelet adhesion (**Chapter 4**). The rate of endothelialization was increased by sustained release of GH from collagen conjugate coating. Biomimetic coatings incorporating the anti-thrombotic agent sodium nitrite and the growth-inducing agent GH provided full endothelial coverage and low platelet adhesion

even in the absence of endothelial cells (**Chapter 5**). These biomimetic coatings also provided high nitrite bioavailability and low thrombus formation even at high shear stress (**Chapter 6**), suggesting that nNitrite-nGH-collagen conjugate coatings are highly promising to promote endothelialization of silicone hollow fibers in biohybrid artificial lungs.

FUTURE PERSPECTIVE

Based on the present thesis several questions can be raised which deserve attention in the future:

1) Does surface modification of silicone hollow fibers affect oxygen transfer through these fibers?

2) Is surface modification with collagen or nNitrite-nGH-collagen conjugate immobilization through AAc grafting also suitable for other polymers that are typically used in the fabrication of hollow fibers used in artificial lungs?

3) Is it possible to improve the method of cell seeding on hollow fibers to promote a homogenous cell layer on the surface of these fibers?

4) How can the endothelialized surface-modified SiHF patches be scaled up to prepare a biohybrid artificial lung with a high number of these SiHF patches?

5) What is the effect of the layout of the SiHF patches on the fluid hydrodynamics characteristics in a biohybrid artificial lung with a high number of SiHF patches?

6) Is the surface modification and fluid hydrodynamics modulation as described in this thesis to develop a stable and functional endothelial cell monolayer on hollow fibers also useful for other blood-contacting devices, e.g. vascular grafts, stents, etc?

ABBREVIATIONS

All abbreviations used in this thesis are provided below:

Abbreviation	Full name
AAc	acrylic acid
AAc Si	acrylic acid-grafted silicone
AAc Si-Col	collagen-immobilized acrylic acid-grafted silicone
AAc Si-Nitrite-Col	sodium nitrite-collagen conjugate immobilized acrylic acid-grafted silicone
AAc Si-nGH-Col	nanoliposomal growth hormone-collagen conjugate immobilized acrylic acid-grafted silicone
AAc Si-nNitrite-Col	nanoliposomal sodium nitrite-collagen conjugate immobilized acrylic acid-grafted silicone
AAc Si-nNitrite-nGH-Col	nanoliposomal sodium nitrite-nanoliposomal growth hormone-collagen conjugate immobilized acrylic acid-grafted silicone
AAc SiHF-Col	collagen-immobilized acrylic acid-grafted silicone hollow fiber
AAc SiHF-nNitrite-nGH-Col	nanoliposomal sodium nitrite-nanoliposomal growth hormone-collagen conjugate immobilized acrylic acid-grafted silicone hollow fiber
AmS	aminosilane
AmS Si	aminosilane-grafted silicone
AmS Si-Col	collagen-immobilized aminosilane-grafted silicone
ECM	extracellular matrix
FE	finite element
GH	growth hormone
nGH	nanoliposomal growth hormone
nGH-Col	nanoliposomal growth hormone-collagen conjugate
nNitrite	nanoliposomal sodium nitrite
nNitrite-Col	nanoliposomal sodium nitrite-collagen conjugate
nNitrite-nGH-Col	nanoliposomal sodium nitrite-nanoliposomal growth hormone-collagen conjugate
NO	nitric oxide
PGI_2	prostaglandin I_2
PSM	plasma surface modification
PSM Si	plasma surface-modified silicone
PSM Si-Col	collagen-immobilized plasma surface-modified silicone
Si	silicone
SiHFs	silicone hollow fibers
Si-Col	collagen-adsorbed silicone
SiHF-Col	collagen-adsorbed silicone hollow fiber

REFERENCES

1 Polk AA, Maul TM, McKeel DT, Snyder TA, Lehocky CA, Pitt B, Stolz DB, Federspiel WJ, Wagner WR. A biohybrid artificial lung prototype with active mixing of endothelialized microporous hollow fibers. Biotechnol Bioeng 2010;106:490-500.

2 Lemon G, Lim ML, Ajalloueian F, Macchiarini P. The development of the bioartificial lung. Br Med Bull 2014;110:35-45.

3 Wagner WR, Griffith BP. Reconstructing the lung. Science 2010;329:519-521.

4 Sawa Y, Ohala T, Takagi M, Suhara H, Matsuda H. Development of hybrid artificial lung with gene transfected biological cells. J Artif Organs 2000;3:1-4.

5 Takagi M, Shiwaku K, Inoue T, Shirakawa Y, Sawa Y, Matsuda H, Yoshida T. Hydrodynamically stable adhesion of endothelial cells onto a polypropylene hollow fiber membrane by modification with adhesive protein. J Artif Organs 2003;6:222-226.

6 Lee SD, Hsiue GH, Chang PCT, Kao CY. Plasma-induced grafted polymerization of acrylic acid and subsequent grafting of collagen onto polymer film as biomaterials. Biomaterials 1996;17:1599-1608.

7 Gupta B, Plummer C, Bisson I, Frey P, Hilborn J. Plasma-induced graft polymerization of acrylic acid onto poly(ethylene terephthalate) films: characterization and human smooth muscle cell growth on grafted films. Biomaterials 2002;2:863-871.

8 Sano S, Kato K, Ikada Y. Introduction of functional groups onto the surface of polyethylene for protein immobilization. Biomaterials 1993;14:817-822.

9 Lee JH, Jung HW, Kang IK, Lee HB. Cell behaviour on polymer surfaces with different functional groups. Biomaterials 1994;15:705-711.

10 Thevenot P, Hu W, Tang L. Surface chemistry influence implant biocompatibility. Curr Top Med Chem 2008;8:270-280.

11 Karkhaneh A, Mirzadeh H, Ghaffariyeh A. Simultaneous graft copolymerization of 2-hydroxyethyl methacrylate and acrylic acid onto polydimethylsiloxane surfaces using a two-step plasma treatment. J Appl Polym Sci 2007;105:2208-2217.

12 Tzoneva R, Seifert B, Alberecht W, Richau K, Lendlein A, Gruth T. Poly(ether imide) membranes: studies on the effect of surface modification and protein pre-adsorption on endothelial cell adhesion, growth and function. J Biomat Sci-Polym E 2008;19:837-852.

13 Farhadi M, Mirzadeh H, Solouk A, Asghari A, Jalessi M, Ghanbari H, Yazdanifard P. Collagen-immobilized patch for repairing small tympanic membrane perforations: In vitro and in vivo assays. J Biomed Mater Res A 2012;100:549-553.

14 Tzoneva R, Faucheux N, Groth T. Wettability of substrata controls cell–substrate and cell–cell adhesions. Biochim Biophys Acta 2007;1770:1538-1547.

15 Siow KS, Britcher L, Kumar S, Griesser HJ. Plasma methods for the generation of chemically reactive surfaces for biomolecule immobilization and cell colonization-A review. Plasma Process Polym 2006;3:392-418.

16 Lin Q, Ding X, Qiu F, Song X, Fu G, Ji J. In situ endothelialization of intravascular stents coated with an anti-CD34 antibody functionalized heparin–collagen multilayer. Biomaterials 2010;31:4017-4025.

17 Wissink MJB, Beernink R, Poot AA, Engbers GH, Beugeling T, van Aken WG, Feijen J. Improved endothelialization of vascular grafts by local release of growth factor from heparinized collagen matrices. J Control Release 2000;64:103-114.

18 Isenberg BC, Williams C, Tranquillo RT. Endothelialization and flow conditioning of fibrin-based media-equivalents. Ann Biomed Eng 2006; 34:971-985.

19 Ott MJ, Ballermann BJ. Shear stress-conditioned, endothelial cell-seeded vascular grafts: improved cell adherence in response to in vitro shear stress. Surgery 1995;117:334-339.

20 Dardik A. Liu A, Ballermann BJ. Chronic in vitro shear stress stimulates endothelial cell retention on prosthetic vascular grafts and reduces subsequent in vivo neointimal thickness. J Vasc Surg 1999;29:157-167.
21 McIlhenny SE, Hager ES, Grabo DJ, DiMatteo C, Shapiro IM, Tulenko TN, DiMuzio PJ. Linear shear conditioning improves vascular graft retention of adipose-derived stem cells by upregulation of the $\alpha_5\beta_1$ integrin. Tissue Eng Part A 2010;16:245-255.
22 Tzima E, del Pozo MA, Shattil SJ, Chien S, Schwartz MA. Activation of integrins in endothelial cells by fluid shear stress mediates Rho-dependent cytoskeletal alignment. EMBO J 2001;20:4639-4647.
23 Frangos JA, Eskin SG, McIntire LV, Ives CL. Flow effects on prostacyclin production by cultured human endothelial cells. Science 1985;227:1477-1479.
24 Hsieh HJ, Liu CA, Huang B, Tseng AH, Wang DL. Shear-induced endothelial mechanotransduction: the interplay between reactive oxygen species (ROS) and nitric oxide (NO) and the pathophysiological implications. J Biomed Sci 2014;21:3-18.
25 Kabirian F, Amoabediny G, Haghighipour N, Salehi-Nik N, Zandieh-Doulabi B. Nitric oxide secretion by endothelial cells in response to fluid shear stress, aspirin, and temperature. J Biomed Mater Res A 2015;103:1231-1237.
26 Brown A, Burke G, Meenan BJ. Modeling of shear stress experienced by endothelial cells cultured on microstructured polymer substrates in a parallel plate flow chamber. Biotechnol Bioeng 2011;108:1148-1158.
27 Lundberg JO, Weitzberg E. NO generation from nitrite and its role in vascular control. Arterioscler Thromb Vasc Biol 2005;25:915-922.
28 Egemnazarov B, Schermuly RT, Dahal BK, Elliott GT, Hoglen NC, Surber MW, Weissmann N, Grimminger F, Seeger W, Ghofrani HA. Nebulization of the acidified sodium nitrite formulation attenuates acute hypoxic pulmonary vasoconstriction. Respir Res 2010;11:81-93.
29 Herring M, Smith J, Dalsing M, Glover J, Compton R, Etchberger K, Zollinger T. Endothelial cell seeding of polytetrafluoroethylene femoral popliteal bypasses: The failure of low-density seeding to improve patency. J Vasc Surg 1994;20:260-265.
30 Maurer AN, Matheis G. The artificial lung, in Advances in tissue engineering. Polak J, Ed. Imperial College Press, 2008.
31 Doi K, Matsuda T. Enhanced vascularization in a microporous polyurethane graft impregnated with basic fibroblast growth factor and heparin. J Biomed Mat Res 1997;34:361-370.
32 Zhang K, Li J, Deng K, Liu T, Chen JY, Huang N. The endothelialization and hemocompatibility of the functional multilayer on titanium surface constructed with type IV collagen and heparin. Colloids Surfaces B 2013;108:295-304.
33 Li G, Yang P, Qin W, Maitz MF, Zhou S, Huang N. The effect of coimmobilizing heparin and fibronectin on titanium on hemocompatibility and endothelialization. Biomaterials 2011;32:4691-4703.
34 Elbayoumi TA, Torchilin VP. Current trends in liposome research. Methods Mol Biol 2010;605:1-27.
35 Jain RA. The manufacturing techniques of various drug loaded biodegradable poly(lactide-co-glycolide) (PLGA) devices. Biomaterials 2000;21:2475-2490.
36 Dominak LM, Omiatek DM, Gundermann EL, Heien ML, Keating CD. Polymeric crowding agents improve passive biomacromolecule encapsulation in lipid vesicles. Langmuir 2010;26:13195-13200.
37 Campbell EJ, O'Byrne V, Stratford PW, Quirk I, Vick TA, Wiles MC, Yianni YP. Biocompatible surfaces using methacryloylphosphorylcholine laurylmethacrylate copolymer. ASAIO J 1994;40:853-857.
38 Thum T, Tsikas D, Frolich JC, Borlak J. Growth hormone induces eNOS expression and nitric oxide release in a cultured human endothelial cell line. FEBS Lett 2003;555:567-571.
39 Plata AM, Sherwin SJ, Krams R. Endothelial nitric oxide production and transport in flow chambers: The importance of convection. Ann Biomed Eng 2010;38:2805-2816.

40 Barbee KA, Jaron D. A computational model of nitric oxide production and transport in a parallel plate flow chamber. Ann Biomed Eng 2009;37:943-954.
41 Mashour GA, Boock RJ. Effects of shear stress on nitric oxide levels of human cerebral endothelial cells cultured in an artificial capillary system. Brain Res 1999;842:233-238.
42 Choi HW, Barakat AI. Modulation of ATP/ADP Concentration at the Endothelial Cell Surface by Flow: Effect of Cell Topography. Ann Biomed Eng 2009;37:2459-2468.
43 Andrews AM, Jaron D, Buerk DG, Kirby PL, Barbee KA. Direct, real-time measurement of shear stress-induced nitric oxide produced from endothelial cells in vitro. Nitric Oxide 2010;23:335-342.

General Summary

GENERAL SUMMARY

The poor biocompatibility of hollow fibers used in artificial lungs is a key limitation for clinical application of these devices. Endothelialized hollow fibers have been suggested as a means to improve artificial lung biocompatibility in new types of artificial lungs, so-called biohybrid artificial lungs. This approach seeks to mimic the *in vivo* function of vascular endothelial cells to yield a biocompatible surface, actively inhibiting platelet activation and deposition for long term blood oxygenation and therefore minimize or eliminate the need for anticoagulants. Synthetic hollow fibers currently used in artificial lungs, such as silicone, do not support endothelial cell adhesion and needs to be surface-modified. The process of endothelial cell adhesion and spreading on hollow fibers *in vitro* has been shown to be facilitated by pre-coating of substrata with the main extracellular matrix protein, collagen. The functional groups, such as peroxide, carboxyl, and amine, are main chemically reactive groups amenable for covalent immobilization of collagen. Endothelial cell retention on collagen-coated hollow fibers in artificial lungs is important since endothelial cell detachment might expose cell-free regions to blood flow and consequently induce platelet adhesion. Controlled exposure of endothelial cells seeded on surface-modified materials to low fluid shear stress, so-called flow preconditioning, remarkably stimulates endothelial cell monolayer retention under high fluid shear stress.

Despite of its positive effects on cell adhesion and proliferation, collagen is highly thrombogenic, and induces platelet adhesion in areas which are not fully covered by endothelial cells. Therefore, suppression of the thrombogenic properties of collagen by using anti-thrombotic agents on the one hand, and promotion of endothelial cell growth using growth-inducing agents to achieve a confluent cell layer on the silicone hollow fibers on the other hand, may result in improved biohybrid artificial lungs performance. Co-immobilization of biomimetic coatings using carbodiimide bonds has been shown to provide resistance against blood flow shear stress. Not only a stable biomimetic coating, but also the bioavailability of anti-thrombotic biomolecules on the hollow fiber-blood interface under shear stress is critical to inhibit thrombus formation. A change in fluid flow modifies the mass transport characteristics at the hollow fiber-blood interface. Therefore, the anti-thrombotic biomolecule concentration at the hollow fiber-blood interface is regulated by the counteraction between the shear stress-dependent production of anti-thrombotic biomolecules and their removal by diffusive and convective transport.

This thesis aimed to improve the biocompatibility of silicone hollow fibers used in artificial lungs by developing a stable and anti-thrombotic functional endothelial cell layer. We hypothesized that silicone surface modification and fluid hydrodynamics modulation improves endothelialization. To test this hypothesis, we

started by surface modification of silicone tubes with three different chemical functional groups, i.e. peroxide, carboxyl, and amine, to determine the surface chemical entity that allows strong collagen immobilization and improvement of endothelialization, cell stability, and anti-thrombotic functionality. The amine groups resulted in the highest concentrations of immobilized collagen on silicone tubes as well as the most optimal collagen-endothelial cell interaction. Although the carboxyl groups on the silicone tubes did not support endothelial cell adhesion, they did improve collagen immobilization thus providing an excellent substrate for endothelial cell attachment and growth. The cell density on collagen-immobilized silicone tubes was higher than on tubes without immobilized collagen. Collagen-immobilized with carbodiimide bonds on silicone tubes with amine or carboxyl groups retained endothelial cells under shear stress. The high nitric oxide (NO) release by endothelial cells on collagen-immobilized silicone tubes indicated an excellent anti-thrombotic functionality of the cells. The collagen immobilization with carboxyl groups was chosen since the amine groups had a limited shelf life and they significantly changed the silicone's physical and mechanical properties (**Chapter 2**).

Collagen immobilization with carboxyl groups was applied to the outside surface of silicone hollow fibers, but 27% of the cells still detached at a high fluid shear stress of 30 dyn/cm^2. This detachment of cells might have occurred as a result of weak bonds between cellular integrins and collagen under high shear stress. Therefore, flow preconditioning was used to increase cell stability under high shear stress. Our results suggest that 24 h preconditioning of endothelial cells on collagen-immobilized silicone hollow fibers with 12 dyn/cm^2 fluid shear stress in a parallel-plate flow chamber significantly increased cell retention and anti-thrombotic function compared with un-preconditioned cells. A finite element model allowed to achieve a detailed and precise flow field computation within the parallel-plate flow chamber, and to correlate the fluid shear stress distribution on the cell surface with the cellular response. Our finite element simulation results showed that by decreasing the cell height after flow preconditioning, the mean and maximum shear stress experienced by the cells also decreased, and therefore a more homogeneous fluid shear stress distribution was obtained at the cell surface, resulting in decreased cell detachment (**Chapter 3**).

Even low endothelial cell detachment from collagen-immobilized materials can stimulate platelet adhesion since collagen is highly thrombogenic. Therefore, incorporation of anti-thrombotic agents into collagen coating can increase its blood compatibility. Nitrite, the stable end-product of NO, has been shown to have anti-thrombogenic properties in acidic environments. Therefore, nitrite and acidified nitrite generating sodium nitrite-collagen conjugate was immobilized on silicone tubes with carboxyl groups and the effect of nitrite and acidified nitrite release on blood compatibility and endothelialization of silicone tubes was investigated.

Sodium nitrite-collagen conjugate coatings with 25-50 μM initial sodium nitrite in conjugate increased endothelial cell proliferation probably via GH production, and also inhibited platelet adhesion (**Chapter 4**).

The ultimate success of endothelialization of materials depends on the degree of confluency of the formed endothelial cell layer. Therefore, development of biomimetic coatings having both anti-thrombotic and growth-inducing properties may result in improved performance of blood-contacting biomedical devices. In addition, sustained release of biomolecules from nanoliposomes improves their biological effect. Nanoliposomes loaded with sodium nitrite (as an anti-thrombotic agent) or GH (as a growth-inducing agent) were prepared, blended with collagen solution, and then co-immobilized on silicone tubes. Encapsulation of sodium nitrite or GH in nanoliposomes increased the controlled release as well as the effectiveness and bioavailability of these bioactive compounds. The presence of nanoliposomal sodium nitrite in the collagen conjugate coating inhibited platelet adhesion more than free sodium nitrite. GH not only affected endothelial cell proliferation, but also the anti-thrombotic function and inhibited platelet aggregation by stimulating endothelial cells to release NO. Nanoliposomal sodium nitrite-nanoliposomal GH-collagen conjugate coating provided full endothelial coverage, and low platelet adhesion on silicone tubes even in the absence of endothelial cells (**Chapter 5**).

The application potential of these biomimetic coatings on the outside surface of silicone hollow fibers was also investigated under fluid shear stress with the aim to improve the performance of biohybrid artificial lungs. The bioavailability of anti-thrombotic biomolecules on the hollow fiber-blood interface, which is of crucial importance to inhibit thrombus formation, strongly depends on transport processes. Measurements of nitric production rate under different shear stresses coupled with simulations of nitrite transport in the parallel-plate flow chamber were used to determine the nitrite bioavailability measured as nitrite concentration on the surface of surface-modified silicone hollow fibers. An increase in fluid velocity increased the magnitude of nitrite production from the endothelialized surface-modified fibers, as well as the velocity of nitrite washing out from the chamber due to convection. Nitrite bioavailability had a direct effect on thrombus deposition on surface-modified fibers under shear stress (**Chapter 6**).

Coating of fibers with nanoliposomal sodium nitrite-nanoliposomal GH-collagen conjugate not only increased endothelial cell proliferation and stability, but also increased nitrite bioavailability and inhibited thrombus formation even under high shear stress, suggesting that this conjugate coating is highly promising to improve the biocompatibility of biohybrid artificial lungs. This, together with new insights in the effects of fluid shear stress on increasing cell stability, and anti-thrombotic functionality, as well as on modifying the bioavailability of anti-thrombotic biomolecules and thrombus deposition, improves our understanding of

how surface modification and fluid hydrodynamics modulation increase material biocompatibility under flow condition. These insights could contribute to the development of biocompatible hollow fibers to use in biohybrid artificial lungs.

Algemene Samenvatting

ALGEMENE SAMENVATTING

De geringe biocompatibiliteit van holle vezels die worden toegepast in kunstmatige longen beperkt de klinische toepassing van deze apparaten in hoge mate. Het bedekken van holle vezels met endotheelcellen is een manier om de biocompatibiliteit van nieuwe generatie kunstmatige longen, zogenaamde biohybride kunstlongen, te verbeteren. Deze benadering beoogt de *in vivo* functie van vasculaire endotheelcellen na te bootsen en tegelijk een biocompatibel oppervlak te creëren. Dit kan leiden tot de remming van de activering van bloedplaatjes en trombosevorming en het bespoedigen van bloedoxygenatie op de lange termijn, waardoor de noodzaak voor toepassing van anticoagulantia wordt geminimaliseerd of uitgesloten. Hechting van endotheelcellen aan synthetische holle vezels die momenteel in kunstlongen worden gebruikt, zoals siliconen, is pas mogelijk na oppervlakte modificatie. Het proces van aanhechting en verspreiding van endotheelcellen op holle vezels *in vitro* wordt aantoonbaar vergemakkelijkt als de substraten vooraf worden bekleed met collageen, het belangrijkste extracellulaire matrix eiwit. Functionele groepen zoals peroxide, carboxyl, en amine zijn de belangrijkste chemisch reactieve groepen geschikt voor de covalente immobilisatie van collageen. Retentie van endotheelcellen op met collageen-bekleedde holle vezels in kunstmatige longen is belangrijk omdat het loslaten van endotheelcellen kan resulteren in blootstelling van celvrije gebieden aan de bloedstroom, met aanhechting van bloedplaatjes als gevolg. Gecontroleerde blootstelling van endotheelcellen uitgezaaid op oppervlakte-gemodificeerde materialen aan lage vloeistofschuifspanning (“fluid shear stress”), zogenaamde “flow preconditioning”, verhoogt de endotheelcelretentie onder hoge vloeistofschuifspanning.

Collageen heeft positieve effecten op de celaanhechting en proliferatie, maar is tegelijkertijd zeer trombogeen, en induceert de aanhechting van bloedplaatjes in gebieden die niet volledig zijn bedekt door endotheelcellen. Het onderdrukken van trombogene eigenschappen van collageen met anti-trombotische middelen enerzijds, en het bevorderen van de groei van endotheelcellen op holle vezels van siliconen met behulp van groeibevorderende middelen anderzijds, kan daarom het functioneren van biohybride kunstmatige longen verbeteren. Co-immobilisatie van biomimetische coatings met behulp van carbodiimide bindingen heeft aantoonbaar geleid tot weerstand tegen bloedstroom-schuifspanning. Niet alleen een stabiele biomimetische coating, maar ook de biologische beschikbaarheid van anti-trombotische biomoleculen op de holle vezel-bloed-interface onder schuifspanning, is kritisch bij het remmen van stolselvorming. Een verandering in de vloeistofstroom wijzigt de kenmerken van massatransport bij de holle vezel-bloed-interface. Daarom wordt de concentratie van anti-trombotische biomoleculen bij de holle vezel-bloed-interface gereguleerd door de tegengestelde

kracht tussen de schuifspanning-afhankelijke productie van anti-trombotische biomoleculen en hun verwijdering door diffusie en convectie transport.

Dit proefschrift was gericht op het verbeteren van de biocompatibiliteit van siliconen holle vezels die gebruikt worden in kunstlongen door een stabiele en anti-trombotische functionele endotheelcellaag te ontwikkelen. Onze hypothese was dat siliconen oppervlakte modificatie en modulatie van vloeistofhydrodynamica de endothelialisatie verbetert. Om deze hypothese te testen, zijn we begonnen met oppervlaktemodificatie van siliconen buisjes met drie verschillende chemische functionele groepen, dat wil zeggen peroxide, carboxyl en amine, om te bepalen welke chemische oppervlakte een sterke collageenimmobilisatie en verbetering van endothelialisatie, celstabiliteit en anti-trombotische functionaliteit mogelijk maakt. De aminegroepen gaven de hoogste concentraties geïmmobiliseerd collageen op de siliconen buisjes en de meest optimale collageen-endotheelcel interacties. Hoewel de carboxylgroepen van de siliconen buisjes geen endotheelcelhechting ondersteunden, verbeterden zij de collageenimmobilisatie om zo een uitstekend substraat te leveren voor endotheelcelhechting en groei. De celdichtheid op collageen-geïmmobiliseerde siliconen buisjes was hoger dan op buisjes zonder geïmmobiliseerd collageen. Collageen geïmmobiliseerd middels carbodiimide bindingen op siliconen buisjes met amine- of carboxylgroepen zorgde voor behoud van endotheelcellen onder schuifspanning. De hoge stikstofoxide (NO) afgifte door endotheelcellen op collageen-geïmmobiliseerde siliconen buisjes wees op een uitstekende anti-trombotische werking van de cellen. Collageen immobilisatie middels carboxylgroepen werd gekozen omdat de aminogroepen een beperkte houdbaarheid hadden en omdat zij de fysieke en mechanische eigenschappen van siliconen aanzienlijk veranderden **(Hoofdstuk 2)**.

Collageen immobilisatie met carboxylgroepen werd toegepast op het buitenoppervlak van siliconen holle vezels. Zevenentwintig % van de cellen liet toch nog los bij hoge vloeistofschuifspanning van 30 dyn/cm^2. Dit loslaten van cellen zou kunnen zijn veroorzaakt door de zwakke banden tussen cellulaire integrines en collageen onder hoge schuifspanning. Om die reden werd “flow preconditioning” gebruikt om de celstabiliteit onder hoge schuifspanning te verhogen. Onze resultaten suggereerden dat 24 uur “flow preconditiong” van endotheelcellen op collageen-geïmmobiliseerde siliconen holle vezels met 12 dyn/cm^2 vloeistofschuifspanning in een parallelle plaat vloeistofstromingkamer leidde tot aanzienlijke toename van celretentie en anti-trombotische werking in vergelijking met cellen die geen “flow preconditioning” hadden ondergaan. Een eindig elementenmodel stelde ons in staat om een gedetailleerde en nauwkeurige stromingsveld-berekening binnen de parallelle plaat vloeistofstroming kamer te maken en om de verdeling van de vloeistofschuifspanning op het celoppervlak te correleren aan de cellulaire respons. De resultaten van de eindige elementen simulaties tonen aan dat door het verlagen van de celhoogte na “flow

preconditioning" de gemiddelde en maximale schuifspanning op de cellen ook verminderde waardoor een homogene vloeistofschuifspanningsverdeling werd verkregen op het celoppervlak, wat resulteerde in verminderde celloslating **(Hoofdstuk 3)**.

Zelfs geringe loslating van endotheelcellen van collageen-geïmmobiliseerde materialen kan de hechting van bloedplaatjes stimuleren, omdat collageen zeer trombogeen is. Derhalve kan incorporatie van anti-trombotische middelen in collageen coating de bloedcompatibiliteit verhogen. Nitriet, het stabiele eindproduct van NO, heeft aantoonbaar anti-trombogene eigenschappen in zure omgevingen. Daarom werd nitriet en aangezuurd nitriet genererend natriumnitriet-collageen conjugaat geïmmobiliseerd op siliconen buisjes met carboxylgroepen, en werd het effect van nitriet en aangezuurd nitriet release op de bloedcompatibiliteit en endothelialisatie van siliconen buisjes onderzocht. Natriumnitriet-collageen conjugaat coatings met 25-50 µM initiële natriumnitriet in conjugaat verhoogden de proliferatie van endotheelcellen, waarschijnlijk door middel van groeihormoon (GH) productie, en remden ook de aanhechting van bloedplaatjes **(Hoofdstuk 4)**.

Het uiteindelijke succes van endothelialisatie van materialen is afhankelijk van de mate van confluentie van de gevormde endotheelcellaag. Daarom kan de ontwikkeling van biomimetische coatings met zowel anti-trombotische en groeibevorderende eigenschappen leiden tot verbeterde prestaties van biomedische apparaten die met bloed in contact komen. Bovendien vergroot de vertraagde afgifte van biomoleculen uit nanoliposomen hun biologische effect. Nanoliposomen geladen met natriumnitriet (als een anti-trombotisch middel) of GH (als groeibevorderend middel) werden geprepareerd, gemengd met collageenoplossing, en vervolgens co-geïmmobiliseerd op siliconen buisjes. Inkapseling van natriumnitriet of GH in nanoliposomen verhoogde de gecontroleerde afgifte als ook de doeltreffendheid en biologische beschikbaarheid van deze bioactieve stoffen. De aanwezigheid van nanoliposomaal natriumnitriet in het met collageen bekleedde conjugaat remde de aanhechting van bloedplaatjes meer dan vrij natrium-nitriet. GH beïnvloedde niet alleen de proliferatie van endotheelcellen maar ook de anti-trombotische werking, en remde de bloedplaatjesaggregatie door de stimulatie van NO productie door endotheelcellen. Nanoliposomaal natriumnitriet-nanoliposomaal GH-collageen conjugaat coating gaf een volledige endotheliale dekking en zeer geringe hechting van bloedplaatjes aan siliconen buisjes, zelfs in de afwezigheid van endotheelcellen **(Hoofdstuk 5)**.

De toepassingsmogelijkheden van deze biomimetische coatings op het buitenoppervlak van siliconen holle vezels werden eveneens onderzocht onder vloeistofschuifspanning teneinde de prestaties van biohybride kunstmatige longen te verbeteren. De biologische beschikbaarheid van anti-trombotische biomoleculen op de holle vezel-bloed-interface, wat van cruciaal belang is voor de remming van

trombusvorming, is sterk afhankelijk van transportprocessen. Metingen van de nitraat productiesnelheid onder verschillende schuifspanningen gekoppeld aan simulaties van nitriet transport in de parallelle plaat stromingkamer werden gebruikt om de biobeschikbaarheid van nitriet, gemeten als nitrietconcentratie op het oppervlak van oppervlakte-gemodificeerde siliconen holle vezels, te bepalen. Een toename van de vloeistofsnelheid verhoogde de nitrietproductie uit de geëndothelializeerde oppervlakte-gemodificeerde vezels, als ook de snelheid van het uitwassen van nitriet uit de kamer als gevolg van convectie. Nitriet biobeschikbaarheid had een direct effect op de trombus depositie op oppervlakte-gemodificeerde vezels onder schuifspanning **(Hoofdstuk 6)**.

Het bekleden van vezels met nanoliposomaal natriumnitriet-nanoliposomaal GH-collageen conjugaat verhoogde niet alleen de endotheelcel proliferatie en stabiliteit maar ook de nitriet biobeschikbaarheid, en remde de trombusvorming, zelfs onder hoge schuifspanning, wat suggereerde dat deze conjugaat coating veelbelovend is om de biocompatibiliteit van biohybride kunstmatige longen te verbeteren. Dit gegeven, tesamen met nieuwe inzichten in de effecten van vloeistofschuifspanning op het vergroten van de celstabiliteit en anti-trombotische functionaliteit en op het modificeren van de biobeschikbaarheid van anti-trombotische biomoleculen en trombus depositie, verbetert ons begrip van hoe oppervlaktemodificatie en modulatie van vloeistof hydrodynamica de materiaalbiocompatibiliteit verhogen onder vloeistofstroming. Deze inzichten kunnen bijdragen aan de ontwikkeling van biocompatibele holle vezels die gebruikt kunnen worden in biohybride kunstmatige longen.

Acknowledgements

ACKNOWLEDGMENTS

First of all, I must thank God for giving me talents and abilities, as well as the ambition, to reach this point in my career. It is truly all due to your glory that I succeeded in pursuing this field of study. This thesis is a result of the hard work of dedicated members of the team. It was a great opportunity for me to be a member of such an enthusiastic team. My gratitude is offered to the University of Tehran and VU University Amsterdam for providing me with the dual degree program that allowed me to perform my PhD research with multidisciplinary research group members from Iran and The Netherlands. I would also like to thank those individuals without whose support I was not in the position that I am today.

It all started with Prof. Ghassem Amoabediny, who afforded me the opportunity to unify the fields of chemical engineering and tissue engineering in order to immerse myself in this interesting research and begin to acquire the required skills in the research profession. Dear Prof. Amoabediny, It was enjoyable to let my scientific immigration grow and mature under the guidance of your scientific yet flexible logic. I really appreciate your invaluable guidance, supervision, encouragement, patience and support throughout my PhD studies.

I would like to express my deepest gratitude to Prof. Dr. Jenneke Klein Nulend, without whom this thesis book would not have been beautifully done. Prof. Dr. Jenneke Klein Nulend, thank you for all the precious time you dedicated to introduce me in the world of science, research, and cell biology. I have learned a lot from you, about how to work as a scientist, to put things into perspective, and write a scientific paper. Thanks for all long calls even late times, explaining simple things to me again and again, correcting my English pronunciation and discussing things together to generate this whole thesis. Sorry to use "I just…" in answering almost all your questions. Your dedication to your PhD students is admirable and this enabled me to submit five papers in two years.

I appreciate the kind support of Prof. Mohammad Ali Shokrgozar, for providing me with the opportunity to work in the warm environment of cell culture lab in Pasteur Institute of Iran and giving me good suggestions that contributed much towards the formation and completion of this thesis. Dear Prof. Shokrgozar, thanks for being approachable all the time and willing to help me throughout my research.

My sincere appreciation will go to Dr. Behrouz Zandieh-Doulabi, my dear compatriot, who always patiently answered the questions I had about my research and also the dual degree rules in VU Amsterdam. He has always been a great listener and lent a caring ear to everyone and also has a big sunny smile. Dear Dr. Zandieh, thank you for being so approachable during my hours of need and supporting me through the tough times. You always made me feel better by saying that "Nasim khanum everything is under control". I will never forget your kindness

to show me the sights of Amsterdam and my surprise birthday party on my first trip to the Netherlands with Fatima.

I also do not forget other professors and scientists whose influence and generous collaboration ever remain invaluable. Dr. Atefeh Solouk, for kindly answering my questions related to surface modification of silicone with carboxyl groups. Dear Atefeh, you always gave me confidence by saying that "go for it". Dr. Jhamak Nourmohammadi for helps and suggestions in introducing amine groups to the silicone surface, and Dr. Nooshin Haghighipour, for helping me kindly and teaching how to work with endothelial cells at Pasteur Institute of Iran.

Especial thanks to all the colleagues from Research Center for New Technologies in Life Science Engineering, University of Tehran (UTLSE). Parnian (Banikarimi), thanks for introducing COMSOL to me and always being with me as a friend and also as a colleague in fluid hydrodynamics part of my research (Chapters 3, and 6). You are a very nice, hard-working young woman with a bright future. Sanaz (Malaie-Blasi), thanks for introducing liposome world to me. You are such a good friend and I really appreciate your valuable contribution to the nanoliposome production part of my thesis work (Chapter 5). Touhid (Hajibabaei), thanks for helping me to modify silicone surface with amine groups. I hope one day I could see your nice Azari dancing. Behdad (Pouran), my dear friend, thank you for sharing so many of your ideas with me about the fluid hydrodynamics via Skype, and helping me in writing and submitting this part of my thesis work (Chapters 3, and 6). Behdad, it has always been a pleasure working with you, and I am sure that one day you will be one of the most famous scientists in the field of regenerative medicine. In addition to coworkers in the UTLSE, I have also met a group of great people while working at Pasteur Institute of Iran that helped me through all of the cell experiments in my thesis work. I would like to thank all members of the cell culture lab, especially Tannaz (Nouri), who taught me cell culture for the first time on my research journey.

I should also appreciate the very kind support that I received from the head of the college of engineering, Prof. Mahmoud Kamarei, and the vice chancellor for research and graduate studies at school of chemical engineering of University of Tehran, Dr Behzad Rostami. They kindly understood my situation as a dual degree student and always helped me through all of the tough times that dual degree threw my way. Dear Dr. Rostami, I wish the universe was full of people like you!

I wish to thank my best friend, Hoda (Heli), for keeping in touch and sharing the ups and downs in life sometimes combined with backbite. Hoda, I would not exchange our friendship for gold. I love you pal! I also like to thank some gorgeous couples who have always made my weekends fantastic and given me more energy to continue my work. Azin and Akbar, Marjan and Ehsan, Hajar and Hadi, and Esi jan thanks for agreeing to our request for going out every time!

Last but most importantly, I would like to express my deepest regards and gratitude to my parents, and my parents-in-law for their encouragement and support. None of my accomplishments would have been possible without the love and prayers of my parents, who constantly pushed me until I learned how to never quit pushing myself. They are the ones who have generously devoted their lives to my success and were been enchanted by my every little success even more than myself. Only and only to remind myself of how much I owe them I would like to dedicate this thesis to my parents. My angel, my little brother, Nima, you are an un-ending source of strength and motivation in my life. I love you so much! My dear sister, Tabassom, thanks to you and your two little girls, Raha and Rasta, for encouraging me to finalize my PhD by saying that "Aunti, when will it be finished? We want to spend more time with you". My special thanks to my husband, my love, Arman for his unconditional love and support. Armanam, you entered my life halfway through this adventure, but you fully embraced it. Your love, concern, support, continuous encouragement, and enthusiasm with every new finding and goal achieved really help me conquer most of the difficulties throughout this work. With you I am not alone in the dawn of my dreams.

CURRICULUM VITAE

Name: Nasim Salehi Nik
Date and place of birth: September 11th, 1984, Tehran, Iran
Nationality: Iranian

Scientific Education

2002-2006 BSc Chemical Engineering, College of Engineering, University of Tehran, Tehran, Iran
Title thesis: Technical and economic studies of disinfectants used in cooling towers of Tehran refinery
Supervisor: Prof.dr. M.A. Mousavian (School of Chemical Engineering, College of Engineering, University of Tehran)
GPA: 16.74/20; Fourth place among 112 students of chemical engineering

2006-2009 MSc Chemical Engineering, College of Engineering, University of Tehran, Tehran, Iran
Title thesis: Determination of fluidization quality in fluidized beds through the sound analysis
Supervisors: Prof.dr. R. Sotudeh-Gharebagh (School of Chemical Engineering, College of Engineering, University of Tehran)
Prof.dr. N. Mostoufi (School of Chemical Engineering, College of Engineering, University of Tehran)
GPA: 17.87/20; First place among 16 students of chemical engineering

2009-2015 PhD student at: 1) Chemical Engineering, College of Engineering, University of Tehran, Tehran, Iran, and 2) Academic Centre for Dentistry Amsterdam, University of Amsterdam and VU University Amsterdam, MOVE Research Institute Amsterdam, Amsterdam, The Netherlands
Title thesis: Improved endothelialisation by silicone surface modification and fluid hydrodynamics modulation: implications for oxygenator biocompatibility

Supervisors: Prof.dr. G. Amoabediny (School of Chemical Engineering, College of Engineering, University of Tehran)
Prof.dr. J. Klein-Nulend (Dept Oral Cell Biology, ACTA-University of Amsterdam and VU University Amsterdam, MOVE Research Institute Amsterdam, Amsterdam, The Netherlands)

Co-supervisors: Prof.dr. M.A. Shokrgozar (National Cell Bank, Pasteur Institute of Iran, Tehran, Iran)
Dr. B. Zandieh Doulabi (Dept Oral Cell Biology, ACTA-University of Amsterdam and VU University Amsterdam, MOVE Research Institute Amsterdam, Amsterdam, The Netherlands)

GPA: 19.2/20

Iranian Patents

2010 Design and construction of a perfusion bioreactor with a new control system for mammalian cell culture

2015 Design and construction of a tubular-perfusion bioreactor for vascular tissue engineering

2015 Design and construction of a parallel-plate flow chamber for mimicking the *in vivo* environment for cultured mammalian cells

International meetings

2014 1st Matrix Biology Congress, June 21-24, 2014, Rotterdam, The Netherlands (poster)

2014 International Conference on Biobased Materials and Composites (ICBMC'14), May 13-16, 2014, Montreal, Canada (poster)

2013 The 6th International Bioengineering Congress (BEC2013), November 12-15, 2013, Izmir, Turkey (2 posters)

2013 9th International Congress on Stem Cell Biology & Technology, September 4-6, 2013, Tehran, Iran (poster)

2013 3rd International Conference on Biomedical Engineering and Technology (ICBET), May 19-20, 2013, Copenhagen, Denmark. (poster-full paper publication). Hydrodynamically stable adhesion of endothelial cells on gelatin electrospun nanofibrous scaffolds. APCBEE Procedia, 2013;7:169-174

2011 7th International Chemical Engineering Congress and Exhibition (IChEC 2011), November 21-24, 2011, Kish, Iran (1 oral presentation, 2 posters)

2010 BIOSPINE 3- 3rd International Congress-Biotechnologies for Spinal Surgery, September 1-4, 2010, Amsterdam, The Netherlands (oral presentation)

2008 2nd International Student Conference of Biotechnology, November 15-17, 2008, Tehran, Iran (1 oral presentation, 1 poster)

PUBLICATIONS

Salehi-Nik N, Amoabediny G, Shokrgozar MA, Mottaghy K, Klein-Nulend J, Zandieh-Doulabi B. Surface modification of silicone tubes by functional carboxyl and amine, but not peroxide groups followed by collagen immobilization improves endothelial cell stability and functionality. Biomedical Materials, 2015;10:015024.

Salehi-Nik N, Amoabediny G, Solouk A, Shokrgozar MA, Zandieh-Doulabi B, Klein-Nulend J. Biomimetic modification of silicone tubes using sodium nitrite-collagen immobilization accelerate endothelialization. Journal of Biomedical Materials Research: Part B, 2015;in press.

Salehi-Nik N, Banikarimi SP, Amoabediny G, Pouran B, Shokrgozar MA, Zandieh-Doulabi B, Klein-Nulend J. Flow preconditioning of endothelial cells on collagen-immobilized silicone fibers enhances cell retention and anti-thrombotic function. Submitted.

Salehi-Nik N, Malaie-Balasi Z, Amoabediny G, Banikarimi SP, Shokrgozar MA, Zandieh-Doulabi B, Klein-Nulend J. Sustained release of growth hormone and sodium nitrite from biomimetic collagen coating immobilized on silicone tubes improves endothelialisation. Submitted.

Salehi-Nik N, Amoabediny G, Banikarimi SP, Pouran B, Zandieh-Doulabi B, Klein-Nulend J. Nanoliposomal growth hormone and sodium nitrite release from silicone fibers reduces thrombus formation under flow. Submitted.

Mokhtari-Jafari F, Amoabediny G, Haghighipour N, Zarghami R, Saatchi A, Akbari J, **Salehi-Nik N**. Mathematical modelling of cell growth in 3D scaffold and validation of static and dynamic culture. Engineering in Life Sciences, 2015;in press.

Kabirian F, Amoabediny G, Haghighipour N, **Salehi-Nik N**, Zandieh-Doulabi B. Nitric oxide secretion by endothelial cells in response to fluid shear stress, aspirin, and temperature. Journal of Biomedical Materials Research: Part A, 2015;103:1231-1237.

Nourmohammadi J, Hajibabaei T, Amoabediny G, Jafari SH, **Salehi-Nik N**. Aminosilane layer formation on the surface of PDMS tubes improves their wettability and cytocompatibility. Trends in Biomaterials and Artificial Organs, 2015;29.

Anisi F, **Salehi-Nik N**, Amoabediny G, Pouran B, Haghighipour N, Zandieh-Doulabi B. Applying shear stress to endothelial cells in a new perfusion chamber: hydrodynamic analysis. Journal of Artificial Organs, 2014;17:329-336.

Salehi-Nik N, Amoabediny G, Pouran B, Tabesh H, Shokrgozar MA, Haghighipour N, Khatibi N, Anisi F, Mottaghy K, Zandieh-Doulabi B. Engineering parameters in bioreactor's design: A critical aspect in tissue engineering. BioMed Research International, 2013;2013:ID 762132.

Tabesh H, Amoabediny G, **Salehi-Nik N**, Heydari M, Yosefifard M, Ranaei Siadat SO, Mottaghy K. The role of biodegradable engineered scaffolds seeded with Schwann cells for spinal cord regeneration. Neurochemistry International, 2009;54:73-83.

Salehi-Nik N, Sotudeh-Gharebagh R, Zarghami R, Mostoufi N, Mahjoob MJ. Determination of hydrodynamic behavior of gas-solid fluidized beds using statistical analysis of acoustic emissions. International Journal of Multiphase Flow, 2009;35:1011-1016.

Book Chapter

Amoabediny G, **Salehi-Nik N**, Heli B. The role of biodegradable engineered scaffold in tissue engineering, In: Biomaterials Science and Engineering, In Tech, 2011: 153-172.

چکیده

پوشش‌دهی سطح فیبرهای توخالی با سلول‌های اندوتلیال در نوع جدیدی از ریه‌های مصنوعی، به نام ریه‌های مصنوعی بیوهیبریدی، روشی مناسب جهت کاهش لخته‌زایی ناشی از جریان خون در این تجهیزات به‌شمار می‌رود. در این پایان‌نامه هدف توسعه یک لایه پایدار و دارای کارایی ضد-انعقادی سلول‌های اندوتلیال بر روی فیبرهای توخالی سیلیکونی با استفاده از تلفیق اصلاح سطح سیلیکون و هیدرودینامیک سیال می‌باشد. به این منظور در ابتدا کلاژن با استفاده از گروه‌های عاملی مختلف روی سطح سیلیکون تثبیت گردید. لوله‌های سیلیکونی حاوی کلاژن تثبیت شده با گروه‌های عاملی کربوکسیل و آمین در مقایسه با لوله سیلیکونی اصلاح نشده سبب ۳-۴ برابر افزایش در تعداد سلول‌های اندوتلیال و نیز حدود ۳ برابر افزایش در ترشح نیتریک‌اکسید توسط سلول‌ها پس از ۶ روز کشت گردیدند. کلاژن با استفاده از گروه‌های کربوکسیل بر سطح خارجی فیبرهای توخالی سیلیکونی تثبیت شد اما با اعمال تنش برشی بالای dyn/cm^2 ۳۰، ۲۷٪ از سلول‌ها از سطح کنده شدند. بنابراین، به منظور بهبود پایداری سلول‌های اندوتلیال تحت تنش‌های برشی بالا، از اعمال پیش‌تنش‌برشی بر سلول‌ها به میزان dyn/cm^2 ۱۲ به مدت ۲۴ ساعت در ظرف جریانی صفحه‌موازی استفاده گردید. اعمال پیش‌تنش‌برشی بر سلول‌های اندوتلیال، کنده شدن سلول‌ها در تنش‌برشی dyn/cm^2 ۳۰ را تا ۸/۲ برابر کاهش داد. شبیه‌سازی تنش برشی بر روی سلول‌ها با استفاده از نرم‌افزار کامسول به همراه نتایج آزمایش‌های سلولی نشان داد که با اعمال پیش‌تنش‌برشی، توزیع تنش‌برشی بر سطح سلول‌ها همگن‌تر شده که سبب افزایش پایداری آن‌ها تحت تنش برشی می‌گردد.

میزان موفقیت در توسعه مواد زیست‌سازگار به خاصیت ضد-انعقادی سطح و درجه همگنی لایه سلول اندوتلیال بستگی دارد. بنابراین، نیتریت سدیم به عنوان عامل ضد-انعقادی و/یا هورمون رشد به عنوان عامل محرک رشد به صورت فرم آزاد و یا نانولیپوزومه شده با محلول کلاژن ترکیب شده و بر سطح لوله‌های سیلیکونی تثبیت شدند. پوشش ترکیبی نیتریت سدیم-کلاژن با μM ۲۵ غلظت اولیه نیتریت‌سدیم پس از ۶ روز کشت، تعداد سلول‌های اندوتلیال را به میزان بیشینه و تا ۲۸٪ افزایش داد. μM ۵۰۰ غلظت اولیه نیتریت‌سدیم نیز چسبندگی پلاکت را به میزان بیشینه و تا ۳ برابر در مقایسه با پوشش کلاژنی کاهش داد. پوشش‌های بیومیمتیکی نیتریت سدیم نانولیپوزومه شده (nNitrite)-هورمون رشد نانولیپوزومه شده (nGH)-کلاژن (Col) پس از ۶ روز کشت ۸۳-۱۱۹٪ همگنی سلول را نتیجه داده و چسبندگی پلاکت‌ها را بین ۵۰-۷۶٪ کاهش دادند.

پتانسیل کاربردی پوشش بیومیمتیکی nNitrite-nGH-Col بر سطح خارجی فیبرهای توخالی سیلیکونی تحت تنش‌برشی سیال خون با هدف بهبود عملکرد ریه‌های مصنوعی بیوهیبریدی مورد بررسی قرار گرفت. به منظور تعیین دسترس‌پذیری‌زیستی نیتریت در مرز مشترک فیبرتوخالی-خون، که اهمیت زیادی در جلوگیری از تشکیل لخته دارد، اندازه‌گیری نرخ تولید نیتریت از فیبرهای اصلاح سطح شده تحت تنش‌های‌برشی مختلف به همراه شبیه‌سازی انتقال نیتریت در ظرف جریانی صفحه‌موازی بوسیله نرم‌افزار کامسول استفاده گردید. نتایج نشان داد که دسترس‌پذیری نیتریت تحت تنش برشی سیال اثر مستقیمی بر رسوب لخته روی فیبرهای اصلاح سطح شده دارد.

پوشش‌دهی فیبرها با ترکیب nNitrite-nGH-Col نه‌تنها تکثیر و پایداری سلول‌های اندوتلیال بلکه دسترس‌پذیری‌زیستی نیتریت و جلوگیری از تشکیل لخته را حتی تحت تنش‌های‌برشی بالا افزایش داد که نشان می‌دهد این پوشش ترکیبی برای بهبود زیست‌سازگاری ریه‌های مصنوعی بیوهیبریدی بسیار مفید است. این نتیجه به همراه نتایج حاصل از تأثیر تنش‌برشی سیال بر افزایش پایداری و کارایی ضد-انعقادی سلول‌ها، و نیز دسترس‌پذیری‌زیستی مولکول‌های ضد-انعقادی و رسوب لخته، چشم‌انداز جدیدی در چگونگی اثر تلفیق اصلاح سطح و هیدرودینامیک سیال در افزایش زیست‌سازگاری مواد تحت شرایط جریان فراهم آورد. این یافته‌ها می‌تواند در توسعه سطح سیلیکونی زیست‌سازگار برای استفاده در ریه‌های مصنوعی بیوهیبریدی یا سایر تجهیزات در تماس با خون بکار گرفته شود.

دانشگاه تهران
پردیس دانشکده‌های فنی
دانشکده مهندسی شیمی

دانشگاه VU آمستردام
مرکز آکادمیک دندانپزشکی آمستردام
انیستیتو تحقیقاتی MOVE آمستردام

"اصلاح سطح سیلیکون و اثر هیدرودینامیک سیال در افزایش پوشش دهی با سلول‌های اندوتلیال جهت کاربرد در زیست‌سازگاری ریه‌مصنوعی"

نسیم صالحی نیک

اساتید راهنما: دکتر قاسم عموعابدینی
دکتر ینکه کلین نولند
اساتید مشاور: دکتر محمدعلی شکرگزار
دکتر بهروز زندیه دولابی

پایان‌نامه برای دریافت درجه‌ی دکتری در رشته‌ی مهندسی شیمی

دانشگاه تهران
پردیس دانشکده های فنی
دانشکده مهندسی شیمی

دانشگاه VU آمستردام
مرکز آکادمیک دندانپزشکی آمستردام
انیستیتو تحقیقاتی MOVE آمستردام

اصلاح سطح سیلیکون و اثر هیدرودینامیک سیال در افزایش پوشش دهی با سلول‌های اندوتلیال جهت کاربرد در زیست‌سازگاری ریه‌مصنوعی

نسیم صالحی نیک

اساتید راهنما: دکتر قاسم عموعابدینی
دکتر ینکه کلین نولند

اساتید مشاور: دکتر محمدعلی شکرگزار
دکتر بهروز زندیه دولابی